Cell replacement therapy for Huntington's disease: what we have learned from post-mortem analyses of grafted patients and mice models

Thèse

Giulia Cisbani

Doctorat en neurobiologie
Philosophiae doctor (Ph.D.)

Québec, Canada

Résumé

La maladie d'Huntington (HD) est un désordre neurodégénératif autosomal dominant qui se manifeste suite à une mutation du gène huntingtin. La maladie est caractérisée par une panoplie de signes cliniques qui incluent des problèmes psychiatriques, cognitifs ainsi que des incapacités motrices, en grande partie des mouvements choréiformes. D'un point vue neuropathologique, les cerveaux des patients touchés par la maladie présentent une atrophie majeure du cortex et du striatum où des pertes cellulaires massives sont observées. Il n'existe aucune cure ni traitements efficaces pour cette maladie, et pour ces raisons, plusieurs efforts sont actuellement déployés afin de développer de nouvelles stratégies thérapeutiques telle, entre autre, la transplantation cellulaire. Ma thèse de Doctorat a donc porté, en grande partie, sur l'analyse de cerveaux de patients huntingtoniens recrutés pour l'essai clinique de l'*University of South Florida*. Ces patients, décédés entre 9 et 12 ans post-transplantation, ont reçus des greffes de tissu dérivé de l'éminence ganglionic latérale de fœtus humains âgés entre 8 et 9 semaines post-conception. Des travaux antérieurs menés dans le laboratoire du Dre Ciccheti ont montré que la survie des greffes est compromise à long terme chez ces patients. L'objectif de mon projet était de mieux comprendre les mécanismes responsables de la survie suboptimale des greffes. Nous avons donc formulé l'hypothèse que 1) la faible vascularisation des greffes, 2) la méthode de transplantation (des morceaux de tissu entier vs. des cellules mécaniquement dissociées) ainsi que 3) la présence de la protéine huntingtin mutée (mHtt) au sein du tissu greffé pouvaient contribuer à la dégénérescence des greffes. En effet, nous avons observé que les éléments de l'unité neurovasculaire étaient largement absents au sein des greffes. Les greffes présentaient une plus faible densité de capillaires et l'absence de larges vaisseaux sanguins, comparativement au cerveau hôte. Nous avons de plus observé un nombre réduit d'astrocytes au sein des greffes et une interaction limitée de ces cellules avec les vaisseaux sanguins, suggérant une défaillance des éléments de la barrière hémato-encéphalique. L'absence d'astrocytes était accompagnée par une carence de la sous-unité connexin 43 des *gap junctions*, importante pour les interactions greffe-hôte. Nous avons ensuite démontré que lorsque des cellules dissociées étaient transplantées dans le striatum de souris YAC128, un modèle murin de la maladie d'Huntington, la survie de la greffe était excellente et ni la vascularisation ou ni l'interaction entre les astrocytes et les vaisseaux était altérée. Finalement, nous avons fait l'extraordinaire découverte d'agrégats de la mHtt au sein du tissu greffé. Nous avons observé ces agrégats exclusivement dans la matrice extracellulaire de la greffe dans les tissus humains tandis qu'ils étaient présents au sein des neurones, de leurs dendrites, de la lame basale des vaisseaux sanguins et de la matrice extracellulaire dans le cerveau du patient. Dans son ensemble, cette thèse met en lumière de nouveaux mécanismes pouvant contribuer à la faible survie des greffes chez les patients souffrant de HD à long-terme. Ces résultats seront fort utiles afin d'améliorer cette approche thérapeutique et aideront à une meilleure compréhension des processus pathologiques de la maladie d'Huntington.

Abstract

Huntington's disease (HD) is a devastating autosomal dominant neurodegenerative disorder which manifests because of a mutation in the huntingtin gene. It is characterized by a variety of clinical signs which include psychiatric and cognitive problems as well as motor disabilities, in large part choreiform movements. Neuropathologically, the brains of patients afflicted with this disease present with a major atrophy of the cortex and striatum where massive cell losses are observed. To this day, cures remain unavailable and for this reason, an enormous amount of energy has been put into the development of experimental approaches, and for example into embryonic neuronal cell transplantation, which aims to replace lost cells. A few clinical trials have thus been initiated to evaluate whether such methodologies would be beneficial to patients. My PhD thesis focused, in large part, on the analysis of a number of brains from patients recruited for the University of South Florida trial and who eventually came to autopsy. These patients (4 analyzed post-mortem) received solid pieces of fetal striatal tissue and died between 9 and 12 years post-transplantation. Previous work carried out in Dr. Cicchetti's laboratory has shown that graft survival is compromised in these patients long-term. The aim of my project was to further understand the mechanisms underlying this suboptimal graft survival. We hypothesized that 1) poor vascularization of the graft, 2) the method of transplantation (solid tissue vs. suspension cells) and 3) the potential presence of mutant huntingtin (mHtt) within the grafted tissue may all contribute to graft demise. Indeed, elements of the neurovascular unit were largely absent within the solid grafts. Grafts presented a lower density of capillaries and absence of large blood vessels compared to the host brain. Moreover, we observed a reduced number of astrocytes within the grafts and a limited interaction of these cells with blood vessels, suggesting impairment in blood brain barrier elements. The absence of astrocytes was accompanied by the lack of the gap junction subunit connexin 43, important for graft-host integration. Interestingly, when dissociated cells were transplanted in the striatum of YAC128 mice, a murine model of HD graft survival was excellent and neither the graft vascularization nor the interaction between astrocytes and vessels was altered. Finally, we describe for the first time the presence of mHtt inclusions within the grafted tissue. In the HD transplanted cases, aggregates were detected only in the extracellular matrix of the graft while in the host brain they co-localized with neurons or other cellular elements, such as the basal lamina of blood vessels. Taken together, this thesis sheds new light onto potential mechanisms contributing to poor long-term graft survival in HD patients. These results will help improve such therapies as well as to better understand disease process in HD.

Table of content

List of tables

List of figures

List of abbreviations

6-OHDA: 6-hydroxydopamine
α-SMA: alpha-smooth muscle actin
α-syn: alpha-synuclein
Aβ: amyloid beta
AChE: acethylcholinesterase
AD: Alzheimer's disease
AEC: 3-amino-9-ethylcarbazole
ASOs: antisense oligonucleotides
ATP: adenosine triphosphate
BBB: blood brain barrier
BDNF: brain derived neurotrophic factor
bFGF: basic fibroblast growth factor
BiFC: biomolecular fluorescence complementation
CA II: carbonic anhydrase II
CD: cluster of differentiation
ChAT: choline acetyltransferase
CNTF: ciliary neurotrophic factor
CNS: central nervous system
CoQ10: co-enzyme Q_{10}
COS7: cells being CV-1 (simian) in origin, and carrying the SV40 genetic material
CSF: cerebrospinal fluid
CX43: connexin-43
D1: dopamine receptor 1
D2: dopamine receptor 2
DAB: 3,3'-Diaminobenzidine
DAPI: 4',6-diamidino-2-phenylindole
DARPP-32: dopamine- and cAMP-regulated phosphoprotein, Mr 32kDa
DCX: doublecortin
EAE: experimental autoimmune encephalitis
ENK: enkephalin
FDA: Food and Drug Administration
FDG-PET: fluorodeoxyglucose positron emission tomography
FGF-2: fibroblast growth factor 2
FLVE: far lateral portion of the lateral ventricular eminence
FTIR-FPA: Fourier transform infrared spectroscopy–focal plane array
GABA: γ-aminobutyric acid
GAD: glutamic acid decarboxylase
GAPDH: glyceraldehyde 3-phosphate dehydrogenase
GDNF: glial derived neurotrophic factor
GFP: green fluorescent protein
GFAP: glial fibrillary acidic protein
GLAST: glutamate aspartate transporter

GLT1: glutamate transporter-1
GP: globus pallidus
GPe: external capsule of the globus pallidus
GPi: internal capsule of the globus pallidus
hASCs: human adipose stem cells
hBM-MSC: human bone marrow derived mesenchymal stem cells
HD: Huntington's disease
HEK293T: human endothelial kidney 293T cells
HLA-DR: human leukocyte antigen-DR
htt: huntingtin
IA: ibotenic acid
Iba1: ionized calcium binding adaptor molecule 1
IGF-1: insulin like growth factor-1
INSERM: Institut national de la santé et de la recherche médicale
IBZM-PET: [^{123}I]iodobenzamide positron emission tomography
KA: kainic acid
KMO: kynurenine 3-monooxygenase
LB: Lewy body
LGE: lateral ganglionic eminence
MAP2: microtubule-associated protein 2
MGE: medial ganglionic eminence
mHtt: mutant huntingtin
MIG-HD: Multicentric Intracerebral Grafting in Huntington's Disease
miRNA: micro RNA
MPs: microparticles
MRI: magnetic resonance imaging
MSNs: medium spiny neurons
NAPDH-d: nicotinamide adenine dinucleotide phosphate-diaphorase
NeuN: neuronal nuclei
NFL-H: neurofilament-H
NGF: nerve growth factor
NMDA: N-Methyl-D-aspartate
NOS: nitric oxide synthase
NRK: normal rat kidney cells
PC12: pheochromocytoma of the rat adrenal medulla
PD: Parkinson's disease
PDGFR-β: platelet derived growth factor receptor beta
PET: positron emission tomography
PolyQ: polyglutamine
PREDICT-HD: The Neurobiological Predictors of Huntington's disease
PROX1: prospero homeobox protein 1
QA: quinolinic acid
RAC-PET: [^{11}C]raclopride positron emission tomography
RNAi: RNA interference

shRNA: short hairpin RNA
siRNA: small interfering RNA
SOX2: (sex determining region Y)-box 2
TH: tyrosine hydroxylase
TNT: tunnelling nanotubes
TP: transplantation
UHDRS: Unified Huntington's disease Rating Scale
VEGF: vascular endothelial growth factor
vGLUT1: vesicular glutamate transporter 1
vWF: von Willebrand factor
WGE: whole ganglionic eminence
XX-FISH: XX- fluorescent *in situ* hybridization
YAC: yeast artificial chromosome

If you can keep your head when all about you
Are losing theirs and blaming it on you,
If you can trust yourself when all men doubt you,
But make allowance for their doubting too;
If you can wait and not be tired by waiting,
Or being lied about, don't deal in lies,
Or being hated, don't give way to hating,
And yet don't look too good, nor talk too wise:

If you can dream - and not make dreams your master;
If you can think - and not make thoughts your aim;
If you can meet with Triumph and Disaster
And treat those two impostors just the same;
If you can bear to hear the truth you've spoken
Twisted by knaves to make a trap for fools,
Or watch the things you gave your life to, broken,
And stoop and build 'em up with worn-out tools:

If you can make one heap of all your winnings
And risk it on one turn of pitch-and-toss,
And lose, and start again at your beginnings
And never breathe a word about your loss;
If you can force your heart and nerve and sinew
To serve your turn long after they are gone,
And so hold on when there is nothing in you
Except the Will which says to them: 'Hold on!'

If you can talk with crowds and keep your virtue,
Or walk with Kings - nor lose the common touch,
If neither foes nor loving friends can hurt you,
If all men count with you, but none too much;
If you can fill the unforgiving minute
With sixty seconds' worth of distance run,
Yours is the Earth and everything that's in it,
And - which is more - you'll be a Man, my son!
Kipling

Acknowledgments

I would like to express my gratitude and thanks to my research supervisor, Dr. Francesca Cicchetti for giving me the possibility of pursuing my studies in Neuroscience. Her patience, the time she dedicated me for constructive suggestions, improving my writing skills and developing a more critical scientific opinion have been invaluable. I would also like to thank her for giving me the chance to work on such a meaningful and unique project. Most importantly, she taught me that persistence pays back!

I would like to thank the members of my doctoral committee, Dr. Jasna Kriz and Dr. Francois Berthod for following the progression of my doctoral studies and for their precious advice. I would like also to thank Dr. André Parent and Dr. Vonsattel for accepting to revise my thesis. I am simply honored to have you on my thesis defense committee.

I would like to acknowledge the scholarships that supported me during my PhD. *In primis* la *bourse de recrutement au doctorat de l'Université Laval*, the *Parkinson Society Canada* and finally a scholarship from the Centre thématique de recherche en neurosciences (CTRN).

I would like to express my great appreciation to Martine, for her assistance, for guiding me through the new techniques at the beginning of the PhD and for her friendship. I would also like to thank all the former and current members of the lab that contributed to my formation. I would like also to acknowledge the members of other research teams that have provided me with suggestions and help along the PhD.

I am most grateful to my friends here in Québec and in Italy that have been supporting and encouraging me throughout my studies. In particular, I would like to thank Serena for her moral support and laughter almost everyday since I moved to Québec.

I wish to deeply thank my family, my father, my mother, Giovanni and Anna for their unconditional love and support. Although distance was not easy, it made us grow stronger. Nothing would have been possible to achieve without all of you.

Last, but by no means least, I wish to thank my beloved JP. You have been on my side, believing in me and giving me the strength and support not to desist, even when everything was falling apart. There are not enough words to thank you.

Avant-propos

Contributions

The core of this thesis is composed of 3 main chapters all published or submitted to peer-review journals. **Chapters II** and **III** consist of the integral versions of two articles published in 2013. *Cisbani et al.* was published in *Brain* and reported the astrocytic response and the vasculature of foetal striatal cells in patients with Huntington's disease (HD), while *Cisbani et al.,* featured in Chapter III and published in *Cell transplantation*, is an *in vivo* study pertaining to the same topic but performed in transplanted animal models of the disease. **Chapter IV** completes the post-mortem analysis of these transplanted HD brains and provides evidence for the presence of mutant huntingtin protein in the genetically unrelated transplanted tissue. The manuscript has been submitted to *Annals of Neurology.* Some sections of the introduction and discussion are derived from 2 review articles that we published in *Cell Death and Differentiation* and *Neuropathology and Applied Neurobiology.*

I would also like to point out that in the course of my PhD, I had the opportunity to work on additional projects not directly in line with my main research theme. In particular, I have been involved in a project aiming to evaluate the effects of immune challenges in pregnant dams and their offspring. These results were recently published in *Brain Behaviour and Immunity* (Arsenault *et al*., 2013) where I appear as third author in the publication. Supported by a scholarship from the Parkinson Society Canada, I also participated to a project evaluating the neurorestorative properties of the compound cystamine using different models of Parkinson's disease, both *in vivo, in vitro* and *ex vivo*. I am co-first author on this publication, which will be submitted shortly to *Journal of Neuroscience.* Finally, I am currently contributing to another project evaluating vascular networks and blood brain barrier impairments in both human and murine models of HD.

List of peer-reviewed publications

Peer-reviewed publications

Cisbani G, Freeman TB, Soulet D, Saint-Pierre M, Gagnon D, Parent M, Hauser RA, Barker RA and Cicchetti F. 2013. Striatal allografts in Huntington's disease patients: impact of diminished astrocytes and vascularization on graft viability. *Brain*, 136:433-43.

Cisbani G, Saint-Pierre M and Cicchetti F. 2013. Single cell suspension methodology favours survival and vascularization of foetal striatal grafts in the YAC128 mouse model of Huntington's disease. *Cell Transplantation,* doi: 10.3727/096368913X668636.

Arsenault D, St-Amour I, **Cisbani G**, Rousseau LS, Cicchetti F. 2013. The different effects of LPS and poly I:C prenatal immune challenges on the behaviour, development and inflammatory responses in pregnant mice and their offspring. *Brain Behaviour and Immunity,* 38:77-90

Cicchetti F, Lacroix S, **Cisbani G**, Vallières N, Saint-Pierre M, St-Amour I, Tolouei R, Skepper JN, Hauser RA, Mantovani D, Barker RA and Freeman TB. 2014. Mutant huntingtin is present in neuronal grafts in Huntington's disease patients. *Annals of Neurology,* 76:31:42

Gratuze M, Noël A, Julien C, **Cisbani G**, Milot-Rousseau P, Morin F, Dickler M, Goupil C, Bezeau F, Poitras I, Bissonnette S, Whittington RA, Hébert SS, Cicchetti F, Parker JA, Samadi P, Planel E. 2014. Tau hyperphosphorylation and deregulation of calcineurin in mouse models of Huntington's disease. *Human Molecular Genetics*, pii: ddu456.

Reviews

Cisbani G & Cicchetti F. 2012. An *in vitro* perspective on the molecular mechanisms underlying mutant huntingtin protein toxicity. *Cell Death and Disease*, 30;3:e382.

Cisbani G & Cicchetti F. 2014. The fate of cell grafts for the treatment of Huntington's disease: the *post-mortem* evidence. *Neuropathology and Applied Neurobiology,* 40(1):71-90.

Papers submitted or in preparation

Cisbani G*, Drouin-Ouellet J*****, Gibrat C*****, Bousquet M, Saint-Pierre M, Lavallée-Bourget MH, Boivin L, Lebel M, and Cicchetti F. 2014. Cystamine rescues neuronal degeneration and promotes behavioural recovery in animal models of Parkinson's disease. *In preparation*
**equal contribution*

Drouin-Ouellet J, Kuan WL, Mason SL, Lagacé M, Alata W, **Cisbani G**, Saint-Pierre M, Francis ST, Hall E, Lacroix S, Calon F, Sawiak S, Gowland RA and Cicchetti F. 2014. Changes in cerebral vasculature and blood brain barrier permeability in Huntington's disease.
In preparation

CHAPTER I

1. Introduction

1.1 Huntington's disease

Huntington's disease (HD) is a devastating neurodegenerative disease of which the prevalence is 5-10 cases per 100 000 people (Conneally, 1984; C. A. Ross and Tabrizi, 2011), although this estimation fluctuates geographically (Mason and Barker, 2009). The symptoms typically manifest between the age of 35 and 50 (Duyao et al., 1993; Foroud et al., 1999), with an average duration of 15 years, translating into a shorter life expectancy (Conneally, 1984). The pathology, inherited in an autosomal-dominant fashion (**Figure 1-1A**), is determined by a single mutation in the huntingtin (*htt*) gene located on the short arm of chromosome 4 (Gusella et al., 1983) (**Figure 1-1B**). The modification consists in the expansion of the CAG stretch located in exon 1 of the gene (**Figure 1-1B**). When the length of the CAG repeat coding for a polyglutamine (polyQ) sequence exceeds a critical threshold (>36 CAG repeats), full penetrance of the disease prevails. This sequence is particularly polymorphic and can range between 36 (partial penetrance) to 200 repeats (full penetrance) with peaks of 250 in the longest repeats reported (Nance et al., 1999). The trinucleotide sequence is highly unstable and the number of CAG repeats can diminish when inherited maternally, and increase when inherited paternally (Duyao et al., 1993; La Spada, 1997; Vonsattel and DiFiglia, 1998). Additionally, a number of studies have reported a negative correlation between the age of onset and the length of the polyQ stretch (Foroud et al., 1999; Gusella and MacDonald, 2000; Squitieri et al., 2001), although the relationship has not been firmly established (Ravina et al., 2008).

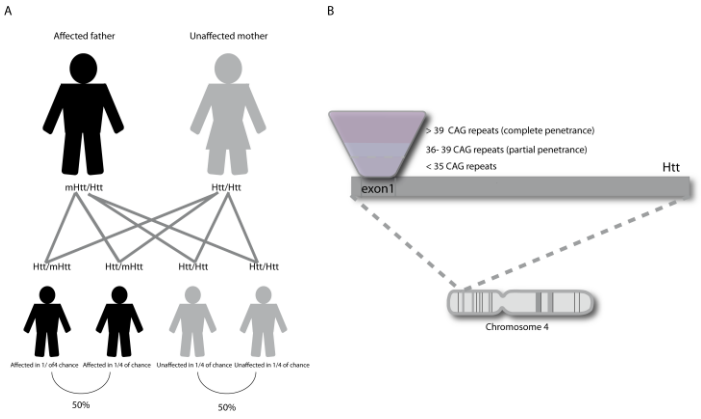

Figure 1-1 HD genetics. (**A**) HD is an autosomal-dominant genetic disorder caused by (**B**) the expansion of the CAG stretch located in the exon 1 of the *htt* gene. The disease manifests when the expansion of the CAG repeats has reached a certain threshold (> 36 CAG repeats). © Giulia Cisbani

1.1.2 Symptomatology

The features which characterize HD include motor dysfunction, cognitive impairments and psychiatric disturbances. The prevalent motor phenotype is chorea, an abnormal and relentless involuntary movement. However, other motor signs such as dystonia, akinesia, bradykinesia and rigidity become predominant with disease progression (Phillips et al., 2008). Cognitive impairments are also observable in HD patients, manifesting even prior to motor decline (Papp et al., 2011). At later stages of the disease, dementia may take place (Mestre and Ferreira, 2012; Peavy et al., 2010; Phillips et al., 2008). Finally, psychiatric symptoms are frequent and manifest as mood disorders, depression, psychosis and insanity that can, in some cases, lead to suicide (Shoulson and Young, 2011) (**Figure 1-2**). In the course of disease progression, patients begin to loose their autonomy in daily activities and accrued care becomes necessary. Death occurs 15-20 years following the appearance of the symptoms and may result from dysphagia, heart failure or respiratory infections (Nance, 2007). It should be noted that juvenile forms of HD also exist. These younger patients do not usually display choreic movements but they present early dysarthria, dystonia, spasticity and ataxia. Cognitive impairments, as well as dementia, can be very severe in these cases and take place early in the disease course (Phillips et al., 2008).

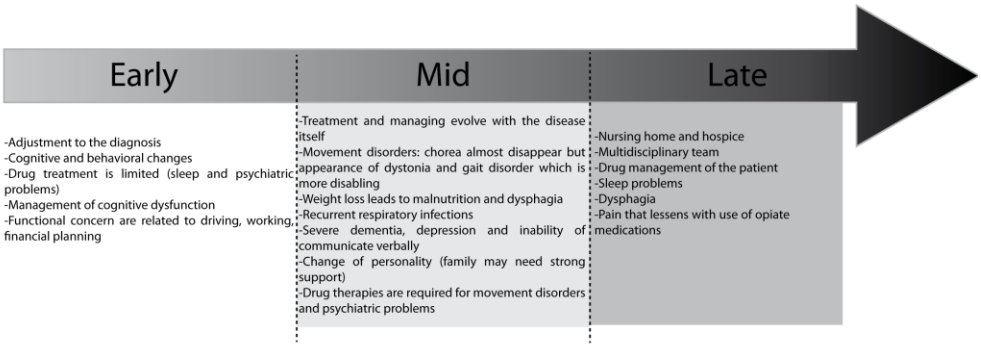

Figure 1-2. Time-line of disease progression. (adapted from (*http://www.stanford.edu/group/hopes/cgi-bin/wordpress/2010/06/the-cognitive-symptoms-of-huntingtons-disease/*, Reuter et al., 2008 and Nance, 2007).

1.1.3 Neuropathology

The main pathological hallmark of the disease is a marked atrophy of the neostriatum, which initially takes place in the caudate nucleus to subsequently involve the putamen. This is due to massive cell loss which reaches 95% in advanced stages (Mann et al., 1993; Myers et al., 1991; Vonsattel and DiFiglia, 1998; Vonsattel et al., 1985). This striatal neuronal degeneration, which largely characterizes the disease, follows a specific topographical pattern, along a caudo-rostral and dorso-lateral/medio-

ventral axis (**Figure 1-3**) (Vonsattel and DiFiglia, 1998). Neuronal degeneration extends to additional structures of the basal ganglia (e.g. thalamus and globus pallidus (GP)) to include deeper cortical layers, all of which are macroscopically visible by a marked enlargement of the lateral ventricles (Vonsattel et al., 1985).

The striatal neuronal degeneration that takes place in HD largely targets the medium spiny neurons (MSNs). During the disease course, the remaining MSNs present dendritic changes, with recurved dendrites, as well as altered shape, size and density of dendritic spines (Vonsattel and DiFiglia, 1998; Vonsattel, 2008). MSNs are GABAergic neurons but they differ in their expression of neuropeptides and their projection target sites (Gerfen, 1992). The GABAergic neurons projecting to the external segment of the globus pallidus (GPe) (Gerfen, 1992), and which express enkephalin (ENK) and D2 receptors, are affected early in the disease. In advanced stages, striatal MSN projecting to the internal segment of the globus pallidus (GPi) and the substantia nigra pars compacta, and expressing substance P and D1 receptors, are targeted (Reiner et al., 2011; Richfield et al., 1995; Sieradzan and Mann, 2001) (**Figure 1-3**). However, striatal interneurons, which are estimated to represent 5% of the striatal cell population (Sieradzan and Mann, 2001; Steiner and Tseng, 2010) - and which include large aspiny cholinergic interneurons and medium aspiny neurons that express somatostatin (Beal et al., 1984; Ferrante et al., 1987), neuropeptide Y (Dawbarn et al., 1985; Ferrante et al., 1987), parvalbumin, calretinin (Cicchetti and Parent, 1996), the enzyme nicotinamide adenine dinucleotide phosphate diaphorase (NADPH-d) (Ferrante et al., 1985), nitric oxide synthase (NOS) and choline acetyltransferase (ChAT) - are largely spared (Cicchetti and Parent, 1996; Cicchetti et al., 2000; Sieradzan and Mann, 2001; Wu and Parent, 2000). However, the remarkable atrophy which characterizes the striatum in the final stages of the disease suggests that both spiny and aspiny neurons may eventually be vulnerable to pathological processes (Vonsattel, 2008).

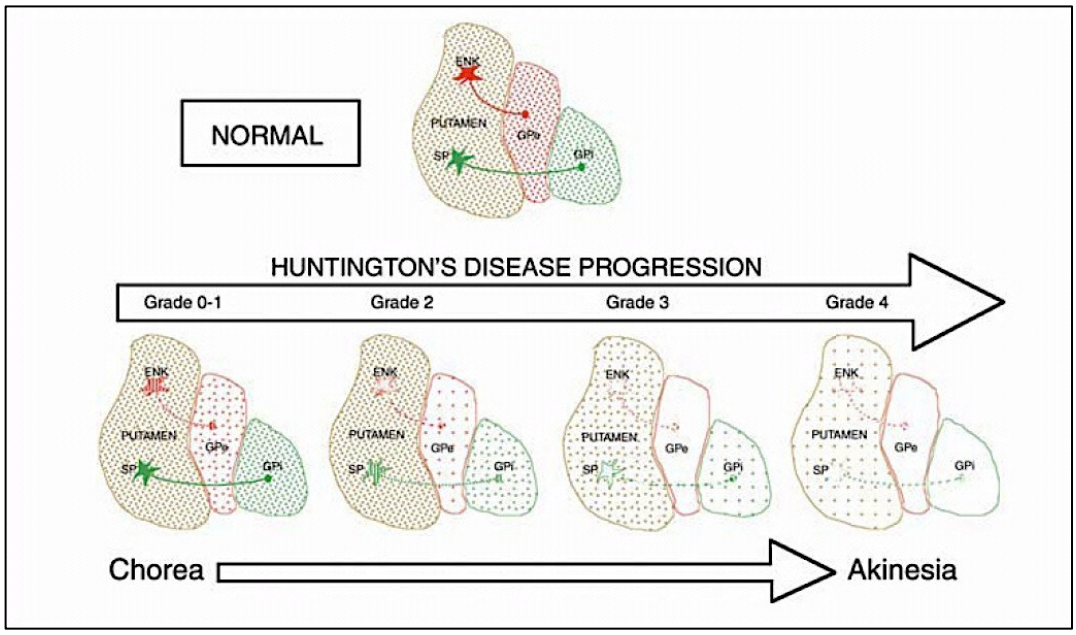

Figure 1-3. Schematic representation of disease progression. Schematic illustration of the preferential loss of ENK+ striato-GPe neurons compared to SP+ striato-GPi neurons during the progression of HD, and the relation of this differential loss to HD symptoms. In brief, the early loss of striato-GPe neurons, which suppresses unwanted movements, explains the early appearance of chorea in HD. Contrary, the later loss of the striato-GPi neurons, which promote desired movement, explain the appearance of akinesia as a later symptom (Reiner et al., 2011).

As the disease progresses, various structures of the brain, and especially the striatum, show increasing atrophy. This striking anatomical feature has served to develop a classification system to stage disease progression. In 1985, Vonsattel *et al*. (Vonsattel et al., 1985) pioneered a disease grading scale (Grades 0 to 4) based on the macroscopic and microscopic post-mortem evaluation of approximately 160 HD brains; a scale which has, since then, become the reference point for grading disease severity (Vonsattel et al., 1985). The macroscopic examination of brain sections is used to evaluate the severity of brain atrophy, while microscopic evaluation helps evaluate the extent of neuronal loss and astrogliosis (Vonsattel et al., 1985) (**Figure 1-4**). At Grade 0 - which corresponds to pre-symptomatic individuals - there is no evidence of brain atrophy at gross examination, although an increased number of oligodendrocytes (Myers et al., 1991) and neurons, which present with aggregates of mHtt protein, are observable in the caudate nucleus. Caudate neuronal loss is approximately 30-40%, although gliosis is still not detected. In Grade 1 patients, measurable atrophy is still not observed but nearly 50% of neurons of the head of the caudate nucleus have died. This is further accompanied by a moderate fibrillary gliosis. Grade 2 is characterized by an evident atrophy of the caudate nucleus while the putamen is slightly atrophied with no signs of ventricular enlargement. Microscopically, neuronal loss, accompanied by fibrillary gliosis, is observed both in the head of the caudate nucleus and in the dorsal putamen. Grade 3 is characterized by a severe atrophy of the caudate nucleus. The putamen is

moderately atrophied but the shape of the ventricles appears rather flatten. Important neuronal loss and astrogliosis are observed both in the caudate nucleus and in the putamen. In the final stages of the disease, referred to as Grade 4, both the caudate nucleus and putamen are marked by an acute atrophy leaving the ventricular surface concave. Almost 95% of neurones have degenerated at this stage (Vonsattel et al., 1985) and severe astrogliosis throughout the neostriatum is present. Finally, atrophy of other brain structures is mild in Grade 1 and 2 patients, while in Grades 3 and 4, it is clearly visible in the GP, neocortex, thalamus (Vonsattel, 2008). It should be noted that greater atrophy and neuronal loss have also been associated to longer trinucleotide repeats (Furtado et al., 1996).

In addition to brain atrophy and increased astrocyte density, microglial activation has been reported in the brains of HD patients. Indeed, while the number of microglial cells is modestly increased between Grades 0 and 3, their density is markedly higher in the brains of Grade 4 patients (Myers et al., 1991; Vonsattel et al., 1985). This microglial response has further been suggested to take place early in disease progression (Pavese et al., 2006; Tai et al., 2007) and to further correlate with the severity of the pathology (Sapp et al., 2001).

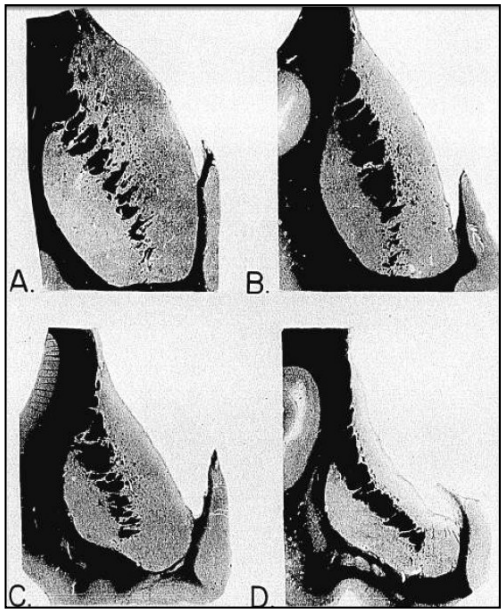

Figure 1-4. Vonsattel grading scale according to macroscopic evaluation. (**A**) Control, Grades 0 and 1: no abnormality on gross examination. (**B**) Grade 2: the caudate nucleus is atrophic but maintains its convex medial outline. (**C**) Grade 3: the striatal atrophy is moderate to severe and the medial outline of the caudate nucleus is now flat, forming a nearly straight line. The cross-section outline of the anterior limb of the internal capsule has likewise lost its medial convexity and putamen is atrophic. (**D**) Grade 4: very severe atrophy of the caudate nucleus and putamen, with markedly concave medial outline of both caudate nucleus and internal capsule (Vonsattel et al., 1985)**.**

1.1.4 Additional pathological features

HD pathology is not limited to the brain but symptom evolution also include a number of peripheral manifestations (Björkqvist et al., 2008; Cisbani and Cicchetti, 2012; Sassone et al., 2009; van der Burg et al., 2009) (**Figure 1-5**). The ubiquitous expression of mHtt leads to abnormalities in the peripheral tissue and alteration in the normal function of various organs. For instance, HD patients can present with metabolic dysfunction, disturbances in sleep and circadian rhythm (Sassone et al., 2009; van der Burg et al., 2009), muscle atrophy, skeletal-muscle waste (Farrer and Meaney, 1985; Ribchester et al., 2004), osteoporosis (Aziz et al., 2009; Hult et al., 2011; Saleh et al., 2009) and in some cases, cardiac failure (van der Burg et al., 2009). Testicular atrophy, but not compromised fertility, has been also reported (Markianos et al., 2005; Van Raamsdonk et al., 2007). Finally, progressive weight loss has been described as a common feature despite adequate calorie intake, which at times further evolves into cachexia (Sanberg et al., 1981; Sassone et al., 2009; Stoy and McKay, 2000; van der Burg et al., 2009). *In vitro* and *in vivo* studies corroborate the role mHtt in impairing the normal physiology of various peripheral cell types. The expression of the mutated protein in myocytes impact transcription and mitochondria function, affecting normal energy metabolism (Ciammola et al., 2006), while expression in pancreatic cells impairs insulin secretion (Lalić et al., 2008). mHtt also interferes with the expression of fat-storage genes and the hormone concentration, such as leptin, in adipocytes (Fain et al., 2001; Phan et al., 2009). In most cases, peripheral symptoms are not secondary to brain-related symptoms but the direct effect of the expression of the mutated protein (van der Burg et al., 2009).

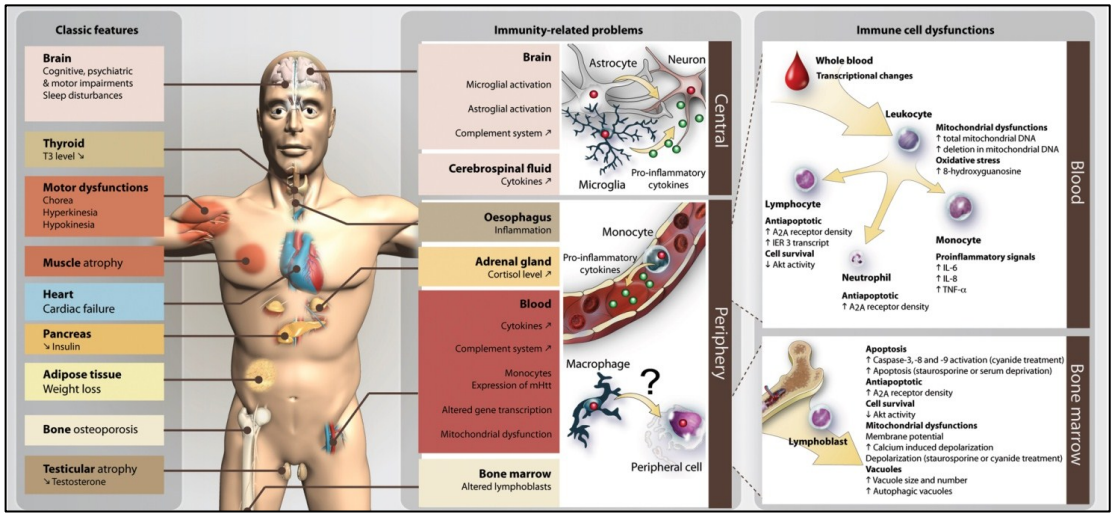

Figure 1-5. HD features. Classic features observed in HD involving several systems (left panel), including immunity-related problems (middle panel) and immune cell dysfunctions (right panel) (Soulet and Cicchetti, 2011).

1.1.5 The huntingtin protein

1.1.5.1 Normal Htt

Normal Htt is a cytoplasmic protein ubiquitously expressed and present both in humans and rodents, with high expression in the brain, cardiovascular system, skeleton, digestive tract and in genital organs (Sassone et al., 2009). Although the cloning of the *htt* gene in 1993 has helped our understanding of HD pathology (The Huntington's Disease Collaborative Research Group, 1993), the role of the protein still remains elusive. The data collected thus far suggests that Htt is associated with several organelles, microtubules and vesicular membranes, pointing to a role of the protein in intracellular trafficking, exocytosis and endocytosis (DiFiglia et al., 1995; Gutekunst et al., 1995). Htt is also associated with proteins involved in synaptic functions (Steffan et al., 2000). It presents anti-apoptotic properties (Cattaneo et al., 2005) and plays a critical role in embryonic development (White et al., 1997). If overexpressed in various systems (cultured striatal cells, primary cultures from HD mouse models (Leavitt 2006) or *in vivo*), normal Htt demonstrates protective properties against apoptosis and excitotoxicity (Cattaneo et al., 2005; Leavitt et al., 2006; Zhang et al., 2003).

1.1.5.2 Mutated Htt

In pathological circumstances, when the mutation takes place, an aberrant protein is synthesized. The polyQ stretch, which is found at the N-terminal of the protein - and which corresponds to approximately 3% of the entire protein content (DiFiglia, 2002) - is released upon proteolytic cleavage by calpains, caspases and metalloproteases (Sieradzan et al., 1999; Tarlac and Storey, 2003). The released polyQ stretches are highly prone to form aggregates, as observed in brain sections immunostained for the polyQ domain of the protein (DiFiglia et al., 1995; 1997). PolyQ tracts may be found in the cytosol as soluble proteins that can further form oligomers and fibrillary structures (Scherzinger et al., 1997). When a certain threshold in intracellular polyQ concentration is reached, these homopolymers form insoluble aggregates (Zuccato et al., 2010). Unlike in normal cells, where the Htt protein is found primarily in the cytoplasm, aggregates are found in both the nucleus and cytoplasm in pathological conditions (Kaytor et al., 2004; Poirier et al., 2005) (Johri and Beal, 2010; Steffan et al., 2000), interfering with various cellular pathways such as transcription, axonal transport, energy metabolism, synaptic transmission and vesicle release (Krainc, 2010; Soulet and Cicchetti, 2011) (**Figure 1-6**).

Figure 1-6. Intracellular targets of mHtt. mHtt that contains a polyQ expansion induces the formation of neuritic, cytoplasmic and nuclear inclusions, leading to dysfunction of the cell, followed ultimately by death. **1**) Calcium homeostasis dysregulation has a central role in this cascade of events. **2**) Under physiological conditions, glutamate stimulates the entry of calcium through NMDA receptors. mHtt interferes with PSD95 and induces the sensitization of NMDA receptors resulting in a massive entry of calcium. **3**) Calcium-dependent proteases (for example, calpains), are thereafter activated, **4**) cleaving the full-length mHtt to release an N-terminal polyQ stretch (Q). **5**) mHtt fragments are ubiquitinated (U) and **6**) inefficiently targeted to the proteasome for degradation. **7**) Intact cytoplasmic polyQ stretches form aggregates, which impair proteasome function. **8**) Degradation of the mHtt also takes place by autophagy, a process involving the formation of double-membrane structures called autophagosomes around a portion of the cytoplasm. **9**) N-terminal fragments containing the polyQ stretch of polyQ-huntingtin are translocated to the nucleus, where they can be ubiquitinated (**10**) in order to be degraded by the proteasome system (**11**). **12**) Spared polyQ-huntingtin forms nuclear aggregates, a hallmark of the disease. Soluble polyQ-huntingtin fragments can interact with transcription factors and lead to transcriptional dysregulation. The mHtt has many intracellular targets. For example, it can impair mitochondrial homeostasis (**13**) and contribute to the release of pro-apoptotic factors, such as Cyt c. Concomitantly, abnormal mitochondrial function causes a reduction of ATP production and disrupts calcium homeostasis (**14**). **16**) The abnormal release of calcium from the endoplasmic reticulum (**15**) also contributes to the massive intracellular calcium build-up (**16**), which is associated with oxidative stress, energy metabolism dysfunction and finally cell death. **17**) mHtt is known to slow down intracellular trafficking and to reduce vesicular transport. For example, mHtt interacts strongly with HAP1, leading to the detachment of the motor protein from the microtubules (**18**). Consequently, vesicular transport is altered, notably the transport of trophic factors such as BDNF. The mHtt interacts also with many proteins involved in exocytosis and endocytosis, and can alter the recycling of vesicles (**19**). Finally, it has recently been suggested that

extracellular mHtt can penetrate into the cell and promote the formation of aggregates (**20**). Abbreviations: ATP, adenosine triphosphate; BDNF, brain-derived neurotrophic factor; Cyt c, cytochrome c; HIPs, huntingtin-interacting proteins; HAPs, huntingtin-associated proteins; mHtt, mutant huntingtin; NMDA, N-methyl-D-aspartic acid; Q, polyQ stretch (Soulet and Cicchetti, 2011).

Purified mHtt fragments reveal that shorter polyQ stretches of the protein tend to adopt a β-structure (β-strand/β-turn), whereas longer polyQ chains yield more globular structures, similar to those produced by a fibrillation process. Globular intermediates can further form protofibrils, which ultimately lead to mature fibres. Conformational changes are important determinants of protein toxicity (Poirier et al., 2002) (**Figure 1-7**). Observations collected in a new model of mHtt aggregation, developed in transiently transfected COS-7 cells, have led to the idea of a dynamic four-step process to explain protein aggregation (Ossato et al., 2010). The *first* phase is the accumulation phase during which only soluble misfolded monomers are present at low concentrations. In the *second* phase, small oligomers are formed and remain in equilibrium with monomers. During the *third* phase, nucleation is triggered at one or more cytoplasmic sites (e.g. nucleation centres), ultimately leading to the formation of larger insoluble inclusions, the *fourth* phase of aggregation (Ossato et al., 2010). Longer polyQ stretches correlate with faster aggregation rates (Lunkes and Mandel, 1998). It should be noted that normal Htt can also contribute to the formation of aggregates (Rajan et al., 2001). Indeed, shorter polyQ stretches are sequestered in mHtt inclusions. Thus, the cells are impoverished of the wild type protein which normally exerts beneficial functions (e.g. anti-apoptotic), leading to loss of function. This provides some explanation as to why the normal protein does not counteract the accumulation of the mutated protein.

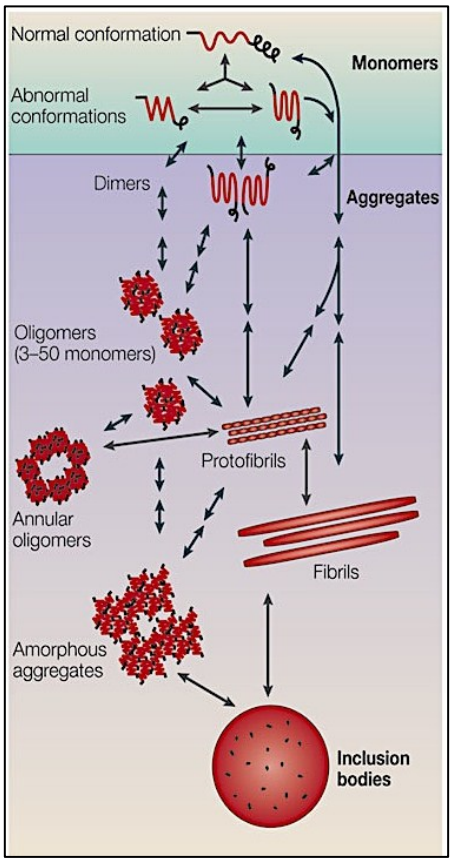

Figure 1-7. Conformational change of the monomer, perhaps with several possible abnormal conformations, initiates the aggregation process. Aggregation begins as soon as there is an association of two or more abnormal proteins or parts of proteins. Amyloid fibrils might be formed by the linear addition of monomers to the growing fibre (arrows on right), or through intermediate oligomeric assemblies, or species called protofibrils, either of which might be 'off' the pathway to fibril formation. Oligomers or protofibrils might be capable of forming annular rings. Furthermore, amorphous aggregates, which do not contain fibrils, can also be formed, possibly through the oligomeric or protofibrillar intermediates as shown, or through precipitation of monomers. If an aggregate becomes large enough, it can be visualized by light microscopy, and large well-demarcated aggregates in cells are often termed inclusion bodies. It is currently proposed that the early species in the aggregation process are more toxic than inclusion bodies or large aggregates. Further research is needed to clarify these pathways, determine similarities and differences between the pathways for different diseases and determine the points where inhibition might be beneficial or detrimental for the disease process. Molecular components are not drawn to scale (C. A. Ross and M.A. Poirier, 2005).

In vitro studies have shown that cells have different susceptibility to mHtt. For example, cells differentiated into neurons present a higher vulnerability than undifferentiated cells (Weiss et al., 2009). The differential susceptibility of various cell types to mHtt cytotoxicity could be due to the differences in their respective cell cycles. Mature neurons, which no longer replicate, have a greater tendency to display aggregates, although there is no correlation between the level of mHtt expression and the rate of cell death *in vivo* (Cisbani and Cicchetti, 2012; Gong et al., 2008). The continuous turnover of proliferating cells can dilute the mutated protein in their progeny, thereby reducing the probability of aggregate accumulation (Tydlacka et al., 2008).

Build-up of aggregates is dependent of the viability of the monomeric mHtt and can thus take place over several years. It is therefore likely to precede the symptomatic manifestation of the pathology. The actual role of aggregate formation and its potential toxicity are still highly controversial (Kaytor et al., 2004; Poirier et al., 2005). Another disputed aspect is whether aggregates, or their soluble forms such as small dimers or oligomers, are the actual cause of cell death (Saudou et al., 1998). Indeed, not all evidence supports a detrimental role of aggregates. For example, it has been shown that neurons die in a dose-dependent manner according to the amount of soluble polyQ present within the cells. Indeed, the presence of aggregates have also been reported to increase cell life-span (Arrasate et al., 2004). Finally, it is still unclear whether the toxicity of aggregates originates from their intra-molecular interactions or from their intra-cellular localization and whether the mutation leads to a gain of toxic function due to the presence of a polyQ stretch or a loss of the beneficial properties of the normal protein, or both (Atwal et al., 2007; Dragatsis et al., 2000; Zuchner and Brundin, 2008).

1.2 Current treatments for HD

Despite the progress that has been made in understanding the pathology of HD and its underlying mechanisms, no effective neuroprotective or disease-modifying therapy has emerged from these findings. Because of its genetic nature, HD can be diagnosed before any signs are observable, unlike other neurodegenerative diseases such as Parkinson's (PD) or Alzheimer's diseases (AD) for which the diagnosis is made when neurodegenerative processes have already been set in motion. Despite the existence of a genetic test for HD, several individuals at risks are reluctant to take such tests and thus disease diagnosis is often made in clinic. Because of that, the Neurobiological Predictors of Huntington's disease group (PREDICT-HD) as well as TRACK-HD have recently proposed a multidimensional diagnosis taking into account both the motor and cognitive dysfunctions, more suitable and efficient for an earlier diagnosis of the pathology (Biglan et al., 2013). Identification of the pathology at the prodromal stage would be advantageous for the development of preventive therapeutic strategies aiming to delay the course or prevent the development of the disease (Biglan et al., 2013; Kordower et al., 1999; 2000).

1.2.1 Current pharmacological treatments for HD

At the present time, the pharmacological management of the disease is the most common alternative available to alleviate symptoms and ameliorate the patients' quality of life (**Figure 1-8**). Dopamine blockers (e.g. neuroleptics), dopamine depleters (e.g. tetrabenazine) and benzodiazepines

(clonazepam, diazepam) are used to control hyperkinetic movements, in particular chorea, especially when they begin to interfere with daily activities (Novak and Tabrizi, 2011). One of the first choice medication - and actually the only one approved by the FDA, according to current literature (**Figure 1-9**) - is tetrabenazine, an anti-choreic agent which improves motor scores without generating side-effects, such as tardive dyskinesia (Mestre and Ferreira, 2012; Novak and Tabrizi, 2011). However, this drug can lead to depression. *Typical* anti-psychotics, such as clozapine, have also been tested to treat chorea but have been dismissed because of their undesirable side effects (e.g. akathisia, dystonia). They have been replaced by *atypical* anti-psychotics (e.g. olanzapine) (Mestre and Ferreira, 2012; Novak and Tabrizi, 2011; Phillips et al., 2008). The latter option is better tolerated, triggers less extrapyramidal side effects and promotes weight gain, which is desirable in HD patients. Benzodiazepines are also used to treat chorea but they induce sedation and depressant effects on cognition (Novak and Tabrizi, 2011). Other agents include the glutamate receptor antagonists riluzole and amantadine, but these drugs have shown limited benefits for the treatment of chorea (**Figure 1-8**).

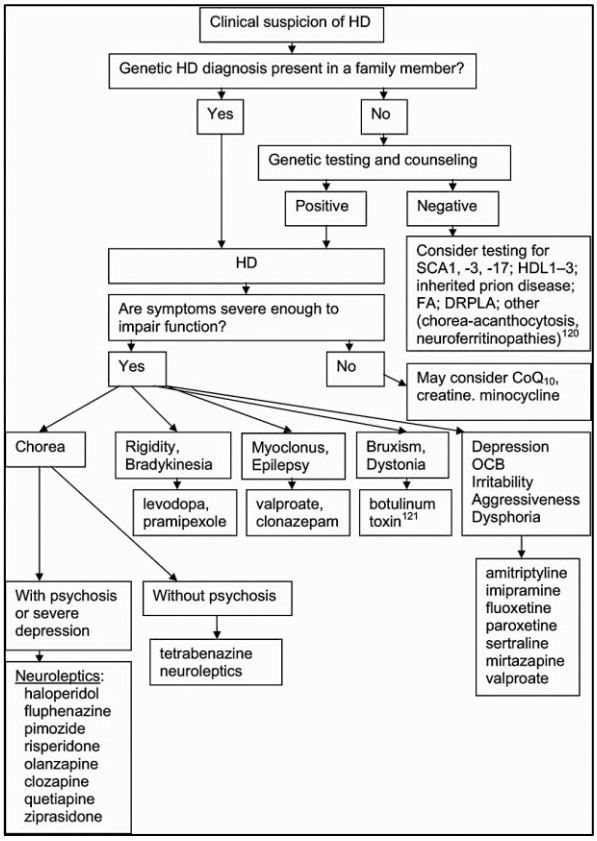

Figure 1-8. Therapeutical strategies for HD. dentatorubropallidoluysian atrophyFriedreich's ataxia(from Adam and Jankovic, 2008).

In addition to the pharmacological approaches currently employed in the clinical practice, various compounds have been tested but have been met with inconsistent results (**Figure 1-9**). To increase GABAergic neurotransmission, GABAergic agonists, GABA mimetics, as well as inhibitors of the GABA transaminase activity (Scigliano et al., 1984; Shoulson et al., 1976; 1978) have all been investigated but failed to reach clinical use due to lack of effects on chorea and the manifestation of undesired side effects (Shoulson et al., 1978). Very limited or the complete absence of effects have been reported with drugs modulating the cannabinoid system (cannabidiol and nabilone) (Mestre and Ferreira, 2012). For the treatment of cognitive decline, acetylcholinesterase inhibitors have been tested in HD following the positive results obtained in AD and Lewy Body (LB) disease but there is still a need for larger clinical trials and longer follow-up to prove their efficacy in HD (Phillips et al., 2008). Finally, HD patients require pharmacotherapy for psychiatric disturbances such as depression and anxiety. A limited number of trials on antidepressants or anti-psychotics have suggested that these drugs might be helpful to fight some of the symptoms of HD, such as irritability and aggression, although further investigation is also required (Phillips et al., 2008). One recent case study has claimed positive effects of combined anti-psychotics on aggressive behaviour and chorea (Edlinger et al., 2013). Finally, despite the prominent role of the immune response observed in HD, all therapies attempting to modulate this response, for example anti-inflammatory therapies (eg. minocycline), did not yield beneficial effects in patients despite promising results collected *in vitro* and *in vivo* (Soulet and Cicchetti, 2011).

Aside from these pharmacological targets, deep brain stimulation of GPi has been tested in a few HD cases. Short-term improvements have been observed both at the motor and psychological levels (Adam and Jankovic, 2008). In one isolated patient, bilateral stimulation of the GPi led to amelioration of chorea and dystonia but worsening of the bradykinesia. However, the long-term efficacy of the procedure is still unknown (Adam and Jankovic, 2008).

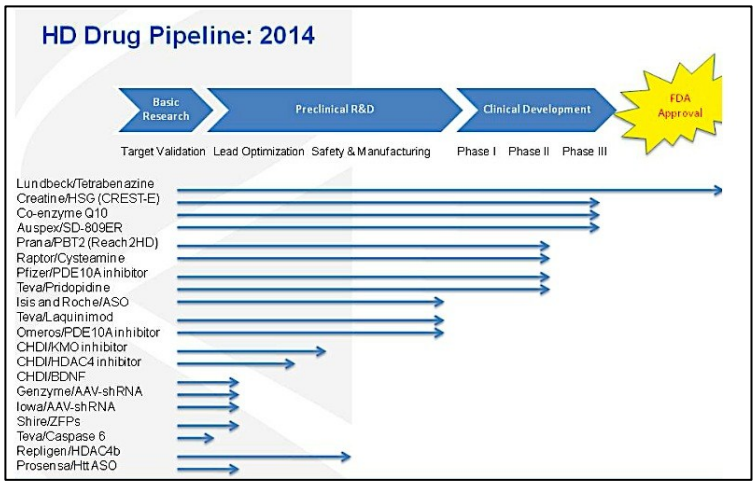

Figure 1-9. HD drug pipeline for 2014. Various drugs have been tested for the treatment of HD. To date, tetrabenazine is the only drug approved by the FDA for its anti-choreic properties. A number of drugs have reached the clinical trial phases and are currently being tested, while others are still in preclinical stages[1].

1.2.2 Experimental strategies being developed for HD

As described in the section above, the current treatments available for HD are extremely limited, not to mention that they are restricted to symptom management (Mestre and Ferreira, 2012; Phillips et al., 2008). However, a number of disease-modifying therapies have been tested in animal models of HD, with the goal of delaying the disease onset. Amongst the strategies developed, a large bulk has focused on modulating the transcription cascade, via histone deacetylase inhibition (Ferrante et al., 2003), to prevent apoptosis via the inhibition of caspase-1 activity (Ona et al., 1999) or to block mHtt aggregation (e.g. clioquinol) (Nguyen et al., 2005). Additional experimental therapies include N-methyl-D-aspartate (NMDA) receptor agonists (Velloso et al., 2009), intake of creatine (to stabilize the bioenergetic deficits) (Hersch et al., 2006), co-enzymeQ_{10} (CoQ10) (for its anti-oxidant properties) (Ferrante et al., 2002) and cystamine (for its inhibitory effects on transglutaminase activity) to impact on mHtt aggregates size and number (Dedeoglu et al., 2002) and stimulating neurotrophic factor release (Borrell-Pagès et al., 2006) (**Figure 1-10**).

Taking into account the impairment in energy production and the reduced mitochondrial complex I-II activity in HD, creatine and CoQ10 were foreseen as potential candidates for treating the disease. Creatine is a substrate for mitochondrial creatine kinase which is capable of modulating the rates of ATP production. CoQ10 is a co-factor of the mitochondrial electron transport chain, accepting electrons

[1] from *http://www.hdsa.org/research/therapies-in-pipeline.html*

from complex I-II. Dietary creatine (Matthews, Yang, Jenkins, et al., 1998) and CoQ10 (Matthews, Yang, Browne, et al., 1998) supplements were shown to exert neuroprotective functions in mitochondrial-neurotoxin lesioned murine models generated by intraparenchymal injections of malonate or 3-nitropropionic acid. These neuroprotective properties were further assessed in the R6/2 transgenic HD model in both pre- (Ferrante et al., 2000; 2002; Schilling et al., 2001) or post-symptomatic stages (Dedeoglu et al., 2003). The combined administration of creatine and CoQ10 prevented striatal volume loss in the 3-nitropropionic-lesioned mice, while an amelioration of the motor performance and extension of the lifespan was recorded in the R6/2 mice (L. Yang et al., 2009). Creatine and CoQ10 moved to clinical trials and proved to be safe and well tolerated (Feigin et al., 1996; Hersch et al., 2006; Huntington Study Group Pre2CARE Investigators et al., 2010). CoQ10 showed a trend towards slowing the motor decline, although it did not reach statistical significance (Huntington Study Group, 2001). Creatine administration slowed brain atrophy (as determined on magnetic resonance imaging (MRI)), but had no effects on cognitive functions (Rosas et al., 2014). A Phase III clinical trial using either creatine or CoQ10 is currently taking place (**Figure 1-10**)[2] Finally, other groups have attempted to modulate the number of mHtt aggregates with cystamine, a small disulphide-containing molecule which is capable of inhibiting transglutaminase activity, an enzyme that mediates the cross-linking of mHtt (Mastroberardino and Piacentini, 2010), promote brain derived neurotrophic factor (BDNF) expression and reduce apoptosis (Borrell-Pagès et al., 2006). Given the positive effects in pre-clinical studies (Dedeoglu et al., 2002; Fox et al., 2004; Karpuj et al., 2002; Y.-L. Wang et al., 2005), the reduced form of cystamine, cysteamine, moved to a phase I clinical trial and was shown to be safe and well-tolerated by HD patients (Dubinsky and Gray, 2006). Phases II/III are currently underway[3].

[2] Huntington Study Group Pre2CARE Investigators et al., 2010, Huntington Study Group Pre2CAREInvestigators, http://www.huntington-studygroup.org/HSGResearch/ClinicalTrials Observational StudiesinProgress /2CARE/tabid/95/Default.aspx.

[3] http://ir.raptorpharma.com/releasedetail.cfm?ReleaseID=633900; http://ir.raptorpharma. com /releasedetail.cfm?ReleaseID=683716

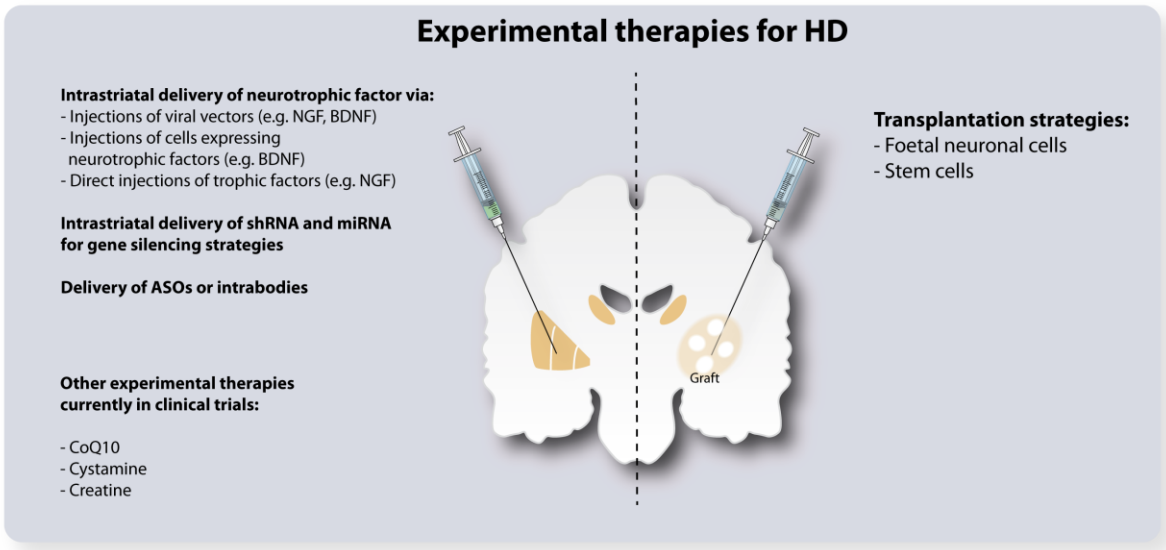

Figure 1-10. Schematic illustrating the potential experimental therapies for HD. Abbreviations: ASOs, antisense oligonucleotides; BDNF, brain derived neurotrophic factor; miRNA, microRNA; NGF, nerve growth factor; shRNA, short hairpin RNA (Adapted from Clelland et al., 2008).

Neurotrophic factor delivery. Neurotrophic factors play critical roles in development as well as in neuronal repair. Treatments with neurotrophins were demonstrated to promote the survival of motor neurons *in vitro* as well as to preserve them following axotomy *in vivo* (Anderson et al., 1996). One of the main features of HD pathology is the impoverishment of cerebral BDNF levels (Zuccato and Cattaneo, 2007). Thus, delivery of trophic support to cells undergoing degeneration (**Figure 1-10**) has been considered for HD.

Various trophic factors, including BDNF, Nerve Growth Factor (NGF), Ciliary Neurotrophic Factor (CNTF) and Glial Derived Neurotrophic Factor (GDNF) have been extensively studied in *in vivo* models of HD (Ramaswamy and Kordower, 2012). These neurotrophins have been delivered directly into the brain as their large size does not allow them to easily cross the blood brain barrier (BBB). Thus far, neurotrophic factors have been delivered through intrastriatal or intraventricular infusions, striatal implantation of cells genetically engineered to over-express these molecules or by the injections of viral vectors. Infusions or viral delivery within the striatum has been reported to have a positive impact in lesioned models of HD, while the few experiments conducted in transgenic HD models have yielded contradictory results (Demeestere and Vandenberghe, 2011). Indeed, some studies failed to report any beneficial effects (Martínez-Serrano and Björklund, 1996) while others demonstrated behavioural and neuropathological improvements (Anderson et al., 1996; Emerich et al., 1996). These discrepancies

may be attributable to the differences in animal models utilized (Demeestere and Vandenberghe, 2011). Cells overexpressing neurotrophic factors have also been tested both in transgenic and lesioned animal models of HD and proved to be efficient in protecting MSNs (Anderson et al., 1996; Emerich et al., 1996; Gharami et al., 2008) as well as improving motor function (Ebert et al., 2010). For instance, overexpression of BDNF in transgenic animal models or in lesion models (Kells et al., 2008) partially reversed motor dysfunction, halted brain volume loss (Dey et al., 2010) and reduced the number of intranuclear mHtt aggregates (Gharami et al., 2008). However, an altered expression of the receptor for BDNF has been reported in HD cases (Ginés et al., 2006) thus the administration of this neurotrophin might not be a suitable therapeutical approach. Thus far, only one isolated pilot study in HD patients has tested the feasibility and safety of intraventricular implantation of encapsulated cells expressing CNTF. Despite the fact that positive electrophysiological changes of neuronal circuits were observed (electrophysiological recordings included palmar sympathetic skin responses, blink reflexes, thenar long latency reflexes, cortical somatosensory evoked potentials and electromyographic silent periods evoked by transcranial magnetic stimulation), no significant clinical benefits were reported (Bloch et al., 2004). Further investigation will be required to assess the safety and feasibility of this method.

Gene silencing. Considering the genetic nature of HD, gene-silencing approaches have been developed to down-regulate the expression of the mutated protein (**Figure 1-10**). The intraparenchymal delivery of virally encoded short-hairpin RNAs (shRNAs), microRNAs (miRNAs) (Franich et al., 2008; Harper et al., 2005; Machida et al., 2006; Rodriguez-Lebron et al., 2005) or synthetic siRNAs (DiFiglia et al., 2007; Y.-L. Wang et al., 2005) are amongst the proposed strategies. Although amelioration of motor symptoms and reduction of mHtt aggregates, both in size and in number, have been reached, the direct impact of these interventions is limited to the site of injection and does not take into account the widespread expression of mHtt. In the long run, it will be essential to consider whether a chronic intraparenchymal administration of viral vectors is feasible over long periods of time and whether the effects are sustainable over time.

Recently, alternative strategies were tested based on the infusion of antisense oligonucleotides (ASOs) in the cerebrospinal fluid (CSF). ASOs are strands of nucleic acid synthesized to bind with specific target mRNAs and mediate their degradation (Kordasiewicz et al., 2012). Transient infusion of ASOs in a HD mouse model, as well as in a non-human primate model, ameliorate motor deficits, prolong survival and reduce the levels of mHtt throughout most of the brain, within the frontal cortex, striatum, thalamus and midbrain. These effects partially persist after the treatment has ended, when the

physiological levels of the mHtt protein are restored. Indeed, the presence of ASOs depleted the cells of mHtt mRNA and consequently of the protein (Kordasiewicz et al., 2012). This study provided strong and promising preclinical evidence in support of the use of ASOs. However, this type of approach also presents important obstacles such as the 1) the route of administration, 2) the indiscriminate binding to both the normal and mutated genes, 3) the need of peripheral biomarkers to monitor the impact of the treatment on the brain and finally 4) the actual feasibility of translating these preclinical results into tangible effects in human subjects (Lu and X. W. Yang, 2012).

Intrabodies delivery. Other than RNA-based approach for modulating mHtt expression, recent advances were made for protein-based methodologies which rely on the use of intrabodies (Butler et al., 2012; Demeestere and Vandenberghe, 2011; Stocks, 2005) (**Figure 1-10**). Intrabodies are recombinant, single chain antibody fragments expressed intracellularly. They are highly specific and capable of distinguishing different conformations of the same protein as well as of modulating the effects of the mutated protein. Intrabodies targeting mHtt were conceived to increase the turnover of the mutated protein (Butler et al., 2012; Southwell et al., 2008, 2009). *In vivo* studies showed that mHtt aggregation is reduced and the degradation of the cytosolic protein is augmented when using intrabodies. Indeed, the interaction between the intrabodies and mHtt favours the ubiquitination of the soluble protein, leading to its subsequent degradation. Moreover, behavioural improvements and prolonged lifespan have also been reported in different transgenic models (Southwell et al., 2009; C.-E. Wang et al., 2008). This is a promising therapeutic strategy especially for the specificity of the interactions between the antibody and the target epitope, reducing the possibility of binding with non-specific alleles. However, intrabodies have yet to be tested in patients.

Cell replacement therapies. Remarkable advancements in the manipulation of cell fate have sparked a massive surge of interest in cell replacement therapies and their application to brain repair (**Figure 1-10**). Cell transplantation strategies were tested in humans 30 years ago by first using adrenal medulla cells (1982-1985) (Backlund et al., 1985; Lindvall et al., 1987; 1989), shortly followed by the use of foetal tissue initiated in Sweden (1985) (Lindvall et al., 1988; 1989). Originally explored for PD (Lindvall and Björklund, 1989; Lindvall et al., 1988; 1989), neural grafting has now been performed in patients with amyotrophic lateral sclerosis (Giordana et al., 2010; H. Huang et al., 2008; Mazzini et al., 2010; 2012), multiple sclerosis (Rice et al., 2013; Uccelli and Mancardi, 2010), stroke (Kondziolka et al., 2003; Savitz et al., 2005), spinal cord injury (Féron et al., 2005; Ramón-Cueto and Santos-Benito, 2001) and HD (Bachoud-Lévi, Bourdet, et al., 2000; Capetian et al., 2009; Gallina et al., 2010; Hauser et al., 2002; Kopyov et al., 1998; Reuter et al., 2008; Rosser et al., 2002). For the purpose of this thesis, I will focus

on the outcome of cell replacement therapies for HD.

1.3 Cell replacement therapies for HD

Poor symptomatic relief achieved with pharmacological treatments, the lack of disease modifying treatments and the neurodegeneration largely circumscribed to the striatum, at least in early stages of the disease, are all factors which have led to the idea that HD patients are good candidates for cell replacement therapies and may thus benefit from it. Cell transplantation approaches have been initiated based on (a) the early success with similar strategies in the treatment of PD (Lindvall and Hagell, 2000; Lindvall et al., 1990), (b) the favorable behavioural and anatomical results obtained from preclinical animal models of HD (Deckel et al., 1986; Isacson et al., 1984; 1986; Sanberg et al., 1986; Schmidt et al., 1981; Wictorin et al., 1988; 1989), and (c) the lack of adequate treatment for HD, which is invariably fatal (Phillips et al., 2008; C. A. Ross and Tabrizi, 2011).

1.3.1 Preclinical studies and rationale

Cell replacement strategies for HD have been largely studied in animal models, including mice, rats (DiFiglia et al., 1988; Döbrössy and Dunnett, 2007; Fricker et al., 1997; Fricker-Gates et al., 2004; Hantraye et al., 1992; Helm et al., 1992; 1993; Isacson et al., 1984; 1985; 1986; 1989; Kendall et al., 1998; Rutherford et al., 1987; Sanberg et al., 1989; Schackel et al., 2013; Tulipan et al., 1986; Wictorin et al., 1988) and primates (Hantraye et al., 1992; Helm et al., 1992; Isacson et al., 1989; Kendall et al., 1998). Initial transplantation studies were based on the use of toxin-induced lesions of the striatum. Kainic acid (KA), an analogue of glutamate, was one of the first toxin used to reproduce the neuropathological and neurochemical characteristics of HD (Coyle and Schwarcz, 1976; E. G. McGeer and P. L. McGeer, 1976). However, KA not only is not physiologically present in the brain but it does not selectively target the GABAergic MSN cell type (Beal and Martin, 1983). For these reasons, KA was quickly substituted by ibotenic acid (IA) and then by quinolinic acid (QA), a metabolite of tryptophan found in the brain. QA is a NMDA receptor agonist that, once injected intrastriatally, produces a selective lesion as compared to other glutamate agonists (Beal et al., 1986). Other toxins such as the 3-nitropropionic acid or malonate, which affect both mitochondrial energy metabolism, were also used to reproduce features of HD in animals (Borlongan et al., 1997). These toxins generate certain pathological events seen in HD patients, including gliosis, degeneration and retraction of axons, shrinkage of the striatum with enlargement of the ventricles, changes in the afferent and efferent projections as well as a compromised functionality of the circuitry, reduction in glucose consumption

and significant decrease of glutamic acid decarboxylase (GAD) and ChAT activities (Isacson et al., 1985). However, lesions do not provoke involuntary choreiform movement in rats but only in primates (Hantraye et al., 1992). Altogether, lesion models fall short to recapitulate the disease likely due to the local lesion, which does not take into account the more generalized aspects of the disorder, including the affectation of other brain regions as well as its genetic nature. However, despite the fact that a number of transgenic animal models of HD exist and that they may be more representative of the disease, very few studies investigating the effects of transplantation in such models are available in the literature (Cisbani, Saint-Pierre, et al., 2013; Dunnett et al., 1998) (**Table 3-1**). The first study on foetal cell transplantation in transgenic models was performed in the R6/2 mouse model (Dunnett et al., 1998). Transplantation in the R6/2 mice, which expresses the truncated *mHtt* gene, yields similar survival to that seen in control animals (Dunnett et al., 1998). However, survival of grafts only yielded modest effects on motor behaviour and had no impact on disease progression. These results were followed by our study (**Chapter III**) performed in the HD YAC128 murine model which was generated to express the full-length *mHtt* gene (Slow et al., 2003). The YAC128 model recapitulates several HD-like features including behavioural and cognitive deficits, selective striatal cell loss, as well as nuclear aggregates, the characteristic neuropathological hallmark of the disease (Slow et al., 2003; Van Raamsdonk, Murphy, et al., 2005). In this study, we observed similar graft viability between transgenic and control mice at 3 months post-transplantation. Importantly, the disease progression did not seemingly impact graft survival.

For cell replacement therapies to be efficient, a number of technical factors will also have to be taken into consideration. Issues which relate to tissue dissection (largely discussed in sections **1.3.2.1** and **1.3.2.2** below), the time-window of donor age as well as the potential of the cells to survive and integrate into the host brain. Cells are chosen according to specific phenotypes and their ability to grow, connect and integrate in the host brain (Dunnett, 2013). To replace the lost striatal MSNs, cells are dissected from the whole ganglionic eminence (WGE) of the embryos, which is composed of the lateral ganglionic eminence (LGE) and the medial ganglionic eminence (MGE). From these two portions emerge different cell populations (**Figure 1-11**) (see paragraph **1.3.2.1**). Foetal cells are collected at the final phases of their mitotic division and when they are committed to a distinct phenotype. It is very important to avoid the implantation of undifferentiated or non-neuronal cells. Indeed, mitotic cells, included inadvertently during dissection, retain the ability to expand and potentially overgrow. The exact developmental stage of the foetal donor is essential to predict the outcome of the transplantation. Various studies testing a range of donor ages (embryonic day (E)13, E14, E15) have established that the embryonic developmental stage has an impact on the cellular composition of the graft as well as on

subsequent functional recovery in HD rodent models (Dunnett, 2013). Younger donors (E13) yield the highest number of striatal-like cells (dopamine-and cAMP-regulated phosphoprotein 32-kDa (DARPP-32) positive) and lead to improvement of motor behaviours in transplanted animals. Indeed, transplants derived from E15 embryos, although initially presenting with a higher number of cells, yield smaller graft volume compared to those derived from the younger donors (Fricker et al., 1997; Schackel et al., 2013).

Overall, the numerous animal studies performed in lesioned models of disease have demonstrated that neurons can survive in the recipient brain, acquire the proper phenotype, form afferent and efferent connections (Isacson et al., 1984). Graft-derived GABAergic cells are capable of connecting and re-innervating the GP (Isacson et al., 1985). Moreover, host afferent connections have been observed to form synaptic connections in the grafts; glutamatergic (Rutherford et al., 1987), dopaminergic (Clarke et al., 1988; Wictorin et al., 1989) as well as serotoninergic projections (Wictorin et al., 1989). Furthermore, transplantation in lesioned murine models of HD can lead to recovery of motor and cognitive impairments (Mazzocchi-Jones et al., 2009), which has been demonstrated using a number of behavioural tests, such as locomotor activity (Deckel et al., 1983; Isacson et al., 1984), rotation (Carli et al., 1985), postural bias (Borlongan et al., 1995), skilled reaching and paw use (Fricker et al., 1997; Montoya et al., 1990) as well as T-maze alternation (Deckel et al., 1986; Isacson et al., 1986) and active or passive avoidance (Piña et al., 1994). Promising results were also obtained with primate models of HD (IA or QA lesions). Indeed, good graft survival (Hantraye et al., 1992; Helm et al., 1992; 1993) as well functional recovery (Kendall et al., 1998) was reported, although it is unclear whether the behavioural ameliorations are sustained over time.

Taken together, this corpus of preclinical work provided evidence for the efficacy and rationale to proceed with clinical trials. However, some investigators still argued against initiating these trials (Brundin et al., 1996) because of the limited number of studies reporting results with human tissue and in large part because of the low number of transplanted cells which survived (Mundt-Petersen et al., 2000) and acquired the right striatal-like phenotype after transplantation (Wictorin et al., 1990). Despite the issues and concerns raised, a number of clinical trials were initiated.

In the following sections, I will describe the human HD transplantation trials which have taken place, discussing various parameters which we feel are important for the success of cell therapy, from patient selection to practical issues which relate to tissue dissection.

1.3.2 Clinical trials

As of now, 7 independent pilot clinical trials have been conducted worldwide (**Table 1-1**), with the purpose of assessing the feasibility and safety of this procedure in HD patients (Bachoud-Lévi, Bourdet, et al., 2000; Capetian et al., 2009; Gallina et al., 2010; Hauser et al., 2002; Kopyov et al., 1998; Reuter et al., 2008; Rosser et al., 2002). The selection of the suitable candidates for surgery is a crucial step. First, the disease has to be confirmed genetically and patients must show motor symptoms excluding any signs of cognitive impairments and psychological fragility (Bachoud-Lévi, Bourdet, et al., 2000). Disease stage is also likely to be critical for the success of the grafts. To this day, trials on cell replacement therapy have largely recruited patients with mild to advanced HD. Advanced brain atrophy could compromise graft placement and create surgical complications (Bachoud-Lévi, Bourdet, et al., 2000; Clelland et al., 2008). A limited number of patients (29 across all studies), with very heterogeneous symptoms and disease course, have been enrolled in these clinical trials, thus rendering very challenging the comparison among studies and difficult to draw conclusions on the efficacy of this procedure.

Table 1-1. Clinical transplantations trials for HD

	California cohort	INSERM Cohort	Cardiff University cohort	Imperial college London cohort	University of South Florida cohort	University of Florence cohort	University of Freiburg cohort
Number of patients	6	5	4	2	7	4	1
Tissue	Solid tissue pieces LGE	Solid tissue pieces WGE	Cell suspension WGE	Cell suspension WGE	Solid tissue pieces FLVE	Cell suspension WGE	Solid tissue pieces WGE
Number of foetuses/age	5–8/ CRL 20–32 mm	1–2/ 7–9 weeks 25–43 mm	1/ 8.5–12 weeks	2-3/ 9–10 weeks	2–8/ 8–9 weeks	1 per site/ 9–12 weeks	2/ 8–9 weeks
Immunosuppression	18 mo	1 y	> 6 mo	1 y	6 mo	1 y	Until death (6 mo)
Reports of surgical procedures and clinical data	Kopyov *et al.*, Exp Neurol 1998 (1 y)	Bachoud-Levi *et al.*, Exp Neurol 2000	Rosser *et al.*, JNNP 2002 (6 mo)	Reuter *et al.*, JNNP 2008 (5 y)	Hauser *et al.*, Neurology 2002 (1 y)	Gallina *et al.*, Exp Neurol 2010 (18 to 34 mo)	Capetian *et al.*, Neuroscience 2009 (6 mo)
Clinical outcome and/or imaging studies	Ross *et al.*, NMR Biomed 1999 (5-100 weeks)	Bachoud-Levi *et al.*, Lancet 2000 (1 y) Gaura *et al.*, Brain 2004 (2 y) Bachoud-Levi *et al.*, Lancet Neurol 2006 (6 y) Krystkowiak *et al.*, PLoS One 2007	Rosser *et al.*, JNNP 2002 (6 mo) Barker *et al.*, JNNP 2013 (3-10 y)	Reuter *et al.*, JNNP 2008 (5 y)	Hauser *et al.*, Neurology 2002 (1y)	Gallina *et al.*, Exp Neurol 2008 (15 mo) Gallina *et al.*, Exp Neurol 2010 (18 to 34 mo)	NA
Post-mortem studies	Keene *et al.*, Neurology 2007 (6-7 y) Keene *et al.*, Acta Neurol 2009 (10 y)	NA	NA	NA	Freeman *et al.*, PNAS 2000 (18 mo) Cicchetti *et al.*, PNAS 2009 (9, 9.5 and 10 y) Cisbani *et al.*, 2013 (9 and 12 y)	NA	Capetian *et al.*, Neuroscience 2009 (6 mo)

Abbreviations: CRL: crown-rump length; FLVE: far lateral ventricular eminence; LGE: lateral ganglionic eminence; mo: months; NA: not available; WGE: whole ganglionic eminence; y: years (adapted from Cisbani and Cicchetti 2014).

1.3.2.1 Tissue dissection

Tissue preparation is essential for successful transplantation. For the HD clinical trials conducted to date, foetuses were retrieved between 7 and 12 weeks of conception, according to reports on the development of human embryonic tissue as well as xenotransplantation studies (human to rat) (Freeman et al., 2011) (**Table 1-1**). The cytoarchitecture of the grafts derived from the LGE, the MGE or the combination of both eminences is very different. In fact, grafts derived from the MGE are poor in striatal markers (at least acetylcholinesterase (AChE)), while LGE grafts are rich in AChE-positive neuropil and DARPP-32-positive neurons and integrate better within the striatum (Deacon et al., 1994; Hauser et al., 2002; Olsson et al., 1995; 1998; Watts, Brasted and Dunnett, 2000a). However, the interneurons present in MGE dissection are important to the survival and development of the grafts (Watts, Brasted and Dunnett, 2000a). Grafting of the WGE has been postulated to be advantageous as grafts derived from the entire ganglionic eminence exhibit a patchy distribution of striatal cells similar to LGE grafts, but have been shown to be particularly rich in DARPP-32-positive cells as well as interneurons (Watts, Brasted and Dunnett, 2000a). Careful selection and dissection of tissue is therefore very important in predicting the future integration and functionality of the graft (Deacon et al., 1994). Notwithstanding the area of the ganglionic eminence chosen for dissection and therefore, transplantation, it is crucial that this procedure be properly and accurately performed to avoid including meningeal tissue, which can lead to graft overgrowth by the proliferation of non-neuronal cells (Barker et al., 2013; Freeman et al., 2011). Serious concerns were raised by the transplantation community (Freeman et al., 2011) when reports of transplanted tissue overgrowth in HD patients were made public (**Table 1-1**) (Gallina et al., 2010; Keene et al., 2009). In one of these reports, graft size had increased by 150-fold 10 years after transplantation (Keene et al., 2009). In this particular case, the authors proposed that a gender-mismatch between the donor tissue and the host could have been responsible for this outcome, but no other group has reported similar results (Keene et al., 2009). To avoid such complications, the INSERM and UK groups (Bachoud-Lévi, Bourdet, et al., 2000; Reuter et al., 2008; Rosser et al., 2002) (**Table1-1**) opted for the use of smaller grafts. However, this approach did not yield measurable clinical benefits in the HD patients of the UK cohorts (Barker et al., 2013; Reuter et al., 2008; Rosser et al., 2002), except for one case reported in Reuter *et al.* (Reuter et al., 2008). Dissection and methods of cell preparation are surely crucial elements for graft outcome and clearly, a consensus on a standardized methodology needs to be reached, although this may not be feasible given the current information available. Despite the fact that some aspects of the protocols utilized in each of the pilot trial were similar in some respect, they are not identical (**Table 1-1**). First, the area of the foetal brain that is dissected to select cells of striatal origin is not the same in these studies. In some cases, the WGE was retrieved (Bachoud-Lévi, Bourdet, et al., 2000; Capetian et al., 2009; Gallina et

al., 2010; Rosser et al., 2002) while others used the LGE (Kopyov et al., 1998) or the far lateral portion of the LGE (Hauser et al., 2002) (**Table 1-1**). Implantation of the WGE allows the implantation of a single foetus per side, while LGE transplantation requires more donors (Bachoud-Lévi et al., 2002). Furthermore, tissue was subsequently implanted either as a cell suspension (Gallina et al., 2010; Reuter et al., 2008; Rosser et al., 2002) or as solid pieces (Bachoud-Lévi, Bourdet, et al., 2000; Capetian et al., 2009; Hauser et al., 2002; Kopyov et al., 1998). All of these differences make comparisons across studies particularly challenging.

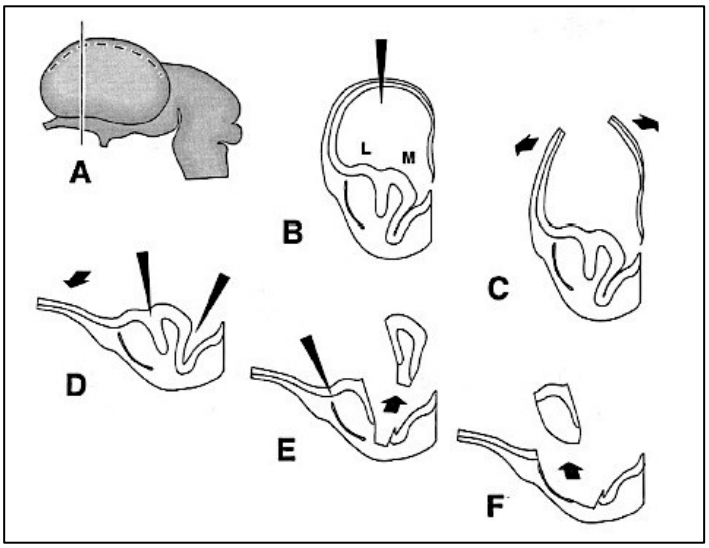

Figure 1-11. Diagram of the steps in the technique used to selectively excise the foetal LGE or MGE. A: lateral view of the foetal brain. The dashed line indicates the placement of the initial incision into the telencephalic vesicle. The solid vertical line indicates the approximate plane of the frontal sections diagrammed in subsequent drawings. **B-F**: drawings of the progressive steps in dissection of LGE from the surrounding foetal brain tissues. Thin triangles indicate orientation of incisions made with microscissors. Arrows indicate reflection of surrounding structures and removal of tissue chunks. L = LGE, M = MGE (Deacon et al., 1994).

1.3.2.2 Tissue preparation

Another crucial aspect which may impact on the outcome of cell transplantation is the methodology used for cell preparation, and more specifically whether the tissue is implanted as solid pieces or as a dissociated cell suspension. Previous studies have demonstrated that solid grafts survive well in the chamber of the eye (Björklund, Hoffer, et al., 1983). On the contrary, limited graft viability was reported in intraparenchymal implantation unless the donor cells were placed near the ventricle or an aspiration cavity, suggesting that a well-vascularized site promotes graft survival. To avoid the problems associated to solid tissue transplant survival, cell suspension preparations, derived from enzymatic digestion and mechanical trituration, were introduced (Björklund, Dunnett, et al., 1980). Both methods

present advantages and disadvantages. In solid pieces of tissue, neurons are mixed together with glial populations, which could help the maturation of the tissue in the host brain (Freeman et al., 2011). Importantly, with the latter approach, cells do not undergo mechanical stress, trauma or necrosis due to axotomy, although cell death may still occur upon dissection of the tissue (Emgård et al., 2002). On the other hand, cell suspensions, which require the mechanical dissociation of the tissue with potential accompanying cell damage, are surgically easier to implant in the brain. Dissociated cells are also more likely to be integrated in the host brain and to form afferent and efferent connections with the latter (Watts, Brasted and Dunnett, 2000b). However, the trituration of the tissue leads to the destruction of the donor vasculature leaving the graft to rely strictly on the vascular supply of the host (Baker-Cairns et al., 1996; Cisbani, Saint-Pierre, et al., 2013; Krum and Rosenstein, 1988). Solid pieces of tissue maintain their own angioarchitecture and will more readily anastomose with surrounding vessels (Baker-Cairns et al., 1996; Broadwell et al., 1990; 1991; Rosenstein and Brightman, 1986). Additionally, cell suspensions trigger a weaker inflammatory response, in part because they are injected through a smaller cannula than solid grafts (Freeman et al., 2011). In clinical trials, the cell suspensions utilized were not completely dissociated and small clusters of cells were maintained, introducing a source of variability with regard to the effective number of cells implanted between transplants. However, the method of cell suspension seems to yield a better outcome (Freeman et al., 2011), as also observed in models of excitotoxic lesion (Watts, Brasted and Dunnett, 2000b).

1.3.2.3 Immunosuppression

The regime of immunosuppression is another parameter that may be predictive of graft outcome and one that is intermingled with the cellular and molecular immune/inflammatory responses against grafted tissue (**Table 1-1**). The early work on transplantation in animal models of disease demonstrated that the long-term survival of dopaminergic xenografts (mouse to rat and human to rat) was improved when the immunosuppressive drug cyclosporine A was administered to the recipient animal, even for a short period of time (Brundin et al., 1985; 1988). However, halting cyclosporine treatment reduced functional effects of grafted tissue at later time points (6 months), although the improvement of the behavioural phenotype of the immunosuppressed animals was still greater than in non-immunosuppressed animals (Brundin et al., 1989).

Clinically, the withdrawal of immunosuppression coincided with the decline of beneficial effects in PD patients (Olanow et al., 2003). It was suggested that this could reflect graft rejection, although grafts survival was confirmed both by positron emission tomography (PET) scans of Fluoro-dopa up-take and

later by post-mortem histological analysis (Olanow et al., 2003), similarly to previous report (Kordower et al., 1997). In other PD cases, the withdrawal of the immunotherapy treatment did not lead to graft rejection (Lindvall et al., 1994; Piccini et al., 1999). Two independent reports have further described graft survival in the absence of any immunosuppressive treatment (Freed et al., 2001; Hauser et al., 1999). Thus, the timing of withdrawal may be more important than the withdrawal per se, or immunotherapy may be needed only for a short period of time post-grafting. In HD, halting immunosuppression did not correlate with graft rejection (Barker and Widner, 2004) at early or later time-points, except in one case (Krystkowiak et al., 2007). Previous post-mortem analyses of HD transplanted cases a decade following grafting revealed a strong immune response cuffing the grafts (Cicchetti et al., 2009), in conditions where the immmunosuppression began 2 weeks before the surgery and continued for 6 months (Hauser et al., 2002). It is possible that solid tissue grafts, following the withdrawal of the immunosuppressive therapy, may present enhanced antigenic stimulation triggering a stronger inflammatory reaction, as compared to cell suspension grafts (Kordower et al., 1997; Mendez et al., 2005; 2008; Olanow et al., 2003; Redmond et al., 2008). Solid grafts may trigger a stronger immune response also because they still contain the donor vasculature which is highly immunogenic (Freeman et al., 2011). Finally, the use of multiple donors may represent another important variable in introducing a number of mismatched human leukocyte antigen (HLA) tissues (Barker and Widner, 2004). Unfortunately, none of the study monitored the immune response via PET neuroimaging with the radioligand PK11195, which is highly selective for the translocator protein (also known as peripheral–type benzodiazepine receptor) abundantly expressed on activated microglia. The use of this ligand would have allowed to monitor the extent of the immune response following transplantation and consequently help understand the host brain reaction to the graft and the potential rejection process (Folkersma et al., 2011; Tai et al., 2007).

In conclusion, immunosuppression is considered a requirement for transplantation procedure. Although immunotherapy has been used to ensure graft survival and development, the treatments might need to be withdrawn to prevent potential side effects for the patients (Barker and Widner, 2004).

1.3.2.4 Imaging of graft placement and functionality

Graft identification by magnetic resonance imaging. In all clinical trials of cell transplantation in HD patients, post-operative MRI has been used to confirm graft placement (**Table 1-1**). In almost all reports, post-operative MRI, conducted as early as one day or as late as 6 years after surgery, indicates that grafts can be found at the location of preselected surgical coordinates, are easily

distinguishable from surrounding tissue, and, for the large part, do not show signs of rejection or of abnormal growth (Bachoud-Lévi, Bourdet, et al., 2000; Cicchetti et al., 2009; Kopyov et al., 1998; Reuter et al., 2008; B. D. Ross et al., 1999; Rosser et al., 2002).

Graft functionality by positron emission tomography. At times, MRI was performed in combination with [^{18}F]fluorodeoxyglucose (FDG) PET scans to assess glucose metabolism (Bachoud-Lévi, Rémy, et al., 2000; Gallina et al., 2010; Hauser et al., 2002), [^{11}C]SCH 23390 for D1 receptor binding and [^{123}I]iodobenzamide (IBZM) or [^{11}C]raclopride (RAC) for D2 receptor binding (Gallina et al., 2010; Hauser et al., 2002; Reiner et al., 2011; Reuter et al., 2008; Rosser et al., 2002), allowing for the evaluation of the extent of grafted cell survival and functionality. For example, Hauser *et al.* reported that putaminal glucose metabolism and D1 receptor binding did not decrease as usually expected with disease progression, although this was not observed in the caudate nucleus. The authors suggested that this was likely due to the small amount of tissue implanted (Hauser et al., 2002). However, they also reported a decrease in D2 receptor binding in the putamen and caudate nucleus, presumably due to the selective survival of transplanted neurons or to differences in the time course or capacity for expression of these receptors (Hauser et al., 2002). Gaura *et al.* reported that at 30 months post-transplantation, brain glucose metabolism was either increased or stable in all parts of the striatum when compared to images obtained immediately post-surgery. Small regions corresponding to the grafts, as identified by MRI, showed a higher metabolic activity compared to the host striatum. Cortical and striatal hypometabolism was ameliorated in 3 patients 2 years post-transplantation, which correlated with functional improvement (Gaura et al., 2004). However, at the 6-year post-transplantation follow-up, glucose metabolism had decreased again (Bachoud-Lévi et al., 2006). Two patients in whom no increase in metabolic activity had been detected at 2 years (Bachoud-Lévi, Rémy, et al., 2000) continued to deteriorate clinically and, accordingly, MRI did not indicate improvements 6 years post-surgery (Bachoud-Lévi et al., 2006). Reuter *et al.* reported increased D2 receptor binding at 6 months in one transplanted patient, which slightly declined afterwards but stayed at levels higher than baseline, whereas another patient did not exhibit any improvement on imaging (Reuter et al., 2008).

Grafting complications and irregularities. Imaging techniques have also been of crucial importance in identifying potential complications and irregularities, although graft complication or unusual grafting patterns remain anecdotal. One single case, which had taken part in a phase II trial conducted by INSERM, was diagnosed with encephalitis and displayed striatal glucose hypometabolism, which were interpreted by the authors as signs of graft rejection. These were identified at 14 months post grafting when the patient had become ill after being taken off a 9-month regime of immunosuppressive drugs

(Krystkowiak et al., 2007). Anti-inflammatory and immunosuppressive medications were reinstated for an additional 7-month period, and follow-up MRI showed recovery from the encephalitis and increased metabolism in striatal areas as compared with images obtained during the putative "rejection" episode or prior to surgery (Krystkowiak et al., 2007). In the reports by Gallina *et al.,* graft overgrowth was observed in all transplanted patients and as early as 4 months post surgery. The latter tissue growth had virtually ceased 9-10 months post-transplantation. However, the grafts had enlarged aberrantly and were not confined to the surgical target sites. In fact, they encompassed regions of the white matter within the overlying cortex and ventral striatum. Hypermetabolic activity was demonstrated by FDG-PET 6-9 months post surgery but had decreased by 12 months after transplantation. Changes in D1 receptor binding varied between patients, which correlated with limited improvement, if any (Gallina et al., 2008; 2010). One additional MRI report showed large cysts and well-delimited masses in one patient 10 years after transplantation (Keene et al., 2009).

1.3.2.5 Impact of grafts on motor function

Cell transplantation trials were initiated to evaluate safety and tolerability of the procedure in HD patients, although motor recovery was monitored (**Figure 1-12**). In the majority of cases, the benefits were only marginal and short-lived. The first clinical trial reported deterioration of the motor symptoms 12 months post-implantation (Kopyov et al., 1998). No significant motor and cognitive amelioration were reported in the seven patients enrolled in the University of South Florida (USF) over a period of 12 months post-surgery (Hauser et al., 2002) as well as in the patients of the Imperial College London and Cardiff University cohorts (Barker et al., 2013; Reuter et al., 2008). Minor motor improvements were reported by Gallina *et al.* (Gallina et al., 2008; 2010) 2 years post-surgery. Only one patient showed improvements lasting over 5 years (Reuter et al., 2008). Sustained improvement and stabilization of the motor symptoms for 4 to 6 years was reported by the INSERM cohort. However, disease course continued 6 year post-surgery (Bachoud-Lévi, Rémy, et al., 2000; Bachoud-Lévi et al., 2006). In addition to anecdotal cases showing long-term motor improvements, there is no evidence that cell transplantation can worsen the pathology (Rosser and Bachoud-Lévi, 2012). However, several factors such as increasing space occupying the site of the transplant, inflammatory infiltrates, vascular glomeruli may be indicators of an altered pathological phenotype, the outcome of which cannot be ascertained.

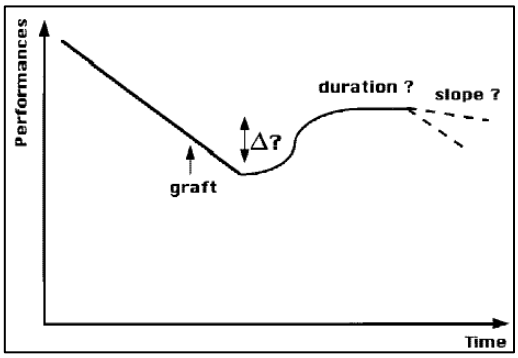

Figure 1-12. Hypothetical course of evolution of clinical symptoms in a grafted HD patient. Using arbitrary coordinates, functions are supposed to decline steadily before and during a short period of time after the graft, while foetal neurons are developing. After that period, three successive steps can be hypothesized: a progressive decrease of the symptoms, characterized by a positive difference (Δ) between the worst and the best functional levels; a stabilization of clinical symptoms, the duration of which has to be determined; then a new decline, best identified by its slope, to be compared with the pre-graft one (Bachoud-Lévi et al., 2002).

1.3.2.6 Post-mortem evidence of graft survival

Although the MRI and PET scans can provide important information regarding the location and the functionality of the grafts, they are limited techniques when it comes to revealing aspects of integration, differentiation and survival of the grafts. To this day, only nine transplanted brains have been analysed post-mortem (**Table 1-2**). The post-mortem studies performed have provided crucial information regarding the short- and long-term survival of the graft. The studies and observations made during my doctorate are based, in large part, on the previous post-mortem reports made by Dr. Cicchetti and collaborators (Cicchetti et al., 2009; Freeman et al., 2000; Hauser et al., 2002), which I will discuss in greater details in the following sections for the purpose of this thesis.

Graft modular organization. Before entering into the details of the post-mortem analyses of the few transplanted HD cases, it is important to introduce some of the terminology related to the graft cytoarchitecture that I will refer to throughout this thesis. Grafts derived from the embryonic ganglionic eminence implanted into the putaminal-caudate sites of the HD brains can be macroscopically identified and present a characteristic compartmentalized architecture (**Figure 1-13**). Indeed, macroscopic patches (p), defined as p-zones, are visible within the graft and embedded in “non-patch” regions (non p-zone) (Graybiel et al., 1989; Isacson et al., 1987). P-zones represent immature striosome and are characterized by high AChE activity, tyrosine hydroxylase (TH) immunoreacitivity and cluster of calbindin- and ENK- positive MSNs, similar to the ones of the host striatum. On the contrary, non p-zones are mainly composed of non striatal-like tissue, presenting a weaker AChE and TH

immunoreactivity and are devoid of calbindin-positive MSNs (Graybiel et al., 1989). This organization of the transplant mirrors the organization of the developing striatum (Graybiel et al., 1989).

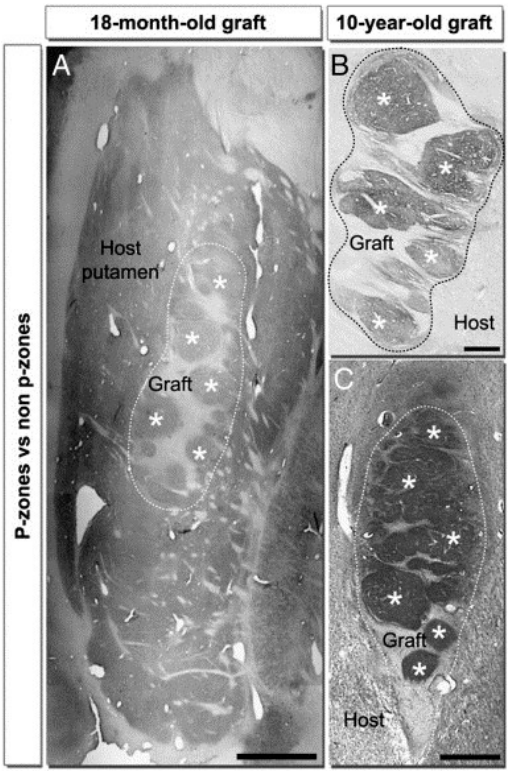

Figure 1-13. Graft modular cytoarchitecture. Graft cytoarchitecture at 18 months vs. 10 years post-transplantation. Immunohistochemical staining for specific striatal markers was performed to identify the proportions of p-zones vs. non p-zones yielded by tissue dissection of the FLVE. **A**. Low power photomicrograph of the entire putamen in an HD patient 18 months post-transplant. Substance P immunohistochemical staining allows the clear identification of the graft borders (dotted line) and reveals several p-zones (white stars). **B–C**. Higher power photomicrographs of two distinct implants in an HD patient at 10 years post-transplantation stained for tyrosine hydroxylase (**B**) and NADPH-diaphorase (**C**). In both cases (18 months vs. 10 years), more than 50% of the graft (SP: 64.8%, TH: 63%; NADPH-d: 73%) is composed of tissue positive for striatal markers. Scale bar in **A**= 1 mm (applies to **C**); **B**= 200 μm (Freeman et al., 2011).

Table 1-2. Patient information across post-mortem studies

	Capetian *et al.*, 2009 6 mo	Freeman *et al.*, 2000 18 mo	Keene *et al.*, 2007 6-7 y		Cicchetti *et al.*, 2009 9-10 y			Keene *et al.*, 2009 10 y		Cisbani *et al.*, 2013 12 y	
Gender	♂	♂	♂	♀	♂	♀	♀	♂	♀	♂	♀
CAG repeats	44	42	45	52	42	42	42	48		53	
Grade	NA	2	NA	NA	3	3	2	NA		4	
Time from diagnosis	NA	7	NA	NA	5	12	5	NA		2	
Symptoms duration (y)	NA	12	7	8	8	17	9	2		6	
Age at transplantation (y)	42	54	47	34	58	64	59	29		28	
Post-operative latency	6 mo	18 mo	6.5 y	6 y	9 y	10.5 y	9.5 y	10 y		12 y	

Abbreviations: mo: months; NA: not available; y: years (Cisbani and Cicchetti 2014)

Early post-mortem evidence of graft survival. The very first post-mortem study of a transplanted HD-affected brain was conducted in a patient who died 18 months after transplantation of causes unrelated to the procedure. This study provided the initial proof of concept that solid foetal striatal grafts could survive in a human HD brain (Freeman et al., 2000) (**Table 1-2**). Large aspiny neurons and MSNs were predominantly seen in the p-zones of the grafts using typical striatal markers such as DARPP-32, calretinin, AChE, calbindin, ENK and substance P. Interneurons positively stained for ChAT, NADPH-d and parvalbumin were also detected within p-zones. Non-p-zones were largely devoid of these markers but were richer in glial fibrillary acidic protein (GFAP)-positive astrocytes. HLA-DR, a marker for macrophages and microglia, was rarely found in the transplant but was abundantly expressed in the host brain. There was no perivascular cuffing or T-cell infiltration, as visualized with CD4 and CD8. mHtt inclusions within the grafted tissue were not detected (Freeman et al., 2000) (**Table 1-3**).

One additional case from the Freiburg University cohort provided a description of graft status at early time interval following transplantation (Capetian et al., 2009) (**Table 1-2**). DARPP-32-positive neurons were found within the grafted tissue and were interspersed with calretinin- and somatostatin-positive interneurons. However, other types of interneurons labelled with either parvalbumin or ChAT were not found within the graft (Capetian et al., 2009). Both these studies with early marker documentation reported ingrowth of TH-positive fibres within the transplanted tissue (Capetian et al., 2009; Freeman et al., 2000). In their report, Capetian *et al*. also discriminated donor cells from host cells within the neural grafts using the XX-FISH technique which allows to distinguish X and Y chromosomes (Capetian et al., 2009). They also noted the presence of a local immune response using CD45 (a marker of lymphocytes and microglia) and CD28 (a marker of macrophages and activated microglia) as well as an astrocytic reaction restricted to the vicinity of the graft borders, which did not have the appearance of a glial scar (Capetian et al., 2009; Soulet and Cicchetti, 2011). Furthermore, Capetian *et al*. investigated mitotic activity of the transplanted cells using the marker Ki67 for dividing cells. Cells within the grafts were also positive for SRY (sex determining region Y)-box 2 (Sox2), which is normally expressed by multipotent neuronal stem cells. The vast majority of the transplanted cells were also positive for doublecortin (DCX), which co-expressed with Sox2, as well as neuronal nuclei (NeuN) and Prospero homeobox protein 1 (Prox1), indicating that multipotent precursors were present within the graft and that grafted cells were committed to a neuronal fate. Cells immunopositive for DCX and Sox2, but not for Ki67, were observed outside the graft boundaries, suggesting that mitotic cells were found exclusively within the solid foetal striatal grafts (Capetian et al., 2009) (**Table 1-3**).

Post-mortem evidence of graft survival long-term. Insight into prolonged graft survival became available with the publication of 7 additional cases for which histological analysis was conducted at much later time points, e.g. between 6 and 12 years after transplantation (Cicchetti et al., 2009; Cisbani, Freeman, et al., 2013; Keene et al., 2007; 2009) (**Tables 1-2 and 1-3**). The report by Keene *et al.* described one HD case 6 years after transplantation and one case 7-year post-transplantation (see **Table 1-2**). In tandem publications (Cicchetti et al., 2009; Cisbani, Freeman, et al., 2013) reported four additional cases from the USF trial, between 9 and 12 years post-transplantation. Finally, the report by Keene *et al.* of their 10-year transplant case indicated the presence of mass lesions and large cysts at all implantation sites (Keene et al., 2009) (**Table 1-3**).

Despite that histological analysis of HD patients transplanted with long-term grafts have generally revealed good graft viability, a closer look at the general appearance of the grafted tissue and health of individual grafted cells argues that survival may be compromised in the long-term. For example, at 6 or 7 years after transplantation, Keene *et al.* (Keene et al., 2007) demonstrated grafted cell survival as shown by the various striatal markers found within the grafted tissue. However, basic markers of cell cytoarchitecture such as hematoxylin & eosin and Nissl reveal that grafted cells depict a morphology very different from host cells (Cicchetti et al., 2009). Cells within p-zones are ballooned, vacuolated, lack structural cytoplasmic integrity and even stain positively for apoptotic markers such as caspase-3. When identical immunohistological stainings are compared between the reports by Keene and Cicchetti, and those published for the 6- (Capetian et al., 2009) and 18-month post-transplantation cases (Freeman et al., 2000), it is apparent that grafted striatal projection neurons exhibit a much weaker staining and that they lack dendritic extensions almost completely (Cicchetti et al., 2009; Keene et al., 2007), pointing to a significant alteration in morphology. In contrast, various subclasses of striatal interneurons including NADPH-d-, ChAT-, parvalbumin- and calretinin-positive cells, show a better long-term survival, suggesting a degeneration or neuronal sparing pattern similar to that observed with HD pathology (Cicchetti et al., 2009; Keene et al., 2007).

Although there may be signs of degeneration within the grafted tissue, ingrowth of host-derived TH fibres can be observed, suggesting connections and interactions between the host and donor cells (Cicchetti et al., 2009; Keene et al., 2007). These results are in accordance with earlier animal model studies as well as transplanted PD patients (Hantraye et al., 1992; Kendall et al., 1998; Scherzinger et al., 1997). Such TH innervation was not found in the 10-year post-transplantation case depicting cysts and mass lesions (Keene et al., 2009), suggesting that TH innervation of grafted tissue is not a random process. However, DARPP-32- and calbindin-positive cells within the grafts do not appear to cross the

graft-host interface, suggesting a limited connectivity of the graft with the host brain (Keene et al., 2009). One study reported the presence of cortical glutamatergic input onto the grafted striatal cells, using both immunohistochemistry and transmission electron microscopy (Cicchetti et al., 2009). Moreover, a notable microglial and astrocytic gliosis was observed in the vicinity of grafted tissue 9-10 years after transplantation (Cicchetti et al., 2009; Cisbani, Freeman, et al., 2013), while such a response was found to be less intense in the graft than in the host at earlier intervals (6 and 7 years) (Keene et al., 2007).

Table 1-3. Summary of post-mortem analyses across studies

		Capetian *et al.*, 2009 6 mo	Freeman *et al.*, 2000 18 mo	Keene *et al.*, 2007 6-7 y	Cicchetti *et al.*, 2009 9-10 y	Keene *et al.*, 2009 10 y	Cisbani *et al.*, 2013 9 and 12 y
Projection neurons	Calbindin		✓	✓	✓	✓	
	DARPP-32	✓	✓	✓			
Interneurons	Calretinin	✓	✓	✓		✓	
	Parvalbumin	✓		✓			
	Somatostatin	✓					
	ChAT	✓					
	NADPH		✓		✓		
Connectivity	TH	✓	✓	✓	✓	✓	✓
	Synaptophysin				✓		
	VGLUT1				✓		
Inflammation	GFAP	✓	✓	✓	✓		✓
	HLA-DR		✓				
	Iba1				✓		
	CD4	✓			✓		
	CD8	✓			✓		
	CD28	✓					
	CD45	✓					
Vasculature	vWF						✓
	PDFGR-β						✓
	α-SMA						✓
Aggregates	mHtt		✓	✓	✓		
	Ubiquitin		✓	✓	✓		
Overall transplant survival		10/10	6/10	13/14	8/10 (9 y) 9/11 (9.5 y) 1/16 (10 y)	None Cysts and mass lesions	8/10 (9 y) 11/11 (12 y)

Abbreviations: α-SMA: alpha-smooth muscle actin; CD: cluster of differentiation; DARPP-32: Dopamine- and cAMP-regulated phosphoprotein, 32 kDa; GFAP: glial fibrillary acidic protein; Iba1: ionized calcium-binding adapter molecule 1; mo: months; NADPH: Nicotinamide adenine dinucleotide phosphate; PDGFR-β: Beta-type platelet-derived growth factor receptor; TH: Tyrosine hydroxylase; VGLUT1: vesicular glutamate transporter 1; vWF: Von Willebrand factor; y: years (Cisbani and Cicchetti, 2014).

1.4 Justification and rationale

Cell therapy offers the possibility of replacing degenerated neurons thereby improving the symptoms of neurodegenerative diseases such as HD. However, in spite of trying various cell replacement protocols, only marginal functional recovery has been reported. The post-mortem analyses of HD transplanted brains began to yield important information as to why patients only show mild and short-lived clinical benefits following these procedures. Understanding why graft survival is compromised long-term is critical to 1) improve this therapeutic strategy in the future and 2) to better understand the pathology itself. For my PhD thesis, I build on this previous work and undertook a series of analyses to further our understanding of graft behaviour in the diseased brains, using both human post-mortem tissue from HD transplanted patients as well as performing grafting studies in animal models of the disease.

1.5 Hypothesis and objectives

1.5.1 Hypotheses

Dr. Cicchetti's laboratory had reported sub-optimal long-term graft survival in HD transplanted patients (Cicchetti et al., 2009; Freeman et al., 2000; Hauser et al., 2002). Despite the identification of a number of factors contributing to graft demise long-term, it is clear that additional elements may be involved complexifing our understanding of these events. We hypothesized that comprised graft vascularization could further contribute to poor graft survival. In addition to post-mortem analyses in the HD cases, we set to test whether methodological issues related to tissue preparation (solid graft vs. cell suspension) could also be responsible for poor graft revascularization. Finally, we hypothesized that the abnormal gene product, the mutant huntingtin protein, could spread from the host diseased brain to the transplant and thereafter, impact graft survival.

1.5.2 Objectives

In order to investigate these two main hypotheses, the project was designed to reach three main objectives:

- Investigate the contribution of the neurovascular unit elements, namely blood vessels and astrocyte, to graft health in HD transplanted patients (**Chapter II**)
- Investigate the survival and revascularization of suspension grafts in the YAC128 mouse model of HD (**Chapter III**)
- Investigate the presence of mHtt within the grafted tissue (**Chapter IV**)

CHAPTER II

2.1 Contributions

The study presented in Chapter II was designed to dissect and understand some of the mechanisms underlying poor graft survival long-term. Specifically, we evaluated the vascularization of foetal striatal allografts 9 and 12 years post-surgery in HD patients and the presence of important elements of the neurovascular unit within the transplanted tissue.

As first author of the paper, I participated to the design of the experiments with Dr Cicchetti and Dr Soulet. I also performed most of the immunofluorescence staining. Martine Saint-Pierre performed part of the staining as well as the optimization of some of the protocols. I acquired the confocal pictures of the immunofluorescence staining with the help of Dave Gagnon (Centre de Recherche Robert Giffard). Moreover, I performed all the quantifications presented in the article and prepared all final figure panels. Finally, I participated in the writing of the initial version of the paper, which was finalized by Dr Cicchetti, Dr Freeman and Dr Barker. Dr Freeman performed the transplantation surgery and provided us with the transplanted tissues. Dr Hauser ensured the clinical follow-up of the patients. Dr Parent provided us with the necessary age-matched control sections for both the HD brains and the transplanted tissue as well as making his confocal microscope available to us.

2.2 Résumé

La transplantation cellulaire fut proposée comme thérapie potentielle pour la maladie de Huntington. La vascularisation et le support trophique sont importants pour la survie des greffes. Cependant, très peu d'études ont fait mention de la vascularisation des greffes chez les patients ayant des désordres neurologiques. Nous avons ici analysé la vasculature du putamen de l'hôte ainsi que celle de greffes de tissu striatal transplanté chez des patients Huntingtoniens 9 à 12 ans auparavant. Les greffes étaient caractérisées par une réduction significative du nombre de vaisseaux sanguins par rapport au cerveau hôte. Nous avons également observé un nombre significativement réduit d'astrocytes et de *gap junctions,* ce qui suggère l'absence d'éléments fonctionnels de la barrière hémato-encéphalique au sein du tissu greffé. De plus, les greffes démontraient une absence quasi complète de péricytes (comparé au striatum de l'hôte), des éléments essentiels dans la stabilisation de la vasculature et de l'angiogenèse. L'impact d'un faible nombre de vaisseaux sanguins de large calibre et d'astrocytes sur la survie des greffes est inconnu. L'augmentation marquée des astrocytes atrophiques dans le cerveau hôte entourant les greffes suggère que la réduction du support trophique de l'hôte pourrait aussi contribuer à la faible survie de greffes dans ce contexte. Une meilleure compréhension de la façon dont ces composantes supportent le tissue greffé est critique au futur développement de thérapies cellulaires pour le traitement de la maladie d'Huntington.

2.3 Striatal allografts in Huntington's disease patients: impact of diminished astrocytes and vascularization on graft viability

[1]Cisbani G, [2,3]Freeman TB, [1,4]Soulet D, [1]Saint-Pierre M, [5]Gagnon D, [4,5]Parent M, [6,7]Hauser RA, [8]Barker RA, *[1,4]Cicchetti F

[1]Centre de Recherche du CHUQ (CHUL), T2-50, 2705 Boulevard Laurier, Québec, QC, Canada, G1V 4G2; [2]Department of Neurosurgery and Brain Repair, [3]Center of Excellence for Aging and Brain Repair, University of South Florida, 2 Tampa General Circle, 7th Floor, Tampa, FL, USA, 33606-3571; [4]Département de Psychiatrie et Neurosciences, Université Laval, Québec, QC, Canada, G1K 7P4; [5]Centre de Recherche Université Laval Robert-Giffard, Room F-6500, 2601 Canardière, Québec, QC, G1J 2G3, Canada; [6]Departments of Neurology; Pharmacology and Experimental Therapeutics, [7]Parkinson's Disease and Movement Disorders National Parkinson's Foundation Center of Excellence, University of South Florida, Tampa, FL, USA, 33606; [8]Cambridge Centre for Brain Repair, Department of Clinical Neurosciences, University of Cambridge, UK, CB2 0PY,

Correspondence
Francesca Cicchetti, PhD
Centre de Recherche du CHUQ (CHUL)
Axe Neurosciences, T2-50
2705, Boulevard Laurier
Québec, QC, Canada, G1V 4G2
Tel #: (418) 656-4141 ext. 48853
Fax #: (418) 654-2753
E-mail: francesca.cicchetti@crchul.ulaval.ca
Running title: Neural transplant vascularization in HD

2.3.1 Abstract

Neuronal transplantation has been proposed as a potential therapy to replace lost neurons in Huntington's disease. Transplant vascularization and trophic support are important for graft survival. However, very few studies have specifically addressed graft vascularization in patients with neurological disorders. In the present study, we analysed the vasculature of the host putamen as well as solid grafts of foetal striatal tissue transplanted into patients with Huntington's disease 9 and 12 years previously. Grafts were characterized by a significantly reduced number of large calibre blood vessels in comparison to the host brain. There were also significantly fewer astrocytes and gap junctions, suggesting a lack of functional blood brain barrier components within the grafted tissue. Additionally, grafts demonstrated a nearly complete absence of pericytes (compared to the striatum) that are considered important for vascular stabilization and angiogenesis. Finally, the host striatum had a marked increase in atrophic astrocytes in comparison to controls and grafts. The extent to which the lower number of large calibre vessels as well as astrocytes within the transplants contributed to suboptimal graft survival is unknown. The marked increase in atrophic astrocytes in the host brain surrounding the grafts suggests that reduced host trophic support may also contribute to poor graft survival in Huntington's disease. A better understanding of the way in which these components support allografted tissue is critical to the future development of cell based therapies for the treatment of Huntington's disease.

Keywords: Huntington's disease, cell transplantation, vascularization, astrocytes, pericytes, glutamate, gap junctions

2.3.2. Introduction

Huntington's disease (HD) is a devastating autosomal dominant neurodegenerative disorder caused by a CAG expansion in exon 1 of the huntingtin gene. The disease is characterized by prominent cell losses in a number of brain structures, particularly in the striatum and cortex. Clinical features include a variety of motor, cognitive and psychiatric deficits (Phillips et al., 2008). Although incurable, there are some partially effective symptomatic treatments and a range of experimental therapies that are being pursued (Qin *et al.*, 2005; Phillips *et al.*, 2008; Nance *et al.*, 2012). Cell transplantation, that aims to replace the neurons of the striatum that are targeted early in the pathogenic process, has yielded some preliminary, modest and short-lived clinical benefits (Bachoud-Lévi, Bourdet, et al., 2000; Bachoud-Lévi et al., 2006; Cicchetti et al., 2009; Gallina et al., 2010; Hauser et al., 2002; Keene et al., 2007; Kopyov et al., 1998; Reuter et al., 2008; Rosser et al., 2002). We have reported previously that graft survival in HD is compromised long-term (Cicchetti et al., 2009; 2011). This raises the possibility that short-term benefits are lost due to compromised graft viability as opposed to the progression of the underlying disease.

We have undertaken post-mortem studies in 5 of the 7 patients with HD who received transplants in the open label study conducted at the University of South Florida (Cicchetti et al., 2009; 2011; Freeman et al., 2000; 2011; Hauser et al., 2002). Our observations suggest that grafted cells undergo degeneration possibly as a result of a chronic inflammatory response to the transplant as well as excitotoxic effects of aberrant host cortical afferents onto the grafted cells (Cicchetti et al., 2009; 2011; Fan and Raymond, 2007; Freeman et al., 2011). In this paper, we additionally examined the relationship between solid neuronal allograft vascularization and astrocytic responses to long-term transplant viability in the brains of two patients with HD.

2.3.3. Material and Methods

2.3.3.1 Patients' characteristics

This report focuses on the histological evaluation of 2 brains (from patients 1 and 7) of the initial 7 HD patient cohort in the open label pilot study on cell transplantation conducted at the University of South Florida (Hauser et al., 2002). These two brains were chosen because they had the best histological evidence of long-term graft survival from our cohort. Patient 1 had 42 CAG repeats (Cicchetti et al., 2009; Hauser et al., 2002), while patient 7 had 53 CAG repeats (Hauser et al., 2002). These two women were transplanted at 58 and 28 yrs of ageand died 9 and 12 yrs post-transplantation

respectively of causes unrelated to surgery. At autopsy, they were classified as having grade 3 and grade 4 disease according to the Vonsattel post-mortem rating scale (Vonsattel et al., 1985).

The age-matched control brain for patient 1 was a 70-yr old woman previously described in (Cicchetti et al., 2009) The age-matched control brain used for patient 7 was a 41-yr old man who died of myocardial infarction. The control brain from a non-HD 12-yr old boy, who died from pulmonary complications of multiple trauma, was used to match the developmental stage of the grafted foetal tissue of both HD transplanted cases (**Figure 2-1B**).

2.3.3.2 Donor tissue preparation and transplantation

Methods for tissue preparation, transplantation and immunosuppression, as well as clinical and radiologic evaluation have been described previously (Björkqvist et al., 2008; Cicchetti et al., 2009; 2011; Freeman et al., 1995; 2011; Hauser et al., 2002; Weiss et al., 2012; 'Freeman et al PNAS 2000', 2000). Briefly, all patients received foetal tissue transplants from 5 to 8 striatal primordia per site. Solid tissue transplants measured 0.5 to 1 mm^3 and were derived from the far lateral portion of the lateral ventricular eminence (FLVE) to optimize the percentage of tissue of striatal origin (Freeman et al., 1995). More specifically, patient 1 received 1 striatal anlage in the left and right caudate and 4 in the left and right putamen. Patient 7 received 1 FLVE in the left and right caudate and 5 and 6 FLVEs in the left and right putamen, respectively. All graft sites could be identified macroscopically on post-mortem evaluation (**Figure 1A**).

2.3.3.3 Tissue preparation for post-mortem histological evaluation

The brains of the transplanted patients were removed within 5 (patient 1) and 2 hrs (patient 7) of death. Briefly, the brains were bisected, cut serially into 1-cm thick slabs and immersed in Zamboni's fixative for 8 days at 4°C. Brain slabs were then placed in a 20% sucrose in 0.1 M phosphate buffered saline (PBS, pH 7.4) cryoprotectant solution (Cicchetti et al., 2009; Freeman et al., 2000). For the control brains, post-mortem delays varied between 10 and 14 hrs. The control brains were also bisected, sliced into 2-cm thick slabs that were fixed by immersion in 4% paraformaldehyde at 4˚C for 3 days. They were then stored at 4°C in a 0.1 M PBS, pH 7.4 containing 15% sucrose and 0.1% sodium azide. Both the transplanted and control brains were sectioned using a freezing microtome (Wallman et al., 2011). These slightly different methods of tissue preservation did not appear to affect the quality of the histological stainings. The protocols for single or double immunohistochemistry as well as for

acetylcholinesterase (AChE) histochemical staining have been described in detailed in (Cicchetti et al., 2009) (see **Table 2-1**).

2.3.3.4 Immunofluorescence

Post-fixation, sections were rinsed three times with KPBS and pre-incubated in a blocking solution containing 0.1% bovine serum albumin (BSA, Bioshop, Burlington, ON), 0.04% Triton X-100 (Sigma), 4% normal goat serum (NGS, Wisent Inc., St-Jean-Baptiste de Rouville, Qc) in KPBS for 30 min. After three further washes with KPBS, they were incubated in a blocking solution overnight at 4 °C with primary antibodies alone or in the following combinations: von Willibrand factor (vWF), platelet-derived growth factor receptor-beta (PDGFR-β)/alpha-smooth muscle actin (α-SMA), vWF/ glial fibrillary acidic protein GFAP (**Table 2-1**). It is important to note that type A pericytes (which emerge and proliferate from the basal lamina, releasing essential components of the extracellular matrix and contributing to the stromal tissue of the glial scar) stain positively for PDGFR-β (Göritz et al., 2011). In contrast, type B pericytes (which attach to blood vessels and fulfil the classic function of pericytes) express PDGFR-β and α-SMA (Göritz et al., 2011).

After washes in KPBS, sections were reincubated with appropriate secondary antibodies in a blocking solution for 90 min at room temperature. After rinsing, sections were incubated in KPBS containing 0.022% DAPI (2mg/mL, Molecular Probes, Eugene, OR), washed and mounted on Superfrost slides (Fisher Scientific, Ottawa, ON), coverslipped with Fluoromount-G (SouthernBiotech, Birmingham, AL) and sealed with nail polish.

2.3.3.5 Confocal laser scanning and brightfield microscopy

Confocal laser scanning microscopy was performed using both an Olympus FV500 (Olympus America Inc., Melville, USA) and LSM 5 PASCAL (Zeiss, Oberkochen, Germany) confocal laser-scanning microscope. Images were acquired by sequential scanning and optimized by a two-frame Kalman filter and analysed using acquisition software from Olympus (Fluoview SV500 imaging software 4.3, Olympus America Inc., Melville, USA) and Zeiss (LSM5 Pascal Image software, Zeiss, Oberkochen, Germany). Acquired z-series images were exported in Imaris Pro Sofware 4.5 (Bitplane AG, Zurich, CH). Reconstructions were performed using ImageJ (version 1.45s, HIH, Maryland, USA), Imaris Surpass module (Apple Corp., Cupertino, CA) and maximum intensity projections. Brightfield photomicrographs were taken by Picture Frame software (Microbrightfield, Vermont, USA) attached to

an E800 Nikon microscope (Nikon Instruments, ON, Canada). Images were prepared for illustration using Adobe Photoshop CS5 and assembled using Adobe Illustrator CS5.

2.3.3.6 Blood vessel quantifications and measurements

Quantifications of blood vessels labelled with vWF (for capillaries) and α-SMA (for large calibre blood vessels) were performed using a series of images collected from the host putamen and grafts at both 10x and 20x on a Zeiss LSM 5 PASCAL confocal laser-scanning microscope. The number of blood vessels (vWF+ or α-SMA+) was calculated in each sampled field of equal area using the standardized method of ImageJ for particle analysis (L. Li et al., 2010; Sen et al., 2011). The results are reported as the number of positive events per field of view and expressed as a mean ± S.E.M. The diameter of vWF+ capillaries or α-SMA+ blood vessels was measured with ImageJ on a sample of 40 vessels each. The diameters are expressed as a mean ± S.E.M. We were unable to measure the density of blood vessels as a function of brain atrophy as the number of brain tissue sections containing the graft were too few to allow this.

2.3.3.7 Quantifications of astrocytic cell types

The perimeters of the p-zones, non p-zones and putamen of the HD and control brains were delineated using the tracing contour option in Stereo Investigator (NeuroExplorer, version 10.0; Microbrightfield, Vermont, USA). Quantifications of GFAP+ cells (both by morphology types and total number of cells) were performed in this entire region using the Optical Fractionator probe (Stereo Investigator, Microbrightfield, Vermont, USA) installed onto an E800 Nikon microscope (Nikon Instruments, Mississauga, ON, Canada).

2.3.3.8 Densitometric quantification of gap junctions

Digitized brain images of the putamen were obtained with a Northern Light Desktop Illuminator (Imaging Research, Ste-Catherine's, ON, Canada) using a Sony Camera Video System (XC-77) and acquired with ScionImage for Windows (*Scion* Corporation, version *Alpha 4.0.3.2*, Maryland, USA). All images were acquired at the same magnification to allow the visualization of the entire putamen in a single field. The entire putaminal structure was delineated and the intensity of connexin-43 staining was assessed using the ImageJ software. Background intensities taken from the corpus callosum devoid of

connexin-43 staining were subtracted from each measurement.

2.3.3.9 Statistical analyses

One-way ANOVA calculations were used to compare the number of GFAP+ cells, vWF+ and α-SMA+ blood vessels in each quantified region. For the GFAP+ cell and vWF+ vessel counts, the assumption of homogeneity was not respected. To solve this, a different variance was estimated for each group. For the number of GFAP+ cells classified by morphology as well as α-SMA+ blood vessels, normality assumption was not respected, thus a negative binomial distribution was used. Step-down Bonferonni correction was further employed to ensure that the overall significance level of the multiple comparison tests was 0.001. The analysis was performed using the MIXED and GENMOD procedures of SAS (version 9.2, Cary, North Carolina). Diameters of vWF+ and α-SMA+ blood vessels were evaluated by a Student *t*-test ($p<0.001$) using PRISM 4 (Graphpad Software, San Diego, CA, USA). All data are expressed as means ± S.E.M.

2.3.4 Results

The majority of transplants could be identified macroscopically (**Figure 2-1A**). The grafts demonstrated a compartmentalized organization with the formation of striatal patchy areas referred to as p-zones that stained positively for AChE, as well as areas where there was no expression of striatal phenotypes (**Figure 2-1A**), referred to as non p-zones (Graybiel et al., 1989). These observations are similar to that which we have described previously (Cicchetti et al., 2009; Freeman et al., 2000; 2011).

2.3.4.1 Diminished number of large calibre blood vessels in grafted tissue

The presence of two distinct blood vessel populations was confirmed using diameter measurements on α-SMA+ large calibre blood vessels and vWF+ capillaries ($p<0,001$; **Figure 2-3F**). The number of large calibre (α-SMA+) blood vessels was lower in grafts compared to host and control brains ($p<0.001$; **Figure 2-2A, B and 2-3A**). Within the grafts themselves, there was a further significant reduction in the number of large vessels in the p-zones compared to the non p-zones of the grafts ($p<0.001$; **Figure 2-2A, B, 2-3A, C**).

Pericytes associated with α-SMA+ blood vessels were found in the host (**Figures 2-3A, B**) and in the graft non p-zones (**Figures 2-3A, D and D'**) but not the p-zones (**Figures 2-3A, C**). Graft p-zones demonstrated PDGFR-β+ pericytes associated only with capillaries (**Figure 2-3C**). Take together, these data suggest that there are diminished blood vessels and pericytes in grafts and that this is more prominent in the graft p-zones than in the non p-zones.

Immunofluorescence for the endothelial marker vWF revealed that the host putamen had a richer capillary network when compared to the grafts or control brains ($p<0.001$; **Figures. 2-2C, D and 2-3E**). These results suggest that there are no significant differences between the number of capillaries in the grafts and age-matched normal brains. However, there is a significant increase in the number of capillaries in the HD putamen in comparison to the normal putamen ($p<0.001$; **Figures 2-2C, D and 2-3E**), although the extent to which this may relate to a degree of atrophy is unclear.

2.3.4.2 Astrocytic subtypes within the host putamen and grafts

There was a significantly higher number of astrocytes in the HD host putamen than in any of the grafts or control putamen ($p<0.001$ and $p<0.05$; **Figures 2-4A, C, 2-5A, C**). In particular, there was a marked increase in the number of atrophic GFAP+ cells in both the host putamen in comparison to grafts or age-matched controls. The host brain was found to have activated atrophic astrocytes typical of what is observed in HD (Vonsattel *et al.*, 1985) ($p<0.001$; **Figures 2-4B, D and 2-5C**).

Within grafts, several different astrocytic subtypes were also evident. Astrocytes at the graft-host border were activated, but had a much more atrophied appearance compared to the ones found in the graft non p-zone and its age-matched control ($p<0.001$; **Figures 2-4B, D, 2-5B, C**). A circumferentially reactive layer of astrocytic processes was found in the transplant non p-zones surrounding the p-zones (**Figures 2-5D, E and G**). This was not a true "glial scar" as host dopaminergic and cortical striatal neurons easily penetrated this reactive layer and innervated the graft (**Figure 2-5F** and (Cicchetti et al., 2009)). Additionally, type A pericytes, typically found in reactive scars (Göritz et al., 2011) were not found in this circumferential reactive layer.

Astrocytes were more concentrated in the periphery than in the core of the p-zones ($p<0.001$ and $p<0.05$; **Figures 2-4A, C, 2-5A, D**). Graft p-zones did not display atrophied GFAP+ cells ($p<0.001$; **Figures 2-4B, D**). A third morphological appearance of astrocytes was found at the interface of the

graft p-zones and graft non p-zones. Resting astrocytes were also observed in both compartments of the grafts, but their number was significantly lower than in the host brain or the 12-yr old control brain ($p<0.01$ and $p<0.05$; **Figures. 2-4B, D, 2-5A, D**). Radially oriented astrocytes were only observed within the graft p-zones (**Figures 2-4B, D and 2-5E**).

2.3.4.3 Blood brain barrier alterations within the grafts

Host blood vessels were almost entirely wrapped by astrocytic end-feet (**Figure 2-6A**). However, astrocytes seem to have an attenuated interaction with the capillaries within graft p-zones (**Figure 2-6C**) compared to the non p-zone (**Figure 2-6B**) and the 12-yr old matched control (**Figure 2-6D**). This suggests that there is a diminished blood brain barrier (BBB) within graft p-zones compared to graft non p-zones or normal brain.

Gap junctions have recently been described to be essential for graft-host cell coupling (Jäderstad et al., 2011). There was a high expression of gap junctions (connexin-43) in the host brain (**Figures 2-6E, H**). Connexin-43 expression was diminished in the graft non p-zones (**Figs. 2-6F, H**) and was even more diminished within the graft p-zones (**Figures 2-6F, H)**. The 12-yr old control brain displayed the highest intensity of connexin-43 staining (**Figures 2-6G, H**), as has been described previously in normal CNS development (Dermietzel et al., 1989).

2.3.5 Discussion

Striatal grafts in patients with HD demonstrate significantly less large blood vessels in comparison to the host and control brains. This may have contributed to poor long-term graft survival (Cicchetti et al., 2009) as blood vessels are necessary for normal cell metabolism. However, while this may relate in some way to the atrophy seen in HD, it more likely reflects a primary abnormality as has been observed in transgenic YAC128 HD models (Franciosi et al., 2012). Diminished vascularization of grafts in comparison to the host has also been described in a Parkinson's disease (PD) patient who had good graft survival (Kordower et al., 1996).

Vascularization of grafted tissue and its integration into the host circulatory system is needed for graft survival (Broadwell et al., 1990; Lindsay and Raisman, 1984). Several factors have been identified to participate in graft revascularization. Blood vessel supply is proportional to the dimension of the graft and method of dissection of the foetal tissue (Freeman et al., 2011). Cell suspension grafts derive vascularization from the host (Baker-Cairns et al., 1996), whereas solid grafts, which have within them

an intact vessel network, anastomose with the host vasculature (Baker-Cairns et al., 1996). Therefore solid grafts, which contain a vascularization from the donor may be more immunogenic than suspension cell transplants (Freeman et al., 2011). In our study, transplants were derived from solid tissue pieces (Cicchetti et al., 2009; Freeman et al., 1995; 2000; Hauser et al., 2002). Additionally, the size of the cannula used for the injection could further trigger inflammation. The smaller cannula used for cell suspension grafting might minimize the brain trauma and thus, the local inflammatory reaction (Freeman et al., 2011). The immunogenicity of the blood vessels in solid grafts combined with the use of a larger needle could lead to increased inflammation which may interfere with the vascularization and viability of grafts (Freeman et al., 2011). However, similar arguments could be made for solid grafts in PD where graft viability has been far less compromised suggesting that other factors are contributing to the loss of viability in HD grafts.

Host factors may have contributed to the diminished graft survival in our HD cases in comparison to previously reported PD cases. Here we noted a marked increase in atrophic astrocytes in the host putamen similar to what has been previously described in other HD patients (Vonsattel et al., 1985). Therefore, it is conceivable that the poor graft survival in our HD patients is due to reduced trophic support from host astrocytes.

We report several differences in the vasculature found within the host, graft non p-zones and p-zones (**Figure 2-7**). First, large blood vessels were more numerous in the host than graft non p-zones, and were almost non-existent in graft p-zones. In this regard, pericytes associated with large blood vessels were found in the host and graft non p-zones but not in the graft p-zones. Taken together, this suggests that the relative absence of large blood vessels and pericytes within the graft p-zones may be contributing to poor graft viability, The presence of large blood vessels is perhaps not expected in the transplant given that typically blood supply comes from locally sprouting smaller vessels (Scott, 1984). We observed no differences between control brains and grafts with regard to capillaries. Therefore, diminished vasculature supply within graft p-zones is specifically limited to the larger blood vessels.

Pericytes and astrocytes are critical elements in the development and maintenance of normal vasculature (Bonkowski et al., 2011; Winkler et al., 2011). The scarcity of these elements in graft p-zones may have further contributed to the diminished graft survival in our patients with HD in comparison to PD. It is also plausible, however, that targeted inflammatory and excitotoxicity aimed at the p-zones within the transplants (Cicchetti et al., 2009; 2011) may have caused degradation of vasculature as a secondary phenomenon. Gap junctions, and in particular connexin-43 that is

abundantly expressed onto astrocytes, have recently been reported to be critical for the proper integration of the grafted cells with the host brain (Jäderstad et al., 2011). Finally in HD, astrocytes show lower levels of some of the transporters that have a high affinity for glutamate, such as the glutamate transporter-1 (GLT1) or the glutamate aspartate transporter (GLAST) (Shin et al., 2005), which could lead to impairments in glutamate buffering, contributing to the excitotoxicity and degeneration of grafted cells (Cicchetti et al., 2009).

We have previously reported that microglia specifically target neurons within the graft p-zones (Cicchetti et al., 2009; 2011). This contrasts with what we have observed here, where astrocytes are distinctly absent within the graft p-zones. As astrocytes participate in the maintenance of the BBB, it may therefore be this which is critically compromised in the p-zone of the transplanted tissue. In addition to the role of astrocytes in maintaining the BBB around blood vessels, several types of astrocytic morphologies were observed within grafts (**Figure 2-7**). A circumferential reactive layer of astrocytic process was found surrounding graft p-zones. Although reminiscent of a glial scar, this layer was highly permeable to the host projections to the grafts including dopaminergic and cortico-striatal glutamatergic fibres. Additionally, type A pericytes, typically found in reactive scars (Göritz et al., 2011) were not found in this circumferential reactive layer. This is therefore not a true scar.

Moreover, radially oriented resting astrocytes within the graft p-zones represented a unique morphology that has never been described in the context of transplantation. The presence of radially oriented glial fibres observed in these transplants in HD patients suggests that these fibres may participate in the internal organization of embryonic graft morphology in response to developmental cues from the host brain, similar to the role of radial glial fibres play in the development of the embryonic brain (Ang et al., 2003; Anthony et al., 2004; Gates et al., 1996; Sidman and Rakic, 1973). In conclusion, diminished graft survival in HD may be influenced by the presence of host atrophic astrocytes and diminished trophic support to grafts, and the relative absence of larger blood vessels and pericytes as well as an abnormal BBB in graft p-zones. The localization of many of these observations to graft p-zones specifically sits well with our previous observations that glutamate toxicity from cortico-striatal projections targets p-zones in grafts as well. These findings suggest that there are complex interactions between inflammatory cells, blood vessels, the BBB and grafts that all contribute to the poor long-term survival of these grafts. Similar interactions may also participate in the development of HD itself.

2.3.6 Funding

This work was supported by Huntington Society Canada and the International Organization of Glutaric Acidemia (IOGA) to Francesca Cicchetti and Denis Soulet. Giulia Cisbani was supported by PhD recruitment scholarship from Université Laval.

2.3.7 Acknowledgements

The authors would like to thank Mr. Gilles Chabot for artwork and the Brain Bank of the Centre de Recherche Université Laval Robert-Giffard (CRULRG), Québec, Canada for providing some of the control brains.

2.3.8 Figures

Figure 2-1. Macroscopic graft identification and patient demographics

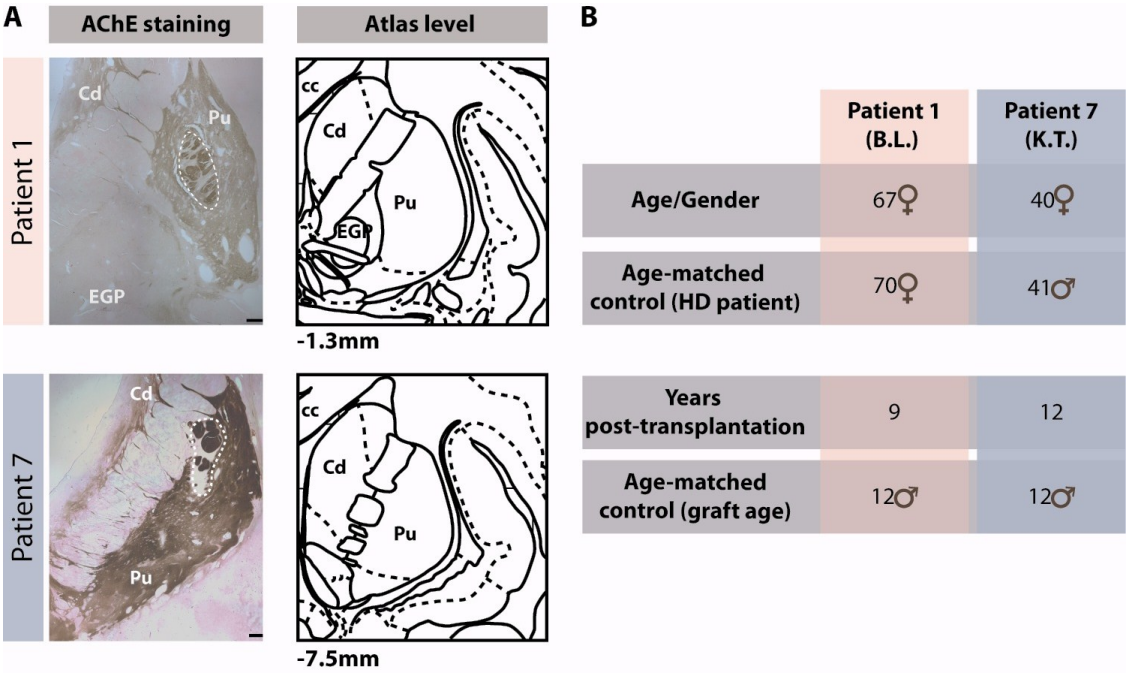

A. Macroscopic identification of the transplants based on AChE staining in two HD patients included in this study, and compared with corresponding atlas levels (Mai et al., 2004). Scale bars: 100µm. **B.** Summary table of all brains analysed in this study. cc: corpus callosum; Cd: caudate; EGP: external globus pallidus; Pu: putamen.

Figure 2-2. Quantifications of vWF-positive capillaries and α-SMA positive blood vessels

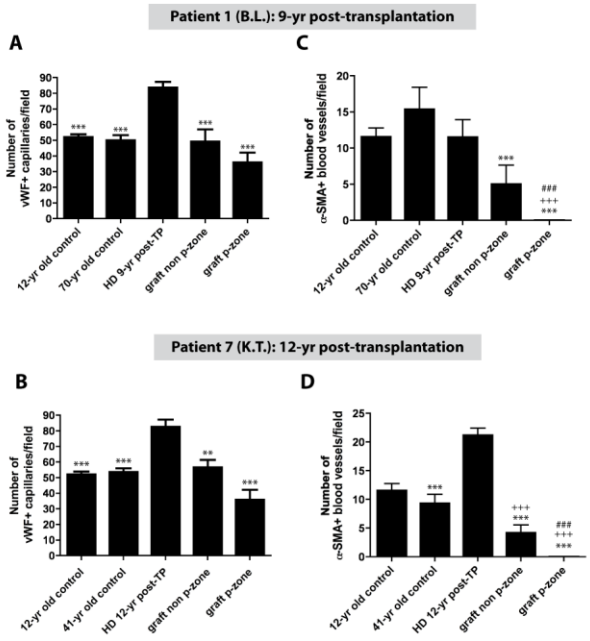

Significant differences were observed between the number of α-SMA+ (**A, B**) and vWF+ (**C, D**) vessels in the host putamen, graft p-zones and non p-zones. Data are expressed as a mean ± S.E.M. All statistical analyses were performed using the Step-down Bonferroni correction method. *** = significant difference compared to the HD transplanted brain ($p<0.001$), ** = $p<0.01$; +++ = significant difference compared to the 12-yr old control brain ($p<0.001$); ### = significant difference compared to the graft non p-zone ($p<0.001$).

Figure 2-3. Discrepancies in vascularization between grafts and host tissue

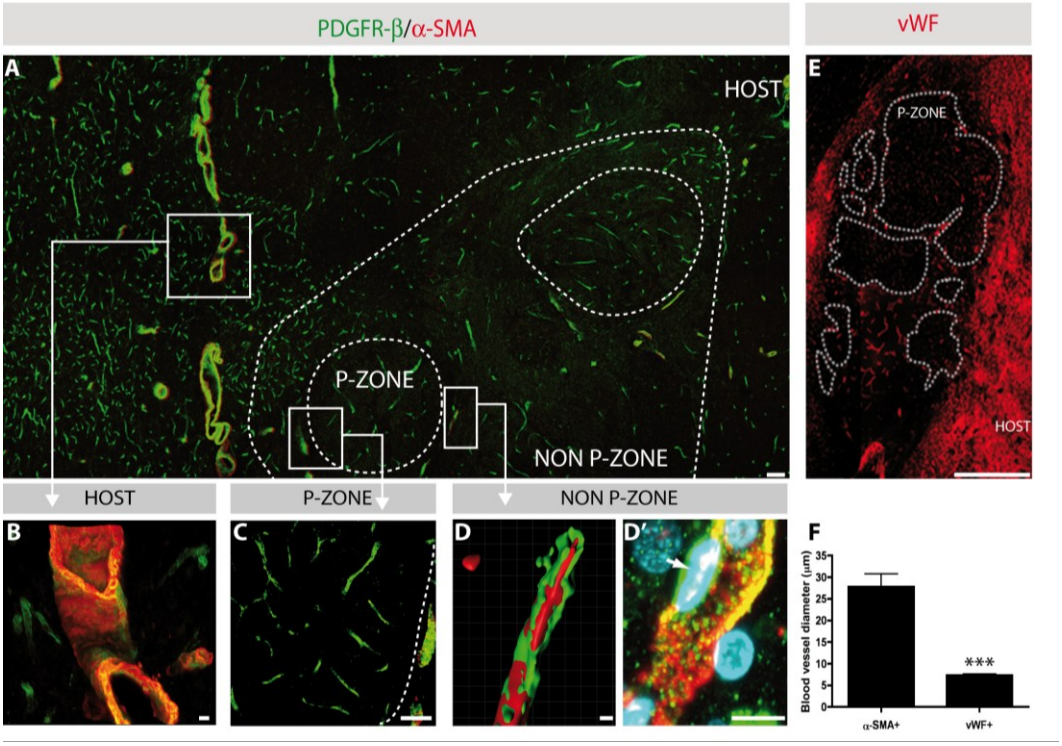

Double immunofluorescence for type A pericytes, labelled with PDGFR-β in green, and type B pericytes, labelled with PDGFR-β and α-SMA+ blood vessels in red (co-labelled in yellow) further revealed that large calibre blood vessels are not present within graft p-zones (dashed lines) (**A, C**), but are detectable in the graft non p-zones (**A, D**, **D'**) as well as in the host (**A**, **B**). Pericytes were observed in the p-zones associated with capillaries but not with large calibre α-SMA blood vessels (**C**). Various examples of blood vessels and blood-associated elements (e.g. pericytes) at higher magnification (**B-D'**). Larger calibre blood vessels, as observed in the host, stained positively for both PDGFR-β and α-SMA (**B**). Photomicrograph illustrating the exclusive presence of capillaries within a graft p-zone (**C**). 3D reconstruction, as performed by confocal microscopy, depicting the presence of pericytes (green) onto a blood vessel (red) (**D**). Higher magnification of a triple staining (PDGFR-β in green, α-SMA in red and DAPI in blue) illustrating pericytes and their relationship to a blood vessel, as visualized in a non p-zone of the grafted tissue (**D'**). Immunofluorescence for the blood glycoprotein von Willibrand Factor (vWF) revealed a significantly greater number of capillaries in the host parenchyma than in the grafted tissue (**E, also see Figs. 2C, D**). To further confirm the presence of distinct blood vessel populations, diameters were measured for 40 sampled vWF+ and α-SMA+ vessels which further revealed a significant difference (**F**). The values are expressed as a mean ± S.E.M (Student's *t*-test; *** = $p<0.001$). Scale bars **A** = 100µm; **B** = 10µm; **C** = 100µm, **D**, **D'** = 10µm; **E** = 1mm.

Figure 2-4. Quantifications of astrocytes according to number and phenotype

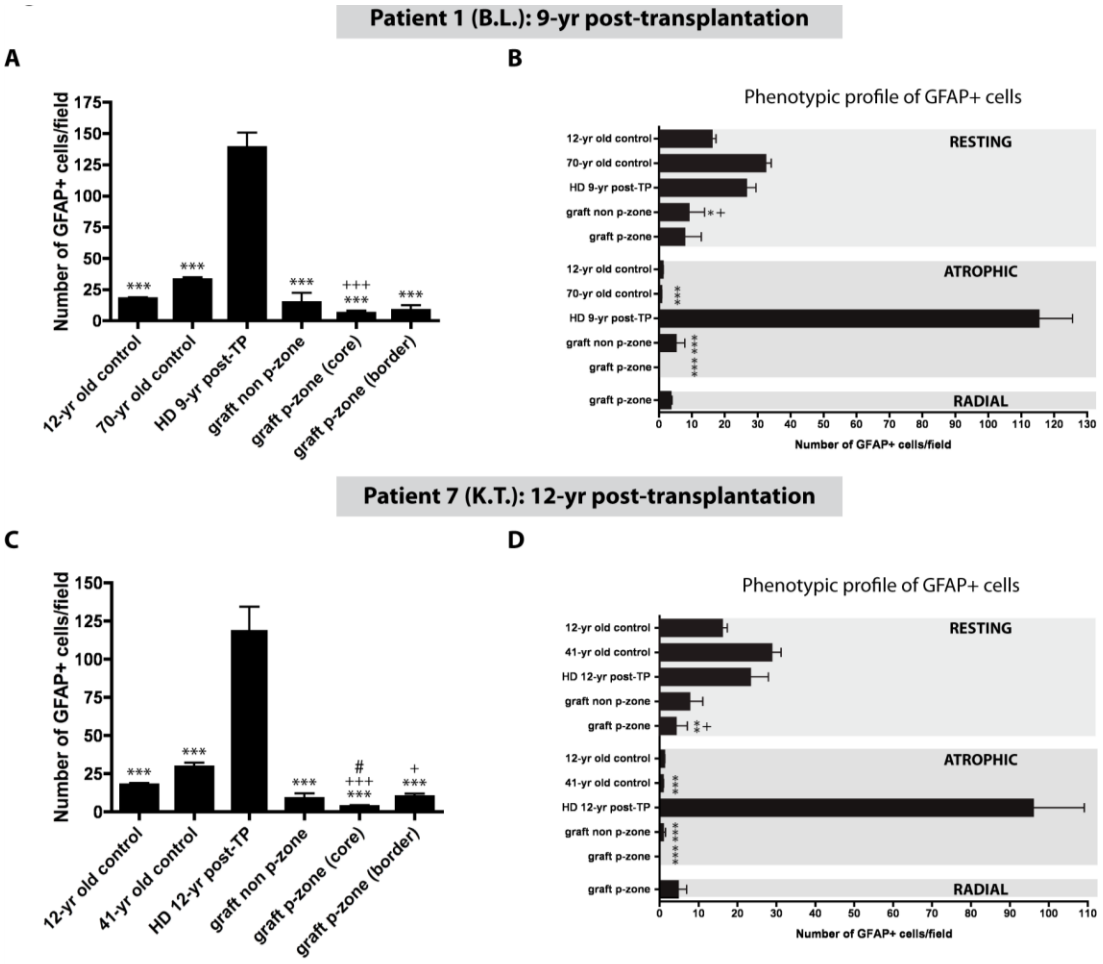

Significant differences were observed between the number of GFAP+ cells in the host putamen, graft p-zones and non p-zones (**A, C**). The subdivision of the p-zones into p-zone border and p-zone core further emphasizes the different distribution of astrocytes in the p-zones as shown in **Figure 5**. Additionally, different astrocytic morphologies (resting, atrophic and radial) were quantified according to their location within the host and graft (**B, D**). The numbers of GFAP+ cells per sampled field of view are expressed as a mean ± S.E.M. All statistical analyses were performed using the Step-down Bonferroni correction method. *** = significant difference compared to the HD transplanted brain ($p<0.001$), ** = $p<0.01$, * = $p<0.05$; +++ = significant difference compared to the 12-yr old control brain ($p<0.001$), + = $p<0.05$; # = significant difference compared to the graft p-zone border ($p<0.05$).

Figure 2-5. Astrocytic subtypes within the graft and surrounding brain

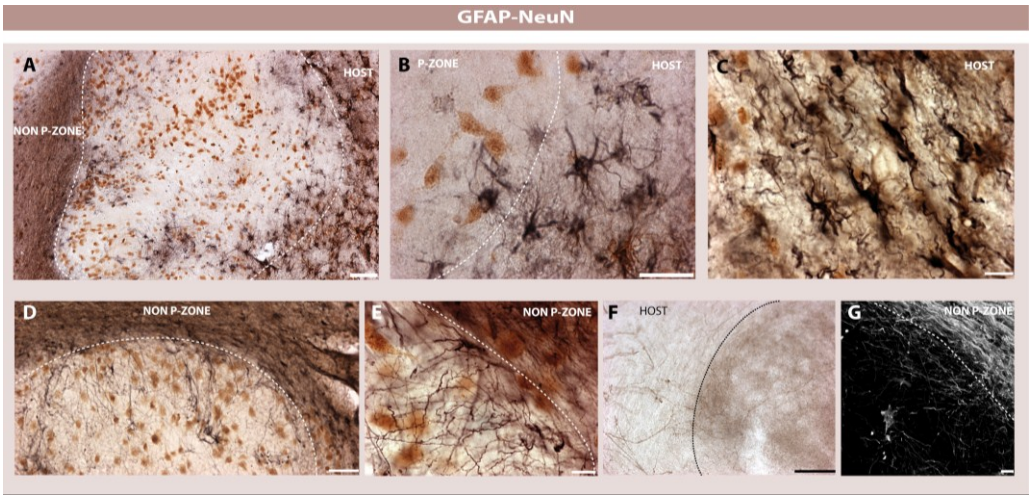

Double immunohistochemistry for neuronal elements (NeuN - revealed with the chromogen DAB in brown) and astrocytes (GFAP - revealed with nickel-intensified DAB in black) (**A-E**). Solid grafts were demarcated by an astrocytic response (**A** and **B**). Astrocytic cells, however, were rarely observed within the p-zones of the grafted tissue (**A**, **B**, **D** and **E**). When present, astrocytes projected radially within the p-zones and depicted the morphology of a resting cell (**D**, **E** and **G**) in comparison to the activated atrophic host astrocytes (**B** and **C**). The morphology of astrocytes differed according to tissue compartments of the graft and surrounding brain (**A-E**). Importantly, the circumferentially oriented astrocytes observed around the graft p-zones did not prevent the infiltration of TH fibres arguing against the presence of a glial scar (**F**). Scale bars **A, B, C** = 100µm; **D** = 100µm; **E** = 15µm; **F** = 25µm; **G** = 10µm.

Figure 2-6. Alteration of BBB components within the grafts

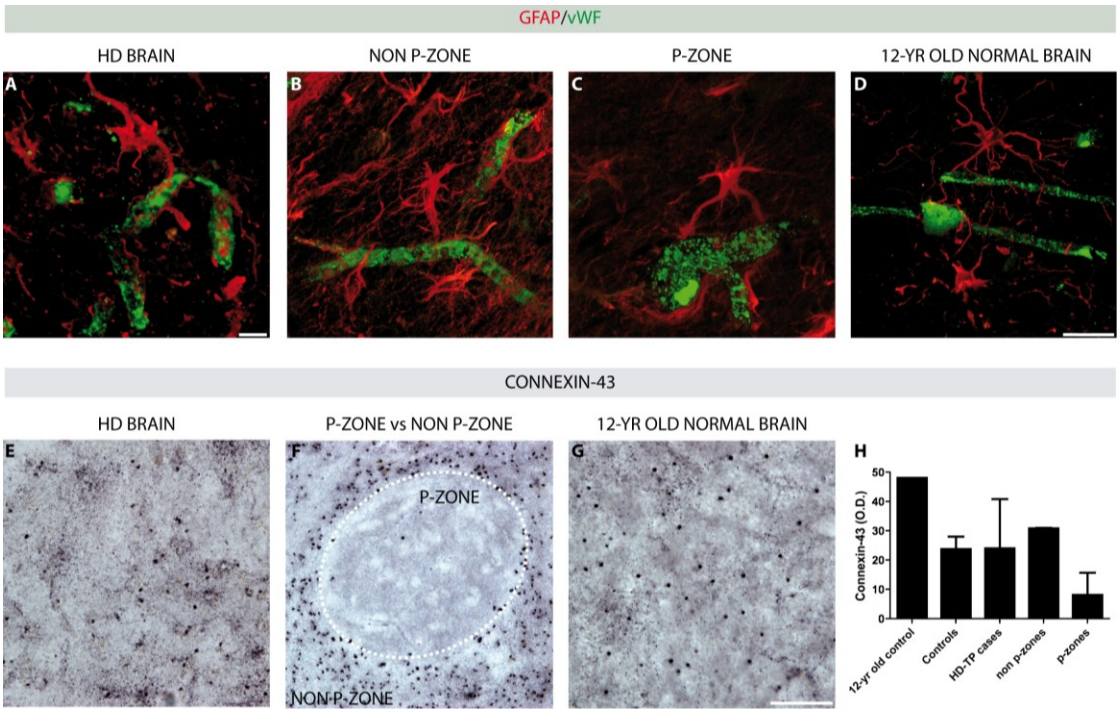

Double immunofluorescence for endothelial cells labelled with vWF in green and astrocytes, stained with GFAP in red (**A-D**). Closer examination of the relationship of astrocytes with blood vessels indicates that astrocytic end-feet are rarely apposed to blood vessels found in the p-zones of the grafted tissue (**C**), in comparison to those found in the host (**A**), the non p-zone (**B**), and the 12-yr old control brain (**D**). Immunohistochemistry for the gap junction subunit connexin-43 (revealed with nickel-intensified DAB in black) demonstrates the markedly reduced expression of gap junctions in the graft p-zone (**F, H**) in comparison to the HD brain (**E, H**), graft non p-zone (**F, H**) and putamen of the 12-yr old control brain (**G, H**). Scale bars **A**= 10 µm; **B**-**D** = 25 µm; **E**-**G** = 100µm.

Figure 2-7. Schematic of astrocytic interaction and vascularization in grafted tissue and surrounding brain

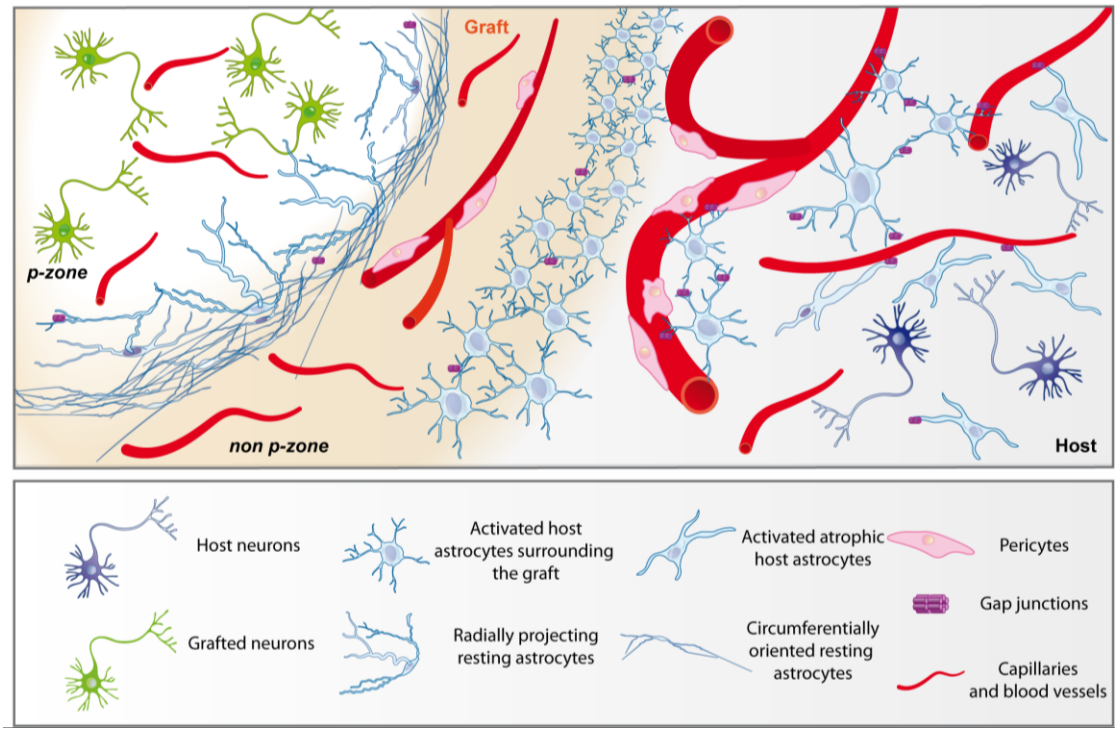

We have observed that foetal allografts in two HD patients a decade post-transplantation are characterized by the absence of critical elements of the neurovascular unit possibly contributing to poor vascularization of the transplanted cells and thus suboptimal graft survival long-term. More specifically, p-zones of the grafted tissue are not supplied by large blood vessels but strictly vascularized by capillaries. Elements associated with vasculature, such as pericytes and astrocytes, are also largely absent within the graft p-zones. In other compartments of the transplant (non p–zones) and in the host, heterogeneous astrocytic populations were identified. For example, host astrocytes were characterized by an activated atrophied morphology. Astrocytes found at the host-graft interface demonstrated an activated morphology. The border p-zone/non p-zone of the graft was demarcated by circumferentially oriented resting astrocytes. On the edge of the graft p-zone, additional radially projecting resting astrocytes were noted. However, this astrogliosis is permeable to the infiltration of TH fibres originating from the host as well as to cortical connection via vGlut1 (Cicchetti et al., 2009; 2011). The absence of astrocytes within the graft is also accompanied by the lack of connexin-43, a subunit of gap junctions.

Table 2-1. List of primary and secondary antibodies

Primary antibody	Company	Catalog number	Dilution
Mouse Cy3 conjugated α-SMA	Sigma	C6198	1:200
Rabbit Connexin- 43	Invitrogen	71-0700	1:100
Mouse GFAP	Sigma	G3893	1:500
Rabbit GFAP	Dako	Z0334	1:500
Mouse Neuronal nuclei	Millipore	MAB377	1:2500
Rabbit PDGFR-β	AbCam	Ab32570	1:100
Rabbit TH	Pel-Freez	P40101	1:2500
Rabbit vWF	Millipore	AB7356	1:500
Secondary antibody	**Company**	**Catalog number**	**Dilution**
Alexa 488 goat anti-mouse	Invitrogen	A11029	1:500
Alexa 633 goat anti-mouse	Invitrogen	A21052	1:500
Alexa 488 goat anti-rabbit	Invitrogen	A11034	1:500
Alexa 546 goat anti-rabbit	Invitrogen	A11035	1:500
Alexa 633 goat anti-rabbit	Invitrogen	A21071	1:500

CHAPTER III

3.1 Contributions

In parallel to the analyses on the human post-mortem brain tissue, we conducted a study in a transgenic mouse model of HD to explore whether the methodology of dissection and tissue preparation may play a role in graft survival. More specifically, we evaluated the survival of the grafts and their revascularization. This study was designed to complement and support the observations made in the human brain (**Chapter II**).

As first author, I performed the transplantation in mice, with Dr. Cicchetti and Martine Saint-Pierre. Dr. Cicchetti also performed the dissection of the foetal tissue. I performed the post-mortem analyses, the image acquisition and all the quantification presented in the article. I also participated to the conception of the project and the writing of the initial version of the article which was finalized by Dr. Cicchetti.

3.2 Résumé

Les thérapies de remplacement cellulaire ont généré des bénéfices variables et de court durée chez les patients souffrant de la maladie d'Huntington. Cet échec est vraisemblablement due au fait que la survie des greffes à long-terme est compromise, car elles sont fort possiblement assujetties à une réponse microgliale inflammatoire de l'hôte, un manque de support trophique adéquat et possiblement à une excitotoxicité véhiculée par des projections corticales glutamatergiques aberrantes. Par contre, la dégénérescence des greffes pourrait aussi être reliée à un problème plus pratique/concret telle la méthodologie de la préparation des cellules greffées (greffes de tissu entier vs. suspension de cellules). Effectivement, nous avons récemment rapporté que les greffes de tissu entier étaient faiblement revascularisées chez les patients huntingtoniens transplantés 9 et 12 ans auparavant. Afin d'évaluer si des problèmes méthodologiques reliés à la préparation cellulaire pouvaient en effet avoir un impact sur la viabilité des greffes, nous avons implanté des suspensions de cellules neuronales striatales provenant de fétus GFP+ dans le striatum de souris YAC128 HD. L'évaluation *post mortem* a permis de constater que la survie de greffes dans les souris YAC128 est comparable aux souris contrôles sauvages à 1 et 3 mois post-transplantation. De plus, le degré de revascularisation dans les souris YAC128 et les souris contrôles sauvages était similaire, avec des capillaires et des vaisseaux sanguins de large calibre observables dans le tissu greffé. Également, les cellules GFP+ interagissaient bien avec les vaisseaux sanguins de l'hôte, indiquant l'intégration des cellules donneuses à l'intérieur du cerveau receveur. Ces observations, combinées à nos données récentes quant à la faible revascularisation des greffes de tissu entier chez les patients huntingtoniens transplantés, suggèrent que le succès de la transplantation cellulaire peut être amélioré par l'optimisation des aspects méthodologiques reliés à la préparation cellulaire.

3.3 Single cell suspension methodology favours survival and vascularization of foetal striatal grafts in the YAC128 mouse model of Huntington's disease

[1]Cisbani G, [1]Saint-Pierre M, [1,2]Cicchetti F

[1]Centre de Recherche du CHU de Québec (CHUL), 2705 Boulevard Laurier, Québec, QC, Canada, G1V 4G2; [2]Département de Psychiatrie et Neurosciences, Université Laval, Québec, QC, Canada, G1K 7P4

Correspondence
Francesca Cicchetti, PhD
Centre de Recherche du CHU de Québec (CHUL)
Axe Neurosciences, T2-50
2705, Boulevard Laurier
Québec, QC, Canada, G1V 4G2
Tel: (418) 656-4141 ext. 48853
Fax: (418) 654-2753
E-mail: francesca.cicchetti@crchul.ulaval.ca

3.3.1 Abstract

Cell replacement therapies have yielded variable and short-lived benefits in HD patients. This suboptimal outcome is likely due to the fact that graft survival is compromised long-term because they are subjected to a host inflammatory microglial response, a lack of adequate trophic support and possibly subjected to cortical excitotoxicity. However, graft demise may also relate to more straightforward issues such as cell preparation methodology (solid grafts vs. cell suspension). Indeed, we recently reported that solid grafts are poorly revascularized in HD patients transplanted 9 and 12 years previously. To evaluate whether methodological issues relating to cell preparation may impact on graft viability, we implanted GFP+ single cell suspensions of foetal striatal neuronal cells into the striatum of YAC128 HD mice. Post-mortem evaluation yielded comparable graft survival in YAC128 mice and their wild type littermates at 1 and 3 months post-transplantation. Additionally, the degree of graft revascularization in the YAC128 and wild type mice was similar, with both capillaries and large calibre vessels observable within the grafted tissue. Furthermore, GFP+ cells interacted well with host blood vessels indicating integration of the donor cells within the recipient brain. These observations, combined with our recent report of poor revascularization of solid grafts in the HD transplanted patients, suggest that the success of cell transplantation can be improved by optimizing methodological aspects relating to cell preparation.

Running title: Survival and vascularization of cell suspension grafts in YAC128 mice

Key words

Huntington's disease, YAC128 mouse model, single-cell suspension grafts, vasculature

3.3.2 Introduction

Huntington's disease (HD) is an autosomal dominant neurodegenerative disorder of the central nervous system (CNS) that is defined by a CAG expansion in exon 1 of the huntingtin gene leading to the production of the mutant huntingtin (mHtt) protein. There is no disease modifying treatment for HD and current clinical interventions are limited to symptom management (Phillips et al., 2008). The development of new therapeutic strategies is thus actively pursued and a number of open label trials have already been conducted to test the feasibility and efficacy of cell replacement approaches in the context of HD. These trials were predicated on the grounds that the major pathology in HD involves the striatum, and thus replacing it with unaffected foetal striatal tissue would be beneficial, as shown experimentally (Deckel et al., 1983; Isacson et al., 1984; Pritzel et al., 1986). However, transplanted HD patients have demonstrated only marginal and short-lived clinical improvements (Cicchetti et al., 2009; 2011; Cisbani, Freeman, et al., 2013).

The reasons for these suboptimal clinical outcomes are not entirely clear but in a unique series of post-mortem analyses of the brains of HD transplanted patients who have come to autopsy, we have observed that graft survival is compromised long-term. The mechanisms underlying this poor graft survival may be numerous, including an important inflammatory microglial response, the lack of adequate trophic support as well as graft demise via cortical excitotoxicity (Cicchetti et al., 2009; 2011; Freeman et al., 2011). However, more easily modifiable technical issues relating to cell preparation, for example the use of solid vs. single cell suspension approaches, have shown diverse outcomes in the revascularization of transplanted neural tissue, a critical factor in long-term graft integration and survival (Freeman et al., 2011). For example, solid grafts show delayed neovascularization, as observed in the parenchyma of both wild type mice (Broadwell et al., 1990; Krum and Rosenstein, 1987) and 6-hydroxydopamine (6-OHDA) lesioned rats (Leigh et al., 1994). Despite the fact that blood vessels of the recipient brain are mitotically active, they rarely penetrate the donor tissue (Broadwell et al., 1990; Krum and Rosenstein, 1987). However, cells placed in an enriched-vascular environment, such as the choroid plexus, survive better than those implanted into the parenchyma (Stenevi et al., 1976).

We have similarly reported significant vasculature disparities between the host brain and solid tissue grafts in HD transplanted patients (Cisbani, Freeman, et al., 2013). In these cases, solid tissue grafts had a vascular network that was much less developed than that of the host brain. While capillaries were observable within the transplants, they were not as frequently encountered as in the host and large calibre blood vessels were almost entirely absent in the transplanted tissue, another important difference with the host brain (Cisbani, Freeman, et al., 2013). We suspect that the compromised revasculature of the solid striatal tissue transplants in HD patients may have further contributed to poor

graft survival long-term. Based on these observations (Cicchetti et al., 2009; Cisbani, Freeman, et al., 2013), we undertook this *in vivo* study in the murine YAC128 model of HD to specifically address whether single cell suspension would favour graft survival and vascularization in the HD diseased brain.

3.3.3 Material and methods

3.3.3.1 Cell preparation

Pregnant hemizygous female mice genetically engineered to express the Green Fluorescent Protein $(GFP)^{+/-}$ (C57BL/6-Tg(ACTB-EGFP)1Osb/J)) (Michaud et al., 2012) (kindly provided by Dr. Serge Rivest from Laval University, Québec, Canada) were subjected to a sub-lethal dose of a ketamine (100mg/mL)/xylazine (1mg/mL) (Vetalar, Bioniche, Belleville, ON/Rompun, Bayer, Toronto, ON) mix at gestational day 13.5. Fetuses were retrieved and placed in sterile ice-cold solution of 20mM glucose (Sigma, Oakville, ON) in Hanks' balanced salt solution (HBSS) 1X (Invitrogen, Burlington, ON). The GFP+ phenotype of each embryo was confirmed using Ultraviolet (UV) lamp illumination. The use of GFP+ tissue allowed for the easy tracking of transplanted cells within the host brain. The lateral ganglionic eminence (LGE), which largely yields foetal cells committed to a striatal phenotype, was dissected and kept in HBSS-glucose solution on ice. The HBSS solution was subsequently replaced by a solution of 0.2% trypsin (Sigma, Oakville, ON) and 0.5mM Ethylenediaminetetraacetic acid (EDTA) (Sigma, Oakville, ON) in HBSS-glucose and incubated for 20 min in a 37ºC water bath to allow enzymatic digestion of the tissue. 0.5ml of 0.2% DNase (Sigma, Oakville, ON) in HBSS-glucose was added, followed by three additional washes of 0.2% DNase. The solution was triturated using a series of fire polished Pasteur pipets of decreasing diameters in order to obtain a single, or near single, cell suspension. Cell viability was assessed using the Trypan Blue (Sigma, Oakville, ON) exclusion assay. The cell suspension was diluted to obtain a concentration of approximately 100,000 cells/µl (Björklund et al., 1983; Holm et al., 2001) (**Figure 3-1A**).

3.3.3.2 Animal model and transplantation procedure

A total of 36 transgenic HD male mice of the YAC128 line and 36 wild-type littermates were purchased from Jackson Laboratories (Bar Harbor, ME) at 2 months of age. They were housed one per cage under standard conditions with free access to food and water, randomized and handled by one investigator. Genotype was confirmed for all mice in the study. Mice were transplanted with GFP+ cell suspensions at 8 months of age - time at which they are reported to be symptomatic (Van Raamsdonk,

Pearson, et al., 2005) - and were sacrificed at 1 or 3 months post-transplantation (total of n=18 mice per experimental group) (**Figure 3-1A**).

To perform intracranial cell implantation, mice were anesthetized with 1.5% isoflurane (Abbott, Saint-Laurent, CA) in 100% oxygen at a rate of 2ml/min and placed in a stereotaxic frame (Kopf Instruments, Tujunga, CA). They received bilateral striatal injection of 1µl of the cell suspension (100,000 cells/µl) per side over a 2 min period using a Hamilton Syringe and a 26-gauge needle (ThermoFisher Scientific, Ottawa, ON). The following striatal coordinates were used: 1) AP +0.5 mm, ML -1.8 mm and DV -3.5 mm; 2) AP +0.5 mm, ML +1.8 mm and DV -3.5 mm (Paxinos and Franklin, 2008). At the completion of cell inoculation, the needle was left in position for 3 min and then slowly removed. The cranial skin was closed using silk 4.0 sutures (Ethicon, Norwalk, CT). Mice were removed from the stereotactic apparatus and put back in their home cage for recovery. They received 0.5ml/day of NaCl 0.9% (Hospira, Montreal, CA) for rehydration and 0.1ml/12 h of buprenorphine (Vetergesic, CDMV, Québec, CA) to reduce pain on the day of surgery and for three subsequent days. All mice were monitored daily for weight loss and general health. All experiments were performed in accordance with the Canadian Guide for the Care and Use of Laboratory animals and all procedures were approved by the Institutional Policy of the Centre Hospitalier de l'Université Laval (CHUL).

3.3.3.3 Post-mortem histological evaluation

At the completion of the experimental protocol, mice were sacrificed by intracardiac perfusion of saline (0.9%) followed by 4% paraformaldehyde (PFA) (Sigma, Oakville, ON), pH 7.4. Brains were collected and post-fixed in the same PFA solution for 6 h and transferred in 20% sucrose (Sigma, Oakville, ON) made in phosphate buffer saline (PBS) (Sigma, Oakville, ON) 0.1M, pH 7.4, for cryoprotection. Coronal sections of 25µm thickness were collected using a freezing microtome (Leica Microsystem, Montreal, Canada), placed in anti-freeze solution (sodium phosphate monobasic 0.2 M, pH 7.3 (Sigma, Oakville, ON); sodium phosphate dibasic 0.2 M, pH 7.3 (Sigma, Oakville, ON); ethylene glycol 30% (Sigma, Oakville, ON); and glycerol 20% (Sigma, Oakville, ON) and stored at -20°C until use.

3.3.3.4 Immunofluorescence

Sections were washed three times in potassium phosphate buffer saline (KPBS) (Sigma, Oakville, ON) 0.1M pH 7.4. The sections stained for GFP were directly incubated in a blocking solution after the initial washes, while sections double stained for GFP and laminin were incubated with proteinase K (Roche Diagnostic, Laval, CA) diluted in a 0.1M Tris (Sigma, Oakville, ON) and 0.5M EDTA (Sigma, Oakville,

ON) buffer diluted in water, at 37°C for 20 min. Sections were cooled down at room temperature (RT), further washed in KPBS and pre-incubated in a blocking solution containing 0.1% bovine serum albumin (BSA, Bioshop, Burlington, ON), 0.04% Triton X-100 (Sigma, Oakville, ON), 4% normal goat serum (NGS, Wisent Inc., St-Jean-Baptiste de Rouville, Qc) in KPBS for 30 min. Sections were next washed with KPBS and incubated overnight at 4ºC in a blocking solution containing the primary antibody anti-GFP (mouse anti-GFP, Invitrogen, 1:1000) alone or in combination with anti-laminin (rabbit anti-laminin, DAKO, 1:1000). After KPBS washes (3 x 10 min), sections were incubated with appropriate secondary antibodies in a blocking solution for 90 min at RT. After an additional three washes, sections were incubated in KPBS containing 0.022% DAPI (2mg/ml, Molecular Probes, Eugene, OR), washed and mounted on Superfrost slides (Fisher Scientific, Ottawa, ON), coverslipped with Fluoromount-G (SouthernBiotech, Birmingham, AL) and sealed with nail polish. Photomicrographs were acquired using Simple PCI version 5.0 (Hamamatsu, Sewickley, PA) software linked to a Nikon eclipse 90i microscope (Nikon Instruments, Toronto, ON). Confocal laser scanning microscopy was performed using an Olympus FV500 confocal laser-scanning microscope (Olympus America Inc., Melville, USA). Images were acquired by sequential scanning and optimized by a two-frame Kalman filter and analysed using acquisition software from Olympus (Fluoview SV500 imaging software 4.3, Olympus America Inc., Melville, USA). All images were prepared for illustration using Adobe Photoshop CS5 and Adobe Illustrator CS5.

3.3.3.5 Assessment of graft survival

All volumetric quantifications were performed by 3 Dimensional (3D) graft reconstruction using GFP-immunofluorescence stained striatal sections. The contours of the grafts as well as the striatum were delineated using the Tracing Contours option in StereoInvestigator (Microbrightfield) operated on a E800 Nikon microscope (Nikon Instruments, Toronto, ON), imported into the software NeuroExplorer (Microbrightfield) and aligned for 3D reconstructions. After delineating the grafts at low magnification (4X objective), GFP+ cells were further stereologically counted using the optical fractionator method at higher magnification (20X objective). In cases of graft misplacement (observed outside the anatomical borders of the striatum), the mouse was discarded from further analyses.

3.3.3.6 Blood vessel measurement and quantification

Diameter measurements as well as quantification of the number of laminin+ blood vessels were performed using 20X magnification images collected with the software Simple PCI version 5.0 linked to

a Nikon eclipse 90i microscope. The diameters of laminin positive vessels were measured from 40 sampled vessels and are expressed as mean ± S.E.M (Cisbani, Freeman, et al., 2013). The number of blood vessels was calculated in each sampled field of equal area using the standardized method of ImageJ for particle analysis (Cisbani, Freeman, et al., 2013). The results are reported as a number of blood vessels per field of view and expressed as mean ± S.E.M.

3.3.3.7 Statistical analyses

A two-way ANOVA was used to compare both graft viability and vasculature in YAC128 and wild type mice at 1 and 3 months post-transplantation. For the total number of GFP+ cells and total graft area analyses, a different variance was estimated for each of the four groups in order to meet the model assumptions. Step-down Bonferonni correction was used for multiple comparison tests and the level of statistical significance was set at $p < 0.05$. Data are expressed as group mean ± SEM. Statistical analyses were performed using the MIXED procedure of SAS (version 9.2, SAS: Cary, North Carolina) and PRISM 4 (Graphpad Software, San Diego, CA).

3.3.4 Results

3.3.4.1 Cell suspension grafts survive well in the YAC128 HD mouse model

All animals in this study were closely monitored throughout the 11-month period of the experimental protocol. YAC128 and wild type mice, transplanted at 8 months of age, recovered well from the grafting procedure as evidenced by progressive weight gain and the absence of any health-related issues (**Figure 3-1B**). Furthermore, the weight gain observed in the YAC128 mice was significantly greater than the wild type controls ($p<0.05$). Similar weight gains have previously been reported in YAC128 mice and have been suggested to be due to levels of full-length Htt and plasma insulin-like growth factor (IGF-1) (Pouladi et al., 2010) (**Figure 3-1B**). At post-mortem, GFP enhanced immunofluorescence staining was performed to confirm graft location. In both YAC128 and non-carriers, GFP+ cell suspension grafts could be identified throughout the rostro-caudal extent of the striatum. A series of quantitative analyses were subsequently performed to determine the extent of graft survival which included calculation of the total number of surviving GFP+ transplanted cells (**Figure 3-1D**), the total graft area (**Figure 3-1E**), the area of the largest transplant found in a single animal (**Figure 3-1F**) and the total graft volume (**Figure 3-1G**). None of these quantifications revealed a significant difference between survival of grafted cells, surface areas nor graft volumes at the time

points evaluated, further suggesting that the evolution of pathology, observed in the YAC128 mice between 8 and 11 months of age, does not significantly impact on the survival of cell suspension grafts.

3.3.4.2 Cell suspension grafts are well vascularized in the YAC128 HD mouse model

We further evaluated whether the methodological transplantation approach of cell suspension grafts would yield adequate vascularization of transplanted cells by the host. Grafts were stained with GFP and blood vessels with laminin, a marker of the basement membrane. Confocal imaging microscopy revealed similar patterns of vascularization of grafted tissue in YAC128 mice and non-carriers, at the two time points studied (**Figure 3-2A, B and C**). In the YAC128 and wild type mice, cell suspension grafts were clearly vascularized by both capillaries and larger calibre blood vessels (**Figure 3-2C**). Importantly, the absence of co-localization of laminin and GFP suggest that the vascular network of the transplanted tissue derived exclusively from the host (**Figures 3-2A, A', A'' and 3-2B, B', B''**). Confocal microscopy further revealed interactions between grafted cells and blood vessels of the host in both YAC128 and non-carrier mice (**Figure 3-2A''' and B'''**).

3.3.5 Discussion

This study was designed to specifically address whether single cell suspension methodology favoured graft survival and vascularization in the context of HD-like pathology. We transplanted dissociated E13.5 LGE cells derived from GFP+ embryos into 8-month old YAC128 and non-carrier mice and performed post-mortem analyses at 1 and 3 months following grafting. In this short communication, we report that similar graft viability and vascularization patterns were observable in both the YAC128 and non-carrier mice. Contrary to our recent observations of poor vascularization of solid foetal striatal allografts in HD patients (Cisbani, Freeman, et al., 2013), single cell suspensions in YAC128 and wild type mice were characterized by a blood network composed of both capillaries and large calibre blood vessels. Furthermore, grafts survived well at 1 and 3 months post-transplantation despite the pathological environment encountered in the YAC128 brain. These results suggest that methodological aspects relating to cell preparation may impact graft survival and therefore the outcome of cell replacement therapy.

Studies investigating the efficacy of neural cell transplantation in transgenic animal models of HD are scarce. We have itemized only 6 publications, which have reported on the survival and efficacy of cell transplantation in *in vivo* HD transgenic mouse models (see **Table 3-1** for summary). These studies

were performed in R6/2 (Dunnett et al., 1998; El-Akabawy et al., 2012; Lee et al., 2009; Y.-T. Lin et al., 2011), YAC128 (Im et al., 2010) and N171-82Q (Snyder et al., 2010) mice and evaluated the efficacy of a variety of cell types including embryonic neuronal cells (Dunnett et al., 1998), adipose stem cells (Im et al., 2010; Lee et al., 2009), mesenchymal stem cells (Y.-T. Lin et al., 2011; Snyder et al., 2010) and more recently human neuronal stem cells (El-Akabawy et al., 2012) (**Table 3-1**). Overall, these studies demonstrated that transplanted cells increased striatal volume and endogenous cell proliferation, likely via heightened trophic support. Our findings are very similar to those reported in the R6/2 mice by Dunnett *et al*. (Dunnett et al., 1998). In their study, the authors demonstrated that intracerebral engraftment of striatal foetal cell suspension in the R6/2 mouse, which expresses the truncated *mHtt* gene, yields similar survival to that seen in control animals (Dunnett et al., 1998). However, their effects on motor behaviour are modest and not observable on disease progression. For the purpose of our study, we chose to utilize the HD YAC128 murine model which was generated to express the full-length *mHtt* gene (Slow et al., 2003). The YAC128 model recapitulates several HD-like features including behavioural and cognitive deficits, selective striatal cell loss, as well as nuclear aggregates, the characteristic neuropathological hallmark of the disease (Slow et al., 2003; Van Raamsdonk, Murphy, et al., 2005). Compared to the R6/2 mouse, the YAC128 presents a more progressive development of pathological features, providing a longer time frame to investigate graft viability and events such as graft vascularization (Crook and Housman, 2011; Slow et al., 2003). We observed similar graft viability in the YAC128 transgenic mice and control littermates at both 1 and 3 months post-transplantation, as previously reported in the R6/2 model (Dunnett et al., 1998). The percentage of grafted surviving cells ranged between 7-8%, which is also similar to previous reports (Sortwell, 2003; Terpstra et al., 2007).

In a recent publication, we have shown limited revascularization of solid tissue grafts in HD patients a decade post-transplantation (Cisbani, Freeman, et al., 2013). The transplants were vascularized by capillaries but not larger blood vessels. Similar results were observed 18 months post-surgery in a Parkinson's disease individual who also received solid foetal tissue transplant (Kordower et al., 1996). Adequate vascular development between the host and donor tissue is essential to graft viability and prevention of ischemic damage (Krum and Rosenstein, 1987; Lindsay and Raisman, 1984) and can have significant implications on overall functional and structural graft integration (Wiegand and Gash, 1988) (**Table 3-2**). Transplants that are rapidly revascularized by the host have indeed a higher survival rate (Krum and Rosenstein, 1987; Lindsay and Raisman, 1984). However, graft reperfusion can be affected by various factors such as graft size (Nikkhah et al., 1994) and techniques of cell preparation (cell suspension vs. solid tissue grafts) (Broadwell et al., 1991). Solid tissue grafts transplanted directly into the parenchyma, have a less rich-vascular environment, and so have poorer survival and

functionality. For example, solid tissue transplants implanted into 6-OHDA lesioned striata require a longer time to develop functional neuronal contacts from the grafted neurons and generate motor improvements when compared to cell suspension grafts (Björklund, Schmidt, et al., 1980). Generally, solid grafts are more slowly revascularized. At 24 hours post-transplantation, there is no integration between the host and the solid tissue transplant vasculature, as observed in PVG rats transplanted with hippocampal tissue (Lawrence et al., 1984). One week post-surgery, marginal vessels start to penetrate the transplant and only by one month following the implantation are the grafts revascularized and depict a vascular organization similar to the host (Lawrence et al., 1984; Scott, 1984). Human neuronal tissue engrafted into the kainic acid-lesioned striatum of rats has demonstrated even greater delayed revascularization. In this particular study, the presence of capillaries was detected only 2 months post-transplantation and revascularization at 3 months post-surgery (Geny et al., 1994). However, endothelial cells originating from the grafts interacted with the host to form blood vessel chimeras and functional revascularization (Baker-Cairns et al., 1996; Lindsay and Raisman, 1984; Wiegand and Gash, 1988).

The connection between host and graft blood networks predominantly takes place at the border of the transplanted tissue and rarely infiltrates the core of the grafts, despite the fact that host blood vessels are mitotically active (Krum and Rosenstein, 1987; Leigh et al., 1994). The method of cell suspension was in fact developed to improve survival and integration of the transplanted cells (Björklund, Schmidt, et al., 1980). However, mechanical trituration, required to prepare cell suspension grafts, compromises the intrinsic vasculature of the dissected tissue (Baker-Cairns et al., 1996). Contrary to solid grafts which maintain their own angioarchitecture but are characterized by sparse blood vessels from the donor (Akalan and Grady, 1994; Baker-Cairns et al., 1996), cell suspension revascularize more rapidly and rely exclusively on the host vasculature and angiogenic process (Baker-Cairns et al., 1996; Broadwell et al., 1991). One study has demonstrated that Nimodipine, a pharmacological approach to promote angiogenesis, can ameliorate the vascular supply and survival of neural grafts in 6-OHDA lesioned mice (Finger and Dunnett, 1989), demonstrating the importance of proper graft revascularization and the possibility to pharmacologically ameliorate the outcome of graft vasculature.

Our findings, combined to our recent observations in transplanted HD patients, support the idea that graft survival may be improved by optimizing methodological aspects of tissue preparation and vascularization.

3.3.6 Acknowledgements

This work was supported by Huntington Society Canada and the International Organization of Glutaric Acidemia (IOGA) to Francesca Cicchetti. Giulia Cisbani was supported by PhD recruitment scholarship from Université Laval. The authors wish to thank Mr. Gilles Chabot for artwork.

3.3.7 Conflict of interests

The authors declare no conflicts of interest.

3.3.8 Figures

Figure 3-1. Comparable graft survival in YAC128 and wild type littermates

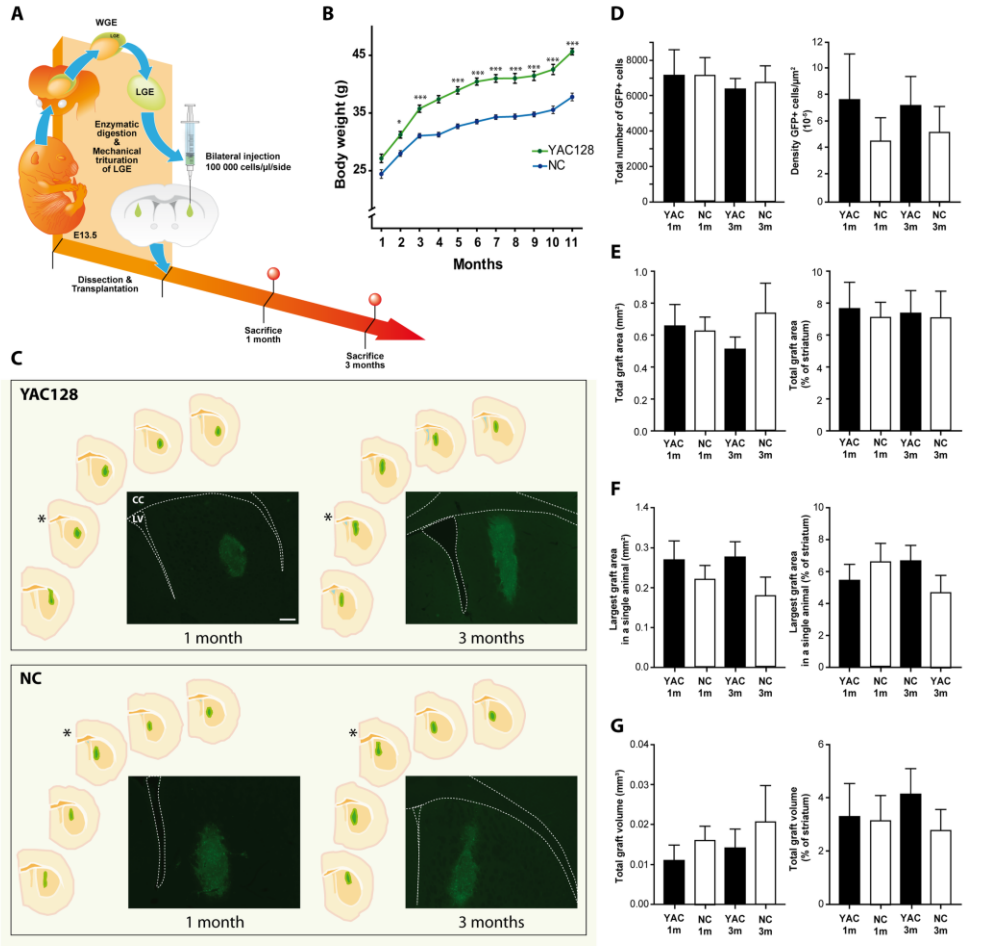

A. 8-month old YAC128 and wild type littermates were sacrificed 1 and 3 months following transplantation of E13.5 GFP+ foetal striatal cell suspensions. **B.** Body weight was monitored for the entire duration of the study (11 months) and neither the YAC128 nor the wild type mice suffered weight loss following the transplantation procedure. In fact, the YAC128 mice demonstrated a greater weight gain than the control animals ($p<0.005$), as previously reported in these animals (Pouladi et al., 2010). **C.** Representative examples of GFP+ grafts, as observed throughout the rostro-caudal extent of the striatum in YAC128 mice and non-carriers at 1 and 3 months post-transplantation. The asterisk next to the schematic drawing of the striatum indicates the location of the transplant for which the photomicrograph has been provided. **D-G.** Plots of the total number of GFP+ surviving cells (**D**), graft area (both total graft area (**E**) and area of the largest graft identified in a single animal (**F**)) as well as the total graft volume (**G**). None of these analyses yielded a significant difference in the extent of graft survival in YAC128 and wild type mice at either 1 or 3 months post-transplantation, indicating that single cell suspensions favour graft viability and that the HD-like diseased environment of the YAC128 mouse model does not impact on graft viability at these time points**.** Scale bar **C**=100µm**.** Abbreviations: WGE: whole ganglionic eminence; LGE: lateral ganglionic eminence; CC: corpus callosum; LV: lateral ventricle; MO: months.

Figure 3-2. Comparable graft vascularization in YAC128 and non-carrier littermates

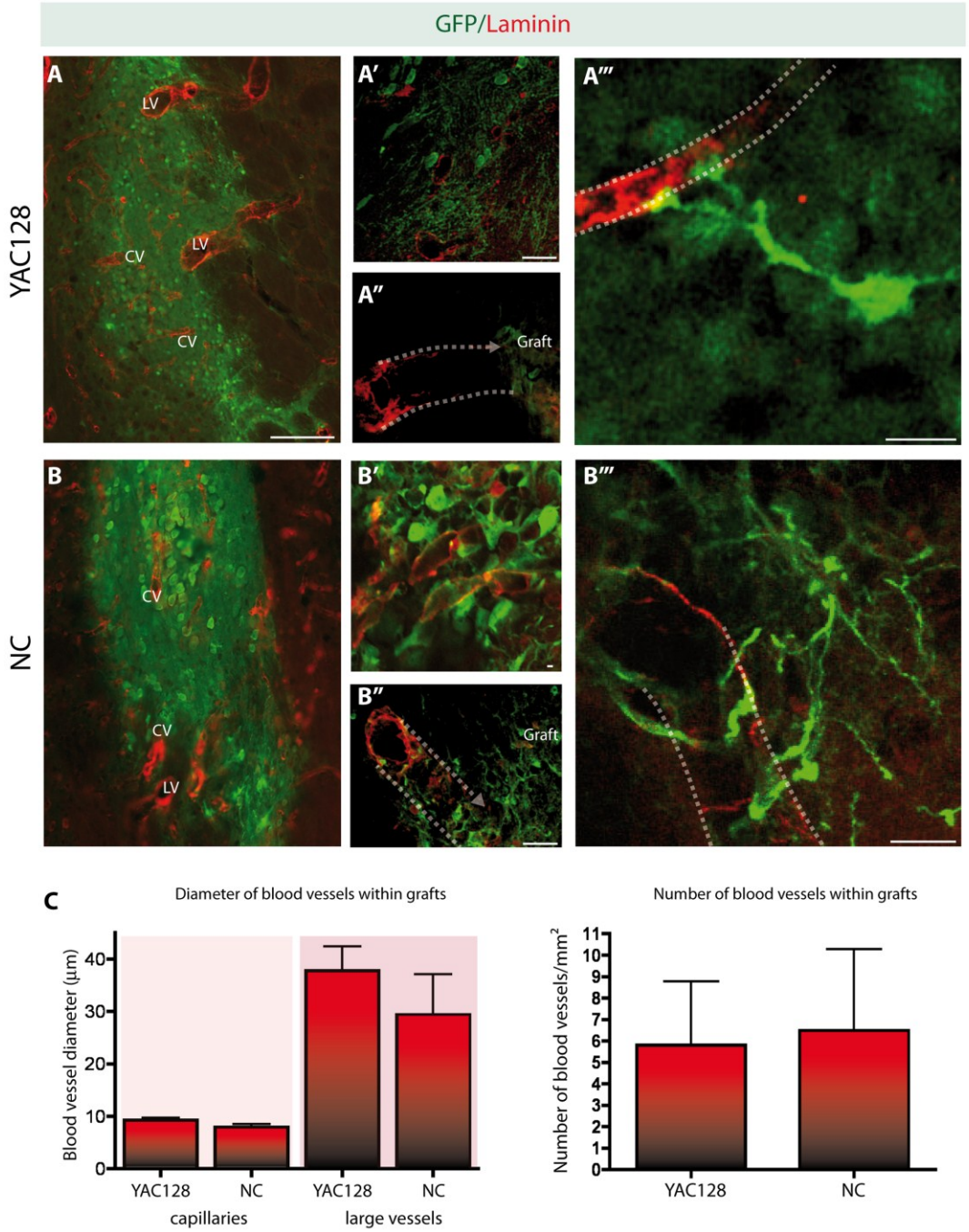

(**A-B**) Single-cell suspension grafts showed similar patterns of vascularization in both the YAC128 and wild type mice. Host blood vessels, identifiable as laminin+ but GFP negative (green) blood vessels, were as frequently encountered in the transplants of the YAC128 than in the wild type mice. The vascularization pattern was similar regardless of the time points evaluated. Both capillaries (diameter size ranging between 6µm and 13µm) and large calibre blood vessels (ranging between 20µm and 45µm) were observed within the transplanted tissue (**A-B**). **(A'' and B")** Confocal images of GFP negative host blood vessels revascularizing the grafts. Dotted lines have been added to indicate the direction of the blood vessels. (**A''' and**

B''') Representative images of interactions observed between GFP+ grafted cells and host blood vessels. (**C**) Quantification of blood vessel diameters, as well as the total number of blood vessels encountered within the grafted tissue of YAC128 and non-carriers revealed similar patterns in each group of animals. Note that the detection of GFP+ grafted cells was further enhanced using GFP immunofluorescence staining (green) while blood vessels were identified using an antibody against the basement membrane protein laminin (red). Scale bars: **A-B**=100μm; **A'-A''**=25μm; **B'-B''**=25μm; **A'''**=10μm; **B'''**=12.5μm. Abbreviations: CV: capillaries vessels; LV: large calibre vessels.

Table 3-1. Summary of transplantation studies performed in transgenic animal models of Huntington's disease

Animal model/age at transplantation	Cell type and methodology	Observations/Results	Ref.
R6/2 10 weeks of age	▪ LGE from E13-14 C57BL/6J mice ▪ Cell suspension ▪ Unilateral striatal implantation	▪ Modest behavioural effects ▪ Good graft survival and integration ▪ No effect on disease progression	(Dunnett et al., 1998)
HD N171-82Q 8 weeks of age	▪ hBM-hMSC derived from healthy donors ▪ Cell suspension ▪ Unilateral striatal implantation	▪ Grafted cells die between 5-15 days post-transplantation ▪ No replacement of cell loss but stimulation of proliferation and differentiation of existing cells ▪ Neuroprotective effects through the release of FGF-2, VEGF, NGF by endogenous neuronal cells persisting for at least 30 days	(Snyder et al., 2010)
R6/2-J2 12 weeks of age C57/B6 (QA lesion) 12 weeks of age	▪ Immortalized hBM-MSC ▪ Cell suspension ▪ Unilateral striatal implantation	▪ R6/2-J2: ▪ No significant motor improvement ▪ No differences in striatal volume ▪ Neuronal proliferation and differentiation within the striatum ▪ Increased life-span ▪ QA-lesioned C57/B6: ▪ Improvement of striatal volume, motor behaviour, neuronal proliferation and differentiation within the striatum ▪ Increased laminin+ vessels and expression of vWF	(Y.-T. Lin et al., 2011)
R6/2 8.5 weeks of age	▪ hASCs derived from healthy donors ▪ Cell suspension ▪ Bilateral striatal implantation	▪ Improvement of motor behaviour ▪ Increase of striatal volume ▪ Disease progression slowed ▪ Positive effects suggested to be due to neurotrophic factor release (FGF-2, VEGF)	(Lee et al., 2009)
YAC128 8 and 12 months of age	▪ hASCs derived from HD patients and healthy donors ▪ Cell suspension ▪ Bilateral striatal implantation	▪ In YAC 128 grafted at 8 months of age, no impact on motor behaviour with hASC derived from normal nor HD donors at 4 months post-transplantation ▪ Better effect 1 and 4 weeks post-transplantation of normal hASC in 12-month old YAC128 mice ▪ Low % of cell survival	(Im et al., 2010)
R6/2 7 weeks of age	▪ Human neuronal stem cells (undifferentiated or pre-differentiated) ▪ Cell suspension ▪ Bilateral striatal implantation	▪ No impact on body weight ▪ No improvement of motor behaviour ▪ No reduction of brain atrophy ▪ Poor graft survival	(El-Akabawy et al., 2012)

Abbreviations: FGF-2: fibroblast growth factor 2; hASCs: human adipose-derived stem cells; hBM-MSC: human bone marrow derived mesenchimal stem cells; HD: Huntington's disease; LGE: lateral ganglionic eminence; NGF: nerve growth factor; QA: quinolinic acid; VEGF: vascular endothelial growth factor; vWF: Von Willebrand factor

Table 3-2. Cell transplantation studies addressing vascularization of grafted tissue in animal models and human cases

Animal models- Patients/age at transplantation	Cell type and methodology	Observations/Results	Ref.
Animal studies			
PVG rats (180-240g ~ 1-2 months of age)	▪ Foetal hippocampal primordia from E17 to P0 PVG rats ▪ Solid tissue grafts ▪ Unilateral hippocampal or septal implantation ▪ Post-mortem analyses performed between 1 day and 3 months post-transplantation	▪ No integration of vasculature between host and solid tissue transplants 24 hours post-transplantation ▪ Host vascularization of the grafts 3-7 days post-transplantation ▪ Presence of mostly capillaries and few larger blood vessels at 1-3 weeks post-transplantation ▪ Core of solid tissue grafts present a vascular density similar to the host 4-5 weeks post-transplantation,	(Lawrence et al., 1984)
PVG rats (180-240g ~ 1-2 months of age)	▪ Foetal hippocampal primordia from E16, E17, E18, E21 and P1 PVG rats ▪ Solid tissue grafts ▪ Bilateral hippocampal implantation ▪ Post-mortem analyses performed 1 month post-transplantation	▪ Formation of blood vessel chimeras 4-5 weeks post-transplantation	(Lindsay and Raisman, 1984)
Brattleboro rats with chronic autosomal homozygous diabetes insipidus Weight/age NA	▪ Foetal anterior hypothalamus from E17 Long-Evans rats ▪ Solid tissue grafts ▪ Third ventricle implantation ▪ Post-mortem analysis performed 3 days, 6 days and 1 month post-transplantation	▪ Vascular organization is incomplete at 3 days post-transplantation ▪ Increase in capillary density at 6 days post-transplantation ▪ Vessels derived from mantle plexus, periventricular stratum and preoptic area ▪ Despite normal vascularization, no improvement of phenotype	(Scott, 1984)
Wistar rats 10-15 days	▪ Foetal neocortex from E17-21 rats ▪ Solid tissue grafts ▪ Fourth ventricular or cortical (control) implantation ▪ Post-mortem analyses performed 24-72 hours and 1-4 weeks post-transplantation	▪ Presence of capillaries in intraventricular grafts 24 hours post-transplantation ▪ Presence of vessels in intraparenchymal grafts 72 hours post-transplantation ▪ More complete vascular network in intraparenchymal grafts 5 days post-transplantation ▪ Host vessels anastomose with intrinsic vessels in both intraventricular and intraparenchymal grafts	(Krum and Rosenstein, 1988)
Brattleboro rats Weight/age NA	▪ Foetal anterior hypothalamus from E16-17 Long-Evans rats ▪ Solid tissue grafts ▪ Lateral, third or fourth ventricular implantation ▪ Post-mortem analyses performed 4 and 6 weeks post-transplantation	▪ Similar vascular density in various transplantation sites ▪ Graft blood vessel density is similar to hypothalamus of control rats	(Wiegand and Gash, 1988)
Kainic acid-lesioned Sprague-Dawley albino rats (200g ~ 2 months of age)	▪ Foetal dorsal thalamic primordial from E15-16 rats ▪ Cell suspension ▪ Unilateral thalamic implantation ▪ Post-mortem analyses performed 10-120 days post-transplantation	▪ Progressive development of graft vascular network ▪ Few capillaries 10 days post-transplantation ▪ Normal vascularization 2 months post-transplantation ▪ Disruption of the pre-existing graft capillaries after mechanical trituration ▪ Revascularization is based on angiogenic process	(Dusart et al., 1989)
6-OHDA-lesioned Sprague-Dawley rats (170-190g ~ 1.5 months of age)	▪ Foetal ventral mesencephalon from E14, E17 and E20 rats ▪ Cell suspension ▪ Unilateral neostriatum implantation	▪ Increased graft vascularization after Nimodipine treatment, further associated with a 2-fold increase in graft volume	(Finger and Dunnett, 1989)

	▪ 2-week Nimodipine treatment ▪ Post-mortem analyses performed 40 days post-transplantation	▪ Donor age impact graft survival: E14 represents optimal conditions while older foetuses give lower survival ▪ Nimodipine ameliorates graft vascularization	
Swiss-Webster mice AKR mice Athimic mice Hypogonadal mice Weight/age NA	▪ Foetal/neonatal neocortex from E16 to P1 rats ▪ Solid tissue grafts ▪ Third ventricular or striatal implantation in Swiss-Webster mice, hypogonadal mice and athimic (nude), AKR mice ▪ Cell suspension of rat astrocytes, PC12 cells, canine glioma, human neuroblastoma or medulloblastoma, fibroblast cell lines ▪ Striatal implantation in athymic (nude) and CD1 mice ▪ Post-mortem analyses performed between 1 and 30 days post-transplantation	▪ Host vascularization of solid tissue grafts 7 days post-transplantation ▪ Host vascularization of cell suspension grafts 3 days post-transplantation ▪ Both donor and host vessels are observed within solid tissue grafts	(Broadwell et al., 1991)
Ibotenic acid-lesioned Sprague-Dawley rats (250-300g ~ 2 months of age)	▪ Foetal basal forebrain from E15-16 Sprague-Dawley rats or Balb/C mice ▪ Cell suspension ▪ Unilateral implantation in lesioned nucleus basalis magnocellularis ▪ Post-mortem analyses performed 2, 4, 8, 24 weeks post-transplantation	▪ BBB formation in both allografts and xenografts 4 weeks post-transplantation ▪ Vasculature supply observed from 2 weeks post-transplantation	(Geist et al., 1991)
Kainic acid-lesioned Sprague-Dawley rats (200-250g ~ 2 months of age)	▪ Human foetal spinal and brainstem - 6-8 weeks of gestation ▪ Solid tissue grafts ▪ Unilateral striatal implantation ▪ Post-mortem analyses performed 1, 2 and 3 months post-transplantation	▪ Delayed graft vascularization ▪ No blood vessels 1 month post-transplantation ▪ Few medium size capillaries 2 months post-transplantation ▪ Graft revascularized 3 months post-surgery, but to a lesser extent than the host	(Geny et al., 1994; Lawrence et al., 1984)
Sprague-Dawley rats (250g ~ 2 months of age)	▪ Foetal basal forebrain from E16 rats ▪ Cell suspension and solid tissue grafts ▪ Corpus callosum implantation ▪ Post-mortem analyses performed 1, 3, 7 and 10 days post-transplantation	▪ BBB formation in solid tissue grafts 7 days post-transplantation ▪ Cell suspension grafts revascularization depends on angiogenic processes of the host	(Akalan and Grady, 1994)
PVG-RT1^{c} and PVG-RT1^{u} rats (200g ~ 2 months of age)	▪ Foetal neocortex from E18 to P1 PVG-RT1^{c} rats ▪ Solid tissue grafts ▪ Lateral ventricles, third ventricle and caudate/putamen implantation ▪ Cell suspension ▪ Caudate/putamen implantation ▪ Post-mortem analyses performed 30 days to 7 months post-transplantation	▪ Host blood vessels found in both solid and cell suspension grafts ▪ Donor vessels found in solid tissue grafts	(Baker-Cairns et al., 1996)
	Human studies		
59-year old PD patient	▪ Foetal ventral mesencephalon at 6.5 -9 weeks post-conception ▪ Solid tissue grafts ▪ Bilateral post-commissural putaminal implantation ▪ Post-mortem analyses performed 18 months post-transplantation	▪ Hypovascularization of grafted tissue compared to the host ▪ BBB formation and normal glucose up-take within the grafts (GLUT-1 staining)	(Kordower et al., 1996)
40- and 67-year old HD patients	▪ Far lateral portion of the lateral ganglionic eminence at 8-9 weeks post- conception ▪ Solid grafts ▪ Bilateral caudate/putamen implantation ▪ Post-mortem analyses performed 9 and 12 years post-transplantation	▪ Discrepancy in graft and host vasculature ▪ Presence of capillaries (vWF+) but not large calibre vessels (α-SMA) in solid tissue grafts	(Cisbani, Freeman, et al., 2013)

Abbreviations: α-SMA: alpha smooth muscle actin; AKR: aldo keto reductase inbred mouse strain; BBB: blood brain barrier; E: embryonic day; GLUT1: glucose transporter 1; NA: Not available; P0: day of birth; P1: postnatal day 1; PC12: pheochromocytoma of the rat adrenal medulla; PVG: Piebald Virol Glaxo inbred rat strain vWF+: Von Willebrand factor

CHAPTER IV

4.1 Contributions

To further understand the mechanisms underlying poor graft survival, we explored the possibility of mHtt transmission to the grafted tissue in HD patients. For this purpose, we used a variety of techniques to demonstrate the presence of the mutated protein within the grafts. The article has been recently submitted to Annals of Neurology.

Dr. Cicchetti made the discovery of mHtt aggregates within the grafted tissue and from there, designed the project. She was involved in experimental designs, image acquisition and data interpretation. She supervised the project and wrote the manuscript. Dr. Lacroix was involved in data interpretation and manuscript writing. I performed most of the immunohistochemical and immunofluorescent stainings, aggregate quantifications, some of the image acquisition and was responsible of assembling all figure panels. Nicolas Vallières helped troubleshoot immunofluorescent protocols and performed all the confocal image acquisition. Martine Saint-Pierre performed some of the immunohistochemical and immunofluorescent stainings as well as some of the image acquisition. Isabelle Saint-Amour performed the western immunoblotting. Ranna Toulei performed the infrared spectroscopy. Jeremy N. Skepper helped with the electron microscopy analyses/interpretation. Dr. Hauser ensured the clinical follow-up of the patients. Dr. Mantovani provided this expertise for the infrared spectroscopy. Dr. Barker was involved in manuscript writing. Dr. Freeman was involved in data interpretation and manuscript writing.

4.2 Résumé

Objectif. La maladie d'Huntington (HD) est causée par une protéine pathologique génétiquement encodée (huntingtin mutée (mHtt)), qu'on croit agir de façon cellule-autonome. Dans cette étude, nous avons testé l'hypothèse selon laquelle la mHtt est capable de se propager dans le tissu cérébral en examinant des greffes de tissus fœtales dans les cerveaux de patients HD. **Méthodes.** La présence d'agrégats de mHtt dans les tissus greffés a été confirmée en utilisant 3 différents types de microscopie (champ clair, fluorescence et électronique), ainsi que des techniques d' immunobuvardage et de spectroscopie infrarouge, et ce en utilisant 4 anticorps distincts ciblant différents épitopes des agrégats de mHtt. **Résultats.** Nous décrivons la présence d'agrégats de mHtt à l'intérieur des allogreffes intracérébrales de tissue striatal chez trois patients HD qui ont reçus leurs transplantations approximativement une décennie auparavant et qui sont décédé de causes reliées à la progression de leur maladie. Les agrégats mHtt+ ont été observés dans la matrice extracellulaire du tissu transplanté tandis que dans le cerveau hôte, ils ont été observés dans les neurones, le neuropile, la matrice extracellulaire et les vaisseaux sanguins. **Interprétation.** Ceci constitue la première démonstration de la présence de mHtt dans une greffe de tissu neuronal génétiquement normal et non relié au receveur. Ces observations soulèvent des questions sur la propagation de protéines dans les désordres neurodégénératifs monogéniques du système nerveux central caractérisés par la formation d'oligomères/agrégats de protéines mutées.

4.3 Mutant huntingtin protein is present in neuronal grafts in Huntington's disease patients

Cicchetti F, PhD*[1,2], Lacroix S, PhD[1,3], Cisbani G, MSc[1], Vallières N, MSc[1,], Saint-Pierre M, DEC[1], St-Amour I, PhD[1], Tolouei R, PhD[4], Skepper JN, PhD[5], Hauser RA, MD[6], Mantovani D, PhD[4], Barker RA, MD, PhD[7], Freeman TB, MD[8,9]

[1]Centre de recherche du CHU de Québec (CHUQ), Québec, QC, Canada G1V 4G2; [2]Département de psychiatrie et neurosciences, Université Laval, Québec, QC, Canada, G1K 7P4; [3]Département de médecine moléculaire, Université Laval, Québec, QC, Canada, G1K 7P4; [4]Laboratoire de biomatériaux et bioingénierie, Hôpital Saint-François d'Assise and Département de génie des mines, de la métallurgie et des matériaux, Université Laval, Québec, QC, Canada G1V 0A6, [5]Cambridge Advanced Imaging Centre, Anatomy building, University of Cambridge, Cambridge, UK, CB2 3DY, [6]Departments of Neurology; Pharmacology and Experimental Therapeutics, Parkinson's Disease and Movement Disorders National Parkinson's Foundation Center of Excellence, University of South Florida, Tampa, FL, USA, 33606, [7]John van Geest Centre for Brain Repair, Department of Clinical Neurosciences, University of Cambridge, Cambridge, UK, CB2 0PY, [8]Department of Neurosurgery and Brain Repair, [9]Center of Excellence for Aging and Brain Repair, University of South Florida, Tampa, FL, USA, 33606

Correspondence
Francesca Cicchetti, PhD
Centre de recherche du CHU de Québec (CHUQ)
Axe Neurosciences, T2-50
2705, Boulevard Laurier
Québec, QC, G1V 4G2, Canada
Tel #: (418) 656-4141 ext. 48853
Fax #: (418) 654-2753
E-mail: Francesca.Cicchetti@crchul.ulaval.ca

4.3.1 Abstract

Objective. Huntington's disease (HD) is caused by a genetically encoded pathological protein (mutant huntingtin (mHtt)), which is thought to exert its effects in a cell-autonomous manner. Here, we tested the hypothesis that mHtt is capable of spreading within cerebral tissue by examining genetically unrelated foetal neural allografts within the brains of patients with advancing HD. **Methods.** The presence of mHtt aggregates within the grafted tissue was confirmed using 3 different types of microscopy (brightfield, fluorescence and electron), 2 additional techniques consisting of western immunoblotting and infrared spectroscopy, and 4 distinct antibodies targeting different epitopes of mHtt aggregates. **Results.** We describe the presence of mHtt aggregates within intracerebral allografts of striatal tissue in three HD patients who received their transplants approximately a decade earlier and then died secondary to the progression of their disease. The mHtt+ aggregates were observed in the extracellular matrix of the transplanted tissue while in the host brain they were seen in neurons, neuropil, extracellular matrix and blood vessels. **Interpretation.** This is the first demonstration of the presence of mHtt in genetically normal and unrelated allografted neural tissue transplanted into the brain of affected HD patients. These observations raise questions on protein spread in monogenic neurodegenerative disorders of the central nervous system characterized by the formation of mutant protein oligomers/aggregates.

4.3.2 Introduction

Huntington's disease (HD) is an autosomal dominant genetic disorder characterized by a clinical triad of a movement disorder, cognitive dysfunction and psychiatric problems (Phillips et al., 2008)combined with a pathological CAG expansion in exon 1 of the huntingtin gene leading to the production of mutant huntingtin protein (mHtt) (Phillips et al., 2008; Zuccato et al., 2010). Wild type Htt is a soluble protein that is ubiquitously expressed but is present in higher concentrations especially in the brain. This cytoplasmic and nuclear protein is associated with several organelles, microtubules and vesicular membranes, pointing to a role in intracellular trafficking, exocytosis, endocytosis and therefore synaptic functions (Phillips et al., 2008; Steffan et al., 2000). In HD, like all genetic trinucleotide disorders of the central nervous system, it has been suggested that the abnormal mutant protein causes cellular dysfunction through a cell-autonomous process in which only genotypically mutant cells exhibit the mutant phenotype. This results in mHtt aggregation, inclusion body formation and cell death, although how these events relate to each other is still debated (Phillips et al., 2008; C. A. Ross and Tabrizi, 2011; Zuccato et al., 2010).

HD is incurable, and different experimental therapeutic strategies have been tested including transplantation of foetal striatal tissue (Freeman et al., 2011; Peschanski et al., 1995). This approach was predicated on the grounds that the primary pathology involves the striatum and that replacing it with unaffected allografts of foetal striatal tissue would be of benefit, as has been shown experimentally in non-transgenic animal models of HD (Deckel et al., 1983; Isacson et al., 1984; Pritzel et al., 1986; Wictorin, 1992). To date, these transplants have generally produced transient or no clinical benefits despite evidence that they survive in the short-term (Freeman et al., 2000). This failure of clinical response to such targeted grafts may relate to the widespread pathology now recognised in HD from an early disease stage, but may also relate to the fact that these grafts survive poorly in HD patients and degenerate in a disease-like manner, as we have described previously (Cicchetti et al., 2009). In this respect, we now show for the first time that mHtt aggregates can be found within the genetically normal transplanted tissue in three HD patients in whom there was long-term graft survival (patients reported previously in (Cicchetti et al., 2009; Cisbani, Freeman, et al., 2013; Freeman et al., 2000; Hauser et al., 2002)).

4.3.3 Methods

4.3.3.1 Patients' information

Female patients one (B.L.), three (M.C.) and five (M.S.) of the original 7 HD patients grafted as part of the transplant trial conducted at the University of South Florida (Cicchetti et al., 2009; Freeman et al., 2000; 2011; Hauser et al., 2002) all had a 42 CAG repeat (previously reported in (Cicchetti et al., 2009; Cisbani, Freeman, et al., 2013; Freeman et al., 2000; Hauser et al., 2002)). They were transplanted at 58, 64 and 59 years of age, respectively. Patient seven (K.T.) was a 28-year old woman who carried 53 CAG repeats. All patients had manifest disease (ranging between 6 and 17 years of symptom duration) at the time that they received bilateral foetal striatal transplants. They all showed mild clinical improvements lasting at most one year, except for patient five (M.S.) whose UHDRS score worsened following grafting (Cicchetti et al., 2009; Freeman et al., 2000; Hauser et al., 2002). They died between 9 and 12 years post-transplantation (Cicchetti et al., 2009; Cisbani, Freeman, et al., 2013) (see **Figure 4-1**). All post-mortem analyses of human brain tissue were approved by the *Comité d'éthique de la recherche du CHU de Québec* (#A13-02-113).

4.3.3.2 Immunohistochemistry

Brains were processed using methods previously published (Cicchetti et al., 2009; Cisbani, Freeman, et al., 2013; Freeman et al., 2000). Standard histology was undertaken to identify the grafts macroscopically. Additional post-mortem analyses included double immunohistochemical staining for neuronal elements using an antibody against neuronal nuclei (NeuN, anti-mouse, MAB377, Millipore, 1:2500) as well as the anti- huntingtin antibodies EM48 (mouse anti-human huntingtin clone EM48, MAB5374, Millipore, 1:2000) and MW7 (mouse anti-human, obtained from the Developmental Studies Hybridoma Bank, 1:100) to identify mHtt+ aggregates. Photomicrographs were taken using Picture Frame software (Microbrightfield) linked to an E800 Nikon microscope (Nikon Instruments).

4.3.3.3 Stereology for EM48+ aggregate count

The density of EM48+ mHtt deposits, reported as the number of aggregates/mm^2 of tissue, was assessed in the cortex and putamen of the host brains as well as in p-zones and non p-zones of the grafts. Each of these structures was delineated using the tracing contour option in *Stereo Investigator* (*NeuroExplorer*, version 10.0; Microbrightfield). Stereological counts were performed using the *Optical Fractionator* probe (Stereo Investigator, Microbrightfield) installed onto an E800 Nikon microscope

(Nikon Instruments). For aggregate size, the perimeter of sampled aggregates were delineated and assessed in the above-mentioned structures.

4.3.3.4 Statistical analyses

To calculate the density of aggregates, a negative binomial distribution was used. Step-down Bonferonni correction was further employed to ensure that the overall significance level of the multiple comparison tests was 0.05. One-way ANOVA was used to compare aggregate size. All statistical analyses were performed using the MIXED and GENMOD procedures of SAS (version 9.2, SAS: Cary, North Carolina).

4.3.3.5 Immunofluorescence

A series of double and triple immunofluorescence stainings was also performed to localize mHtt, using either EM48 (1:200) or MW7 (1:100) (see **Table 4-S1**). The following antibodies were used for the detection of specific cell populations: astrocytes (rabbit anti-GFAP, Z0334, Dako Cytomation, 1:500), microglia (rabbit anti-Iba1, 019-19741, Wako Chemicals, 1:800), neurons (rabbit anti-MAP2, 17490-1-AP, Protein Tech, 1:500 or anti-chicken Neurofilament H (NFL-H), AB5539, Millipore, 1:400), oligodendrocytes (rabbit anti-CAII, 1:2000), perivascular macrophages (rabbit anti-CD163, NBP1-30148, Novus biological), vascular endothelium (rabbit anti-Laminin, Z0097, Dako Cytomation, 1:500) and extracellular matrix (rat anti-phosphocan, MAB2688, R&D system, 1:100) . Ubiquitinated aggregates were also identified using an anti-rabbit ubiquitin antibody (Z0458, DAKO, 1:100). Some of these antibodies required an additional post-fixation with paraformaldehyde (PFA) 4% pH 7.4 (Sigma-Aldrich) for 1 hr prior to staining (**Table 4-S1**). Sections were stained using standard procedures (see X for more details) All sections were observed at 60X and imaged on a Fluoview FV1000 confocal microscope system equipped with 559nm and 635nm laser diodes and an Ar 488nm laser (Olympus Canada Inc.).

All immunohistochemistry and immunofluorescence experiments included multiple controls such as normal and HD matched brain sections (both free floating and paraffin embedded sections; provided by the NIHR funded Cambridge Brain Bank, UK) and negative controls where the primary antibody was omitted from the incubation media. Control conditions further included a range of dilutions for the EM48 antibody (1:50 to 1:5000), all of which yielded positive immunoreactivity for mHtt aggregates in the

grafted tissue as revealed with the nickel intensified DAB method and an optimized DAB protocol which was different from that used previously by us (Cicchetti et al., 2009; Freeman et al., 2000).

4.3.3.6 Sequential method for chromogenic immunohistochemistry

We undertook an additional series of experiments to investigate the co-localization of EM48 with MW7 and ubiquitin. In order to do this, we applied a sequential staining protocol using the chromogen 3-amino-9-ethylcarbazole (AEC) (Becher et al., 1998; G. Glass et al., 2009; Kim et al., 2012; Pirici et al., 2009). To confirm the complete removal of the primary antibody, the sections were also incubated solely in the secondary antibody. Photomicrographs were taken by Picture Frame software (Microbrightfield) linked to an E800 Nikon microscope (Nikon Instruments).

4.3.3.7 Electron microscopy

For electron microscopy, specific areas of a 30µm DAB-stained brain section were prepared by flat embedding in epoxy resin (Hayat, M.A.) The embedded samples were then serially sectioned in parallel at 60nm with a diamond knife (DDK, Delaware, USA) on an ultramicrotome (Ultracut E, Reichert-Jung, Austria). The sections were placed onto a single-hole copper/formvar grid and stained with 3% aqueous uranyl acetate for 5 min. After drying, observation was performed with an electron microscope, JEM-1230 (JEOL, Japan) set at 80 kV (Cicchetti et al., 2009).

4.3.3.8 Protein extraction from fixed tissue

Brain sections were selected and dissected to isolate pieces of the cortex in both HD and control patients, as well as the grafted tissue. This was performed on 15 sections for each condition. The dissected tissue was collected into eppendorf tubes, weighed and frozen on dry ice and homogenized in 4 volumes of extraction buffer (50mM HEPES, 150mM NaCl, 10mM EDTA, 1% triton X-100 (Sigma-Aldrich), 0.5% deoxycholate (Sigma-Aldrich), 0.1% BSA (Bishop), 200mM DTT, 2% SDS (Sigma-Aldrich), 20mM Tris HCl pH 8.8 (Sigma-Aldrich),(Addis et al., 2009; Weiss et al., 2012) containing a cocktail of protease (Roche) and phosphatase inhibitors (Sigma-Aldrich)) and sonicated. The homogenate was then incubated at 100°C for 20 min followed by an incubation of 1 h at 80°C on a shaker (80rpm). Finally, the tubes were spun for 20 min at 4°C at 13000rpm and the supernatant was

collected and stored at -80°C until used. Total protein concentration was determined using the Pierce 660nm protein assay (Thermo Fisher).

4.3.3.9 Western blotting

All reagents and chemicals used for immunoblotting were purchased from Sigma-Aldrich, unless otherwise specified. Fifteen µg of protein was prepared in the sample buffer (250 mM Tris-HCl, 2% w/v lithium dodecyl sulphate, 100 mM DTT, 0.4 mM EDTA, 10% v/v glycerol (Fisher Scientific), 0.2 mM bromophenol red, 0.2 mM Brilliant Blue G, pH 8.5) and heated for 10 min at 70°C. The proteins were then separated for 5 hrs at 150 V on a 3 - 8% gradient hand-cast polyacrylamide gel (37.5:1 acrylamide: bisacrylamide solution (J.T. Baker) in 0.2 M Tris-acetate buffer, pH 7.4 using a midi electrophoresis system (15 x 15 cm) in an electrophoresis buffer (50 mM Tricine, 50 mM Tris, 0.1% SDS, 1.3 mM sodium bisulfite, pH 8.2), as previously described.(Cubillos-Rojas et al., 2010) Proteins were electroblotted onto 0.45 µm Immobilon PVDF membranes (EMD Millipore, Billerica, MA, USA) overnight at 15V in the transfer buffer (20% methanol (Fisher Scientific) 25 mM Bicine, 25 mM Bis-Tris, 1 mM EDTA, 1.3 mM sodium bisulfite, pH 7.2). After being blocked in a solution of 5% skimmed milk, 0.5% bovine serum albumin (Bioshop Canada Inc, Burlington, ON, Canada) in PBS, 0.1% Tween-20 (Thermo Scientific) the membranes were immunoblotted with MW1 (anti-mouse antibody, 1:1000) overnight at 4°C followed with horseradish peroxidase (HRP)-conjugated goat anti-mouse antibody (Jackson Immunoresearch, 1:30,000) and detected by the addition of chemiluminescence reagents (Luminata forte, EMD Millipore). The membranes were then stripped and reprobed for total Htt (anti-mouse, clone: 1HU-4C8, MAB2166, EMD Millipore, 1:1000), glyceraldehyde 3-phosphate dehydrogenase (anti-mouse GAPDH, G041, Applied Biological Materials Inc, 1:7500), and neuronal nuclei (anti-mouse NeuN, MAB377, EMD Millipore, 1:1000). Images of the membranes were acquired using myEcl Imager (Thermo Fisher). Band intensities were quantified using Carestream Molecular Imaging Software (version 4.0.5f7, Eastman Kodak). The graphs were generated using the Prism software (version 4.0, GraphPad Software Inc.) and assembled in illustrator CS5.

4.3.3.10 Infrared spectroscopy

Infrared spectroscopy was used to detect structural protein changes such as the β-sheets of mHtt within the HD host brain and grafted tissue of unstained sections.(W. André et al., 2013; Khare et al., 2005) Fourier transform infrared spectroscopy–focal plane array (FTIR-FPA) maps were acquired using a 32 × 32 detector with a pixel size of 5.5 µm giving 1024 spectra/map. The IR spectra were collected

on a Nicolet Magna-IR 550 FT spectrometer (Thermo Nicolet, Madison, WI, USA) equipped with a deuterated triglycine sulfate (DTGS) detector and a germanium-coated KBr beam splitter. IR data were treated with Omnic E.S.P. 5.1 (Thermo Nicolet, Madison, WI, USA) and Grams 32 (Spectral Notebase version 4.11, Galactic Industries Corporation, Salem, NH, USA).

4.3.3.11 Image preparation

All the images were prepared using Adobe Photoshop CS5 and assembled using Adobe Illustrator CS5.

4.3.4 Results

Surviving neuronal transplants with a compartmentalized organization were observed in three of four transplant recipient brains that we have reported previously (Cicchetti et al., 2009; Cisbani, Freeman, et al., 2013; Freeman et al., 2000) (**Figures. 4-1 and 4-2**). Within the surviving transplants of all three patients, we observed patches of striatal-like neuronal tissue referred to as p-zones, as well as areas where there was no expression of striatal phenotypes (non p-zones) (Graybiel et al., 1989). In the fourth patient (patient three (M.C.) from our original series), no surviving transplants were found (Cicchetti et al., 2009).

Aggregated mHtt protein was observed in the genetically unrelated transplanted tissue in all three HD patients with surviving grafts (**Figures 4-1 and 4-2**). Aggregates identified with either EM48 or MW7 were frequently found within both the p-zones (**Figures 4-1A-C, F-I, 4-2A-C**) and non p-zones of the grafts (**Figures 4-1A-D, F-I, 4-2C-D**). These aggregates occurred with similar frequency and size in both the grafts and surrounding non-transplanted putamen and cortex in these HD patients (**Figure 4-1,** bar graphs).

Within the transplanted tissue, mHtt+ aggregates were localized to the extracellular matrix of both the p- and non p-zone throughout the grafts, as confirmed using two distinct antibodies (EM48 and MW7, **Figure 4-3A-B**). EM48+ and MW7**+** aggregates within transplants were not observed in neurons (**Figure 4-3A-B**), microglia (**Figures 4-3C, 4-4A**), astrocytes (**Figures 4-3D, 4B**), perivascular macrophages (**Figures 4-3E, 4-4C**), oligodendrocytes (data not shown), endothelial cells (data not shown) or blood vessels (**Fig. 3F,** data not shown for MW7).

In contrast in these same patients, mHtt protein aggregates found within the non-transplanted cortex were localized to the neurons and neuropil (**Figure 4-5A-D**), as previously described.(DiFiglia et al., 1997; Gutekunst et al., 1998) mHtt was also frequently observed within the extracellular matrix of the host cortex (**Figure 4-5E**), a finding that has not been previously reported. Additionally, aggregates of mHtt protein were observed within the vascular space of the HD brain (**Figure 4-5F**) including cells (**Figure 4-5F inset –** EM48/DAPI staining). Aggregates of mHtt protein (stained either with EM48 or MW7) were not observed in host microglia (**Figures 4-4E and 4-5G**), astrocytes (**Figures 4-4F and 4-5H**), perivascular macrophages (**Figures 4-4G and 4-5I**), oligodendrocytes (**Figure 4-5J**) nor within endothelial cells (data not shown).

Co-localization of EM48+ aggregates and the protein ubiquitin was confirmed within the grafted tissue (**Figure 4-6A**) and the cortex (**Figure 4-6B**). Using a technique of chromogen stripping, (G. Glass et al., 2009; Kim et al., 2012; Pirici et al., 2009) we further demonstrated that EM48, ubiquitin and MW7 co-localize in the cortical tissue of transplanted HD patients (**Figure 4-7**). In order to confirm the presence of these aggregates, we further performed electron microscopy (**Figure 4-8**), western immunoblotting (**Figure 4-9**) and infrared spectroscopy (**Figure 4-10**), all of which corroborated our original immunohistochemical findings of aggregates in the graft and host brain.

4.3.5 Discussion

Here we describe for the first time that mHtt can be found within genetically unrelated tissue grafted into the brains of patients with advancing HD. The mHtt was localized to the extracellular matrix of the transplants. This differs from the localization of mHtt within the non-grafted regions of the brain of patients with HD, where the mHtt protein is primarily localized to neurons and the neuropil – as has been described before in HD (DiFiglia et al., 1997; Gutekunst et al., 1998).

The foetal striatal allografts implanted in these patients with HD are derived from normal donors not carrying the mutant gene and thus mHtt. This raises two questions: 1) how did the mHtt protein from the patient become localized within the transplanted tissue and 2) did this localization of mHtt within the transplants contribute to their compromised survival (Cicchetti et al., 2009; Cisbani, Freeman, et al., 2013; Freeman et al., 2000)? Several possible mechanisms can be put forward to explain these findings.

mHtt protein transmission, deposition or diffusion into the transplant. In another neurodegenerative disorder of the central nervous system, Parkinson's disease (PD), it has been demonstrated that the pathologically associated protein α-synuclein (i.e. Lewy body pathology) could spread into the allografted ventral mesencephalic tissue (Kordower et al., 2008; J. Y. Li et al., 2008). This was hypothesized to occur in a prion-like fashion (Brundin et al., 2010; Goedert et al., 2013; Kordower et al., 2008; Olanow and Prusiner, 2009; Soto, 2012). Both *in vitro* and *in vivo* studies have subsequently demonstrated that α-synuclein can be released and taken up by neurons (Desplats et al., 2009; Hansen et al., 2011) and seed pathology. Indeed, intracerebral inoculation of brain homogenates derived from α-synuclein transgenic mice, or injection of synthetic α-synuclein preformed fibrils accelerates the formation of α-synuclein protein aggregates and precipitates neurological dysfunction in animals (Luk et al., 2012). A similar propagation of tau pathology has been described in a model of early Alzheimer's disease (AD) and tauopathies (Clavaguera et al., 2013; de Calignon et al., 2012). It is therefore possible that mHtt was transferred from the patients' brains to the grafts via a similar mechanism. However, unlike the host brain, where mHtt aggregates were mainly seen within the neuropil, inclusions in the grafts were only observed within the extracellular matrix and not within any cellular elements. Therefore, within these case reports, we do not have direct evidence of cell-to-cell propagation of mHtt.

Results from *in vivo* models of AD suggest that neurodegeneration in AD may result from tau pathology being spread via transynaptic connections (Liu et al., 2012; Soto, 2012). It is possible that mHtt could similarly be transmitted transynaptically to the transplants from the diseased cortex, and in this respect we have previously demonstrated synaptic connections between the diseased cortex and the grafted neurons in these HD patients (Cicchetti et al., 2009; 2011). Although we did not observe mHtt within grafted neurons, the extracellular localization of aggregates within the p-zones could be derived from dying cortico-striatal synaptic terminals that innervated the transplant (Cicchetti et al., 2009) and expressed mHtt, possibly leading to graft cell lysis and degeneration with release of the aggregates within transplant neuropil. However, extracellular localization of mHtt was also observed within non p-zones of the grafts, structures that do not receive direct projections from cortical neurons. This would suggest that, at most, this mechanism is partially involved in the mHtt spread and other mechanisms of protein transport may exist.

An alternative possibility related to this is that aberrant cortical striatal neurons containing the mHtt protein may leave axonal debris within transplant extracellular spaces in the process of undergoing cell

death. In support of this hypothesis, a large number of aggregates that did not colocalize with MAP2+ grafted neurones were nonetheless found in close proximity to these neuronal elements.

In vivo models of AD have also demonstrated that pathology may be associated with diffusion of the soluble form of Aβ in the extracellular space with uptake by cells in the vicinity (Meyer-Luehmann et al., 2003; Soto, 2012). Ren et al. (Ren et al., 2009) also described that fibrillar polyglutamine peptide aggregates can be internalized by mammalian cells *in vitro*. It is similarly possible that the localization of mHtt in our transplants results from diffusion of mHtt from the putamen to the transplants via the extracellular matrix. Uptake of this mutant protein may then compromise the viability of the cells in the graft that have endocytosed it. However, in our post-mortem samples we have no evidence of mHtt in any cell type within the graft, which would argue against such a mechanism compromising the transplants.

Oxidative stress, excitotoxicity, inflammation and poor trophic support. These mechanisms have been implicated in neuronal transplant pathology in both PD and HD (Brundin and Kordower, 2012; Cicchetti et al., 2011; Cisbani and Cicchetti, 2014; Freeman et al., 2011). CAG repeat length gains may occur in non-dividing cells,(Kennedy et al., 2003; Shelbourne et al., 2007) independent of the DNA replication process. It is possible that oxidative stress, excitotoxicity, inflammation or a poor trophic milieu may induce pathological polyglutamine expression in the transplants. However, Shelbourne et al. (Shelbourne et al., 2007) and Kennedy et al. (Kennedy et al., 2003) noted this CAG expansion within neurons and glia whereas we only saw the abnormal CAG in the extracellular milieu of the grafts. Furthermore, if such a mechanism was dominant, one would expect to see similar inclusions in other types of grafts such as ventral mesencephalon transplants in PD, which is not the case.

Hematogenous transport of mHtt. mHtt aggregates were occasionally observed within the HD cerebral blood vessels (**Figure 4-3F**), within cells of these blood vessels (**Figure 4-3F, insert**) and possibly within perivascular macrophages of the host brain (**Figure 4-8**). These new observations raise the possibility that mHtt could be transported from the host to the transplant via blood-borne cells such as those of the immune system. Interestingly, it was recently shown that certain types of immune cells can contribute to disease progression in animal models of HD (Bouchard et al., 2012; Kwan et al., 2012). This mechanism is further supported by the diffuse localization of mHtt within both the p-zone and non p-zone aspects of the graft. This mechanism is mitigated by the lack of direct evidence of mHtt aggregates within blood vessels and perivascular macrophages of the graft but the fact that we did not

observe this rare event within the transplants does not eliminate this possible mechanism, and further research is needed to address this issue.

Previously, we and others have reported the absence of mHtt aggregates within transplants in HD patients (Cicchetti et al., 2009; Freeman et al., 2000; Keene et al., 2007). Our new observation that mHtt inclusions are indeed present within grafts differs from these previous reports and can be explained in two ways. As in foetal ventral mesencephalon grafts in PD, α-synuclein depositions developed in a time-dependent manner and were only observed in grafts exposed to the disease process for over a decade (Kordower et al., 2008; J. Y. Li et al., 2008). Likewise, Freeman et al. (Freeman et al., 2000) and Keene et al. (Keene et al., 2007) examined transplants in HD patients that were exposed to the disease process for comparatively short-times (18 months, 6 and 7 years respectively). In Cicchetti et al., 2009 (Cicchetti et al., 2009), one of the 3 patients did not show graft survival precluding histological evaluation. However, in the other 2 subjects in this paper, we did not observe mHtt aggregates using standard techniques of the time. We therefore sought to re-examine these cases in this report using several techniques that were not available at the time of the original publication, including some techniques developed for this study, and we now can show that these grafts do indeed contain mHtt.

In genetic disorders such as HD, pathogenesis is thought to occur via cell-autonomous mechanisms. The exclusive localization of mHtt expression within the extracellular matrix of the grafted tissue, combined with the novel observation of mHtt expression within the host extracellular matrix suggest that other mechanisms may exist for mHtt spread within the HD brain. Further research is needed to determine the scientific, clinical and therapeutic implications of this finding to the normal disease process in HD.

4.3.6 Acknowledgments

This work was supported by a grant from the International Organization of Glutaric Acidemia (IOGA) awarded to Francesca Cicchetti. Salary support for Francesca Cicchetti and Steve Lacroix was provided by the Fonds de recherche du Québec en santé (FRQS). Giulia Cisbani was supported by the Bourse d'excellence du Centre thématique de recherche en neurosciences (Université Laval). The Cambridge Brain Bank is supported by an NIHR funded Biomedical Research Centre to the University of Cambridge/Addenbrooke's Hospital. The authors would like to thank Mr. Richard Janvier for his very skilful electron microscopy sample preparation and analyses, Marie Leroy (MSc), Pascale Chevalier (PhD), Lucie Levesque (MSc) and Gaétan Laroche (PhD) for FTIR analysis as well as Greg Sutter and Pamela Pierce who participated in the procurement of the brain from patient seven. The MW7 and MW1 antibodies developed by Dr P.H. Patterson were obtained from the Developmental Studies Hybridoma Bank developed under the auspices of the NICHD and maintained by The University of Iowa, Department of Biology, Iowa City, IA 52242.

4.3.7 Authorship

FC made the observation of the presence of mHtt within the grafted tissue, was involved in experimental designs, image acquisition and data interpretation. She supervised the project and wrote the manuscript. SL was involved in data interpretation and manuscript writing.

GC performed most of the immunohistochemical and immunofluorescent stainings, aggregate quantifications, some of the image acquisition and was responsible of assembling all figure panels. NV helped troubleshoot immunofluorescent protocols and performed all the confocal image acquisition. MSP performed some of the immunohistochemical and immunofluorescent stainings as well as some of the image acquisition. ISA performed the western immunoblotting. RT performed the infrared spectroscopy. JNS helped with the electron microscopy analyses/interpretation. RAH ensured the clinical follow-up of the patients. DM provided this expertise for the infrared spectroscopy. RAB was involved in manuscript writing. TBF was involved in data interpretation and manuscript writing.

4.3.8 Figures

Figure 4-1. EM48+ mHtt aggregates in grafted tissue

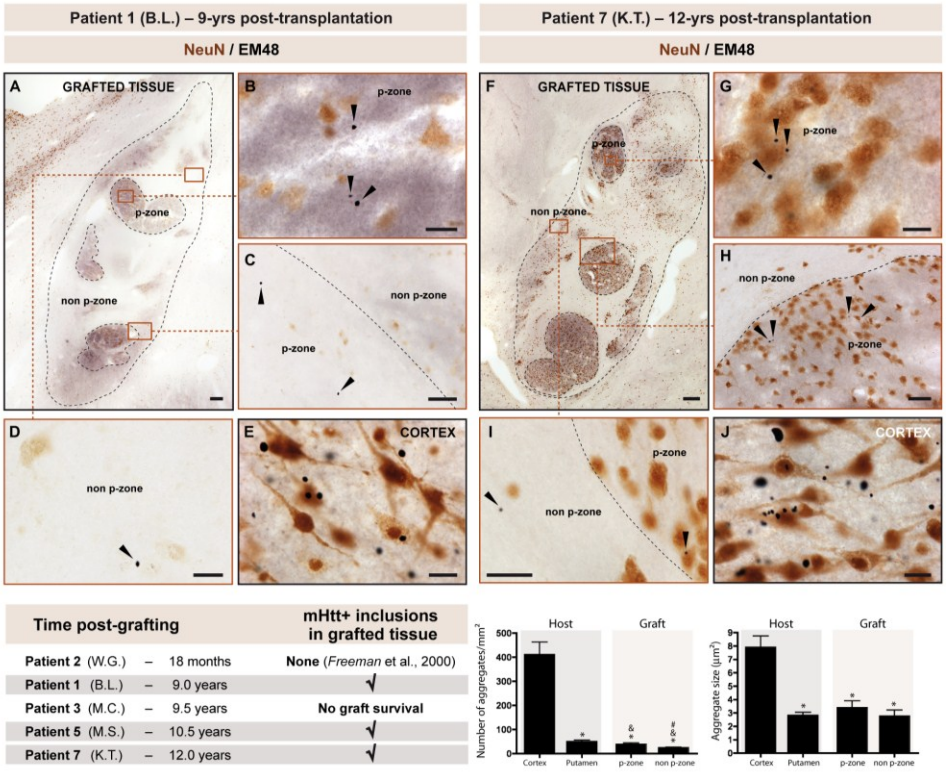

Double immunohistochemistry staining for the neuronal marker NeuN (revealed with the chromogen DAB - brown color) and EM48 (that stains for mHtt aggregates) (revealed with nickel intensified DAB – black color) in two late-stage (Grades three and four) HD cases 9.5 years (patient 1 (B.L.); left panel) and 12 years post-transplantation (patient seven (K.T.); right panel). Low magnification of representative grafts stained for NeuN/EM48 in patient one (**A**) and patient seven (**F**). Typical striatal morphology within the grafts is evident in both cases. EM48+ aggregates were found in transplanted tissue both within the p-zones (**B,C,G,H,I**) and non p-zones (**D,I**). In the host HD brain, and particularly in the cortex (**E,J**), several EM48+ aggregates could be identified. Scale bars **A**,**F**=200µm, **B**,**D**,**E**=25µm, **C**=50µm, **G**=25µm, **H**=50µm, **I**,**J**=25µm. Table summarizing the demographics of patients from the University of South Florida HD transplant trial who have come to post-mortem. All patients that had surviving grafts a decade post-transplantation also demonstrated mHtt aggregates within these grafts. Graphs illustrate stereological counts of EM48+ aggregates in the host cortex and putamen, as well as in the two compartments of the transplanted tissue, p-zones and non p-zones. EM48+ aggregate size was also measured. Data are expressed as a mean ± SEM. All statistical analyses were performed using the step-down Bonferroni correction method. * p< 0.05 compared to the cortex; & p< 0.05 compared to the putamen; # p< 0.05 compared to the transplant p-zone.

Figure 4-2. MW7+ mHtt aggregates in grafted tissue

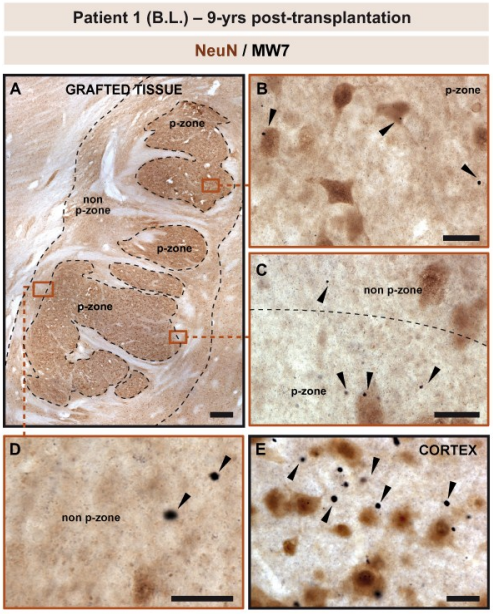

(**A**) Low magnification of double immunohistochemical staining for the neuronal marker NeuN (revealed with the chromogen DAB – brown color) and MW7 (mHtt aggregates) (revealed with nickel intensified DAB – black color) in patient 1 (B.L). MW7+ aggregates were found in transplanted tissue both within the p-zones (**B,C**) and non p-zones (**C**,**D**). Several MW7+ aggregates were also identified in the host HD cortex (**E**). Scale bars **A**=300µm, **B-E**=20µm.

Figure 4-3. Localization of EM48+ and MW7+ mHtt aggregates in grafted tissue

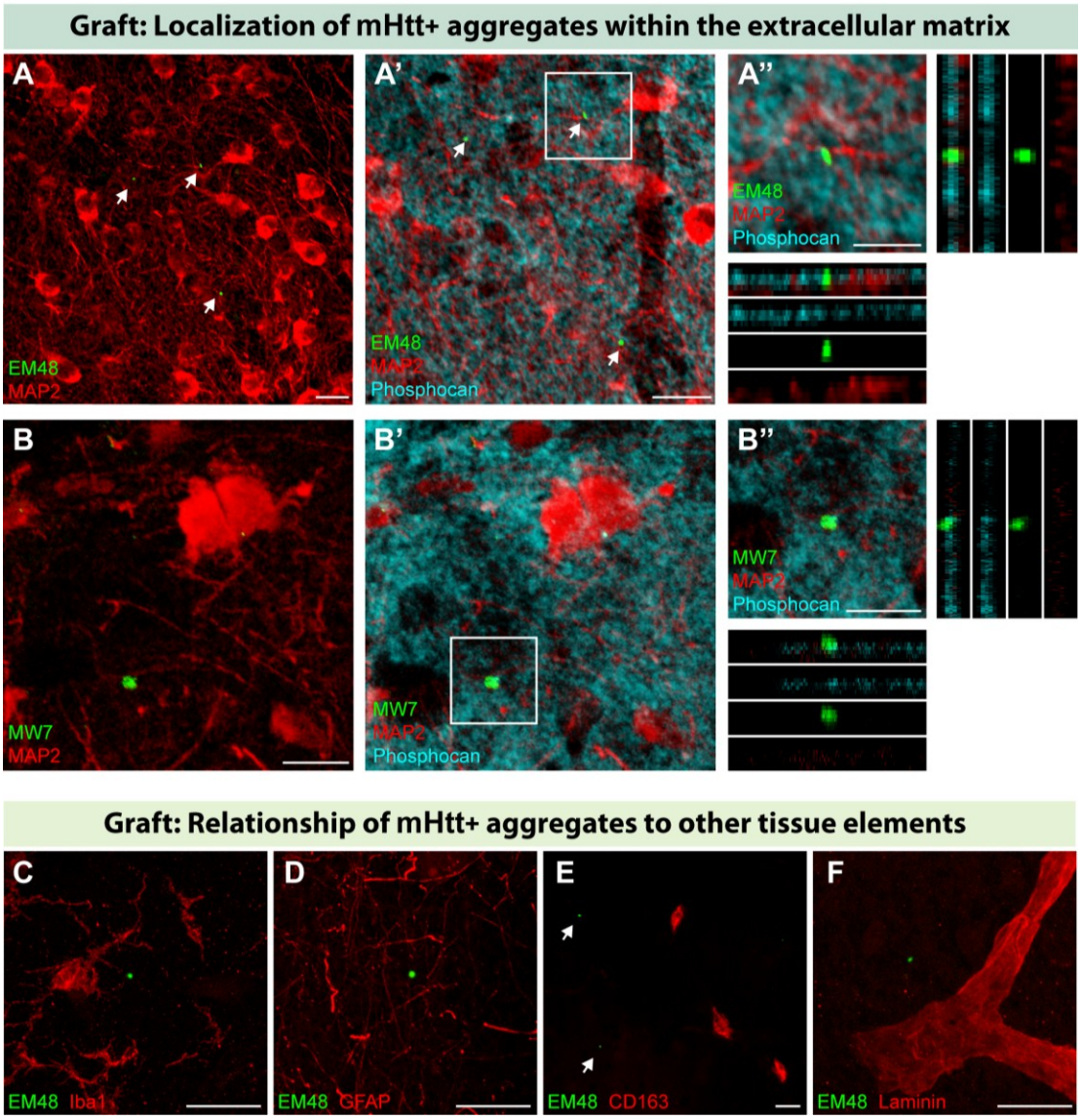

(**A**) Triple immunofluorescence for EM48 mHtt+ aggregates (green), MAP2 (neuronal marker in red) and phosphocan (extracellular matrix in cyan) depicting the localization of EM48 mHtt+ aggregates within the extracellular matrix. (**B**) Triple immunofluorescence for MW7 mHtt+ aggregates (green), MAP2 (red) and phosphocan (cyan) depicting the localization of MW7 mHtt+ aggregates within the extracellular matrix. Double immunofluorescence for EM48 with Iba1 (microglia) (**C**), GFAP (astrocyte) (**D**), CD163 (perivascular macrophage) (**E**) and laminin (basal lamina of blood vessels) (**F**) depicting the absence of co-localization of EM48+ aggregates with any of these makers within the grafted tissue. Scale bars **A**,**A'**=20µm, **A"**=10µm, **B**,**B'**,**B"**=20µm, **C-F**=20µm.

Figure 4-4. Localization of MW7+ mHtt aggregates in grafts and in the HD host cortex

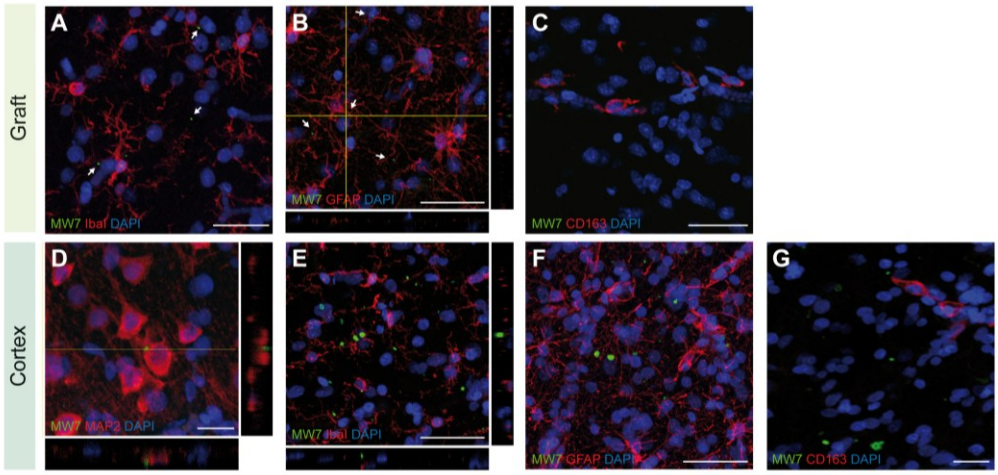

As observed for EM48+ staining, MW7+ aggregates identified within the grafts did not co-localize with neurones (MAP2 **– see Figure 2B**), microglia (Iba1, **A**), astrocytes (GFAP, **B**) and perivascular macrophages (CD163, **C**). In the HD host cortex, MW7+ aggregates (similar to EM48+ aggregates) were localized within neuronal elements (MAP2, **D**) but not found within microglia (Iba1, **E**), astrocytes (GFAP, **F**) or perivascular macrophages (CD163, **G**). Scale bars **A-D**=20µm, **E-G**=50µm.

Figure 4-5. Localization of EM48 mHtt+ aggregates in the HD host cortex

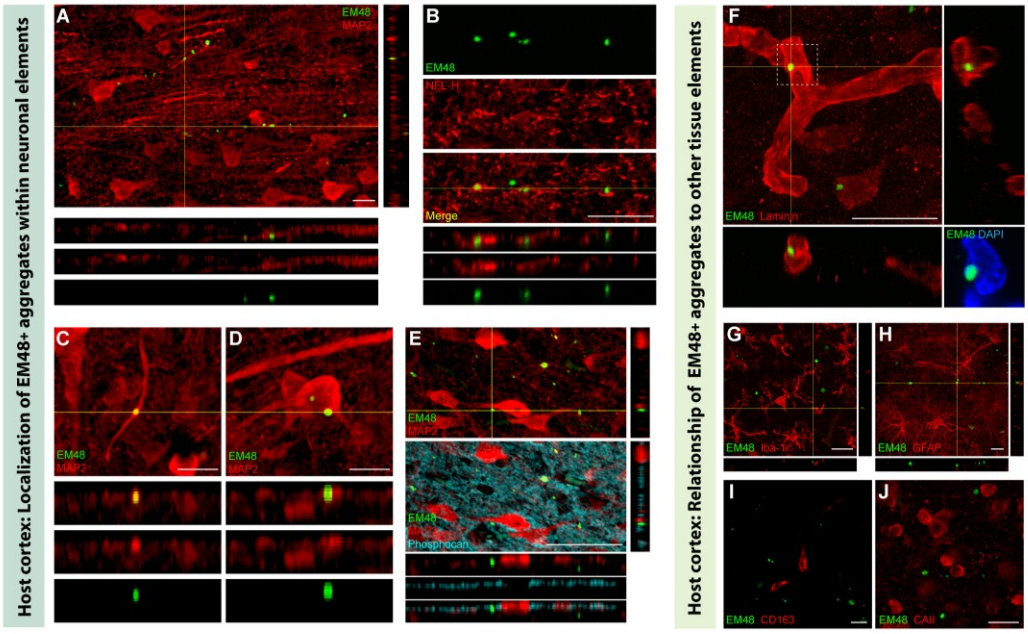

Double immunofluorescence for MAP2 (red) and EM48 (green) (**A**-**D**) demonstrating the co-localization of mHtt+ aggregates in dendrites (**A,C**) and soma (**D**) of cortical cells, as visualized in the brains of HD transplanted patients. The presence of EM48+ aggregates within dendrites of cortical cells was further demonstrated using a double immunofluorescent staining with Neurofilament H (**B**). A significant number of EM48+ aggregates were also found within the extracellular matrix of the host cortex, as demonstrated with the marker phosphocan (cyan) (**E**). EM48+ mHtt aggregates were also found in the basal lamina of blood vessels (**F**). Inset depicts an EM48+ inclusion within the nucleus of a cell-type associated with a blood vessel (DAPI staining in blue). EM48+ mHtt aggregates were not found in microglia (Iba1, **G**), astrocytes (GFAP, **H**), perivascular macrophages (CD163, **I**) nor in oligodendrocytes (CAII, **J**). Scale bars **A-J**=20µm.

Figure 4-6. Co-localization of EM48 and ubiquitin in grafts and in the HD host cortex

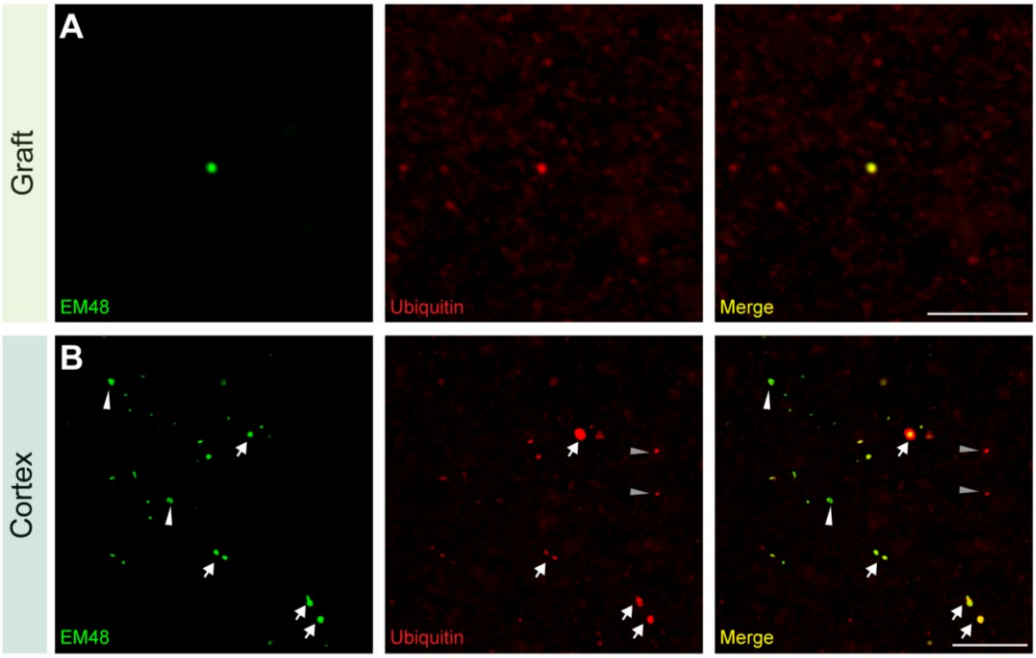

Double immunofluorescence staining depicting the co-localization of EM48 (in green) with the protein ubiquitin (in red) in both the graft (**A**) and the cortex of the HD patient (**B**). White arrows point to aggregates expressing both EM48 and ubiquitin, white arrowheads point to examples of singly labeled EM48 aggregates whereas gray arrowheads identify singly labeled ubiquitin+ elements. Scale bars in **A**=20µm, **B**= 50µm.

Figure 4-7. Co-localization of MW7, ubiquitin and EM48 in the HD host cortex

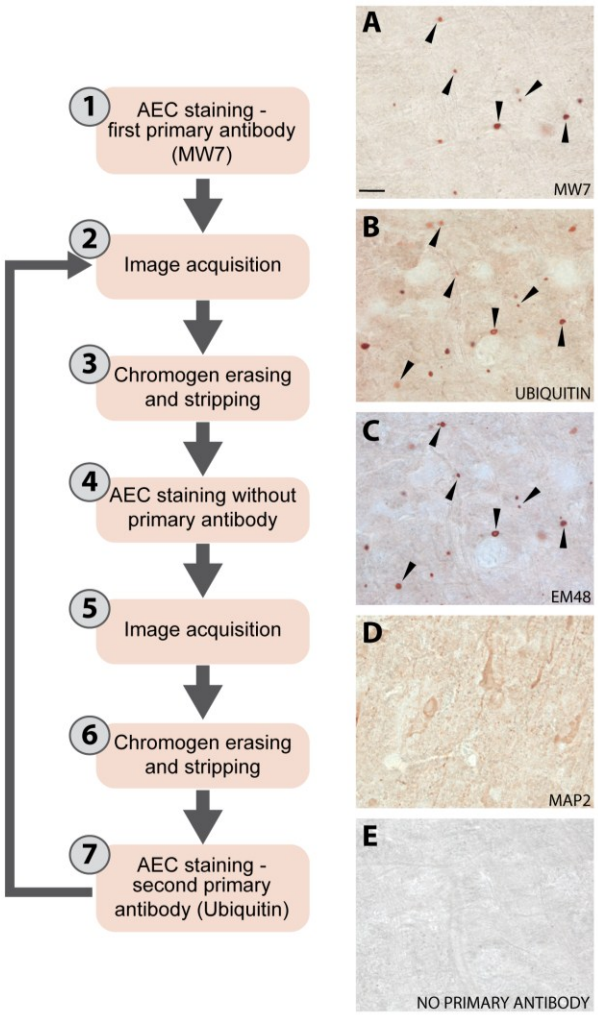

Sequential method for chromogenic immunohistochemistry demonstrates the co-localization (arrows) of MW7 (**A**), ubiquitin (**B**) and EM48 (**C**) in the HD host cortex. The MAP2 staining (**D**) or the image collected with no primary antibody (**E**) demonstrates the efficacy of the stripping method to completely erase the staining between steps. Scale bars in **A-E**= 50µm.

Figure 4-8. Detection of EM48+ mHtt aggregates by electron microscopy in grafts and in the HD host cortex

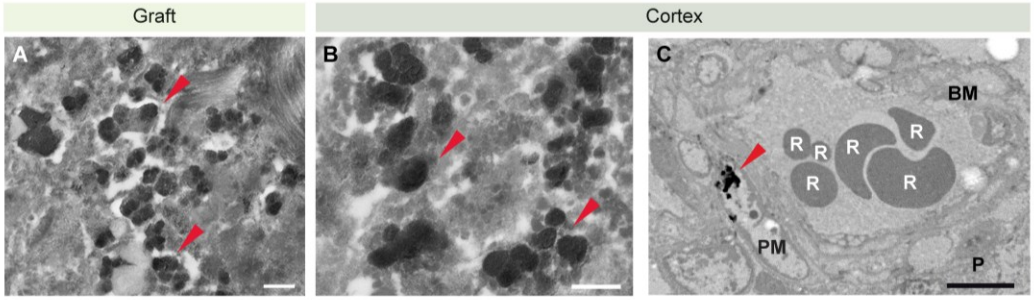

Electron microscopy revealed EM48 aggregates stained with nickel-intensified DAB (deposits pointed by red arrows) in the grafted tissue (**A**) as well as in the HD brain (**B**). Some of the nickel deposits (EM48 aggregates) appeared to be localized within perivascular macrophages in the HD brain (**C**). Scale bars **A**,**B**= 500nm, **C**= 5µm. Abbreviations. BM: Basal membrane; P: Pericytes; PM: Perivascular macrophage; R: red blood cell.

Figure 4-9. Detection of the mHtt protein by western immunoblotting in grafts and in the HD host cortex

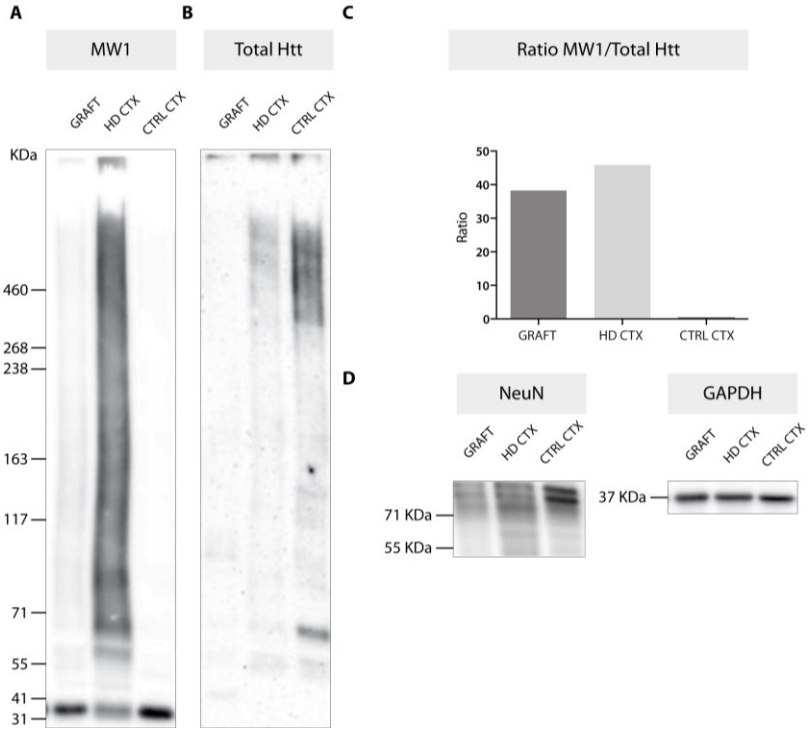

The expression of mutant (MW1, **A**) and total Htt (**B**) in samples extracted from fixed tissue derived from the cortex (CTX) of controls (CTRL), HD patients as well as in the allografted tissue (GRAFT) was quantified by western blot analyses. The ratio of mutant/total Htt (**C**) revealed higher levels in the HD CTX and GRAFT as compared to the CTRL brain. Neuronal Nuclei (NeuN) staining was used as a marker for neurons (**D**) and confirmed the quality of the extraction. The homogeneity of sample loading was determined by protein quantification and glyceraldehyde 3-phosphate dehydrogenase (GAPDH) staining (**D**).

Figure 4-10. Detection of mHtt aggregates by infrared spectroscopy in grafts and in the HD host cortex

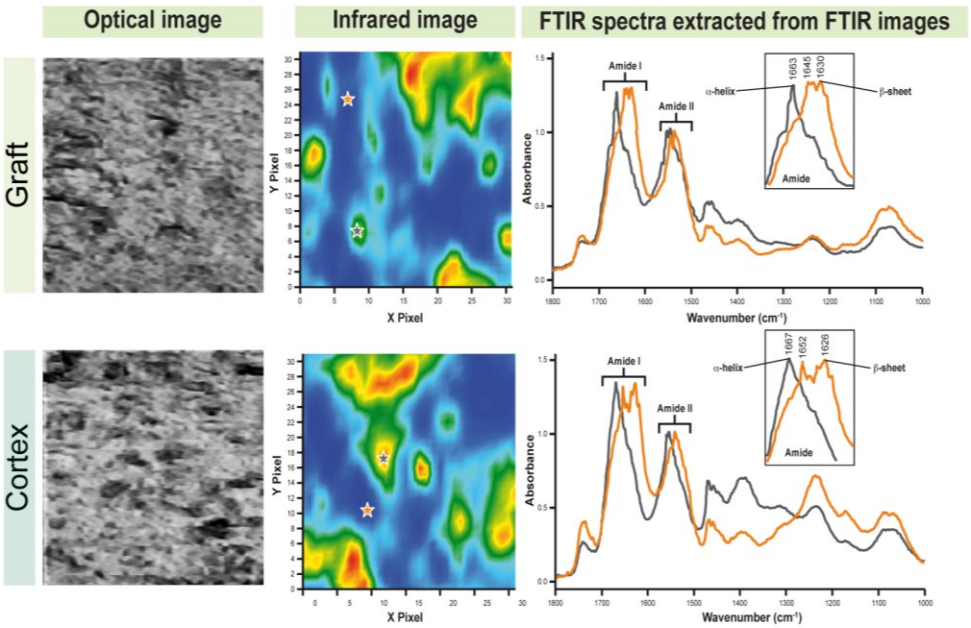

Optical images of unstained brain tissue sections (from the striatal graft and the transplant recipient's cortex) (left panels). Full spectral FTIR maps of the same tissue sections (175x175 µm) processed for the intensity of the protein at 1400cm^{-1} and FTIR spectra collected from the areas marked with asterisks (orange and gray, for HD cortical tissue and protein aggregates, respectively). Amide I mode (inset) discloses conformational changes in the samples due to the detection of protein aggregates. These characteristic spectroscopic changes, i.e. the increase in β-sheet content within the spectra, are evident from the unique fingerprint of a double peak at ~1630 cm^{-1} in the Amide I region (orange spectra), which indicates the presence of proteins with a β-sheet conformation. A similar fingerprint was seen in the grafted tissue, thus confirming a high content of β-sheet.

4.3.9 Supplementary table

Table 4-S1. List of primary and secondary antibodies

Primary antibody	Source	Catalog #	Host	Dilution	Note
Carbonic anhydrase II (CA II)	Dr. Said Ghandour	N/A	Rabbit	1:2000	IF – no PFA post-fixation
Cluster of differentiation 163 CD163 (K20-T)	Novus biological	NBP1-30148	Rabbit	1:100	IF – 4% PFA post-fixation
Various forms of mutant huntingtin protein (EM48)	Millipore	MAB5374	Mouse	1:200 IF	IF – Additional 4% PFA post-fixation if required for the antibody used in double immunofluorescence
				1:2000 IHC	IHC – 4% PFA post-fixation
Glial fibrillary acid protein (GFAP)	Dako Cytomation	Z0334	Rabbit	1:500	IF – 4% PFA post-fixation
Glyceraldeide 3-phosphate dehydrogenase (GAPDH)	Applied Biological Materials Inc.	G041	Mouse	1:7500	IB
Ionized calcium-binding adaptor molecule 1 (Iba1)	Wako Chemicals	019-19741	Rabbit	1:800	IF – 4% PFA post-fixation
Laminin (Associated with type IV collagen networks)	Dako Cytomation	Z0097	Rabbit	1:500	IF – 4% PFA post-fixation
Microtubule-Associated Protein 2 (MAP2)	Protein Tech	17490-1-AP	Rabbit	1:500	IF - 4% PFA post-fixation
Polyglutamine stretch (MW1)	Developmental Study Hybridoma Bank	N/A	Mouse	1:1000	IB
Polyproline stretch (MW7)	Developmental Study Hybridoma Bank	N/A	Mouse	1:100	IF - 4% PFA post-fixation IHC - 4% PFA post-fixation
Neurofilament H (NFL-H)	Millipore	AB5539	Chicken	1:400	IF – 4%PFA post-fixation
Neuron-specific nuclear protein (NeuN)	Millipore	MAB377	Mouse	1:2500	IHC – 4% PFA post-fixation
				1:1000	IB
Phosphocan (Clone 279244)	R&D system	MAB2688	Rat	1:100	IF – 4%PFA post-fixation
Total Htt (clone 1HU-4C8)	Millipore	MAB2166	Mouse	1:1000	IB
Ubiquitin	DAKO	Z0458	Rabbit	1:100	IF – 4%PFA

					post-fixation
				1:1000	IHC – 4%PFA post-fixation

Secondary antibody	Source	Catalog #	Host	Dilution	Note
Alexa 488 anti-mouse	Life Technologies	A21202	Donkey	1:500	N/A
Alexa 488 anti-rat	Life Technologies	A21208	Donkey	1:500	N/A
Alexa 546 anti-mouse	Life Technologies	A10036	Donkey	1:500	N/A
Alexa 546 anti-rabbit	Life Technologies	A10040	Donkey	1:500	N/A
Alexa 647 anti-rabbit	Life Technologies	A31573	Donkey	1:500	N/A
Biotinylated anti-mouse	Vector Laboratories	BA-9200	Goat	1:1500	N/A
Biotinylated anti-rabbit	Vector Laboratories	BA-1000	Goat	1:1500	N/A
Cy5 anti-chicken	Jackson Immunoresearch	103-175-155	Goat	1:500	N/A
HRP-conjugated anti-mouse	Jackson Immunoresearch	115-035-174	Goat	1:30000	IB

Abbreviations: IB: Immunoblot; IF: Immunofluorescence; IHC: Immunohistochemistry; N/A: not applicable

CHAPTER V

5. Discussion

During the course of my research project, I performed post-mortem histological analyses on brain tissue derived from HD transplanted patients taking part in the USF trial (Hauser et al., 2002). Initiated by Dr Thomas B. Freeman more than a decade ago, this pilot clinical trial comprised 7 HD patients who meet the eligibility criteria (see paragraph **1.3.2**) for cell transplantation (Hauser et al., 2002). Recruited patients received bilateral foetal striatal grafts derived from the far lateral ganglionic eminence. Five out the 7 patients came to autopsy between 18 months (Freeman et al., 2000) and 12 years post-transplantation (Cicchetti et al., 2009; Cisbani, Freeman, et al., 2013), providing the largest cohort of transplanted patients analysed post-mortem as well as the longest time point ever evaluated (12 years post-transplantation). My PhD dissertation builds on the initial observations reported by Dr. Cicchetti and her co-workers (Cicchetti et al., 2009). Before I began my PhD thesis, post-mortem analyses of the transplanted brain tissue had already revealed poor graft viability long-term. Based on these initial observations, we set out to investigate additional putative causes of graft demise in HD patients. **Chapter II** provides evidence for the lack of astrocytes as well as proper blood networks within the p-zones of the solid pieces of grafted tissue which could contribute to poor graft survival. To further address this, we transplanted a murine HD model, the YAC128, with cell suspension to investigate graft vasculature using this methodology (**Chapter III**). Contrary to the results obtained in the human brain, the grafts in the HD mouse brains was well-vascularized and showed good survival comparable to that seen in transplanted wild type mice. These observations suggest that the method of transplantation (cell suspension vs. solid graft) plays a role in revascularization and thus graft survival. In addition to this work, we have recently reported the presence of mHtt aggregates within the genetically unrelated grafted tissue. Although the mechanisms by which this may occur are still unknown, this is the first report of mutant protein transmission *in vivo*. In the following section, I will further discuss the putative mechanisms that may underlie poor graft survival long-term.

5.1 Putative mechanisms underlying compromised long-term graft survival

Previous published work by Cicchetti and colleagues suggested a series of mechanisms by which grafts could degenerate long-term (Cicchetti et al., 2009; 2011) (**Figure 5-1**). Amongst these mechanisms, it was suggested that aberrant glutamatergic cortical projections, connecting onto the grafted cells, could create excitotoxicity (1). It was further suggested that the absence of astrocytes within the grafted tissue, astrocytes which play a critical function in glutamate buffering, could exacerbate the excitotoxic phenomenon (2). An important microglial response was also observed around the grafts, which was proposed to further participate to graft degeneration via the release of

cytokines and pro-inflammatory molecules (3) or the impoverishment in neurotrophic support (4) (Cicchetti et al., 2009). Observations collected during my doctoral research project provided evidence for additional mechanisms of action underlying poor graft survival long-term. These include 5) poor graft-host interaction; 6) paucity of blood vessels within the grafted tissue (**Chapter II**) and 7) the presence of mHtt aggregates within grafts (**Chapter IV**) (**Figure 5-1**).

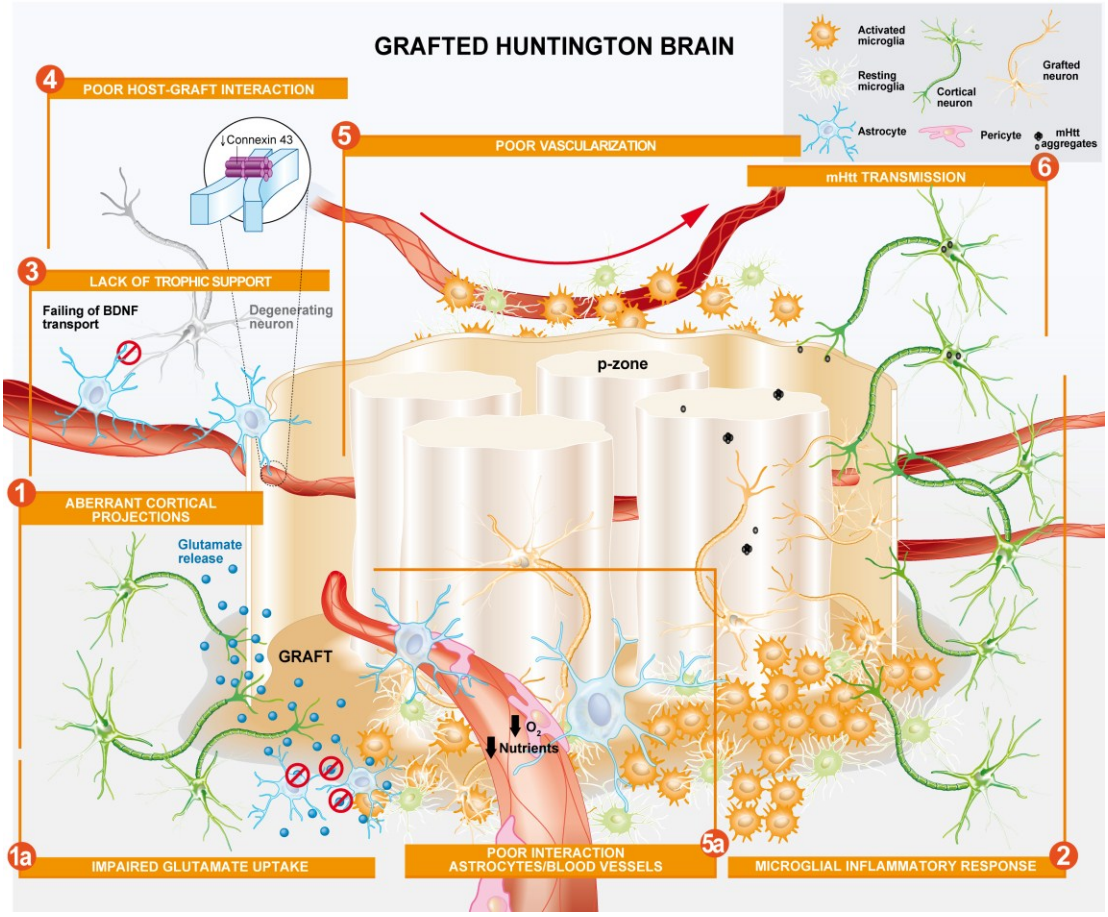

Figure 5-1. Putative mechanisms of action for compromised long-term graft survival. A compendium of the post-mortem analyses performed in 5 HD patients enrolled in the USF trial suggests that grafts survive up to 12 years. However, their survival appears compromised in the long-term and various mechanisms might be implicated in such poor graft survival. **1**) Grafts appear to receive aberrant cortical projections (**1**) which may lead to excitotoxicity within the transplant. This is associated with a lack of astrocytes within the grafted tissue. Given that these cells are critical for glutamate up-take, their apparent absence within the grafted tissue may further contribute to excitotoxic phenomenon (**1a**). The scarcity of astrocytes within the transplant also translates into the absence of the gap junction unit connexin 43, important in host-graft communication (**2**). The microglial inflammatory response observed around the graft, and more particularly around the p-zones, may further participate to graft degeneration through cytokine release and lack of trophic support (**3-4**). The lack of vasculature within the transplants may further compromise their integrity and ability to survive long-term (**5-5a**). Finally, the presence of mHtt aggregates within the grafted tissue could also impact graft viability (adapted from (Cisbani and Cicchetti, 2014).

5.1.1 Excitotoxicity and impaired glutamate up-take

Excitotoxicity is a very detrimental phenomenon that has been associated with the pathogenesis of HD. This event has been identified as one of the main cause of MSNs degeneration. Indeed, HD brains are characterized by abnormal levels of glutamate (Taylor-Robinson et al., 1996), especially in the striatum, which are likely to originate from the cortical-striatal projection neurons (Cowan and Raymond, 2006). The chronic exposure to abnormal levels of the neurotransimitter, concurrent with the impairment in re-uptake mechanisms (Levine et al., 2010), the high influx of ions that are neurotoxic at high concentration (Fan and Raymond, 2007) and the increased vulnerability of mHtt-expressing neurons to excitotoxic insults (Cowan and Raymond, 2006; Okamoto et al., 2009), may act in concert to render striatal neurons particularly vulnerable to degeneration (Cross et al., 1986; Levine et al., 2010).

Glutamatergic projection neurons of the cortex form synaptic contacts with the grafted striatal neurons, as previously shown both by immunohistochemistry and electron microscopy (Cicchetti et al., 2009) (**Figure 5-1**). Interestingly, the transplant seems to be more affected by pathological processes than the host striatum given the fact that the grafts are younger and genetically unrelated to the HD patient and that they have been exposed to the disease for about a decade. Instead of a positive influence of grafts on the cortex, the pathology affecting the cortex appears to induce neuronal degeneration within the grafts (Cicchetti et al., 2009). Despite recent evidence supporting the latter hypothesis in animal studies (Stack et al., 2007), the functional significance of this interaction remains unknown. It is also possible that glutamate is not the sole agent of striatal excitotoxicity (V. M. André et al., 2010; Raymond et al., 2011). For instance, dopamine released by nigral dopaminergic projections might act concomitantly with glutamate to generate oxidative stress and modulate glutamate release itself (Tang et al., 2007). In fact, decortication or 6-hydrohydopamine (6-OHDA) lesioning of the substantia nigra in R6/2 mice leads to behavioural improvements and significant increases in longevity. Animals also exhibit lower striatal glutamate concentrations, suggesting overall that the cortical and nigral pathways may act synergistically to induce excitotoxicity (Stack et al., 2007).

Astrocytes are key players in glutamate up-take and clearance, which takes place mainly via the gap junction (Scheckenbach et al., 2011). In HD brains, there is an increase in the density of astrocytes (Vonsattel et al., 1985) which correlates with an increase in the expression of the gap junction unit, connexin 43 (Cx43) (Vis et al., 1998). In HD, astrocytes also show lower levels of glutamate transporters such as glutamate transporter-1 (GLT1) or the glutamate-aspartate transporter (GLAST) (Hassel et al., 2008; Shin et al., 2005), which might impair glutamate buffering, thereby contributing to the excitotoxicity and degeneration of grafted cells (Cicchetti et al., 2009).

Interestingly, we observed that p-zones were impoverished in astrocytes, although different astrocyte morphologies were observed in non p-zones of the grafts (**Figure 2-7**). For example, higher densities of circumferential reactive astrocytic process occurred at the boarders of p-zones and non p-zones. Few atrophic astrocytes were also observed in the non p-zones and abundantly in the host striatum. Although the organization of the astrocytes surrounding the graft might be reminiscent of a glial scar, dopaminergic and cortical projections are penetrating in the transplanted tissue (Cicchetti et al., 2009; Cisbani, Freeman, et al., 2013), excluding this hypothesis. The observation of various types of astrocytes around the graft is very peculiar and the quasi absence of this cell type within the grafted tissue even more surprising, especially given that the dissection and implantation of a solid piece of tissue should contain a diversity of cell types, including astrocytes. This certainly raises questions about the involvement of astrocytes to graft demise (**Figure 5-1**).

5.1.2 Poor host-graft interaction: the role of gap junction

Functional interactions between donor and host cells have also been reported to occur via gap junction formation (Jäderstad et al., 2010; 2011). The interplay between neurons and astrocytes can provide neuroprotection, especially in early phases of donor-host interaction (Jäderstad et al., 2011). Cx43 is expressed at very low levels within the grafted tissue due to the almost complete lack of astrocytes, which might contribute to a compromised host-graft communication (**Figures 2-5 and 5-1**) (Cisbani, Freeman, et al., 2013). Glutamate and other neurotransmitters are normally taken up by astrocytes and extensively diluted in the astrocytic network through gap junction channels (Eugenin et al., 2012; Maragakis and Rothstein, 2006; Theis and Giaume, 2012). Because of the limitations inherent to post-mortem histological analyses, we cannot determine whether connexins expressed by glial cells around the p-zones are functional. However, it has been demonstrated that in pathologic conditions, gap junction channel formation is compromised and molecules such as glutamate can become toxic (Rose and Ransom, 1997; Wallraff et al., 2006). Changes in connexin expression in pathological conditions are not fully understood, but may contribute to the intercellular propagation of apoptotic signals. For example, mice heterozygous for Cx43 have a high risk of ischemia (Iadecola and Nedergaard, 2007; Maragakis and Rothstein, 2006). Cx43 also contributes to glucose transport from blood vessels to neurons (Maragakis and Rothstein, 2006; Tabernero et al., 2006), and therefore, its near absence within p-zones might result in poor nutrient support to donor cells.

5.1.3 Microglial response

One of the most critical steps in neuronal degeneration may originate from an adverse interaction with surrounding microglia (**Figure 5-1**) (C. K. Glass et al., 2010). Microglial activation against grafted tissue has long been described as an early event following neuronal grafting (Date et al., 1988; Lawrence et al., 1990; Shinoda et al., 1996). Soon following transplant, microglial cells have been found within the grafted tissue in non-immunized rats, although the response fades with time (Shinoda et al., 1996). Immune responses have been suggested to undermine viability and graft development (Lawrence et al., 1990).

In long-term post-mortem assessment of transplants in HD patients, one report showed that the microglial response was particularly centered around the p-zones of the grafts (Cicchetti et al., 2009). The specificity of the microglial response correlated with areas where grafted neuronal degeneration was most prominent. Conversely, microglial infiltration was minimal in graft regions rich in glial cell types despite their immunological similarity (Cicchetti et al., 2009). These data suggest that the phenotypic determinant of the cell type is the main factor responsible for the triggering of the microglial response rather than immunological aspects of the allografted tissue. In addition, grafted neuronal elements were closely associated with microglial cells. However, microglia play a dual role and can exert both beneficial or detrimental effects on grafted neurons (Cicchetti et al., 2011; C. K. Glass et al., 2010). Resting microglia may have a beneficial role by providing neurotrophic support or sensing the environment to clear cell debris and misfolded proteins (C. K. Glass et al., 2010). On the other hand, they can migrate to the site of injury and release various pro-inflammatory factors, which can become detrimental when delivered in a chronic and uncontrolled fashion (Garden and Möller, 2006; Nimmerjahn et al., 2005; Simard et al., 2006). It should be noted that similar observations were made in a transplanted PD patient where solid tissue grafts were also surrounded by an inflammatory response as early as 18 months post-surgery (Kordower et al., 1996).

5.1.4 Lack of trophic support

Adequate trophic support is also necessary for graft survival (Brundin et al., 2000; Cicchetti et al., 2011). Several studies in PD and HD animal models have repeatedly emphasized that only low number of cells survive transplantation (Cisbani, Saint-Pierre, et al., 2013; Sortwell, 2003; Terpstra et al., 2007). The reason for this is not well understood but it has been hypothesized that deficient trophic support may be implicated. For example, both pretreatment of cells derived from foetal ventral mesencephalon with basic fibroblast growth factor (bFGF) or GDNF and repeated parenchymal infusion of trophic

factors in transplanted 6-OHDA-lesioned rats significantly ameliorate dopaminergic cell survival and promote fibre outgrowth (Apostolides et al., 1998; Mayer et al., 1993; Y. Wang et al., 1996). GDNF pre-treatment of embryonic dopaminergic cells implanted in PD patients showed good survival and led to beneficial effects clinically (Mendez et al., 2000). However, animal studies in 6-OHDA-lesioned mice have reported that implanted dopaminergic cells pre-treated with BDNF show a lower survival rate, albeit leading to improved behavioural recovery (Zhou et al., 1997). Importantly, treatment with trophic factors favour a TH phenotype in foetal cells *in vitro* (Du and Iacovitti, 1995; Du et al., 1995).

BDNF has been shown to promote survival and to afford protection from excitotoxicity both *in vitro* (Almeida et al., 2005; Melo et al., 2013) and *in vivo* (Bemelmans et al., 2006). In normal conditions, BDNF is highly expressed in the cortex, especially in layer V, and retrogradely transported to the striatum (Altar et al., 1997; Baquet et al., 2005). The expression of mHtt interferes both with normal BDNF transcription (Zuccato and Cattaneo, 2009) and with the transport of vesicles along the microtubules (Cicchetti et al., 2011; Zuccato and Cattaneo, 2007), resulting in the depletion of BDNF derived from the cortical layer in the caudate and putamen (Ferrer et al., 2000). Mice depleted of cortical BDNF show reduced striatal volume and an altered dendritic morphology of the MSNs similarly to HD mouse models (Baquet et al., 2005). Since mHtt aggregates are found especially in layer V (Cicchetti et al., 2009) of the cortex, which projects onto the graft p-zones (Cicchetti et al., 2009; Raju and Smith, 2005), grafts may not receive adequate trophic support, making the grafted cells more susceptible to harmful factors derived from the diseased brain (**Figure 5-1**). In their report, Keene *et al*. suggested that incompatible and dissimilar expression of growth factors could promote the development of an intrinsic neuronal network within the transplant tissue but restricted to the boundaries of the cell implant (Keene et al., 2007). In HD brains, BDNF levels are reduced particularly in the caudate nucleus and the putamen (Ferrer et al., 2000; Zuccato et al., 2011), creating a detrimental environment for the graft. Similar decreases in BDNF and GDNF have been reported in the brain parenchyma of PD patients. The absence of appropriate neurotrophic support has long been suggested to lead to compromised homeostasis of the grafted neurons, including suitable defence mechanisms against oxidative stress (Brundin et al., 2008) and could further explain the low rate of dopaminergic cells survival in PD transplants (Deacon et al., 1997; Freed et al., 2001; Kordower et al., 1996; Lindvall and Hagell, 2000; Schumacher et al., 2000).

5.1.5 Poor graft vascularization

Grafted tissue that is promptly connected to the circulatory system and vascularized in the host has a better likelihood of survival (Lindsay and Raisman, 1984). Although brain foetal tissue is characterized by a well developed vasculature, it becomes strictly dependent on the host vascular network after implantation (Geny et al., 1994). Vascular perfusion of the graft is determined not only by the size of the transplant but also by the method of tissue preparation (solid tissue vs. cell suspension) (Broadwell et al., 1991; Nikkhah et al., 1994). Indeed, cell suspension favours graft vascularization (**Figure 3-2**) as we have shown in the HD mouse model YAC128 (Cisbani, Saint-Pierre, et al., 2013) (**Chapter III**). The importance of a well vascularized site of implantation has been previously demonstrated in rodent models (Stenevi et al., 1976). However, genetic disparity between the host and the graft, as well as the slow migration of endothelial cells of the host brain, which provide pro-angiogenic factors, may impact and delay the revascularization of the graft as demonstrated in a xenotransplant of human brain tissue into the rat (Geny et al., 1994).

Several years after transplantation, grafts in HD patients show reduced vascularization compared to host brain (Cisbani, Freeman, et al., 2013) (**Figure 5-1**). This is in agreement with previous observations in a PD patient also transplanted with foetal tissue chunks (Kordower et al., 1996). In the HD transplants, p-zones were completely devoid of large blood vessels, which may be expected given the blood supply derived from small vessel sprouts (Scott, 1984). Excitotoxicity from the cortico-striatal pathway, along with a significant microglial inflammatory response, may potentially further damage the vasculature (Cisbani, Freeman, et al., 2013). Reduced vascularization also translates into the absence of important cell types and important elements such as glucose transporters, which are necessary to maintain normal brain function. Furthermore, elements essential for the maintenance of BBB integrity, such as pericytes and astrocytes, are virtually absent within the grafts. The absence of pericytes, which are crucial in stabilizing the angioarchitecture during both development and adulthood, and which are involved in angiogenesis (Dore-Duffy et al., 2000), may very well contribute to poor revascularization of the graft (see **Chapter II**).

5.1.6 Pathological protein spreading

The last study presented in **Chapter IV** provides the first *in vivo* demonstration for the transfer of mHtt protein from the diseased brain to genetically unrelated neuronal grafted tissue. To date, only *in vitro* studies have demonstrated the possible cell-cell transfer of mHtt (Costanzo et al., 2013; Herrera et al., 2011; Ren et al., 2009; W. Yang et al., 2002).

5.1.6.1 Pathological protein spread

After the discovery of prion, the idea that protein can spread and act as a transmissible pathogen emerged (Brundin et al., 2010; Soto, 2012). A growing body of evidence now suggests that pathological misfolded proteins, such as amyloid β (Aβ), Tau and α-synuclein (α-syn) are capable of spreading in a prion-like fashion (Soto, 2012). For example, it has been demonstrated that Aβ can diffuse extracellularly and can be found within wild type neuronal grafts in a transplanted AD mouse model (Meyer-Luehmann et al., 2003). Additionally, an increased and accelerated burden in Aβ has been reported following the inoculation of brain extracts from AD patients or from aged AD mouse models into a transgenic model expressing the human amyloid precursor protein (Kane et al., 2000; Meyer-Luehmann et al., 2006). Similarly, implantation of brain extracts derived from a transgenic mouse model expressing a human Tau isoform into the hippocampus of a second transgenic mouse expressing the longer Tau isoform and that usually do not present inclusions, promoted the spreading of aggregation from the site of implantation to the neighbour regions (Clavaguera et al., 2009). The observation of LB in transplanted tissue in PD patients (Kordower et al., 2008; J. Y. Li et al., 2008) further supports the idea that the protein α-syn has the capacity to propagate throughout the brain. The observations made in the human PD transplanted brain were subsequently replicated in a mouse model. Transgenic mice expressing human α-syn were transplanted with GFP+ cortical neuronal stem cells in the hippocampus. The number of grafted cells containing inclusion bodies increased over time (Desplats et al., 2009). Furthermore, inoculations of brain extracts from aged α-syn expressing mice can seed aggregation in the recipient mouse and propagate in the brain regions via anatomically connected structures (Luk et al., 2012). The propagation properties of α-syn, Aβ and Tau have all been confirmed *in vitro.* The proteins can be taken-up by neuronal cells and have detrimental consequences (Danzer et al., 2011; Desplats et al., 2009). Overall, these observations indicate a prion-like spread of pathological proteins that could contribute to neurodegenerative processes (Brundin et al., 2010). Pathological proteins retain the ability to propagate from cell to cell, likely sharing some properties of the infectious misfolded prion proteins (Goedert et al., 2010). Importantly, this process may be common to all sporadic neurodegenerative disorders (de Calignon et al., 2012; Meyer-Luehmann et al., 2003; Olanow and Prusiner, 2009; Soto, 2012).

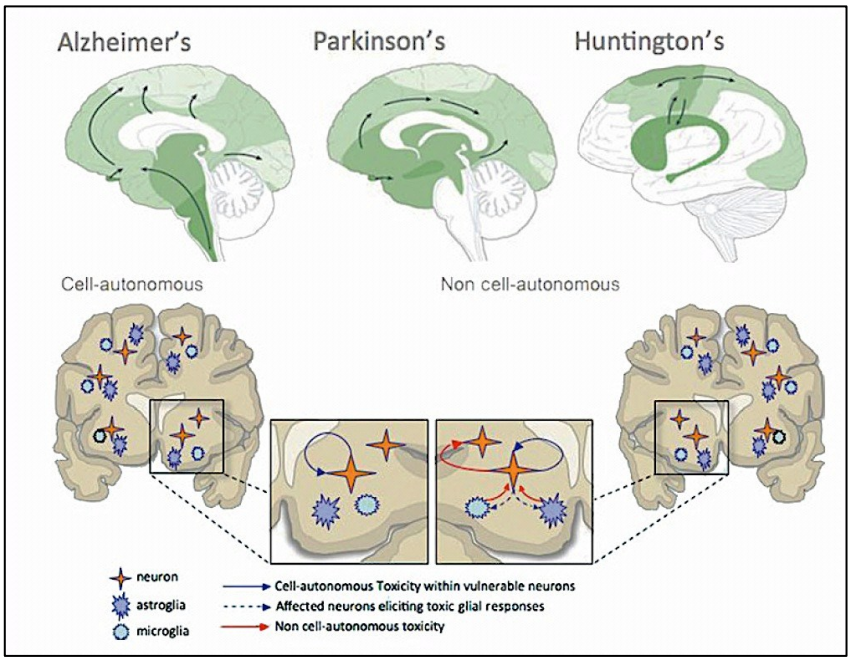

Figure 5-2. Progression of pathological changes in neurodegenerative diseases. Upper panel, schematic representation of the spatiotemporal progression of neuropathological changes during AD, PD and HD. A mid-sagittal view is shown for AD and PD and a lateral view for HD. Darker shading represents areas of the brain in which neuropathology develops earlier and the spreading patterns are indicated by arrows. In PD Lewy bodies and Lewy neurites appear first in the brainstem and the anterior olfactory structures. In AD, neurofibrillary tangles appear first in the hippocampus, the basal nucleus of Meynert and the brainstem. In HD, cortical degeneration seems to precede degeneration in the striatum. In each disorder, from the initial affected areas neuropathology progresses following predictable anatomical pathways. Lower panel, graphic representation of the concept of cell-autonomous and non-cell-autonomous degeneration with no anatomical reference to specific brain areas. Neurodegenerative diseases are traditionally viewed as diseases mainly affecting the most vulnerable neurons thus defining the characteristic feature of a given disorder. Selective degeneration and death occurs in neurons that are selectively susceptible to the disease-related alterations (indicated by the solid blue arrows, left-hand inset) and alone suffices to produce disease. Some brain areas are more resilient than others and resist the disease longer (cell-autonomous diseases, left-hand panel). Increasing evidence indicates that the convergence of damage occurring in multiple cell types, including neighbouring neuronal and non-neuronal cells (e.g. astroglia, microglia) (red arrows and broken blue arrows, right-hand inset) is crucial to determine the specific clinical picture of various neurodegenerative diseases (non-cell-autonomous diseases, right-hand panel). This synergistic form of cellular dysfunction may possibly account for selective neuronal loss in neurodegenerative diseases and in this frame prion-like transmission of protein aggregates might contribute to the gradual spreading of the pathology (Costanzo and Zurzolo, 2013).

5.1.6.2 mHtt protein transmission

The hypothesis that mHtt can propagate from cell to cell has been suggested by a very limited number of *in vitro* studies (Costanzo et al., 2013; Herrera et al., 2011; Ren et al., 2009; W. Yang et al., 2002). It has been reported that different cell types, such as neurons (COS7, HEK293T and PC12 cell lines) can take up and internalize synthetic mHtt aggregates exogenously delivered in the culture milieu (Ren et al., 2009; W. Yang et al., 2002). In these experiments, aggregates were localized within the cytoplasm, associated with proteins involved in the quality control of the cell, such as ubiquitin (Ren et al., 2009). When the synthetic protein was tagged with a sequence mediating its import into the nuclear compartment (nuclear localization signal), aggregates were translocated in the nucleus, leading to cell

death (W. Yang et al., 2002). These observations led to the conclusion that membranes are permeable to large fibrillar structures (Ren et al., 2009; W. Yang et al., 2002). Subsequently, another group developed a Biomolecular Fluorescence Complementation (BiFC)-based assay using non-fluorescent halves of the Venus protein tagged to mHtt. When mHtt oligomerized, a fluorescent signal was detected. To evaluate whether mHtt was able to propagate from cell to cell, the two halves were expressed independently in two separate cell populations and then mixed together. The mixed population presented a significant number of fluorescent cells, which demonstrated the capacity of the protein to migrate from cell to cell and act as a seed for further aggregation (Herrera et al., 2011).

The actual mechanisms underlying the propagation of mHtt to the grafts are still poorly understood. Here, I will discuss potential routes we believe may be involved in mHtt spread (**Figure 5-3**).

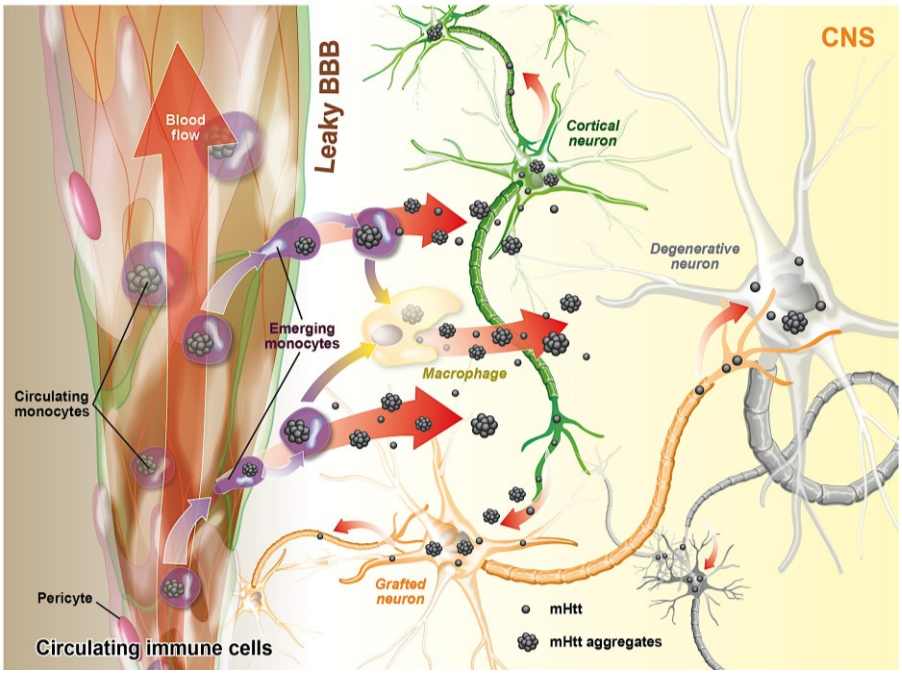

Figure 5-3. Potential routes for mHtt spread. Based on our combined observation, we hypothesize that mhtt spread could take place via transynaptic propagation, especially between cortical neurons which we have shown make contacts with grafted cells. The presence of mHtt in the circulatory monocytes ad some of our observation on BBB leakage in HD further support the potential spread of mHtt through immune cells. Finally, we also propose that microparticles which can be detach from circulatory immune cells in pathological conditions could also carry mHtt from the periphery to the brain (Conceptualization and design of the schema by Dr. Cicchetti and myself. Artwork completed by art designer Gilles Chabot).

5.1.6.3 Trans-synaptic propagation

Transynaptic transmission of mHtt from cortical projection neurons to the graft may be one of the routes of disease spread. This hypothesis is in part supported by the abundant expression of mHtt in the layer V of the cortex (Fusco et al., 1999) as well as by the evidence of synaptic connections between cortical neurons and grafted cells (Cicchetti et al., 2009). The ability of misfolded proteins to transfer

transynaptically has been previously reported in an AD model (de Calignon et al., 2012; Liu et al., 2012). Selective expression of Tau in the entorhinal cortex showed the propagation of the protein in other brain regions anatomically linked (de Calignon et al., 2012; Liu et al., 2012), where targeted cells were also reported to degenerate (de Calignon et al., 2012). Similarly, inoculation of brain lysates from aged α-syn-expressing mice or α-syn preformed fibrils in the brain of recipient mice, accelerated the formation of aggregates and protein spread in different regions. The protein was found in structures remote to the injection sites but which followed the anatomical circuits (Luk et al., 2012). It is thus plausible that mHtt aggregates are released into the graft through anatomical connections, and more specifically from cortical projections. Htt is indeed associated with axonal transport (Trushina et al., 2004) and synaptic transmission (Sun et al., 2001). However, we did not observe mHtt aggregates within any specific cell types of the graft, but exclusively within the extracellular matrix. It is thus also possible aggregates found in the grafted tissue are left behind from dying/dead cells.

5.1.6.4 mHtt propagation via tunnelling nanotubes

An alternative mechanism which has been recently suggested to take place in protein transmission is the tunnelling nanotubes (TNTs) that allow the direct transfer between the cytosolic compartments of adjacent cells. TNTs were first described during a live-imaging session of PC12 cells (Rustom et al., 2004) and subsequently described in other cell types such as the human embryonic kidney (HEK) 293T or normal rat kidney (NRK) cells (Rustom et al., 2004), macrophages, T cells, activated B cells and human glioblastomas cells (Gupta and DeFranco, 2003; Onfelt et al., 2004; 2006; Sowinski et al., 2008). TNTs are actin-rich cellular processes and they guarantee cell-cell continuity and communication, allowing the selective passage of vesicles and organelles (Rustom et al., 2004). The demonstration that mHtt can spread between neuronal cells through direct cell contact via TNTs was recently reported (Costanzo et al., 2013). Direct cell contact is required for the *in vitro* neuronal transfer of mHtt between cells carrying the mutated protein and those containing the normal protein. When the two cell populations are cultured separately and the culture media of the cells expressing the normal protein is substituted with the one derived from mHtt carrying cells, the transfer of the mutated protein is no longer observable (Costanzo et al., 2013). Importantly, it has been observed that prion transmission occurs via TNTs (Gousset et al., 2009) and similarly TNTs-transfer has also been suggested to occur for Aβ monomer and protofibrils (Y. Wang et al., 2011). Although TNTs represent a potential mechanism for pathology spread, there are still several questions that remain unanswered, especially those relating to the formation of TNTs, the directionality of the exchange and most importantly the frequency of the connections *in vivo* (Sherer, 2013).

5.1.6.5 Potential contribution of exomes and microparticles to mHtt propagation

Among the various hypotheses of disease spread, the possible involvement of extracellular vesicles, exosomes and microparticles (MPs) has also recently been suggested (Soto, 2012). Exosomes are small membrane vesicles (<100nm) derived from the fusion of multivesicular late endosome/lysosome with the plasma membrane. Unlike exosomes, which are released from intracellular compartments, MPs are larger (200-1000 nm), released from cytoplasmic membrane blebbing which carry part of the cytosolic and nuclear components of the parent cells (Beyer and Pisetsky, 2010; Boilard et al., 2012). Exosomes are secreted constitutively or in a regulated manner by a variety of cell types, both of hematopoietic (e.g. monocytes) or non-hematopoietic origins (e.g. neurons and neuroglia) (Lakkaraju and Rodriguez-Boulan, 2008; Théry et al., 2002; van Niel et al., 2006). They are found in physiological fluids, such as plasma, which may further serve as disease-specific biomarkers (Caby et al., 2005). The protein composition of the exosomes is dependent on the cell of origin. They are biologically active entities and they can interact with the target cells in different ways, such as by endocytosis or fusion with the plasma membrane (Lakkaraju and Rodriguez-Boulan, 2008; van Niel et al., 2006). MPs derived from platelet cells were the first to be described (Wolf, 1967), however MPs can be secreted by neutrophils, endothelial cells and fibroblasts (Beyer and Pisetsky, 2010; Boilard et al., 2012). MPs are released during cell activation or apoptosis (Beyer and Pisetsky, 2010; Boilard et al., 2012) and the expression of adhesion molecules favours their interaction with the recipient cells (Théry et al., 2009). The functions of the extracellular vesicles are not fully understood but several roles have been attributed to them. Of particular interest, exosomes have been identified as a vehicle of transmission for prions (Février et al., 2005). More recently, exosomes have been suggested to offer a route for the release of α-syn (Danzer et al., 2012; Emmanouilidou et al., 2010), Aβ (Rajendran et al., 2006; Vingtdeux et al., 2012) and SOD1 (Basso et al., 2013; Gomes et al., 2007) into the extracellular space. Extracellular vesicles do not have migratory activities, so one mechanism of transport into the central nervous system (CNS) may simply rely on their small dimensions. Small gaps in the leaky BBB may lead to diffusion of leukocyte-derived mHtt-containing vesicles, as it was recently shown in the synovial vasculature in murine models of arthritis (Boilard et al., 2012; Cloutier et al., 2013). Thus, extracellular vesicles found in the circulation could act as conveyors of mHtt. This topic remains unexplored in HD, thus further investigation will be necessary to evaluate whether exosomes and/or microparticles could be a route for disease propagation for this pathology as well.

5.1.6.6 mHtt spread via peripheral immune cells

To date, several studies have demonstrated the implication of peripheral immune dysfunction in HD progression. Elevated expression of the mutated protein have been detected in monocytes of HD patients, and its levels in leukocytes vary according to disease stage (Weiss et al., 2012), with increased levels of pro-inflammatory cytokines and chemokines in the early phases of the pathology (Björkqvist et al., 2008; Weiss et al., 2012 and unpublished observation). Lowering mHtt levels in immune cells of HD patients *ex vivo* via RNA interference (RNAi) reduced the cytokine production and limited transcriptional changes (Träger et al., 2014). Additionally, depletion of bone marrow cells and their replacement with wild type cells normalizes the levels of cytokines and chemokines in the murine model of HD, the YAC128 mouse, further generating moderate behavioural benefits (Kwan et al., 2012).

Although the BBB plays an important role in limiting the passage of large molecules and leukocytes to the brain parenchyma, peripheral immune cells can transmigrate during pathological conditions, such as multiple sclerosis and stroke, when the BBB integrity is compromised (Engelhardt, 2008; Ransohoff and Engelhardt, 2012; Wilson et al., 2010). Peripheral leukocytes (such as monocytes and neutrophils) that reach the brain parenchyma could partecipate to the deposition of mHtt into the brain by exocytosis (Batrakova et al., 2011). Infiltrated leukocytes could further contribute to mHtt spread by apoptosis and the consequential local release of the toxic non-degraded protein. In line with this hypothesis, it was recently reported that monocytes recruited to the brain following a stroke underwent apoptosis as early as 3 days post-infiltration (T. Li et al., 2013). Likewise, recruited monocytes to the brain following experimental autoimmune encephalitis (EAE) progression (a model of multiple sclerosis) are ultimately lost by apoptosis (Ajami et al., 2011). Finally, another study demonstrated that almost all cells died locally a few days following stroke or heart infarct, further inducing myeloid leukocyte recruitment (Leuschner et al., 2012). Therefore, it is possible that similarly in HD, monocytes carrying mHtt could be recruited to the brain (and grafted tissue) where local cell death may occur via apoptosis. Cell debris resulting from this could either be cleared phagocytic cells or left over as a mHtt aggregate deposit within the extracellular matrix.

Similarly to other proteins, such as Aβ (Tapiola et al., 2009) and α-syn (Parnetti et al., 2013; Tinsley et al., 2010), mHtt is also detected in plasma and CSF (Weiss et al., 2009) of patients. Therefore, plasma and CSF could facilitate the transmission of these proteins throughout the body. Interestingly, a recent study demonstrated the ability of radiolabelled Aβ to enter into the parenchyma via paravascular routes once injected into the CSF of the cisterna magna (Iliff et al., 2012). The study demonstrated the role of

astrocytes and aquaporine-4, a water channel localized on astrocytic end-feet, in mediating the clearance of the Aβ deposits. The absence of aquaporine 4 increased the Aβ burden (Iliff et al., 2012). We could speculate that the presence of mHtt aggregates within the graft may also derive from an impaired clearance mediated by astrocytes which, as we have described in previous chapters, are largely absent within the transplanted tissue. The cerebrovascular unit is still largely unexplored in HD, except for few reports (Franciosi et al., 2012; C.-Y. Lin et al., 2013), therefore, we do not know the extent of BBB leakage in this disease. Taken together a lot of work remains to be done to understand the role of immune response in the mechanisms of mHtt propagation.

5.2 Additional factors predicting graft success

Based on the large body of evidence for poor graft survival long-term as well as the suboptimal clinical benefits recorded, the future of cell transplantation for HD is questionable. Nonetheless, extensive research is currently ongoing to find alternative and suitable sources of cells to implant in the diseased brain. Some positive results have been already obtained in animal models of HD with stem cells (Lee et al., 2005; 2009; McBride et al., 2004; Ryu et al., 2004). However, the translation of these studies to the clinical practice will face the same problems encountered by foetal neuronal cells. A number of factors need to be taken into account to insure the success of the transplants. To some extent, graft outcomes can also be predicted by technical factors relating to the harvesting and preparation of donor tissue (see paragraphs **1.3.2.1** and **1.3.2.2**). Patient selection is also paramount and each characteristic, for example age at the time of transplantation, symptom duration, number of CAG repeats, time of transplantation from diagnosis and Unified Huntington's disease Rating Scale (UHDRS) motor score – if not chosen carefully, may jeopardize the significant clinical benefits that could be derived from this therapy.

Drawing conclusions from the very limited number of studies currently available is obviously a difficult task. Patients recruited so far show important variability regarding their age at the time of transplantation, their symptom duration, their number of CAG repeats, the time of transplantation from diagnosis and their UHDRS motor score. Nevertheless, we have attempted to analyze these parameters to determine whether any factor might account for the various behaviours observed for transplants between studies. For this purpose, we have excluded the cases analyzed at early time points after transplantation (Cicchetti et al., 2009; Cisbani, Freeman, et al., 2013; Keene et al., 2007; 2009). We thus arbitrarily assessed graft survival giving a score from 0 (no graft survival) to 5 (all grafts having survived) and performed Spearman correlation analysis with the selected parameters. These

analyses, although performed on a very limited number of cases (*n*=7), suggested that grafts survived better when implanted in younger patients (**Figure 5-4A**; Spearman *r* = -0.97101, *p* = 0.0012) who manifested symptoms for a shorter period of time (**Figure 5-4B**; Spearman *r* = -0.9255, *p* = 0.008). Surprisingly, patients with the higher number of CAG repeats showed better graft survival (**Figure 5-4C**; Spearman *r* = 0.93796, *p* = 0.0057). Although it is difficult to explain how higher CAG repeats may not be detrimental to graft survival, our analysis suggests that younger patients at earlier phases of disease progression may be better candidates for transplantation, as severe brain atrophy may represent a less than favorable niche for graft survival and integration.

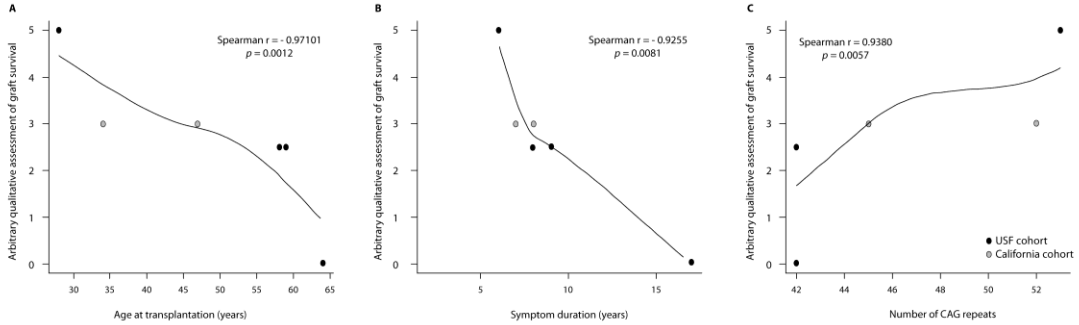

Figure 5-4. Correlations of graft survival with age at the time of transplantation, symptom duration and CAG repeats. Spearman correlation analyses were performed between the qualitative assessment of graft survival (see method below) and various parameters related to the HD patients, namely the age of at the time of transplantation, the symptom duration (years), the number of CAG repeats, the time of transplantation from diagnosis and their UHDRS motor score (see also Table 2). Linear regression analysis was only performed using the transplanted HD cases that were analyzed several years after transplantation, which included 7 patients from 2 distinct trials (Hauser et al., 2002; Kopyov et al., 1998). Despite the limited number of patients, graft survival correlated with age at transplantation, suggesting that grafts survive better in younger patients (A; Spearman *r* = -0.97101, *p* = 0.0012). Graft survival also positively correlated with symptom duration (B; Spearman *r* = -0.9255, *p* = 0.008) and it negatively correlated with CAG repeats, indicating that patients with a higher number of CAG repeats presented better graft survival (C; Spearman *r* = 0.93796, *p* = 0.0057). *Method:* Graft survival was determined arbitrarily using a scale from 0 (no grafts surviving in the patient brain) to 5 (all grafts surviving in the patient brain). The strength of the relationships between the arbitrary qualitative assessment of graft survival and the other variables was investigated using the non-parametric Spearman correlation. This type of correlation was chosen to evaluate the presence of a monotonic relation between variables instead of a simple linear relationship, as estimated with parametric Pearson correlations. Another advantage of the Spearman correlation is that no assumption is made on the type of probability distribution for the variables studied. However, the power of the test is relatively low since only 7 patients were included, but correlations may still be studied from an exploratory point of view. For instance, if we applied a Bonferroni correction to control for the type I error rate, the correlations would have to be >0.8586 to be significant (Sokal and Rohlf, 1995). This cut-off value was obtained using the Fisher *z*-transformation applied to the sample correlation coefficient. All statistical analyses were performed by the *Service de Consultation Statistique* of *Université Laval* using SAS (version 9.3, SAS, Cary, NC) and the graphs generated with R software (2013). Abbreviation: USF: University of South Florida (Cisbani and Cicchetti, 2014).

5.3 Consequences for the presence of mHtt in the genetically unrelated grafts in HD patients

In addition to neurons, it is highly plausible that other cell types also participate to mHtt propagation and degenerative processes (La Spada et al., 2011; Polymenidou and Cleveland, 2011). Recently, a new transgenic mouse model was generated to express the N-terminal domain of mHtt under the GFAP

promoter, promoting the selective expression of the protein in astroglial cells. Although the protein expression was lower than endogenous levels, the mice developed neurological symptoms in an age-dependent manner with weight loss, motor decline and reduced lifespan (Bradford et al., 2009). In our study, we were not able to detect the presence of mHtt aggregates within glial cells of the host brain nor of the transplant. Our observations are in agreement with previous studies reporting the absence (Becher et al., 1998; Sapp et al., 1997; Sieradzan et al., 1999) or rare occurrence (Herndon et al., 2009; Sieradzan et al., 1999) of mHtt staining in glial cells. This is also consistent with previous observations describing low expression of *htt* mRNA in glial cells (Landwehrmeyer et al., 1995). However, we cannot totally exclude the presence of soluble mHtt in glial cells, which we were not able to identify because specific antibodies were unavailable (see paragraph **5.2.1**). Additionally, the mHtt turnover might be different in glial cells and neurons. A more efficient ubiquitin proteasome system was reported in glial cells which may account for the preferential accumulation of the aggregates in neuronal cells (Tydlacka et al., 2008).

New insights into the pathology of HD can be acquired from the presence of mHtt aggregates into the grafted normal tissue. mHtt propagation from cell to cell might play a role in the disease development and progression. However, the implications of this event are still unclear. The transmission of the mutated form of the protein from the host brain could contribute to the aggregation burden, also recruiting the normal Htt protein from the donor tissue as previously demonstrated in *in vivo* (Wheeler et al., 2000) and *in vitro* models (de Cristofaro et al., 2000). Interestingly, it has been shown that aggregates might have a protective role, while cells containing the soluble form of the mutant protein are more prone to die (Arrasate et al., 2004). The role of mHtt aggregates and the soluble oligomers is still highly debated (Kaytor et al., 2004; Poirier et al., 2005; Saudou et al., 1998). For example, we were not able to identify the soluble mHtt within the grafted tissue because of the lack of suitable antibody detecting this form of the protein (see paragraph **5.2.1**). Understanding the implications for the presence of mHtt aggregates within the grafts will require further *in vitro* and *in vivo* experiments.

5.3.1 Challenges in the post-mortem detection of mHtt aggregates: technical considerations

The detection of mHtt is particularly challenging, due to the limited availability of suitable antibodies, especially for differentiating between the soluble and aggregated form of the protein. Antibodies recognizing various fragments of the protein have been developed (Becher et al., 1998; DiFiglia et al., 1995; 1997; Gutekunst et al., 1995; 1998; Hoffner et al., 2005; Persichetti et al., 1996; Sapp et al., 1997; Sieradzan et al., 1999; Trottier et al., 1995) with the intent of discerning and characterizing the

mutated and normal Htt using immunocytochemical and biochemical techniques (**Figure 5-5**). Only N-terminal antibodies are able to detect inclusions (Becher et al., 1998; DiFiglia et al., 1997; Sieradzan et al., 1999), leading to the conclusion that the aggregates are constituted only of the regions upstream of the cleavage sites (Sieradzan et al., 1999). C-terminal antibodies do not detect aggregates nor can they discern between the normal and mutated protein (Sapp et al., 1997), suggesting that this portion of the protein is not present within the inclusions. Interestingly, antibodies recognizing specifically the polyQ stretch, such as 1C2, MW1 and 3BH10, are able to selectively detect the mutated fragment but only using immunoblotting techniques (Ko et al., 2001; Sapp et al., 2012; Weiss et al., 2012). In post-mortem immunohistochemical analyses these antibodies can detect the cytoplasmic soluble Htt but it is not possible to differentiate between the normal and mutated protein nor to recognize aggregates (Herndon et al., 2009; Khoshnan et al., 2013; Sieradzan et al., 1999). However, the antibody MW1 allowed us to detect the presence of the polyQ fragments in the graft and in the host tissue by immunoblotting (**Figure 4-9**). One of the most used antibody for mHtt aggregates is EM48 (Kuemmerle et al., 1999), which encompasses the first 256 amino acids (Gutekunst et al., 1998; 1999). Additionally, EM48 is capable of detecting a larger number of aggregates compared to other similar antibodies (Becher et al., 1998; DiFiglia et al., 1997). Recently, the group of Patterson developed a number of antibodies to detect mHtt. Amongst them, MW7 and MW8 are able to detect mHtt aggregates on mouse tissue by immunohistochemistry (Ko et al., 2001). MW7 recognizes the polyproline stretch that follows the polyQ sequence in the protein while the binding of MW8 is within the polyQ region. These antibodies were not tested on human tissue, but we successfully stained aggregates using MW7 on our human transplanted tissue. We were further able to demonstrate that MW7 recognizes EM48+ and Ubiquitin+ aggregates (**Figure 4-6**). In our study, we used the strength of a number of techniques (immunofluorescence, immunohistochemistry, electron microscopy, infrared spectroscopy and immunoblot) to prove the presence of mHtt within the grafted tissue.

A

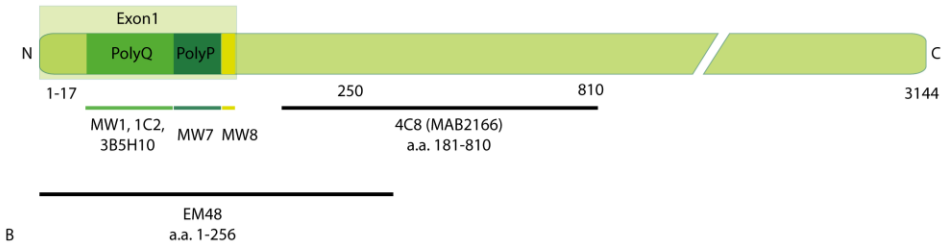

B

Antibody	Epitope	Specificity	IHC/IF	IB
1C2	PolyQ	Recognizes both wt Htt and mHtt	Punctuated staining within the cytoplasm of various brain cells (unlike aggregate) (works on free floating and parrafin sections)	Detects mHtt but not wt Htt
3BH510	PolyQ	Recognizes both wt Htt and mHtt	Punctuated staining within the cytoplasm of various brain cells (unlike aggregate) (works on free floating and parrafin sections)	NI
MW1	PolyQ	Recognizes both wt Htt and mHtt	Punctuated staining within the cytoplasm of various brain cells (unlike aggregate) (works on free floating and parrafin sections)	Detects mHtt but not wt Htt
MW7	PolyP	Binds all peptides with >5 consecutive prolines	Stains aggregates within neuronal and non-neuronal elements throughout the brain (works on free floating and parrafin sections)	Does not work
MW8	AEEPLHRPK stretch next to PolyP	Recognizes the aggregated form of mHtt Epitope not detectable in the soluble form	Stains aggregates within neuronal and non-neuronal elements throughout the brain (works only on paraffin sections)	Detects wrong MW
EM48	a.a. 1-256	Recognizes the aggregated form of mHtt	Stains aggregates within neuronal and non-neuronal elements throughout the brain (works on free floating and parrafin sections)	Does not work
4C8	a.a. 181-810	Recognizes both wt Htt and mHtt	NI	Detects mHtt and wt Htt
Ubiquitin	Ubiquitin	Recognizes the ubiquitinated form of mHtt aggregates	Stains aggregates within neuronal and non-neuronal elements throughout the brain (works on free floating and parrafin sections)	Does not work

Figure 5-5. List of mHtt antibodies utilized to detect mHtt. Map of Htt protein (**A**) and list of the antibodies, epitopes recognized as well as their specificity (**B**). The columns IHC/IF and IB report personal observations collected following the staining of HD and control tissue. Abbreviations: IB, immunoblot; IF, immunofluorescence; IHC, immunohistochemistry; mHtt, mutant huntingtin; MW, molecular weight; NI, not investigated; PolyP, polyproline stretch; Poly Q, polyglutamine stretch; wt Htt, wild type huntingtin.

5.4 Perspectives

mHtt propagation is a fairly novel concept in HD compared to the extensive research already performed in other neurodegenerative diseases, such as AD and PD. The investigation of mHtt transmission in the CNS via the different routes proposed in this thesis is likely to provide new insights into the properties of the mutated protein and into the disease progression. As we have discussed throughout this thesis, one possible route of disease transmission may occur via transynaptic connections. The development of *in vivo* models based on the focal expression of mHtt within the cortex, via injections of lentiviral vectors or the injection of mHtt-expressing brain lysate, will allow to evaluate the potential of mHtt to

travel to synaptically connected sites. Additional routes of disease transmission may occur via leukocytes and exosomes/microparticles. Research strategies aiming to determine whether leukocytes-derived mHtt or vesicles-associated mHtt are capable of spreading into the CNS will need to be developed. Despite the fact that mHtt expression in leukocytes has been reported to correlate with both disease progression and brain atrophy, it has not been explored whether they contribute to development of the brain pathology. A single study has reported limited beneficial effects on the disease progression following bone marrow cell transplantation in two animal models of HD (Kwan et al., 2012). Experiments using chimeric approaches with transplantation of bone marrow cells expressing fluorescent protein will allow to better understand whether leukocytes expressing mHtt are capable to migrate to the brain and whether they contribute to mHtt aggregate burden. Monocytes are also capable of releasing exosomes/microparticles. The analysis of these vesicles from human plasma samples will be critical to support this hypothesis of their involvement in disease progression.

5.5 Conclusions

HD is a devastating fatal neurodegenerative disease without effective treatments. Neuronal cell transplantation is one of the sole treatments that has resulted in temporary beneficial effects. The post-mortem study of transplanted HD patients provides the unique opportunity to understand why grafts have yielded sub-optimal clinical outcomes. This is essential to improve the long-term efficacy of this approach, particularly if such therapies will be applied in young patients with an expectation of lifetime benefit or for future stem cell therapy, which will be facing the same challenges. We believe that our analyses will have direct impact on patients suffering of HD. Our observations will be useful for the new clinical trials in cell transplantation currently ongoing in Europe (Multicentric Intracerebral Grafting in Huntington's Disease; MIG-HD). Additionally, this new knowledge can be extended to other neurodegenerative diseases, such as PD and amyotrophic lateral sclerosis.

References

Adam OR, Jankovic J. Symptomatic treatment of Huntington disease. Neurotherapeutics 2008; 5: 181–197.

Addis MF, Tanca A, Pagnozzi D, Crobu S, Fanciulli G, Cossu-Rocca P, et al. Generation of high-quality protein extracts from formalin-fixed, paraffin-embedded tissues. Proteomics 2009; 9: 3815–3823.

Ajami B, Bennett JL, Krieger C, McNagny KM, Rossi FMV. Infiltrating monocytes trigger EAE progression, but do not contribute to the resident microglia pool. Nat. Neurosci. 2011; 14: 1142–1149.

Akalan N, Grady MS. Angiogenesis and the blood-brain barrier in intracerebral solid and cell suspension grafts. Surgical neurology 1994; 42: 517–522.

Almeida CG, Tampellini D, Takahashi RH, Greengard P, Lin MT, Snyder EM, et al. Beta-amyloid accumulation in APP mutant neurons reduces PSD-95 and GluR1 in synapses. Neurobiol. Dis. 2005; 20: 187–198.

Altar CA, Cai N, Bliven T, Juhasz M, Conner JM, Acheson AL, et al. Anterograde transport of brain-derived neurotrophic factor and its role in the brain. Nature 1997; 389: 856–860.

Anderson KD, Panayotatos N, Corcoran TL, Lindsay RM, Wiegand SJ. Ciliary neurotrophic factor protects striatal output neurons in an animal model of Huntington disease. Proc. Natl. Acad. Sci. U.S.A. 1996; 93: 7346–7351.

André VM, Cepeda C, Levine MS. Dopamine and glutamate in Huntington's disease: A balancing act. CNS Neurosci. Ther. 2010; 16: 163–178.

André W, Sandt C, Dumas P, Djian P, Hoffner G. Structure of Inclusions of Huntington's Disease Brain Revealed by Synchrotron Infrared Microspectroscopy: Polymorphism and Relevance to Cytotoxicity. Anal. Chem. 2013; 85: 3765-3773.

Ang ESBC, Haydar TF, Gluncic V, Rakic P. Four-dimensional migratory coordinates of GABAergic interneurons in the developing mouse cortex. J. Neurosci. 2003; 23: 5805–5815.

Anthony TE, Klein C, Fishell G, Heintz N. Radial glia serve as neuronal progenitors in all regions of the central nervous system. Neuron 2004; 41: 881–890.

Apostolides C, Sanford E, Hong M, Mendez I. Glial cell line-derived neurotrophic factor improves intrastriatal graft survival of stored dopaminergic cells. Neuroscience 1998; 83: 363–372.

Arrasate M, Mitra S, Schweitzer ES, Segal MR, Finkbeiner S. Inclusion body formation reduces levels of mutant huntingtin and the risk of neuronal death. Nature 2004; 431: 805–810.

Atwal RS, Xia J, Pinchev D, Taylor J, Epand RM, Truant R. Huntingtin has a membrane association signal that can modulate huntingtin aggregation, nuclear entry and toxicity. Hum. Mol. Genet. 2007; 16: 2600–2615.

Aziz NA, Pijl H, Frölich M, van der Graaf AWM, Roelfsema F, Roos RAC. Increased hypothalamic-pituitary-adrenal axis activity in Huntington's disease. J. Clin. Endocrinol. Metab. 2009; 94: 1223–1228.

Bachoud-Lévi A, Bourdet C, Brugières P, Nguyen JP, Grandmougin T, Haddad B, et al. Safety and tolerability assessment of intrastriatal neural allografts in five patients with Huntington's disease. Exp. Neurol. 2000; 161: 194–202.

Bachoud-Lévi A-C, Gaura V, Brugières P, Lefaucheur J-P, Boissé M-F, Maison P, et al. Effect of fetal neural transplants in patients with Huntington's disease 6 years after surgery: a long-term follow-up study. Lancet Neurol. 2006; 5: 303–309.

Bachoud-Lévi A-C, Hantraye P, Peschanski M. Fetal neural grafts for Huntington's disease: a prospective view. Mov. Disord. 2002; 17: 439–444.

Bachoud-Lévi AC, Rémy P, Nguyen JP, Brugières P, Lefaucheur JP, Bourdet C, et al. Motor and cognitive improvements in patients with Huntington's disease after neural transplantation. Lancet 2000; 356: 1975–1979.

Backlund EO, Granberg PO, Hamberger B, Knutsson E, Mårtensson A, Sedvall G, et al. Transplantation of adrenal medullary tissue to striatum in parkinsonism. First clinical trials. J. Neurosurg. 1985; 62: 169–173.

Baker-Cairns BJ, Sloan DJ, Broadwell RD, Puklavec M, Charlton HM. Contributions of donor and host blood vessels in CNS allografts. Exp. Neurol. 1996; 142: 36–46.

Baquet ZC, Bickford, P. C., Jones KR. Brain-derived neurotrophic factor is required for the establishment of the proper number of dopaminergic neurons in the substantia nigra pars compacta. J. Neurosci. 2005; 25: 6251–6259.

Barker RA, Mason SL, Harrower TP, Swain RA, Ho AK, Sahakian BJ, et al. The long-term safety and efficacy of bilateral transplantation of human fetal striatal tissue in patients with mild to moderate Huntington's disease. J. Neurol. Neurosurg. Psychiatr. 2013; 84: 657:665

Barker RA, Widner H. Immune problems in central nervous system cell therapy. NeuroRx 2004; 1: 472–481.

Basso M, Pozzi S, Tortarolo M, Fiordaliso F, Bisighini C, Pasetto L, et al. Mutant copper-zinc superoxide dismutase (SOD1) induces protein secretion pathway alterations and exosome release in astrocytes: implications for disease spreading and motor neuron pathology in amyotrophic lateral sclerosis. J. Biol. Chem. 2013; 288: 15699–15711.

Batrakova EV, Gendelman HE, Kabanov AV. Cell-mediated drug delivery. Expert Opin. Drug Deliv. 2011; 8: 415–433.

Beal MF, Bird ED, Langlais PJ, Martin JB. Somatostatin is increased in the nucleus accumbens in Huntington's disease. Neurology 1984; 34: 663–666.

Beal MF, Kowall NW, Ellison DW, Mazurek MF, Swartz KJ, Martin JB. Replication of the neurochemical characteristics of Huntington's disease by quinolinic acid. Nature 1986; 321: 168–171.

Beal MF, Martin JB. Effects of lesions on somatostatin-like immunoreactivity in the rat striatum. Brain Res. 1983; 266: 67–73.

Becher MW, Kotzuk JA, Sharp AH, Davies SW, Bates GP, Price DL, et al. Intranuclear neuronal inclusions in Huntington's disease and dentatorubral and pallidoluysian atrophy: correlation between the density of inclusions and IT15 CAG triplet repeat length. Neurobiol. Dis. 1998; 4: 387–397.

Bemelmans A-P, Husson I, Jaquet M, Mallet J, Kosofsky BE, Gressens P. Lentiviral-mediated gene transfer of brain-derived neurotrophic factor is neuroprotective in a mouse model of neonatal excitotoxic challenge. J. Neurosci. Res. 2006; 83: 50–60.

Beyer C, Pisetsky DS. The role of microparticles in the pathogenesis of rheumatic diseases. Nat. Rev. Rheumatol. 2010; 6: 21–29.

Biglan KM, Zhang Y, Long JD, Geschwind M, Kang GA, Killoran A, et al. Refining the diagnosis of Huntington disease: the PREDICT-HD study. Front Aging Neurosci. 2013; 5: 12.

Björklund A, Dunnett SB, Stenevi U, Lewis ME, Iversen SD. Reinnervation of the denervated striatum by substantia nigra transplants: functional consequences as revealed by pharmacological and sensorimotor testing. Brain Res. 1980; 199: 307–333.

Björklund H, Hoffer BJ, Palmer MR, Seiger A, Olson L. Survival and growth of neurons with enkephalin-like immunoreactivity in fetal brain areas grafted to the anterior chamber of the eye. Neuroscience. 1983; 10:1387-98

Björklund A, Schmidt RH, Stenevi U. Functional reinnervation of the neostriatum in the adult rat by use of intraparenchymal grafting of dissociated cell suspensions from the substantia nigra. Cell Tissue Res. 1980; 212: 39–45.

Björklund A, Stenevi U, Schmidt RH, Dunnett SB, Gage FH. Intracerebral grafting of neuronal cell suspensions. I. Introduction and general methods of preparation. Acta Physiol. Scand. Suppl. 1983; 522: 1–7.

Björkqvist M, Wild EJ, Thiele J, Silvestroni A, Andre R, Lahiri N, et al. A novel pathogenic pathway of immune activation detectable before clinical onset in Huntington's disease. J. Exp. Med. 2008; 205: 1869–1877.

Bloch J, Bachoud-Lévi AC, Déglon N, Lefaucheur JP, Winkel L, Palfi S, et al. Neuroprotective gene therapy for Huntington's disease, using polymer-encapsulated cells engineered to secrete human ciliary neurotrophic factor: results of a phase I study. Hum. Gene Ther. 2004; 15: 968–975.

Boilard E, Blanco P, Nigrovic PA. Platelets: active players in the pathogenesis of arthritis and SLE. Nat. Rev. Rheumatol. 2012; 8: 534–542.

Bonkowski D, Katyshev V, Balabanov RD, Borisov A, Dore-Duffy P. The CNS microvascular pericyte: pericyte-astrocyte crosstalk in the regulation of tissue survival. Fluids Barriers CNS 2011; 8: 8.

Borlongan CV, Cahill DW, Sanberg PR. Asymmetrical behavior in rats following striatal lesions and fetal transplants: the elevated body swing test. Restor. Neurol. Neurosci. 1995; 9: 15–19.

Borlongan CV, Koutouzis TK, Sanberg PR. 3-Nitropropionic acid animal model and Huntington's disease. Neurosci. Biobehav. Rev. 1997; 21: 289–293.

Borrell-Pagès M, Canals JM, Cordelières FP, Parker JA, Pineda JR, Grange G, et al. Cystamine and cysteamine increase brain levels of BDNF in Huntington disease via HSJ1b and transglutaminase. J. Clin. Invest. 2006; 116: 1410–1424.

Bouchard J, Truong J, Bouchard K, Dunkelberger D, Desrayaud S, Moussaoui S, et al. Cannabinoid Receptor 2 Signaling in Peripheral Immune Cells Modulates Disease Onset and Severity in Mouse Models of Huntington's Disease. J. Neurosci. 2012; 32: 18259–18268.

Bradford J, Shin J-Y, Roberts M, Wang C-E, Li X-J, Li S. Expression of mutant huntingtin in mouse brain astrocytes causes age-dependent neurological symptoms. Proc. Natl. Acad. Sci. U.S.A. 2009; 106: 22480–22485.

Broadwell RD, Charlton HM, Ebert P, Hickey WF, Villegas JC, Wolf AL. Angiogenesis and the blood-brain barrier in solid and dissociated cell grafts within the CNS. Prog. Brain Res. 1990; 82: 95–101.

Broadwell RD, Charlton HM, Ebert PS, Hickey WF, Shirazi Y, Villegas J, et al. Allografts of CNS tissue possess a blood-brain barrier. II. Angiogenesis in solid tissue and cell suspension grafts. Exp. Neurol. 1991; 112: 1–28.

Brundin P, Fricker RA, Nakao N. Paucity of P-zones in striatal grafts prohibit commencement of clinical trials in Huntington's disease. Neuroscience 1996; 71: 895–897.

Brundin P, Karlsson J, Emgård M, Schierle GS, Hansson O, Petersén A, et al. Improving the survival of grafted dopaminergic neurons: a review over current approaches. Cell transplant. 2000; 9: 179–195.

Brundin P, Kordower JH. Neuropathology in transplants in Parkinson's disease: implications for disease pathogenesis and the future of cell therapy. Prog. Brain Res. 2012; 200: 221–241.

Brundin P, Li JY, Holton JL, Lindvall O, Revesz T. Research in motion: the enigma of Parkinson's disease pathology spread. Nat. Rev. Neurosci. 2008; 9: 741–745.

Brundin P, Melki R, Kopito R. Prion-like transmission of protein aggregates in neurodegenerative diseases. Nat. Rev. Mol. Cell Biol. 2010; 11: 301–307.

Brundin P, Nilsson OG, Gage FH, Björklund A. Cyclosporin A increases survival of cross-species intrastriatal grafts of embryonic dopamine-containing neurons. Exp. Brain Res. 1985; 60: 204–208.

Brundin P, Strecker RE, Widner H, Clarke DJ, Nilsson OG, Astedt B, et al. Human fetal dopamine

neurons grafted in a rat model of Parkinson's disease: immunological aspects, spontaneous and drug-induced behaviour, and dopamine release. Exp. Brain Res. 1988; 70: 192–208.

Brundin P, Widner H, Nilsson OG, Strecker RE, Björklund A. Intracerebral xenografts of dopamine neurons: the role of immunosuppression and the blood-brain barrier. Exp. Brain Res. 1989; 75: 195–207.

Butler DC, McLear JA, Messer A. Engineered antibody therapies to counteract mutant huntingtin and related toxic intracellular proteins. Prog. Neurobiol. 2012; 97: 190–204.

Caby M-P, Lankar D, Vincendeau-Scherrer C, Raposo G, Bonnerot C. Exosomal-like vesicles are present in human blood plasma. Int. Immunol. 2005; 17: 879–887.

Capetian P, Knoth R, Maciaczyk J, Pantazis G, Ditter M, Bokla L, et al. Histological findings on fetal striatal grafts in a Huntington's disease patient early after transplantation. Neuroscience 2009; 160: 661–675.

Carli M, Evenden JL, Robbins TW. Depletion of unilateral striatal dopamine impairs initiation of contralateral actions and not sensory attention. Nature 1985; 313: 679–682.

Cattaneo E, Zuccato C, Tartari M. Normal huntingtin function: an alternative approach to Huntington's disease. Nat. Rev. Neurosci. 2005; 6: 919–930.

Ciammola A, Sassone J, Alberti L, Meola G, Mancinelli E, Russo MA, et al. Increased apoptosis, Huntingtin inclusions and altered differentiation in muscle cell cultures from Huntington's disease subjects. Cell Death Differ. 2006; 13: 2068–2078.

Cicchetti F, Parent A. Striatal interneurons in Huntington's disease: selective increase in the density of calretinin-immunoreactive medium-sized neurons. Mov. Disord. 1996; 11: 619–626.

Cicchetti F, Prensa L, Wu Y, Parent A. Chemical anatomy of striatal interneurons in normal individuals and in patients with Huntington's disease. Brain Res. Brain Res. Rev. 2000; 34: 80–101.

Cicchetti F, Saporta S, Hauser RA, Parent M, Saint-Pierre M, Sanberg PR, et al. Neural transplants in patients with Huntington's disease undergo disease-like neuronal degeneration. Proc. Natl. Acad. Sci. U.S.A. 2009; 106: 12483–12488.

Cicchetti F, Soulet D, Freeman TB. Neuronal degeneration in striatal transplants and Huntington's disease: potential mechanisms and clinical implications. Brain 2011; 134: 641–652.

Cisbani G, Cicchetti F. An in vitro perspective on the molecular mechanisms underlying mutant huntingtin protein toxicity. Cell Death Dis. 2012; 3: e382.

Cisbani G, Cicchetti F. The fate of cell grafts for the treatment of Huntington's disease: the post-mortem evidence. Neuropathol. Appl. Neurobiol. 2014; 40: 71–90.

Cisbani G, Freeman TB, Soulet D, Saint-Pierre M, Gagnon D, Parent M, et al. Striatal allografts in

patients with Huntington's disease: impact of diminished astrocytes and vascularization on graft viability. Brain 2013; 136: 433–443.

Cisbani G, Saint-Pierre M, Cicchetti F. Single cell suspension methodology favours survival and vascularization of fetal striatal grafts in the YAC128 mouse model of Huntington's disease. Cell transplant. 2013; doi: 10.3727/096368913X668636.

Clarke DJ, Dunnett SB, Isacson O, Sirinathsinghji DJ, Björklund A. Striatal grafts in rats with unilateral neostriatal lesions--I. Ultrastructural evidence of afferent synaptic inputs from the host nigrostriatal pathway. Neuroscience 1988; 24: 791–801.

Clavaguera F, Akatsu H, Fraser G, Crowther RA, Frank S, Hench J, et al. Brain homogenates from human tauopathies induce tau inclusions in mouse brain. Proc. Natl. Acad. Sci. U.S.A. 2013; 110: 9535–9540.

Clavaguera F, Bolmont T, Crowther RA, Abramowski D, Frank S, Probst A, et al. Transmission and spreading of tauopathy in transgenic mouse brain. Nat. Cell Biol. 2009; 11: 909–913.

Clelland CD, Barker RA, Watts C. Cell therapy in Huntington disease. Neurosurg. Focus 2008; 24: E9.

Cloutier N, Tan S, Boudreau LH, Cramb C, Subbaiah R, Lahey L, et al. The exposure of autoantigens by microparticles underlies the formation of potent inflammatory components: the microparticle-associated immune complexes. EMBO Mol. Med. 2013; 5: 235–249.

Conneally PM. Huntington disease: genetics and epidemiology. Am. J. Hum. Genet. 1984; 36: 506–526.

Costanzo M, Abounit S, Marzo L, Danckaert A, Chamoun Z, Roux P, et al. Transfer of polyglutamine aggregates in neuronal cells occurs in tunneling nanotubes. J. Cell. Sci. 2013; 126: 3678–3685.

Costanzo M, Zurzolo C. The cell biology of prion-like spread of protein aggregates: mechanisms and implication in neurodegeneration. Biochem. J. 2013; 452: 1-17

Cowan CM, Raymond LA. Selective neuronal degeneration in Huntington's disease. Curr. Top. Dev. Biol. 2006; 75: 25–71.

Coyle JT, Schwarcz R. Lesion of striatal neurones with kainic acid provides a model for Huntington's chorea. Nature 1976; 263: 244–246.

Crook ZR, Housman D. Huntington's disease: can mice lead the way to treatment? Neuron 2011; 69: 423–435.

Cross AJ, Slater P, Reynolds GP. Reduced high-affinity glutamate uptake sites in the brains of patients with Huntington's disease. Neurosci. Lett. 1986; 67: 198–202.

Cubillos-Rojas M, Amair-Pinedo F, Tato I, Bartrons R, Ventura F, Rosa JL. Simultaneous electrophoretic analysis of proteins of very high and low molecular mass using Tris-acetate

polyacrylamide gels. Electrophoresis 2010; 31: 1318–1321.

Danzer KM, Kranich LR, Ruf WP, Cagsal-Getkin O, Winslow AR, Zhu L, et al. Exosomal cell-to-cell transmission of alpha synuclein oligomers. Mol. Neurodegener. 2012; 7: 42.

Danzer KM, Ruf WP, Putcha P, Joyner D, Hashimoto T, Glabe C, et al. Heat-shock protein 70 modulates toxic extracellular α-synuclein oligomers and rescues trans-synaptic toxicity. FASEB J. 2011; 25: 326–336.

Date I, Kawamura K, Nakashima H. Histological signs of immune reactions against allogeneic solid fetal neural grafts in the mouse cerebellum depend on the MHC locus. Exp. Brain. Res. 1988; 73: 15–22.

Dawbarn D, De Quidt ME, Emson PC. Survival of basal ganglia neuropeptide Y-somatostatin neurones in Huntington's disease. Brain Res. 1985; 340: 251–260.

de Calignon A, Polydoro M, Suarez-Calvet M, William C, Adamowicz DH, Kopeikina KJ, et al. Propagation of tau pathology in a model of early Alzheimer's disease. Neuron 2012; 73: 685–697.

de Cristofaro T, Affaitati A, Feliciello A, Avvedimento EV, Varrone S. Polyglutamine-mediated aggregation and cell death. Biochem. Biophys. Res. Commun. 2000; 272: 816–821.

Deacon T, Schumacher J, Dinsmore J, Thomas C, Palmer P, Kott S, et al. Histological evidence of fetal pig neural cell survival after transplantation into a patient with Parkinson's disease. Nat. Med. 1997; 3: 350–353.

Deacon TW, Pakzaban P, Isacson O. The lateral ganglionic eminence is the origin of cells committed to striatal phenotypes: neural transplantation and developmental evidence. Brain Res. 1994; 668: 211–219.

Deckel AW, Moran TH, Coyle JT, Sanberg PR, Robinson RG. Anatomical predictors of behavioral recovery following fetal striatal transplants. Brain Res. 1986; 365: 249–258.

Deckel AW, Robinson RG, Coyle JT, Sanberg PR. Reversal of long-term locomotor abnormalities in the kainic acid model of Huntington's disease by day 18 fetal striatal implants. Eur. J. Pharmacol. 1983; 93: 287–288.

Dedeoglu A, Kubilus JK, Jeitner TM, Matson SA, Bogdanov M, Kowall NW, et al. Therapeutic effects of cystamine in a murine model of Huntington's disease. J. Neurosci. 2002; 22: 8942–8950.

Dedeoglu A, Kubilus JK, Yang L, Ferrante KL, Hersch SM, Beal MF, et al. Creatine therapy provides neuroprotection after onset of clinical symptoms in Huntington's disease transgenic mice. J. Neurochem. 2003; 85: 1359–1367.

Demeestere J, Vandenberghe W. Experimental surgical therapies for Huntington's disease. CNS Neurosci. Ther. 2011; 17: 705–713.

Dermietzel R, Traub O, Hwang TK, Beyer E, Bennett MV, Spray DC, et al. Differential expression of three gap junction proteins in developing and mature brain tissues. Proc. Natl. Acad. Sci. U.S.A. 1989; 86: 10148–10152.

Desplats P, Lee HJ, Bae EJ, Patrick C, Rockenstein E, Crews L, et al. Inclusion formation and neuronal cell death through neuron-to-neuron transmission of alpha-synuclein. Proc. Natl. Acad. Sci. U.S.A. 2009; 106: 13010–13015.

Dey ND, Bombard MC, Roland BP, Davidson S, Lu M, Rossignol J, et al. Genetically engineered mesenchymal stem cells reduce behavioral deficits in the YAC 128 mouse model of Huntington's disease. Behav. Brain Res. 2010; 214: 193–200.

DiFiglia M, Sapp E, Chase K, Schwarz C, Meloni A, Young C, et al. Huntingtin is a cytoplasmic protein associated with vesicles in human and rat brain neurons. Neuron 1995; 14: 1075–1081.

DiFiglia M, Sapp E, Chase KO, Davies SW, Bates GP, Vonsattel JP, et al. Aggregation of huntingtin in neuronal intranuclear inclusions and dystrophic neurites in brain. Science 1997; 277: 1990–1993.

DiFiglia M, Schiff L, Deckel AW. Neuronal organization of fetal striatal grafts in kainate- and sham-lesioned rat caudate nucleus: light- and electron-microscopic observations. J. Neurosci. 1988; 8: 1112–1130.

DiFiglia M, Sena-Esteves M, Chase K, Sapp E, Pfister E, Sass M, et al. Therapeutic silencing of mutant huntingtin with siRNA attenuates striatal and cortical neuropathology and behavioral deficits. Proc. Natl. Acad. Sci. U.S.A. 2007; 104: 17204–17209.

DiFiglia M. Huntingtin fragments that aggregate go their separate ways. Mol. Cell 2002; 10: 224–225.

Dore-Duffy P, Owen C, Balabanov R, Murphy S, Beaumont T, Rafols JA. Pericyte migration from the vascular wall in response to traumatic brain injury. Microvasc. Res. 2000; 60: 55–69.

Döbrössy MD, Dunnett SB. The corridor task: striatal lesion effects and graft-mediated recovery in a model of Huntington's disease. Behav. Brain Res. 2007; 179: 326–330.

Dragatsis I, Dietrich P, Zeitlin S. Expression of the Huntingtin-associated protein 1 gene in the developing and adult mouse. Neurosci. Lett. 2000; 282: 37–40.

Du X, Iacovitti L. Synergy between growth factors and transmitters required for catecholamine differentiation in brain neurons. J. Neurosci. 1995; 15: 5420–5427.

Du X, Stull ND, Iacovitti L. Brain-derived neurotrophic factor works coordinately with partner molecules to initiate tyrosine hydroxylase expression in striatal neurons. Brain Res. 1995; 680: 229–233.

Dubinsky R, Gray C. CYTE-I-HD: phase I dose finding and tolerability study of cysteamine (Cystagon) in Huntington's disease. Mov. Disord. 2006; 21: 530–533.

Dunnett SB, Carter RJ, Watts C, Torres EM, Mahal A, Mangiarini L, et al. Striatal transplantation in a

transgenic mouse model of Huntington's disease. Exp. Neurol. 1998; 154: 31–40.

Dunnett SB. Neural tissue transplantation, repair, and rehabilitation. Handb. Clin. Neurol. 2013; 110: 43–59.

Dusart I, Nothias F, Roudier F, Besson JM, Peschanski M. Vascularization of fetal cell suspension grafts in the excitotoxically lesioned adult rat thalamus. Brain Res. Dev. Brain Res. 1989; 48: 215–228.

Duyao M, Ambrose C, Myers R, Novelletto A, Persichetti F, Frontali M, et al. Trinucleotide repeat length instability and age of onset in Huntington's disease. Nat. Genet. 1993; 4: 387–392.

Ebert AD, Barber AE, Heins BM, Svendsen CN. Ex vivo delivery of GDNF maintains motor function and prevents neuronal loss in a transgenic mouse model of Huntington's disease. Exp. Neurol. 2010; 224: 155–162.

Edlinger M, Seppi K, Fleischhacker W, Hofer A. Treatment of psychotic and behavioral symptoms with clozapine, aripiprazole, and reboxetine in a patient with Huntington's disease. Int. Clin. Psychopharmacol. 2013; 28: 214–216.

El-Akabawy G, Rattray I, Johansson SM, Gale R, Bates G, Modo M. Implantation of undifferentiated and pre-differentiated human neural stem cells in the R6/2 transgenic mouse model of Huntington's disease. BMC Neurosci. 2012; 13: 97.

Emerich DF, Lindner MD, Winn SR, Chen EY, Frydel BR, Kordower JH. Implants of encapsulated human CNTF-producing fibroblasts prevent behavioral deficits and striatal degeneration in a rodent model of Huntington's disease. J. Neurosci. 1996; 16: 5168–5181.

Emgård M, Blomgren K, Brundin P. Characterisation of cell damage and death in embryonic mesencephalic tissue: a study on ultrastructure, vital stains and protease activity. Neuroscience 2002; 115: 1177–1187.

Emmanouilidou E, Melachroinou K, Roumeliotis T, Garbis SD, Ntzouni M, Margaritis LH, et al. Cell-produced alpha-synuclein is secreted in a calcium-dependent manner by exosomes and impacts neuronal survival. J. Neurosci. 2010; 30: 6838–6851.

Engelhardt B. Immune cell entry into the central nervous system: involvement of adhesion molecules and chemokines. J. Neurol. Sci. 2008; 274: 23–26.

Eugenin EA, Basilio D, Sáez JC, Orellana JA, Raine CS, Bukauskas F, et al. The role of gap junction channels during physiologic and pathologic conditions of the human central nervous system. J. Neuroimmune Pharmacol. 2012; 7: 499–518.

Fain JN, Del Mar NA, Meade CA, Reiner A, Goldowitz D. Abnormalities in the functioning of adipocytes from R6/2 mice that are transgenic for the Huntington's disease mutation. Hum. Mol. Genet. 2001; 10: 145–152.

Fan MMY, Raymond LA. N-methyl-D-aspartate (NMDA) receptor function and excitotoxicity in

Huntington's disease. Prog. Neurobiol. 2007; 81: 272–293.

Farrer LA, Meaney FJ. An anthropometric assessment of Huntington's disease patients and families. Am. J. Phys. Anthropol. 1985; 67: 185–194.

Feigin A, Kieburtz K, Como P, Hickey C, Claude K, Abwender D, et al. Assessment of coenzyme Q10 tolerability in Huntington's disease. Mov. Disord. 1996; 11: 321–323.

Ferrante RJ, Andreassen OA, Dedeoglu A, Ferrante KL, Jenkins BG, Hersch SM, et al. Therapeutic effects of coenzyme Q10 and remacemide in transgenic mouse models of Huntington's disease. J. Neurosci. 2002; 22: 1592–1599.

Ferrante RJ, Andreassen OA, Jenkins BG, Dedeoglu A, Kuemmerle S, Kubilus JK, et al. Neuroprotective effects of creatine in a transgenic mouse model of Huntington's disease. J. Neurosci. 2000; 20: 4389–4397.

Ferrante RJ, Kowall NW, Beal MF, Martin JB, Bird ED, Richardson EP. Morphologic and histochemical characteristics of a spared subset of striatal neurons in Huntington's disease. J. Neuropathol. Exp. Neurol. 1987; 46: 12–27.

Ferrante RJ, Kowall NW, Beal MF, Richardson EP, Bird ED, Martin JB. Selective sparing of a class of striatal neurons in Huntington's disease. Science 1985; 230: 561–563.

Ferrante RJ, Kubilus JK, Lee J, Ryu H, Beesen A, Zucker B, et al. Histone deacetylase inhibition by sodium butyrate chemotherapy ameliorates the neurodegenerative phenotype in Huntington's disease mice. J. Neurosci. 2003; 23: 9418–9427.

Ferrer I, Goutan E, Marín C, Rey MJ, Ribalta T. Brain-derived neurotrophic factor in Huntington disease. Brain Res. 2000; 866: 257–261.

Féron F, Perry C, Cochrane J, Licina P, Nowitzke A, Urquhart S, et al. Autologous olfactory ensheathing cell transplantation in human spinal cord injury. Brain 2005; 128: 2951–2960.

Février B, Vilette D, Laude H, Raposo G. Exosomes: a bubble ride for prions? Traffic 2005; 6: 10–17.

Finger S, Dunnett SB. Nimodipine enhances growth and vascularization of neural grafts. Exp. Neurol. 1989; 104: 1–9.

Folkersma H, Foster Dingley JC, van Berckel BNM, Rozemuller A, Boellaard R, Huisman MC, et al. Increased cerebral (R)-[(11)C]PK11195 uptake and glutamate release in a rat model of traumatic brain injury: a longitudinal pilot study. J Neuroinflammation 2011; 8: 67.

Foroud T, Gray J, Ivashina J, Conneally PM. Differences in duration of Huntington's disease based on age at onset. J. Neurol. Neurosurg. Psychiatr. 1999; 66: 52–56.

Fox JH, Barber DS, Singh B, Zucker B, Swindell MK, Norflus F, et al. Cystamine increases L-cysteine levels in Huntington's disease transgenic mouse brain and in a PC12 model of polyglutamine

aggregation. J. Neurochem. 2004; 91: 413–422.

Franciosi S, Ryu JK, Shim Y, Hill A, Connolly C, Hayden MR, et al. Age-dependent neurovascular abnormalities and altered microglial morphology in the YAC128 mouse model of Huntington disease. Neurobiol. Dis. 2012; 45: 438–449.

Franich NR, Fitzsimons HL, Fong DM, Klugmann M, During MJ, Young D. AAV vector-mediated RNAi of mutant huntingtin expression is neuroprotective in a novel genetic rat model of Huntington's disease. Mol. Ther. 2008; 16: 947–956.

Freed CR, Greene PE, Breeze RE, Tsai WY, DuMouchel W, Kao R, et al. Transplantation of embryonic dopamine neurons for severe Parkinson's disease. N. Engl. J. Med. 2001; 344: 710–719.

Freeman TB, Cicchetti F, Bachoud-Lévi AC, Dunnett SB. Technical factors that influence neural transplant safety in Huntington's disease. Exp. Neurol. 2011; 227: 1–9.

Freeman TB, Cicchetti F, Hauser RA, Deacon TW, Li XJ, Hersch SM, et al. Transplanted fetal striatum in Huntington's disease: phenotypic development and lack of pathology. Proc. Natl. Acad. Sci. U.S.A. 2000; 97: 13877–13882.

Freeman TB, Sanberg PR, Nauert GM, Boss BD, Spector D, Olanow CW, et al. The influence of donor age on the survival of solid and suspension intraparenchymal human embryonic nigral grafts. Cell transplant. 1995; 4: 141–154.

Fricker RA, Torres EM, Dunnett SB. The effects of donor stage on the survival and function of embryonic striatal grafts in the adult rat brain. I. Morphological characteristics. Neuroscience 1997; 79: 695–710.

Fricker-Gates RA, White A, Gates MA, Dunnett SB. Striatal neurons in striatal grafts are derived from both post-mitotic cells and dividing progenitors. Eur. J. Neurosci. 2004; 19: 513–520.

Furtado S, Suchowersky O, Rewcastle B, Graham L, Klimek ML, Garber A. Relationship between trinucleotide repeats and neuropathological changes in Huntington's disease. Ann. Neurol. 1996; 39: 132–136.

Fusco FR, Chen Q, Lamoreaux WJ, Figueredo-Cardenas G, Jiao Y, Coffman JA, et al. Cellular localization of huntingtin in striatal and cortical neurons in rats: lack of correlation with neuronal vulnerability in Huntington's disease. J. Neurosci. 1999; 19: 1189–1202.

Gallina P, Paganini M, Lombardini L, Mascalchi M, Porfirio B, Gadda D, et al. Human striatal neuroblasts develop and build a striatal-like structure into the brain of Huntington's disease patients after transplantation. Exp. Neurol. 2010; 222: 30–41.

Gallina P, Paganini M, Lombardini L, Saccardi R, Marini M, De Cristofaro MT, et al. Development of human striatal anlagen after transplantation in a patient with Huntington's disease. Exp. Neurol. 2008; 213: 241–244.

Garden GA, Möller T. Microglia biology in health and disease. J. Neuroimmune Pharmacol. 2006; 1: 127–137.

Gates MA, Laywell ED, Fillmore H, Steindler DA. Astrocytes and extracellular matrix following intracerebral transplantation of embryonic ventral mesencephalon or lateral ganglionic eminence. Neuroscience 1996; 74: 579–597.

Gaura V, Bachoud-Lévi A-C, Ribeiro M-J, Nguyen J-P, Frouin V, Baudic S, et al. Striatal neural grafting improves cortical metabolism in Huntington's disease patients. Brain 2004; 127: 65–72.

Geist MJ, Maris DO, Grady MS. Blood-brain barrier permeability is not altered by allograft or xenograft fetal neural cell suspension grafts. Exp. Neurol. 1991; 111: 166–174.

Geny C, Naimi-Sadaoui S, Jény R, Belkadi AM, Juliano SL, Peschanski M. Long-term delayed vascularization of human neural transplants to the rat brain. J. Neurosci. 1994; 14: 7553–7562.

Gerfen CR. The neostriatal mosaic: multiple levels of compartmental organization. Trends Neurosci. 1992; 15: 133–139.

Gharami K, Xie Y, An JJ, Tonegawa S, Xu B. Brain-derived neurotrophic factor over-expression in the forebrain ameliorates Huntington's disease phenotypes in mice. J. Neurochem. 2008; 105: 369–379.

Ginés S, Bosch M, Marco S, Gavaldà N, Díaz-Hernández M, Lucas JJ, et al. Reduced expression of the TrkB receptor in Huntington's disease mouse models and in human brain. Eur. J. Neurosci. 2006; 23: 649–658.

Giordana MT, Grifoni S, Votta B, Magistrello M, Vercellino M, Pellerino A, et al. Neuropathology of olfactory ensheathing cell transplantation into the brain of two amyotrophic lateral sclerosis (ALS) patients. Brain Pathol. 2010; 20: 730–737.

Glass CK, Saijo K, Winner B, Marchetto MC, Gage FH. Mechanisms underlying inflammation in neurodegeneration. Cell 2010; 140: 918–934.

Glass G, Papin JA, Mandell JW. SIMPLE: a sequential immunoperoxidase labeling and erasing method. J. Histochem. Cytochem. 2009; 57: 899–905.

Goedert M, Clavaguera F, Tolnay M. The propagation of prion-like protein inclusions in neurodegenerative diseases. Trends Neurosci. 2010; 33: 317–325.

Goedert M, Spillantini MG, Del Tredici K, Braak H. 100 years of Lewy pathology. Nat. Rev.Neurol. 2013; 9: 13–24.

Gomes C, Keller S, Altevogt P, Costa J. Evidence for secretion of Cu,Zn superoxide dismutase via exosomes from a cell model of amyotrophic lateral sclerosis. Neurosci. Lett. 2007; 428: 43–46.

Gong B, Lim MCY, Wanderer J, Wyttenbach A, Morton AJ. Time-lapse analysis of aggregate formation in an inducible PC12 cell model of Huntington's disease reveals time-dependent aggregate formation

that transiently delays cell death. Brain Res. Bull. 2008; 75: 146–157.

Gousset K, Schiff E, Langevin C, Marijanovic Z, Caputo A, Browman DT, et al. Prions hijack tunnelling nanotubes for intercellular spread. Nat. Cell Biol. 2009; 11: 328–336.

Göritz C, Dias DO, Tomilin N, Barbacid M, Shupliakov O, Frisén J. A pericyte origin of spinal cord scar tissue. Science 2011; 333: 238–242.

Graybiel AM, Liu FC, Dunnett SB. Intrastriatal grafts derived from fetal striatal primordia. I. Phenotypy and modular organization. J. Neurosci. 1989; 9: 3250–3271.

Gupta N, DeFranco AL. Visualizing lipid raft dynamics and early signaling events during antigen receptor-mediated B-lymphocyte activation. Mol. Biol. Cell 2003; 14: 432–444.

Gusella JF, MacDonald ME. Molecular genetics: unmasking polyglutamine triggers in neurodegenerative disease. Nat. Rev. Neurosci. 2000; 1: 109–115.

Gusella JF, Wexler NS, Conneally PM, Naylor SL, Anderson MA, Tanzi RE, et al. A polymorphic DNA marker genetically linked to Huntington's disease. Nature 1983; 306: 234–238.

Gutekunst CA, Levey AI, Heilman CJ, Whaley WL, Yi H, Nash NR, et al. Identification and localization of huntingtin in brain and human lymphoblastoid cell lines with anti-fusion protein antibodies. Proc. Natl. Acad. Sci. U.S.A. 1995; 92: 8710–8714.

Gutekunst CA, Li SH, Yi H, Ferrante RJ, Li XJ, Hersch SM. The cellular and subcellular localization of huntingtin-associated protein 1 (HAP1): comparison with huntingtin in rat and human. J. Neurosci. 1998; 18: 7674–7686.

Gutekunst CA, Li SH, Yi H, Mulroy JS, Kuemmerle S, Jones R, et al. Nuclear and neuropil aggregates in Huntington's disease: relationship to neuropathology. J. Neurosci. 1999; 19: 2522–2534.

Hansen C, Angot E, Bergström A-L, Steiner JA, Pieri L, Paul G, et al. alpha-Synuclein propagates from mouse brain to grafted dopaminergic neurons and seeds aggregation in cultured human cells. J. Clin. Invest. 2011; 121: 715–725.

Hantraye P, Riche D, Maziere M, Isacson O. Intrastriatal transplantation of cross-species fetal striatal cells reduces abnormal movements in a primate model of Huntington disease. Proc. Natl. Acad. Sci. U.S.A. 1992; 89: 4187–4191.

Harper SQ, Staber PD, He X, Eliason SL, Martins IH, Mao Q, et al. RNA interference improves motor and neuropathological abnormalities in a Huntington's disease mouse model. Proc. Natl. Acad. Sci. U.S.A. 2005; 102: 5820–5825.

Hassel B, Tessler S, Faull RLM, Emson PC. Glutamate uptake is reduced in prefrontal cortex in Huntington's disease. Neurochem. Res. 2008; 33: 232–237.

Hauser RA, Freeman TB, Snow BJ, Nauert M, Gauger L, Kordower JH, et al. Long-term evaluation of

bilateral fetal nigral transplantation in Parkinson disease. Arch. Neurol. 1999; 56: 179–187.

Hauser RA, Furtado S, Cimino CR, Delgado H, Eichler S, Schwartz S, et al. Bilateral human fetal striatal transplantation in Huntington's disease. Neurology 2002; 58: 687–695.

Helm GA, Palmer PE, Simmons NE, diPierro C, Bennett JP. Descriptive morphology of developing fetal neostriatal allografts in the rhesus monkey: a correlated light and electron microscopic Golgi study. Neuroscience 1992; 50: 163–179.

Helm GA, Palmer PE, Simmons NE, diPierro CG, Bennett JP. Degeneration of long-term fetal neostriatal allografts in the rhesus monkey: an electron microscopic study. Exp. Neurol. 1993; 123: 174–180.

Herndon ES, Hladik CL, Shang P, Burns DK, Raisanen J, White CL. Neuroanatomic profile of polyglutamine immunoreactivity in Huntington disease brains. J. Neuropathol. Exp. Neurol. 2009; 68: 250–261.

Herrera F, Tenreiro S, Miller-Fleming L, Outeiro TF. Visualization of cell-to-cell transmission of mutant huntingtin oligomers. PLoS Curr. 2011; 3: RRN1210.

Hersch SM, Gevorkian S, Marder K, Moskowitz C, Feigin A, Cox M, et al. Creatine in Huntington disease is safe, tolerable, bioavailable in brain and reduces serum 8OH2'dG. Neurology 2006; 66: 250–252.

Hoffner G, Island M-L, Djian P. Purification of neuronal inclusions of patients with Huntington's disease reveals a broad range of N-terminal fragments of expanded huntingtin and insoluble polymers. J. Neurochem. 2005; 95: 125–136.

Holm KH, Cicchetti F, Bjorklund L, Boonman Z, Tandon P, Costantini LC, et al. Enhanced axonal growth from fetal human bcl-2 transgenic mouse dopamine neurons transplanted to the adult rat striatum. Neuroscience 2001; 104: 397–405.

Huang CC, Faber PW, Persichetti F, Mittal V, Vonsattel JP, MacDonald ME, et al. Amyloid formation by mutant huntingtin: threshold, progressivity and recruitment of normal polyglutamine proteins. Somat. Cell Mol. Genet. 1998; 24: 217–233.

Huang H, Chen L, Xi H, Wang H, Zhang J, Zhang F, et al. Fetal olfactory ensheathing cells transplantation in amyotrophic lateral sclerosis patients: a controlled pilot study. Clin. Transplant. 2008; 22: 710–718.

Hult S, Soylu R, Björklund T, Belgardt BF, Mauer J, Brüning JC, et al. Mutant huntingtin causes metabolic imbalance by disruption of hypothalamic neurocircuits. Cell Metab. 2011; 13: 428–439.

Huntington Study Group Pre2CARE Investigators, Hyson HC, Kieburtz K, Shoulson I, McDermott M, Ravina B, et al. Safety and tolerability of high-dosage coenzyme Q10 in Huntington's disease and healthy subjects. Mov. Disord. 2010; 25: 1924–1928.

Huntington Study Group. A randomized, placebo-controlled trial of coenzyme Q10 and remacemide in Huntington's disease. Neurology 2001; 57: 397–404.

Iadecola C, Nedergaard M. Glial regulation of the cerebral microvasculature. Nat. Neurosci. 2007; 10: 1369–1376.

Iliff JJ, Wang M, Liao Y, Plogg BA, Peng W, Gundersen GA, et al. A paravascular pathway facilitates CSF flow through the brain parenchyma and the clearance of interstitial solutes, including amyloid β. Sci. Transl. Med. 2012; 4: 147ra111.

Im W, Lee S-T, Park JE, Oh HJ, Shim J, Lim J, et al. Transplantation of patient-derived adipose stem cells in YAC128 Huntington's disease transgenic mice. PLoS Curr. 2010; 2

Isacson O, Brundin P, Gage FH, Björklund A. Neural grafting in a rat model of Huntington's disease: progressive neurochemical changes after neostriatal ibotenate lesions and striatal tissue grafting. Neuroscience 1985; 16: 799–817.

Isacson O, Brundin P, Kelly PA, Gage FH, Björklund A. Functional neuronal replacement by grafted striatal neurones in the ibotenic acid-lesioned rat striatum. Nature 1984; 311: 458–460.

Isacson O, Dawbarn D, Brundin P, Gage FH, Emson PC, Björklund A. Neural grafting in a rat model of Huntington's disease: striosomal-like organization of striatal grafts as revealed by acetylcholinesterase histochemistry, immunocytochemistry and receptor autoradiography. Neuroscience 1987; 22: 481–497.

Isacson O, Dunnett SB, Björklund A. Graft-induced behavioral recovery in an animal model of Huntington disease. Proc. Natl. Acad. Sci. U.S.A. 1986; 83: 2728–2732.

Isacson O, Riche D, Hantraye P, Sofroniew MV, Maziere M. A primate model of Huntington's disease: cross-species implantation of striatal precursor cells to the excitotoxically lesioned baboon caudate-putamen. Exp. Brain Res. 1989; 75: 213–220.

Jäderstad J, Jäderstad LM, Herlenius E. Dynamic changes in connexin expression following engraftment of neural stem cells to striatal tissue. Exp. Cell Res. 2011; 317: 70–81.

Jäderstad J, Jäderstad LM, Li J, Chintawar S, Salto C, Pandolfo M, et al. Communication via gap junctions underlies early functional and beneficial interactions between grafted neural stem cells and the host. Proc. Natl. Acad. Sci. U.S.A. 2010; 107: 5184–5189.

Johri A, Beal MF. Hunting-ton for new proteases: MMPs as the new target? Neuron 2010; 67: 171–173.

Kane MD, Lipinski WJ, Callahan MJ, Bian F, Durham RA, Schwarz RD, et al. Evidence for seeding of beta-amyloid by intracerebral infusion of Alzheimer brain extracts in beta -amyloid precursor protein-transgenic mice. J. Neurosci. 2000; 20: 3606–3611.

Karpuj MV, Becher MW, Steinman L. Evidence for a role for transglutaminase in Huntington's disease and the potential therapeutic implications. Neurochemistry international 2002; 40: 31–36.

Kaytor MD, Wilkinson KD, Warren ST. Modulating huntingtin half-life alters polyglutamine-dependent aggregate formation and cell toxicity. J. Neurochem. 2004; 89: 962–973.

Keene CD, Chang RC, Leverenz JB, Kopyov O, Perlman S, Hevner RF, et al. A patient with Huntington's disease and long-surviving fetal neural transplants that developed mass lesions. Acta Neuropathol. 2009; 117: 329–338.

Keene CD, Sonnen JA, Swanson PD, Kopyov O, Leverenz JB, Bird TD, et al. Neural transplantation in Huntington disease: long-term grafts in two patients. Neurology 2007; 68: 2093–2098.

Kells AP, Henry RA, Connor B. AAV-BDNF mediated attenuation of quinolinic acid-induced neuropathology and motor function impairment. Gene Ther. 2008; 15: 966–977.

Kendall AL, Rayment FD, Torres EM, Baker HF, Ridley RM, Dunnett SB. Functional integration of striatal allografts in a primate model of Huntington's disease. Nat. Med. 1998; 4: 727–729.

Kennedy L, Evans E, Chen C-M, Craven L, Detloff PJ, Ennis M, et al. Dramatic tissue-specific mutation length increases are an early molecular event in Huntington disease pathogenesis. Hum. Mol. Genet. 2003; 12: 3359–3367.

Khare SD, Ding F, Gwanmesia KN, Dokholyan NV. Molecular origin of polyglutamine aggregation in neurodegenerative diseases. PLoS Comput. Biol. 2005; 1: 230–235.

Khoshnan A, Ou S, Ko J, Patterson PH. Antibodies and intrabodies against huntingtin: production and screening of monoclonals and single-chain recombinant forms. Methods Mol. Biol. 2013; 1010: 231–251.

Kim M, Soontornniyomkij V, Ji B, Zhou X. System-wide immunohistochemical analysis of protein co-localization. PLoS ONE 2012; 7: e32043.

Ko J, Ou S, Patterson PH. New anti-huntingtin monoclonal antibodies: implications for huntingtin conformation and its binding proteins. Brain Res. Bull. 2001; 56: 319–329.

Kondziolka D, Wechsler L, Gebel J, DeCesare S, Elder E, Meltzer CC. Neuronal transplantation for motor stroke: from the laboratory to the clinic. Phys. Med. Rehabil. Clin. N. Am. 2003; 14: S153–60– xi.

Kopyov OV, Jacques S, Lieberman A, Duma CM, Eagle KS. Safety of intrastriatal neurotransplantation for Huntington's disease patients. Exp. Neurol. 1998; 149: 97–108.

Kordasiewicz HB, Stanek LM, Wancewicz EV, Mazur C, McAlonis MM, Pytel KA, et al. Sustained therapeutic reversal of Huntington's disease by transient repression of huntingtin synthesis. Neuron 2012; 74: 1031–1044.

Kordower JH, Chu Y, Hauser RA, Freeman TB, Olanow CW. Lewy body-like pathology in long-term embryonic nigral transplants in Parkinson's disease. Nat. Med. 2008; 14: 504–506.

Kordower JH, Isacson O, Emerich DF. Cellular delivery of trophic factors for the treatment of

Huntington's disease: is neuroprotection possible? Exp. Neurol. 1999; 159: 4–20.

Kordower JH, Isacson O, Leventhal L, Emerich DF. Cellular delivery of trophic factors for the treatment of Huntington's disease: is neuroprotection possible? Prog. Brain Res. 2000; 127: 414–430.

Kordower JH, Rosenstein JM, Collier TJ, Burke MA, Chen EY, Li JM, et al. Functional fetal nigral grafts in a patient with Parkinson's disease: chemoanatomic, ultrastructural, and metabolic studies. J. Comp. Neurol. 1996; 370: 203–230.

Kordower JH, Styren S, Clarke M, DeKosky ST, Olanow CW, Freeman TB. Fetal grafting for Parkinson's disease: expression of immune markers in two patients with functional fetal nigral implants. Cell transplant. 1997; 6: 213–219.

Krainc D. Huntington's disease: tagged for clearance. Nat. Med. 2010; 16: 32–33.

Krum JM, Rosenstein JM. Patterns of angiogenesis in neural transplant models: I. Autonomic tissue transplants. J. Comp. Neurol. 1987; 258: 420–434.

Krum JM, Rosenstein JM. Patterns of angiogenesis in neural transplant models: II. Fetal neocortical transplants. J. Comp. Neurol. 1988; 271: 331–345.

Krystkowiak P, Gaura V, Labalette M, Rialland A, Remy P, Peschanski M, et al. Alloimmunisation to donor antigens and immune rejection following foetal neural grafts to the brain in patients with Huntington's disease. PLoS ONE 2007; 2: e166.

Kuemmerle S, Gutekunst CA, Klein AM, Li XJ, Li SH, Beal MF, et al. Huntington aggregates may not predict neuronal death in Huntington's disease. Ann. Neurol. 1999; 46: 842–849.

Kwan W, Magnusson A, Chou A, Adame A, Carson MJ, Kohsaka S, et al. Bone marrow transplantation confers modest benefits in mouse models of Huntington's disease. J. Neurosci. 2012; 32: 133–142.

La Spada AR. Trinucleotide repeat instability: genetic features and molecular mechanisms. Brain Pathol. 1997; 7: 943–963.

La Spada AR, Weydt P, Pineda VV. Huntington’s Disease Pathogenesis: Mechanisms and Pathways. Neurobiology of Huntington's Disease: Applications to Drug Discovery. Boca Raton (FL): CRC Press; 2011. Chapter 2

Lakkaraju A, Rodriguez-Boulan E. Itinerant exosomes: emerging roles in cell and tissue polarity. Trends Cell Biol. 2008; 18: 199–209.

Lalić NM, Marić J, Svetel M, Jotić A, Stefanova E, Lalić K, et al. Glucose homeostasis in Huntington disease: abnormalities in insulin sensitivity and early-phase insulin secretion. Arch. Neurol. 2008; 65: 476–480.

Landwehrmeyer GB, McNeil SM, Dure LS, Ge P, Aizawa H, Huang Q, et al. Huntington's disease gene: regional and cellular expression in brain of normal and affected individuals. Ann. Neurol. 1995; 37:

218–230.

Lawrence JM, Huang SK, Raisman G. Vascular and astrocytic reactions during establishment of hippocampal transplants in adult host brain. Neuroscience 1984; 12: 745–760.

Lawrence JM, Morris RJ, Wilson DJ, Raisman G. Mechanisms of allograft rejection in the rat brain. Neuroscience 1990; 37: 431–462.

Leavitt BR, Van Raamsdonk JM, Shehadeh J, Fernandes H, Murphy Z, Graham RK, et al. Wild-type huntingtin protects neurons from excitotoxicity. J. Neurochem. 2006; 96: 1121–1129.

Lee S-T, Chu K, Jung K-H, Im W-S, Park JE, Lim H-C, et al. Slowed progression in models of Huntington disease by adipose stem cell transplantation. Ann. Neurol. 2009; 66: 671–681.

Lee S-T, Chu K, Park J-E, Lee K, Kang L, Kim SU, et al. Intravenous administration of human neural stem cells induces functional recovery in Huntington's disease rat model. Neurosci. Res. 2005; 52: 243–249.

Leigh K, Elisevich K, Rogers KA. Vascularization and microvascular permeability in solid versus cell-suspension embryonic neural grafts. J. Neurosurg. 1994; 81: 272–283.

Leuschner F, Rauch PJ, Ueno T, Gorbatov R, Marinelli B, Lee WW, et al. Rapid monocyte kinetics in acute myocardial infarction are sustained by extramedullary monocytopoiesis. J. Exp. Med. 2012; 209: 123–137.

Levine MS, Cepeda C, André VM. Location, location, location: contrasting roles of synaptic and extrasynaptic NMDA receptors in Huntington's disease. Neuron 2010; 65: 145–147.

Li JY, Englund E, Holton JL, Soulet D, Hagell P, Lees AJ, et al. Lewy bodies in grafted neurons in subjects with Parkinson's disease suggest host-to-graft disease propagation. Nat. Med. 2008; 14: 501–503.

Li L, Welser JV, Milner R. Absence of the alpha v beta 3 integrin dictates the time-course of angiogenesis in the hypoxic central nervous system: accelerated endothelial proliferation correlates with compensatory increases in alpha 5 beta 1 integrin expression. J. Cereb. Blood Flow Metab. 2010; 30: 1031–1043.

Li T, Pang S, Yu Y, Wu X, Guo J, Zhang S. Proliferation of parenchymal microglia is the main source of microgliosis after ischaemic stroke. Brain 2013; 136: 3578–3588.

Lin C-Y, Hsu Y-H, Lin M-H, Yang T-H, Chen H-M, Chen Y-C, et al. Neurovascular abnormalities in humans and mice with Huntington's disease. Exp. Neurol. 2013; 250: 20–30.

Lin Y-T, Chern Y, Shen C-KJ, Wen H-L, Chang Y-C, Li H, et al. Human mesenchymal stem cells prolong survival and ameliorate motor deficit through trophic support in Huntington's disease mouse models. PLoS ONE 2011; 6: e22924.

Lindsay RM, Raisman G. An autoradiographic study of neuronal development, vascularization and glial cell migration from hippocampal transplants labelled in intermediate explant culture. Neuroscience 1984; 12: 513–530.

Lindvall O, Backlund EO, Farde L, Sedvall G, Freedman R, Hoffer B, et al. Transplantation in Parkinson's disease: two cases of adrenal medullary grafts to the putamen. Ann. Neurol. 1987; 22: 457–468.

Lindvall O, Björklund A. Transplantation strategies in the treatment of Parkinson's disease: experimental basis and clinical trials. Acta Neurol. Scand., Suppl.c 1989; 126: 197–210.

Lindvall O, Brundin P, Widner H, Rehncrona S, Gustavii B, Frackowiak R, et al. Grafts of fetal dopamine neurons survive and improve motor function in Parkinson's disease. Science 1990; 247: 574–577.

Lindvall O, Hagell P. Clinical observations after neural transplantation in Parkinson's disease. Prog. Brain Res. 2000; 127: 299–320.

Lindvall O, Rehncrona S, Brundin P, Gustavii B, Astedt B, Widner H, et al. Human fetal dopamine neurons grafted into the striatum in two patients with severe Parkinson's disease. A detailed account of methodology and a 6-month follow-up. Arch. Neurol. 1989; 46: 615–631.

Lindvall O, Rehncrona S, Gustavii B, Brundin P, Astedt B, Widner H, et al. Fetal dopamine-rich mesencephalic grafts in Parkinson's disease. Lancet 1988; 2: 1483–1484.

Lindvall O, Sawle G, Widner H, Rothwell JC, Björklund A, Brooks D, et al. Evidence for long-term survival and function of dopaminergic grafts in progressive Parkinson's disease. Ann. Neurol. 1994; 35: 172–180.

Liu L, Drouet V, Wu JW, Witter MP, Small SA, Clelland C, et al. Trans-synaptic spread of tau pathology in vivo. PLoS ONE 2012; 7: e31302.

Lu X-H, Yang XW. ‘Huntingtin holiday’: progress toward an antisense therapy for Huntington's disease. Neuron 2012; 74: 964–966.

Luk KC, Kehm V, Carroll J, Zhang B, O'Brien P, Trojanowski JQ, et al. Pathological alpha-synuclein transmission initiates Parkinson-like neurodegeneration in nontransgenic mice. Science 2012; 338: 949–953.

Lunkes A, Mandel JL. A cellular model that recapitulates major pathogenic steps of Huntington's disease. Hum. Mol. Genet. 1998; 7: 1355–1361.

Machida Y, Okada T, Kurosawa M, Oyama F, Ozawa K, Nukina N. rAAV-mediated shRNA ameliorated neuropathology in Huntington disease model mouse. Biochem. Biophysical. Res. Commun. 2006; 343: 190–197.

Mai JK, Assheuer J, Paxinos G. Mai: Atlas of the human brain. 2nd edn. London: Elsevier Academic

Press; 2004.

Mann DM, Oliver R, Snowden JS. The topographic distribution of brain atrophy in Huntington's disease and progressive supranuclear palsy. Acta Neuropathol. 1993; 85: 553–559.

Maragakis NJ, Rothstein JD. Mechanisms of Disease: astrocytes in neurodegenerative disease. Nat. Clin. Pract. Neurol. 2006; 2: 679–689.

Markianos M, Panas M, Kalfakis N, Vassilopoulos D. Plasma testosterone in male patients with Huntington's disease: relations to severity of illness and dementia. Ann. Neurol. 2005; 57: 520–525.

Martínez-Serrano A, Björklund A. Protection of the neostriatum against excitotoxic damage by neurotrophin-producing, genetically modified neural stem cells. J. Neurosci. 1996; 16: 4604–4616.

Mason SL, Barker RA. Emerging drug therapies in Huntington's disease. Expert Opin. Emerg. Drugs 2009; 14: 273–297.

Mastroberardino PG, Piacentini M. Type 2 transglutaminase in Huntington's disease: a double-edged sword with clinical potential. J. Intern. Med. 2010; 268: 419–431.

Matthews RT, Yang L, Browne S, Baik M, Beal MF. Coenzyme Q10 administration increases brain mitochondrial concentrations and exerts neuroprotective effects. Proc. Natl. Acad. Sci. U.S.A. 1998; 95: 8892–8897.

Matthews RT, Yang L, Jenkins BG, Ferrante RJ, Rosen BR, Kaddurah-Daouk R, et al. Neuroprotective effects of creatine and cyclocreatine in animal models of Huntington's disease. J. Neurosci. 1998; 18: 156–163.

Mayer E, Fawcett JW, Dunnett SB. Basic fibroblast growth factor promotes the survival of embryonic ventral mesencephalic dopaminergic neurons--II. Effects on nigral transplants in vivo. Neuroscience 1993; 56: 389–398.

Mazzini L, Ferrero I, Luparello V, Rustichelli D, Gunetti M, Mareschi K, et al. Mesenchymal stem cell transplantation in amyotrophic lateral sclerosis: A Phase I clinical trial. Exp. Neurol. 2010; 223: 229–237.

Mazzini L, Mareschi K, Ferrero I, Miglioretti M, Stecco A, Servo S, et al. Mesenchymal stromal cell transplantation in amyotrophic lateral sclerosis: a long-term safety study. Cytotherapy 2012; 14: 56–60.

Mazzocchi-Jones D, Döbrössy M, Dunnett SB. Embryonic striatal grafts restore bi-directional synaptic plasticity in a rodent model of Huntington's disease. Eur. J. Neurosci. 2009; 30: 2134–2142.

McBride JL, Behrstock SP, Chen E-Y, Jakel RJ, Siegel I, Svendsen CN, et al. Human neural stem cell transplants improve motor function in a rat model of Huntington's disease. J. Comp. Neurol. 2004; 475: 211–219.

McGeer EG, McGeer PL. Duplication of biochemical changes of Huntington's chorea by intrastriatal

injections of glutamic and kainic acids. Nature 1976; 263: 517–519.

Melo CV, Okumoto S, Gomes JR, Baptista MS, Bahr BA, Frommer WB, et al. Spatiotemporal resolution of BDNF neuroprotection against glutamate excitotoxicity in cultured hippocampal neurons. Neuroscience 2013; 237: 66–86.

Mendez I, Dagher A, Hong M, Hebb A, Gaudet P, Law A, et al. Enhancement of survival of stored dopaminergic cells and promotion of graft survival by exposure of human fetal nigral tissue to glial cell line--derived neurotrophic factor in patients with Parkinson's disease. Report of two cases and technical considerations. J. Neurosurg. 2000; 92: 863–869.

Mendez I, Sanchez-Pernaute R, Cooper O, Viñuela A, Ferrari D, Björklund L, et al. Cell type analysis of functional fetal dopamine cell suspension transplants in the striatum and substantia nigra of patients with Parkinson's disease. Brain 2005; 128: 1498–1510.

Mendez I, Viñuela A, Astradsson A, Mukhida K, Hallett P, Robertson H, et al. Dopamine neurons implanted into people with Parkinson's disease survive without pathology for 14 years. Nat. Med. 2008; 14: 507–509.

Mestre TA, Ferreira JJ. An evidence-based approach in the treatment of Huntington's disease. Parkinsonism Relat. Disord. 2012; 18: 316–320.

Meyer-Luehmann M, Coomaraswamy J, Bolmont T, Kaeser S, Schaefer C, Kilger E, et al. Exogenous induction of cerebral beta-amyloidogenesis is governed by agent and host. Science 2006; 313: 1781–1784.

Meyer-Luehmann M, Stalder M, Herzig MC, Kaeser SA, Kohler E, Pfeifer M, et al. Extracellular amyloid formation and associated pathology in neural grafts. Nat. Neurosci. 2003; 6: 370–377.

Michaud J-P, Richard KL, Rivest S. Hematopoietic MyD88-adaptor Protein Acts as a Natural Defense Mechanism for Cognitive Deficits in Alzheimer's Disease. Stem Cell Rev. 2012

Montoya CP, Astell S, Dunnett SB. Effects of nigral and striatal grafts on skilled forelimb use in the rat. Prog. Brain Res. 1990; 82: 459–466.

Mundt-Petersen U, Petersén A, Emgård M, Dunnett SB, Brundin P. Caspase inhibition increases embryonic striatal graft survival. Exp. Neurol. 2000; 164: 112–120.

Myers RH, Vonsattel JP, Paskevich PA, Kiely DK, Stevens TJ, Cupples LA, et al. Decreased neuronal and increased oligodendroglial densities in Huntington's disease caudate nucleus. J. Neuropathol. Exp. Neurol. 1991; 50: 729–742.

Nance MA, Mathias-Hagen V, Breningstall G, Wick MJ, McGlennen RC. Analysis of a very large trinucleotide repeat in a patient with juvenile Huntington's disease. Neurology 1999; 52: 392–394.

Nance MA. Comprehensive care in Huntington‘s disease: a physician’s perspective. Brain Res. Bull. 2007; 72: 175–178.

Narain Y, Wyttenbach A, Rankin J, Furlong RA, Rubinsztein DC. A molecular investigation of true dominance in Huntington's disease. J. Med. Genet. 1999; 36: 739–746.

Nguyen T, Hamby A, Massa SM. Clioquinol down-regulates mutant huntingtin expression in vitro and mitigates pathology in a Huntington's disease mouse model. Proc. Natl. Acad. Sci. U.S.A. 2005; 102: 11840–11845.

Nikkhah G, Cunningham MG, Jödicke A, Knappe U, Björklund A. Improved graft survival and striatal reinnervation by microtransplantation of fetal nigral cell suspensions in the rat Parkinson model. Brain Res. 1994; 633: 133–143.

Nimmerjahn A, Kirchhoff F, Helmchen F. Resting microglial cells are highly dynamic surveillants of brain parenchyma in vivo. Science 2005; 308: 1314–1318.

Novak MJU, Tabrizi SJ. Huntington's disease: clinical presentation and treatment. Int. Rev. Neurobiol. 2011; 98: 297–323.

Okamoto S-I, Pouladi MA, Talantova M, Yao D, Xia P, Ehrnhoefer DE, et al. Balance between synaptic versus extrasynaptic NMDA receptor activity influences inclusions and neurotoxicity of mutant huntingtin. Nat. Med. 2009; 15: 1407–1413.

Olanow CW, Goetz CG, Kordower JH, Stoessl AJ, Sossi V, Brin MF, et al. A double-blind controlled trial of bilateral fetal nigral transplantation in Parkinson's disease. Ann. Neurol. 2003; 54: 403–414.

Olanow CW, Prusiner SB. Is Parkinson's disease a prion disorder? Proc. Natl. Acad. Sci. U.S.A. 2009; 106: 12571–12572.

Olsson M, Björklund A, Campbell K. Early specification of striatal projection neurons and interneuronal subtypes in the lateral and medial ganglionic eminence. Neuroscience 1998; 84: 867–876.

Olsson M, Campbell K, Wictorin K, Björklund A. Projection neurons in fetal striatal transplants are predominantly derived from the lateral ganglionic eminence. Neuroscience 1995; 69: 1169–1182.

Ona VO, Li M, Vonsattel JP, Andrews LJ, Khan SQ, Chung WM, et al. Inhibition of caspase-1 slows disease progression in a mouse model of Huntington's disease. Nature 1999; 399: 263–267.

Onfelt B, Nedvetzki S, Benninger RKP, Purbhoo MA, Sowinski S, Hume AN, et al. Structurally distinct membrane nanotubes between human macrophages support long-distance vesicular traffic or surfing of bacteria. J. Immunol. 2006; 177: 8476–8483.

Onfelt B, Nedvetzki S, Yanagi K, Davis DM. Cutting edge: Membrane nanotubes connect immune cells. J. Immunol. 2004; 173: 1511–1513.

Ossato G, Digman MA, Aiken C, Lukacsovich T, Marsh JL, Gratton E. A two-step path to inclusion formation of huntingtin peptides revealed by number and brightness analysis. Biophys. J. 2010; 98: 3078–3085.

Papp KV, Kaplan RF, Snyder PJ. Biological markers of cognition in prodromal Huntington's disease: a review. Brain Cogn. 2011; 77: 280–291.

Parnetti L, Castrioto A, Chiasserini D, Persichetti E, Tambasco N, El-Agnaf O, et al. Cerebrospinal fluid biomarkers in Parkinson disease. Nat. Rev. Neurol. 2013; 9: 131–140.

Pavese N, Gerhard A, Tai YF, Ho AK, Turkheimer F, Barker RA, et al. Microglial activation correlates with severity in Huntington disease: a clinical and PET study. Neurology 2006; 66: 1638–1643.

Paxinos, G.; Franklin, K. B. J. Mouse Brain in Stereotaxic Coordinates, 3rd edition, compact version CD-ROM, Third Edition: A comprehensive brain atlas with an introduction to stereotaxic surgery and the use of stereotaxic coordinates in the laboratory, 3rd ed. San Diego: Academic Press; 2008.

Peavy GM, Jacobson MW, Goldstein JL, Hamilton JM, Kane A, Gamst AC, et al. Cognitive and functional decline in Huntington's disease: dementia criteria revisited. Mov. Disord. 2010; 25: 1163–1169.

Persichetti F, Carlee L, Faber PW, McNeil SM, Ambrose CM, Srinidhi J, et al. Differential expression of normal and mutant Huntington's disease gene alleles. Neurobiol. Dis. 1996; 3: 183–190.

Peschanski M, Cesaro P, Hantraye P. Rationale for intrastriatal grafting of striatal neuroblasts in patients with Huntington's disease. Neuroscience 1995; 68: 273–285.

Phan J, Hickey MA, Zhang P, Chesselet M-F, Reue K. Adipose tissue dysfunction tracks disease progression in two Huntington's disease mouse models. Hum. Mol. Genet. 2009; 18: 1006–1016.

Phillips W, Shannon KM, Barker RA. The current clinical management of Huntington's disease. Mov. Disord. 2008; 23: 1491–1504.

Piccini P, Brooks DJ, Björklund A, Gunn RN, Grasby PM, Rimoldi O, et al. Dopamine release from nigral transplants visualized in vivo in a Parkinson's patient. Nat. Neurosci. 1999; 2: 1137–1140.

Piña AL, Ormsby CE, Bermúdez-Rattoni F. Differential recovery of inhibitory avoidance learning by striatal, cortical, and mesencephalic fetal grafts. Behav. Neural Biol. 1994; 61: 196–201.

Pirici D, Mogoanta L, Kumar-Singh S, Pirici I, Margaritescu C, Simionescu C, et al. Antibody elution method for multiple immunohistochemistry on primary antibodies raised in the same species and of the same subtype. J. Histochem. Cytochem. 2009; 57: 567–575.

Poirier MA, Jiang H, Ross CA. A structure-based analysis of huntingtin mutant polyglutamine aggregation and toxicity: evidence for a compact beta-sheet structure. Hum. Mol. Genet. 2005; 14: 765–774.

Poirier MA, Li H, Macosko J, Cai S, Amzel M, Ross CA. Huntingtin spheroids and protofibrils as precursors in polyglutamine fibrilization. J. Biol. Chem. 2002; 277: 41032–41037.

Polymenidou M, Cleveland DW. The seeds of neurodegeneration: prion-like spreading in ALS. Cell

2011; 147: 498–508.

Pouladi MA, Xie Y, Skotte NH, Ehrnhoefer DE, Graham RK, Kim JE, et al. Full-length huntingtin levels modulate body weight by influencing insulin-like growth factor 1 expression. Hum. Mol. Genet. 2010; 19: 1528–1538.

Pritzel M, Isacson O, Brundin P, Wiklund L, Björklund A. Afferent and efferent connections of striatal grafts implanted into the ibotenic acid lesioned neostriatum in adult rats. Exp. Brain Res. 1986; 65: 112–126.

Rajan RS, Illing ME, Bence NF, Kopito RR. Specificity in intracellular protein aggregation and inclusion body formation. Proc. Natl. Acad. Sci. U.S.A. 2001; 98: 13060–13065.

Rajendran L, Honsho M, Zahn TR, Keller P, Geiger KD, Verkade P, et al. Alzheimer's disease beta-amyloid peptides are released in association with exosomes. Proc. Natl. Acad. Sci. U.S.A. 2006; 103: 11172–11177.

Raju DV, Smith Y. Differential localization of vesicular glutamate transporters 1 and 2 in the rat striatum. The Basal Ganglia VIII. Singapore: Springer. 2005. 601-610.

Ramaswamy S, Kordower JH. Gene therapy for Huntington's disease. Neurobiol. Dis. 2012; 48: 243–254.

Ramón-Cueto A, Santos-Benito FF. Cell therapy to repair injured spinal cords: olfactory ensheathing glia transplantation. Restor. Neurol. Neurosci. 2001; 19: 149–156.

Ransohoff RM, Engelhardt B. The anatomical and cellular basis of immune surveillance in the central nervous system. Nat. Rev. Immunol. 2012; 12: 623–635.

Ravina B, Romer M, Constantinescu R, Biglan K, Brocht A, Kieburtz K, et al. The relationship between CAG repeat length and clinical progression in Huntington's disease. Mov. Disord. 2008; 23: 1223–1227.

Raymond LA, André VM, Cepeda C, Gladding CM, Milnerwood AJ, Levine MS. Pathophysiology of Huntington's disease: time-dependent alterations in synaptic and receptor function. Neuroscience 2011; 198: 252–273.

Redmond DE, Vinuela A, Kordower JH, Isacson O. Influence of cell preparation and target location on the behavioral recovery after striatal transplantation of fetal dopaminergic neurons in a primate model of Parkinson's disease. Neurobiol. Dis. 2008; 29: 103–116.

Reiner A, Dragatsis I, Dietrich P. Genetics and neuropathology of Huntington's disease. Int. Rev. Neurobiol. 2011; 98: 325–372.

Ren P-H, Lauckner JE, Kachirskaia I, Heuser JE, Melki R, Kopito RR. Cytoplasmic penetration and persistent infection of mammalian cells by polyglutamine aggregates. Nat. Cell Biol. 2009; 11: 219–225.

Reuter I, Tai YF, Pavese N, Chaudhuri KR, Mason S, Polkey CE, et al. Long-term clinical and positron

emission tomography outcome of fetal striatal transplantation in Huntington's disease. J. Neurol. Neurosurg. Psychiatr. 2008; 79: 948–951.

Ribchester RR, Thomson D, Wood NI, Hinks T, Gillingwater TH, Wishart TM, et al. Progressive abnormalities in skeletal muscle and neuromuscular junctions of transgenic mice expressing the Huntington's disease mutation. Eur. J. Neurosci. 2004; 20: 3092–3114.

Rice CM, Kemp K, Wilkins A, Scolding NJ. Cell therapy for multiple sclerosis: an evolving concept with implications for other neurodegenerative diseases. Lancet 2013; 382: 1204–1213.

Richfield EK, Maguire-Zeiss KA, Vonkeman HE, Voorn P. Preferential loss of preproenkephalin versus preprotachykinin neurons from the striatum of Huntington's disease patients. Ann. Neurol. 1995; 38: 852–861.

Rodriguez-Lebron E, Denovan-Wright EM, Nash K, Lewin AS, Mandel RJ. Intrastriatal rAAV-mediated delivery of anti-huntingtin shRNAs induces partial reversal of disease progression in R6/1 Huntington's disease transgenic mice. Mol. Ther. 2005; 12: 618–633.

Rosas HD, Doros G, Gevorkian S, Malarick K, Reuter M, Coutu J-P, et al. PRECREST: A phase II prevention and biomarker trial of creatine in at-risk Huntington disease. Neurology 2014

Rose CR, Ransom BR. Regulation of intracellular sodium in cultured rat hippocampal neurones. J. Physiol. 1997; 499: 573–587.

Rosenstein JM, Brightman MW. Alterations of the blood-brain barrier after transplantation of autonomic ganglia into the mammalian central nervous system. J. Comp. Neurol. 1986; 250: 339–351.

Ross BD, Hoang TQ, Blüml S, Dubowitz D, Kopyov OV, Jacques DB, et al. In vivo magnetic resonance spectroscopy of human fetal neural transplants. NMR Biomed. 1999; 12: 221–236.

Ross CA, Poirier MA. Opinion: What is the role of protein aggregation in neurodegeneration? Nat. Rev. Mol. Cell Biol. 2005; 6: 891–898.

Ross CA, Tabrizi SJ. Huntington's disease: from molecular pathogenesis to clinical treatment. Lancet Neurol. 2011; 10: 83–98.

Rosser AE, Bachoud-Lévi A-C. Clinical trials of neural transplantation in Huntington's disease. Prog. Brain Res. 2012; 200: 345–371.

Rosser AE, Barker RA, Harrower T, Watts C, Farrington M, Ho AK, et al. Unilateral transplantation of human primary fetal tissue in four patients with Huntington's disease: NEST-UK safety report ISRCTN no 36485475. J. Neurol. Neurosurg. Psychiatr. 2002; 73: 678–685.

Rustom A, Saffrich R, Markovic I, Walther P, Gerdes H-H. Nanotubular highways for intercellular organelle transport. Science 2004; 303: 1007–1010.

Rutherford A, Garcia-Munoz M, Dunnett SB, Arbuthnott GW. Electrophysiological demonstration of host

cortical inputs to striatal grafts. Neurosci. Lett. 1987; 83: 275–281.

Ryu JK, Kim J, Cho SJ, Hatori K, Nagai A, Choi HB, et al. Proactive transplantation of human neural stem cells prevents degeneration of striatal neurons in a rat model of Huntington disease. Neurobiol. Dis. 2004; 16: 68–77.

Saleh N, Moutereau S, Durr A, Krystkowiak P, Azulay J-P, Tranchant C, et al. Neuroendocrine disturbances in Huntington's disease. PLoS ONE 2009; 4: e4962.

Sanberg PR, Fibiger HC, Mark RF. Body weight and dietary factors in Huntington's disease patients compared with matched controls. Med. J. Aust. 1981; 1: 407–409.

Sanberg PR, Giòrdano M, Henault MA, Nash DR, Ragozzino ME, Hagenmeyer-Houser SH. Intraparenchymal striatal transplants required for maintenance of behavioral recovery in an animal model of Huntington's disease. J. Neural. Transplant. 1989; 1: 23–31.

Sanberg PR, Henault MA, Deckel AW. Locomotor hyperactivity: effects of multiple striatal transplants in an animal model of Huntington's disease. Pharmacol. Biochem. Behav. 1986; 25: 297–300.

Sapp E, Kegel KB, Aronin N, Hashikawa T, Uchiyama Y, Tohyama K, et al. Early and progressive accumulation of reactive microglia in the Huntington disease brain. J. Neuropathol. Exp. Neurol. 2001; 60: 161–172.

Sapp E, Schwarz C, Chase K, Bhide PG, Young AB, Penney J, et al. Huntingtin localization in brains of normal and Huntington's disease patients. Ann. Neurol. 1997; 42: 604–612.

Sapp E, Valencia A, Li X, Aronin N, Kegel KB, Vonsattel J-P, et al. Native mutant huntingtin in human brain: evidence for prevalence of full-length monomer. J. Biol. Chem. 2012; 287: 13487–13499.

Sassone J, Colciago C, Cislaghi G, Silani V, Ciammola A. Huntington's disease: the current state of research with peripheral tissues. Exp. Neurol. 2009; 219: 385–397.

Saudou F, Finkbeiner S, Devys D, Greenberg ME. Huntingtin acts in the nucleus to induce apoptosis but death does not correlate with the formation of intranuclear inclusions. Cell 1998; 95: 55–66.

Savitz SI, Dinsmore J, Wu J, Henderson GV, Stieg P, Caplan LR. Neurotransplantation of fetal porcine cells in patients with basal ganglia infarcts: a preliminary safety and feasibility study. Cerebrovasc. Dis. 2005; 20: 101–107.

Schackel S, Pauly M-C, Piroth T, Nikkhah G, Döbrössy MD. Donor age dependent graft development and recovery in a rat model of Huntington's disease: Histological and behavioral analysis. Behav. Brain Res. 2013; 256: 56-63.

Scheckenbach KEL, Crespin S, Kwak BR, Chanson M. Connexin channel-dependent signaling pathways in inflammation. J. Vasc. Res. 2011; 48: 91–103.

Scherzinger E, Lurz R, Turmaine M, Mangiarini L, Hollenbach B, Hasenbank R, et al. Huntingtin-

encoded polyglutamine expansions form amyloid-like protein aggregates in vitro and in vivo. Cell 1997; 90: 549–558.

Schilling G, Coonfield ML, Ross CA, Borchelt DR. Coenzyme Q10 and remacemide hydrochloride ameliorate motor deficits in a Huntington's disease transgenic mouse model. Neurosci. Lett. 2001; 315: 149–153.

Schmidt RH, Björklund A, Stenevi U. Intracerebral grafting of dissociated CNS tissue suspensions: a new approach for neuronal transplantation to deep brain sites. Brain Res. 1981; 218: 347–356.

Schumacher JM, Ellias SA, Palmer EP, Kott HS, Dinsmore J, Dempsey PK, et al. Transplantation of embryonic porcine mesencephalic tissue in patients with PD. Neurology 2000; 54: 1042–1050.

Scigliano G, Giovannini P, Girotti F, Grassi MP, Caraceni T, Schechter PJ. Gamma-vinyl GABA treatment of Huntington's disease. Neurology 1984; 34: 94–96.

Scott DE. Fetal hypothalamic transplants: neuronal and neurovascular interrelationships. Neurosci. Lett. 1984; 51: 93–98.

Sen A, Capitano ML, Spernyak JA, Schueckler JT, Thomas S, Singh AK, et al. Mild elevation of body temperature reduces tumor interstitial fluid pressure and hypoxia and enhances efficacy of radiotherapy in murine tumor models. Cancer Res. 2011; 71: 3872–3880.

Shelbourne PF, Keller-McGandy C, Bi WL, Yoon S-R, Dubeau L, Veitch NJ, et al. Triplet repeat mutation length gains correlate with cell-type specific vulnerability in Huntington disease brain. Hum. Mol. Genet. 2007; 16: 1133–1142.

Sherer NM. Long-distance relationships: do membrane nanotubes regulate cell-cell communication and disease progression? Mol. Biol. Cell 2013; 24: 1095–1098.

Shin J-Y, Fang Z-H, Yu Z-X, Wang C-E, Li S-H, Li X-J. Expression of mutant huntingtin in glial cells contributes to neuronal excitotoxicity. J. Cell Biol. 2005; 171: 1001–1012.

Shinoda M, Hudson JL, Strömberg I, Hoffer BJ, Moorhead JW, Olson L. Microglial cell responses to fetal ventral mesencephalic tissue grafting and to active and adoptive immunizations. Exp. Neurol. 1996; 141: 173–180.

Shoulson I, Goldblatt D, Charlton M, Joynt RJ. Huntington's disease: treatment with muscimol, a GABA-mimetic drug. Ann. Neurol. 1978; 4: 279–284.

Shoulson I, Kartzinel R, Chase TN. Huntington's disease: treatment with dipropylacetic acid and gamma-aminobutyric acid. Neurology 1976; 26: 61–63.

Shoulson I, Young AB. Milestones in huntington disease. Mov. Disord. 2011; 26: 1127–1133.

Sidman RL, Rakic P. Neuronal migration, with special reference to developing human brain: a review. Brain Res. 1973; 62: 1–35.

Sieradzan KA, Mann DM. The selective vulnerability of nerve cells in Huntington's disease. Neuropathol. Appl. Neurobiol. 2001; 27: 1–21.

Sieradzan KA, Mechan AO, Jones L, Wanker EE, Nukina N, Mann DM. Huntington's disease intranuclear inclusions contain truncated, ubiquitinated huntingtin protein. Exp. Neurol. 1999; 156: 92–99.

Simard AR, Soulet D, Gowing G, Julien J-P, Rivest S. Bone marrow-derived microglia play a critical role in restricting senile plaque formation in Alzheimer's disease. Neuron 2006; 49: 489–502.

Slow EJ, van Raamsdonk J, Rogers D, Coleman SH, Graham RK, Deng Y, et al. Selective striatal neuronal loss in a YAC128 mouse model of Huntington disease. Hum. Mol. Genet. 2003; 12: 1555–1567.

Snyder BR, Chiu AM, Prockop DJ, Chan AWS. Human multipotent stromal cells (MSCs) increase neurogenesis and decrease atrophy of the striatum in a transgenic mouse model for Huntington's disease. PLoS ONE 2010; 5: e9347.

Sokal RR, Rohlf FJ. Biometry. 3rd Edn. Macmillan; 1995.

Sortwell CE. Strategies for the augmentation of grafted dopamine neuron survival. Front. Biosci. 2003; 8: s522–32.

Soto C. Transmissible proteins: expanding the prion heresy. Cell 2012; 149: 968–977.

Soulet D, Cicchetti F. The role of immunity in Huntington's disease. Mol. Psychiatry 2011; 16: 889–902.

Southwell AL, Khoshnan A, Dunn DE, Bugg CW, Lo DC, Patterson PH. Intrabodies binding the proline-rich domains of mutant huntingtin increase its turnover and reduce neurotoxicity. J. Neurosci. 2008; 28: 9013–9020.

Southwell AL, Ko J, Patterson PH. Intrabody gene therapy ameliorates motor, cognitive, and neuropathological symptoms in multiple mouse models of Huntington's disease. J. Neurosci. 2009; 29: 13589–13602.

Sowinski S, Jolly C, Berninghausen O, Purbhoo MA, Chauveau A, Köhler K, et al. Membrane nanotubes physically connect T cells over long distances presenting a novel route for HIV-1 transmission. Nat. Cell Biol. 2008; 10: 211–219.

Squitieri F, Cannella M, Giallonardo P, Maglione V, Mariotti C, Hayden MR. Onset and pre-onset studies to define the Huntington's disease natural history. Brain Res. Bull. 2001; 56: 233–238.

Stack EC, Dedeoglu A, Smith KM, Cormier K, Kubilus JK, Bogdanov M, et al. Neuroprotective effects of synaptic modulation in Huntington's disease R6/2 mice. J. Neurosci. 2007; 27: 12908–12915.

Steffan JS, Kazantsev A, Spasic-Boskovic O, Greenwald M, Zhu YZ, Gohler H, et al. The Huntington's disease protein interacts with p53 and CREB-binding protein and represses transcription. Proc. Natl.

Acad. Sci. U.S.A. 2000; 97: 6763–6768.

Steiner H, Tseng KY. Handbook of Basal Ganglia Structure and Function. Academic Press; 2010; 151-154.

Stenevi U, Björklund A, Svendgaard NA. Transplantation of central and peripheral monoamine neurons to the adult rat brain: techniques and conditions for survival. Brain Res. 1976; 114: 1–20.

Stocks M. Intrabodies as drug discovery tools and therapeutics. Curr. Opin Chem. Biol. 2005; 9: 359–365.

Stoy N, McKay E. Weight loss in Huntington's disease. Ann. Neurol. 2000; 48: 130–131.

Sun Y, Savanenin A, Reddy PH, Liu YF. Polyglutamine-expanded huntingtin promotes sensitization of N-methyl-D-aspartate receptors via post-synaptic density 95. J. Biol. Chem. 2001; 276: 24713–24718.

Tabernero A, Medina JM, Giaume C. Glucose metabolism and proliferation in glia: role of astrocytic gap junctions. J. Neurochem. 2006; 99: 1049–1061.

Tai YF, Pavese N, Gerhard A, Tabrizi SJ, Barker RA, Brooks DJ, et al. Imaging microglial activation in Huntington's disease. Brain Res. Bull. 2007; 72: 148–151.

Tang T-S, Chen X, Liu J, Bezprozvanny I. Dopaminergic signaling and striatal neurodegeneration in Huntington's disease. J. Neurosci. 2007; 27: 7899–7910.

Tapiola T, Alafuzoff I, Herukka S-K, Parkkinen L, Hartikainen P, Soininen H, et al. Cerebrospinal fluid {beta}-amyloid 42 and tau proteins as biomarkers of Alzheimer-type pathologic changes in the brain. Arch. Neurol. 2009; 66: 382–389.

Tarlac V, Storey E. Role of proteolysis in polyglutamine disorders. J. Neurosci. Res. 2003; 74: 406–416.

Taylor-Robinson SD, Weeks RA, Bryant DJ, Sargentoni J, Marcus CD, Harding AE, et al. Proton magnetic resonance spectroscopy in Huntington's disease: evidence in favour of the glutamate excitotoxic theory. Mov. Disord. 1996; 11: 167–173.

Terpstra BT, Collier TJ, Marchionini DM, Levine ND, Paumier KL, Sortwell CE. Increased cell suspension concentration augments the survival rate of grafted tyrosine hydroxylase immunoreactive neurons. J. Neurosci. methods 2007; 166: 13–19.

The Huntington’s Disease Collaborative Research Group. A novel gene containing a trinucleotide repeat that is expanded and unstable on Huntington‘s disease chromosomes. T. Cell 1993; 72: 971–983.

Theis M, Giaume C. Connexin-based intercellular communication and astrocyte heterogeneity. Brain Res. 2012; 1487: 88–98.

Théry C, Ostrowski M, Segura E. Membrane vesicles as conveyors of immune responses. Nat. Rev. Immunol. 2009; 9: 581–593.

Théry C, Zitvogel L, Amigorena S. Exosomes: composition, biogenesis and function. Nat. Rev. Immunol. 2002; 2: 569–579.

Tinsley RB, Kotschet K, Modesto D, Ng H, Wang Y, Nagley P, et al. Sensitive and specific detection of α-synuclein in human plasma. J. Neurosci. Res. 2010; 88: 2693–2700.

Träger U, Andre R, Lahiri N, Magnusson-Lind A, Weiss A, Grueninger S, et al. HTT-lowering reverses Huntington's disease immune dysfunction caused by NFκB pathway dysregulation. Brain 2014

Trottier Y, Devys D, Imbert G, Saudou F, An I, Lutz Y, et al. Cellular localization of the Huntington's disease protein and discrimination of the normal and mutated form. Nat. Genet. 1995; 10: 104–110.

Trushina E, Dyer RB, Badger JD, Ure D, Eide L, Tran DD, et al. Mutant huntingtin impairs axonal trafficking in mammalian neurons in vivo and in vitro. Mol. Cell Biol. 2004; 24: 8195–8209.

Tulipan N, Huang S, Whetsell WO, Allen GS. Neonatal striatal grafts prevent lethal syndrome produced by bilateral intrastriatal injection of kainic acid. Brain Res. 1986; 377: 163–167.

Tydlacka S, Wang C-E, Wang X, Li S, Li X-J. Differential activities of the ubiquitin-proteasome system in neurons versus glia may account for the preferential accumulation of misfolded proteins in neurons. J. Neurosci. 2008; 28: 13285–13295.

Uccelli A, Mancardi G. Stem cell transplantation in multiple sclerosis. Curr. Opin. Neurol. 2010; 23: 218–225.

van der Burg JMM, Björkqvist M, Brundin P. Beyond the brain: widespread pathology in Huntington's disease. Lancet Neurol. 2009; 8: 765–774.

van Niel G, Porto-Carreiro I, Simoes S, Raposo G. Exosomes: a common pathway for a specialized function. J. Biochem. 2006; 140: 13–21.

Van Raamsdonk JM, Murphy Z, Selva DM, Hamidizadeh R, Pearson J, Petersén Å, et al. Testicular degeneration in Huntington disease. Neurobiol. Dis. 2007; 26: 512–520.

Van Raamsdonk JM, Murphy Z, Slow EJ, Leavitt BR, Hayden MR. Selective degeneration and nuclear localization of mutant huntingtin in the YAC128 mouse model of Huntington disease. Hum. Mol. Genet. 2005; 14: 3823–3835.

Van Raamsdonk JM, Pearson J, Slow EJ, Hossain SM, Leavitt BR, Hayden MR. Cognitive dysfunction precedes neuropathology and motor abnormalities in the YAC128 mouse model of Huntington's disease. J. Neurosci. 2005; 25: 4169–4180.

Velloso NA, Dalmolin GD, Gomes GM, Rubin MA, Canas PM, Cunha RA, et al. Spermine improves recognition memory deficit in a rodent model of Huntington's disease. Neurobiol. Learn. Mem. 2009; 92:

574–580.

Vingtdeux V, Sergeant N, Buée L. Potential contribution of exosomes to the prion-like propagation of lesions in Alzheimer's disease. Front. Physiol. 2012; 3: 229.

Vis JC, Nicholson LF, Faull RL, Evans WH, Severs NJ, Green CR. Connexin expression in Huntington's diseased human brain. Cell Biol. Int. 1998; 22: 837–847.

Vonsattel JP, DiFiglia M. Huntington disease. J. Neuropathol. Exp. Neurol. 1998; 57: 369–384.

Vonsattel JP, Myers RH, Stevens TJ, Ferrante RJ, Bird ED, Richardson EP. Neuropathological classification of Huntington's disease. J. Neuropathol. Exp. Neurol. 1985; 44: 559–577.

Vonsattel JPG. Huntington disease models and human neuropathology: similarities and differences. Acta Neuropathol. 2008; 115: 55–69.

Wallman M-J, Gagnon D, Parent M. Serotonin innervation of human basal ganglia. Eur. J. Neurosci. 2011; 33: 1519–1532.

Wallraff A, Köhling R, Heinemann U, Theis M, Willecke K, Steinhäuser C. The impact of astrocytic gap junctional coupling on potassium buffering in the hippocampus. J. Neurosci. 2006; 26: 5438–5447.

Wang C-E, Zhou H, McGuire JR, Cerullo V, Lee B, Li S-H, et al. Suppression of neuropil aggregates and neurological symptoms by an intracellular antibody implicates the cytoplasmic toxicity of mutant huntingtin. J. Cell Biol. 2008; 181: 803–816.

Wang Y, Cui J, Sun X, Zhang Y. Tunneling-nanotube development in astrocytes depends on p53 activation. Cell Death Differ. 2011; 18: 732–742.

Wang Y, Tien LT, Lapchak PA, Hoffer BJ. GDNF triggers fiber outgrowth of fetal ventral mesencephalic grafts from nigra to striatum in 6-OHDA-lesioned rats. Cell Tissue Res. 1996; 286: 225–233.

Wang Y-L, Liu W, Wada E, Murata M, Wada K, Kanazawa I. Clinico-pathological rescue of a model mouse of Huntington's disease by siRNA. Neurosci. Res. 2005; 53: 241–249.

Watts C, Brasted PJ, Dunnett SB. Embryonic donor age and dissection influences striatal graft development and functional integration in a rodent model of Huntington's disease. Exp. Neurol. 2000a; 163: 85–97.

Watts C, Brasted PJ, Dunnett SB. The morphology, integration, and functional efficacy of striatal grafts differ between cell suspensions and tissue pieces. Cell transplant. 2000b; 9: 395–407.

Weiss A, Abramowski D, Bibel M, Bodner R, Chopra V, DiFiglia M, et al. Single-step detection of mutant huntingtin in animal and human tissues: a bioassay for Huntington's disease. Anal. Biochem. 2009; 395: 8–15.

Weiss A, Träger U, Wild EJ, Grueninger S, Farmer R, Landles C, et al. Mutant huntingtin fragmentation

in immune cells tracks Huntington's disease progression. J. Clin. Invest. 2012; 122: 3731–3736.

Wheeler VC, White JK, Gutekunst CA, Vrbanac V, Weaver M, Li XJ, et al. Long glutamine tracts cause nuclear localization of a novel form of huntingtin in medium spiny striatal neurons in HdhQ92 and HdhQ111 knock-in mice. Hum. Mol. Genet. 2000; 9: 503–513.

White JK, Auerbach W, Duyao MP, Vonsattel JP, Gusella JF, Joyner AL, et al. Huntingtin is required for neurogenesis and is not impaired by the Huntington's disease CAG expansion. Nat. Genet. 1997; 17: 404–410.

Wictorin K, Brundin P, Gustavii B, Lindvall O, Björklund A. Reformation of long axon pathways in adult rat central nervous system by human forebrain neuroblasts. Nature 1990; 347: 556–558.

Wictorin K, Clarke DJ, Bolam JP, Björklund A. Host Corticostriatal Fibres Establish Synaptic Connections with Grafted Striatal Neurons in the Ibotenic Acid Lesioned Striatum. Eur. J. Neurosci. 1989; 1: 189–195.

Wictorin K, Isacson O, Fischer W, Nothias F, Peschanski M, Björklund A. Connectivity of striatal grafts implanted into the ibotenic acid-lesioned striatum--I. Subcortical afferents. Neuroscience 1988; 27: 547–562.

Wictorin K. Anatomy and connectivity of intrastriatal striatal transplants. Prog. Neurobiol. 1992; 38: 611–639.

Wiegand SJ, Gash DM. Characteristics of vasculature and neurovascular relations in intraventricular anterior hypothalamic transplants. Brain Res. Bull. 1988; 20: 105–124.

Wilson EH, Weninger W, Hunter CA. Trafficking of immune cells in the central nervous system. J. Clin. Invest. 2010; 120: 1368–1379.

Winkler EA, Bell RD, Zlokovic BV. Central nervous system pericytes in health and disease. Nat. Neurosci. 2011; 14: 1398–1405.

Wolf P. The nature and significance of platelet products in human plasma. Br. J. Haematol. 1967; 13: 269–288.

Wu Y, Parent A. Striatal interneurons expressing calretinin, parvalbumin or NADPH-diaphorase: a comparative study in the rat, monkey and human. Brain Res. 2000; 863: 182–191.

Yang L, Calingasan NY, Wille EJ, Cormier K, Smith K, Ferrante RJ, et al. Combination therapy with coenzyme Q10 and creatine produces additive neuroprotective effects in models of Parkinson‘s and Huntington’s diseases. J. Neurochem. 2009; 109: 1427–1439.

Yang W, Dunlap JR, Andrews RB, Wetzel R. Aggregated polyglutamine peptides delivered to nuclei are toxic to mammalian cells. Hum. Mol. Genet. 2002; 11: 2905–2917.

Zhang Y, Li M, Drozda M, Chen M, Ren S, Mejia Sanchez RO, et al. Depletion of wild-type huntingtin in

mouse models of neurologic diseases. J. Neurochem. 2003; 87: 101–106.

Zhou J, Bradford HF, Stern GM. Influence of BDNF on the expression of the dopaminergic phenotype of tissue used for brain transplants. Brain Res. Dev. Brain Res. 1997; 100: 43–51.

Zuccato C, Cattaneo E. Role of brain-derived neurotrophic factor in Huntington's disease. Prog. Neurobiol. 2007; 81: 294–330.

Zuccato C, Cattaneo E. Brain-derived neurotrophic factor in neurodegenerative diseases. Nat. Rev. Neurol. 2009; 5: 311–322.

Zuccato C, Marullo M, Vitali B, Tarditi A, Mariotti C, Valenza M, et al. Brain-derived neurotrophic factor in patients with Huntington's disease. PLoS ONE 2011; 6: e22966.

Zuccato C, Valenza M, Cattaneo E. Molecular mechanisms and potential therapeutical targets in Huntington's disease. Physiol. Rev. 2010; 90: 905–981.

Zuchner T, Brundin P. Mutant huntingtin can paradoxically protect neurons from death. Cell Death Differ. 2008; 15: 435–442.